To the Graduate Council

I am submitting herewith a dissertation written by Keith Eric Roberson entitled "Depositional History and Early Freshwater Diagenesis of Basal Middle Ordovician Peritidal Carbonate Rocks, East Tennessee". I have examined the final copy of this dissertation for form and content and recommend that it be accepted for the degree of Doctor of Philosophy, with a major in Geology.

Kenneth R. Walker

Kenneth R. Walker, Major Professor

We have read this dissertation and recommend its acceptance

Robert C. Kopp

Steven G. Driese

Walid Alawan

Accepted for the council

Lew Minkel

Associate Vice Chancellor and Dean of the Graduate School

DEPOSITIONAL HISTORY AND EARLY FRESHWATER DIAGENESIS OF BASAL MIDDLE ORDOVICIAN PERITIDAL CARBONATE ROCKS, EAST TENNESSEE

A Dissertation
Presented for the
Doctor of Philosophy
Degree
The University of Tennessee, Knoxville

Keith Eric Roberson
May, 1994

DEDICATION

This dissertation is dedicated to my extraordinarily patient wife, Jennifer Tobola Roberson. You've been with me since I started this project, and the accomplishment is yours as much as it is mine. Thank you so much for hanging in there.

ACKNOWLEDGMENTS

I wish to express my appreciation to Dr. Kenneth R. Walker for his constant moral and financial support while serving as my dissertation chairman; to Drs. Steven G. Driese, Otto C. Kopp, and Vahid Alavian for serving on my committee; to present and former members of the "Carbonate Bank"--Dr. J. Lincoln Foreman, Dr. R. Eric Johnson, Dr. D. Mark Steinhauff, Dr. Krishnan Srinivasan, Dr. J. Dan Walker, Dr. L. James Weber, and the future Dr. Kenneth J. Tobin for always being available for technical support and stimulating discussions of our research; to Drs. L. A. Hardie, E. A. Shinn, and R.N. Ginsburg for their pioneering work on tidal flat sedimentation and on the Andros Island tidal flat in particular; to Dr. Anita G. Harris and the U.S. Geological Survey for help with conodont biostratigraphy (again); to International Technology Corporation (IT) for financial assistance and allowing me time off from work to complete my degree; to Chris Olson, Andy Stefaniak, Ian Richards, Marvin Bennett, and Krishnan Srinivasan for assistance and hospitality during the completion of this dissertation; and to all my friends at school and at work, and all the people I've played music with over the past years, for the moral support and recreational therapy necessary to get me through this. Finally, I'd like to extend special thanks to my parents, Manley C. and Louise Roberson, for always stressing education as the way to a better life.

This research was supported by grants from the National Science Foundation to Dr. Ken Walker, and by the University of Tennessee Department of Geological Sciences discretionary fund.

ABSTRACT

The basal Middle Ordovician strata in the Valley and Ridge province of eastern Tennessee signify the resumption of carbonate deposition after post-Knox exposure in depositional environments that paralleled the eastern shoreline of the North American continent. The Douglas Lake Member of the Lenoir Formation and the Blackford Member of the Five Oaks Formation are the basal stratigraphic units of this peritidal sequence, and were deposited in isolated topographic depressions on the Knox surface in a variety of isolated nearshore terrestrial and paralic environments. The Mosheim Member of the Lenoir Formation and the main body of the Five Oaks Formation comprise a complex tidal-flat facies that developed and migrated across the Knox surface during continued marine transgression after topographic depressions were filled. The Lincolnshire Formation and the main body of the Lenoir Formation overlie the tidal-flat facies, and represent deposition in the shallow subtidal marine environment that lay just offshore from the tidal flat. The vertical succession of these three facies defines a deepening-upward, transgressive sequence that resulted from the landward migration of the package of peritidal environments.

The Mosheim/Five Oaks tidal-flat facies is a close ancient analogue to the Holocene tidal flat on Andros Island in the Bahamas. This tidal flat consists of three major subfacies, each of which is analogous to a subenvironment of the Andros Island tidal flat. The highly fenestral, laminated basal portion of the Mosheim/Five Oaks facies was deposited in a supratidal environment analogous to the inland algal marsh, the most landward portion of the Andros Island tidal flat complex. The majority of the Mosheim/ Five Oaks facies consists of a random arrangement of shallow subtidal, intertidal, and supratidal lithologies that represent deposition in a complex mosaic of ponds, channels, algal marshes, and levees, that collectively represent an Andros Island-type channeled

belt. The uppermost layers of the sequence at many outcrops represent supratidal deposition on a beach ridge that formed the seaward margin of the tidal flat. The vertical succession of subfacies within the Mosheim/Five Oaks tidal-flat facies defines a transgressive sequence that contains no evidence of progradational, shallowing-upward cycles.

The Mosheim/Five Oaks tidal-flat facies and the overlying adjacent offshore subtidal marine facies do not interfinger, and the contact between the two facies signifies the final flooding of the tidal flat due to transgression by the offshore marine environment. The upper surface of the tidal-flat facies is typically sharp and erosional, and exhibits evidence of subaerial exposure, early lithification, and wave scour, and probably formed through a combination of subaerial (karst) dissolution and tidal erosion. Despite evidence of vadose alteration and erosion, paleontologic data indicate that this surface represents only a brief break in deposition, and is not a major disconformity. This erosional surface is not a depositional sequence boundary, because the vertical sequence of facies predicted by Walther's Law for transgressive superpositioning of adjacent peritidal facies is not disrupted at the surface. Also, the development of the surface is diachronous across strike belts, and therefore cannot be the result of eustatic sea level fall, but is merely the result of transgression of the subtidal offshore environment over the tidal flat. An analogous erosional surface is presently forming without sea level fall in a very similar stratigraphic setting on the northwest side of Andros Island as a result of transgressive migration of peritidal environments.

Diagenetic alteration of the tidal flat facies is overwhelmingly dominated by features that indicate alteration by meteoric water in unsaturated (vadose) and saturated (phreatic) zones. Subaerial exposure and vadose alteration is indicated by several features, including: (1) abundant fenestral fabrics and rare shrinkage cracks; (2) progressive alteration of fenestral fabrics to diagenetic grainstone/pisolite fabrics;

(3) exposure surfaces and thin bleached zones within and at the top of supra- and intertidal lithologies; (4) localized zones of incipient caliche development, typically just below exposure surfaces; (5) pendant and meniscus cement distributions; and (6) geopetal crystal silt in fenestrae and vugs. Additional evidence of meteoric diagenesis that may have begun in the vadose zone and continued in the phreatic realm includes dissolution features such as fossil molds and solution-enlarged molds and vugs; stabilization of lime mud to micrite; and the ubiquitous presence of clear, non-ferroan, compositionally-zoned, equant calcite cement. Stable oxygen isotope ratios for these cements show depletion in ^{18}O relative to Ordovician seawater values. Virtually all porosity is occluded by equant calcite cement; other types of cement and other authigenic minerals are volumetrically negligible.

Dolomite within the tidal-flat sequence is uncommon, and generally occurs as isolated rhombs disseminated widely through the muddy matrix. As a rule, dolomite abundance decreases upward within the tidal flat facies, and the only pervasively dolomitized lithologies occur within a meter of the base of the facies, where magnesium was available from several sources, including mobilization of Mg^{++} from the underlying Knox dolostones and movement of burial fluids along the Knox unconformity. Above the basal strata, dolomite abundance is related to depositional subenvironment, and is most abundant in burrowed, subtidal lithologies and least abundant in supratidal fenestral lithologies. Dolomitization of subtidal pond sediment may have occurred by interaction with mixed meteoric / marine fluids in the coastal mixing zone.

Most diagenetic alteration within the tidal-flat facies occurred very early, beginning immediately upon deposition and being largely concluded before deep burial. Most diagenesis occurred in the tidal-flat depositional environment. The upper surface of the tidal-flat facies, and likely other subaerially exposed horizons within the facies, were at least partially lithified prior to deposition of the overlying strata. Evidence for early

diagenetic alteration and lithification of inter- and supratidal lithologies occurs in the form of 1) paleokarst features on the upper erosion surface; 2) truncation of cements at erosional surfaces; 3) borings and vugs extending downward from erosion surfaces; and 4) encrustation of the upper erosion surface by calcareous marine organisms. The timing of diagenetic alteration of subtidal lithologies is less well constrained, but probably was largely completed during shallow burial in the phreatic environment. Hydrologically, the setting in which deposition and early diagenesis occurred was a zone of mixing of seawater and freshwater in an unconfined coastal aquifer. The composition of the fluids that covered this tidal flat and saturated the sediment beneath the water table (and mean sea level) probably fluctuated between meteoric and normal marine end members, but the diagenetic features and geochemical data indicate that the predominant water chemistry was probably closer in composition to freshwater than to seawater.

TABLE OF CONTENTS

Chapter Page

1. INTRODUCTION 1
   Methods 4

2. GEOLOGIC SETTING AND STRATIGRAPHY OF THE BASAL MIDDLE ORDOVICIAN CARBONATE SEQUENCE, EAST TENNESSEE 6
   Geologic Setting 6
      Tectonic Framework 6
      Study Area 8
   Stratigraphy 10
      Across-Strike Variations in Middle Ordovician Stratigraphy 10
      Ages of Basal Middle Ordovician Units 12
      Correlation with Units Outside the Study Area 15

3. DEPOSITIONAL HISTORY OF THE BASAL MIDDLE ORDOVICIAN PERITIDAL CARBONATE ROCKS, EAST TENNESSEE: DEVELOPMENT AND MIGRATION OF AN ANDROS ISLAND-TYPE TIDAL FLAT WITHIN A TRANSGRESSIVE SEDIMENTARY SEQUENCE 19
   Introduction 19
   Geologic Setting 20
   Lithofacies Descriptions and Environmental Interpretations 21
      Nearshore Terrestrial / Paralic Lithofacies 23
      Tidal Flat Lithofacies 40
      Adjacent Offshore Marine Lithofacies 70
   Nature of Tidal Flat Deposition 74
      Summary of Sedimentological Features and Environmental Interpretations 74
      Vertical Arrangement of Subfacies Within the Tidal Flat Facies 80
      Discussion: Absence of Progradational Cycles Within the Mosheim/Five Oaks Tidal Flat Facies 89
   Summary: Depositional Model 93
   Conclusions 94

4. EARLY DIAGENESIS OF A MIDDLE ORDOVICIAN CARBONATE TIDAL FLAT IN A FRESHWATER-DOMINATED COASTAL MIXING ZONE 96
   Introduction 96
   Geologic Setting 97
      Depositional History and Environments of Deposition 97

Burial History 98

Diagenetic Features and Processes 101
Porosity Development 101
Porosity Occlusion 115
Matrix Alteration 133
Burial Diagenesis 158
Diagenetic History 161
Constraints on Timing of Diagenetic Events 161
Paragenetic Sequence 165
Diagenetic Environments 165
Relationship Between Diagenesis of the Basal Peritidal Limestones and the Overlying Middle Ordovician Strata 167
Paleohydrologic Model 169
Sources and Travel Pathways of Fluids 171
Zones of Diagenetic Alteration 172
Controls on Later Fluid Migration and Economic Implications 173
Conclusions 174

5. A REGIONAL APPALACHIAN EROSIONAL SURFACE PRODUCED SOLELY BY ENVIRONMENTAL MIGRATION WITHIN A MIDDLE ORDOVICIAN TRANSGRESSIVE SEDIMENTARY SEQUENCE 177
Introduction 177
Description of the Erosional Surface 178
Distribution and Stratigraphic Position 178
Classification and Terminology 180
Physical Description 184
Model for Development of the Erosional Surface 189
Conclusions 196

6. CONCLUSIONS 198

REFERENCES 204

APPENDIX: SAMPLE DESCRIPTIONS 222

VITA 268

LIST OF FIGURES

Figure — Page

2.1 Location map of the study area, showing strike belts between major northwest-directed thrust faults and locations of outcrops used in the study . . . 9

2.2 Basal Middle Ordovician stratigraphy of the study area 11

3.1 Outcrop photographs of representative lithologies of the Douglas Lake Member 25

3.2 Thin-section photomicrographs of the Douglas Lake and Blackford Member subfacies 27

3.3 Aerial photograph of the Three Creeks area, northwestern Andros Island tidal flat, Bahamas 43

3.4 Block diagram showing the major depositional environments of the northwestern portion of the Andros Island tidal flat 45

3.5 Detailed map showing subenvironments of the beach ridge and the algal marshes and ponds of the channeled belt that occur on the landward side of the beach ridge, Andros Island 46

3.6 Profile across a portion of the Andros Island tidal flat, from beach ridge (or channel levee) to a tidal pond, showing the major depositional subenvironments relative to mean tide level (MTL), mean high water (MHW), and mean low water (MLW) 47

3.7 Lithologies of the Mosheim Member 51

3.8 Lithologies of the Five Oaks Formation 63

3.9 Stratigraphic sections of basal Middle Ordovician strata at outcrops in the study area 81

3.10 Depositional model for the basal Middle Ordovician peritidal strata in East Tennessee 86

4.1 Burial history curves for the Middle Ordovician sequence of East Tennessee 100

4.2 Stratigraphic variation in porosity-type abundance, Thorn Hill section 103

4.3 Primary and secondary porosity types in the Mosheim/Five Oaks sequence . 104

4.4 Secondary porosity types and internal sediments 112

4.5 Photomicrograph pair showing a cement-filled fenestra (left side) that is truncated by a vein (right half of photo), from just beneath the top of the Mosheim, Baptist Hospital 122

4.6 Stable isotopic signatures of various diagenetic and depositional materials in the Mosheim 126

4.7 Progressive development of diagenetic grainstone/pisolite texture 129

4.8 Matrix alteration in the Mosheim/Five Oaks tidal flat sequence 137

4.9 The erosional surface at the top of the Mosheim Member 159

4.10 Paragenetic sequence of diagenetic processes in the Mosheim/Five Oaks tidal flat facies 166

4.11 Paleohydrologic model for diagenetic alteration of the Mosheim/Five Oaks tidal flat facies 170

5.1 Location map of the southern Appalachian Valley and Ridge Province, showing noted exposures of the erosional disconformity between the basal Middle Ordovician tidal flat facies and the overlying shallow subtidal marine facies 179

5.2 Biostratigraphic correlation of basal Middle Ordovician peritidal facies in Alabama and East Tennessee, based on conodont biostratigraphy 183

LIST OF TABLES

Table Page

3.1 Lamination Types on the Andros Island Tidal Flat 48

4.1 Stable Isotope Data 125

4.2 Elemental Geochemistry of Tidal Flat Dolomicrites 144

4.3 Summary of Mosheim/Five Oaks Tidal Flat Diagenesis 168

5.1 Features Indicative of Meteoric Diagenesis 188

Chapter 1

INTRODUCTION

This dissertation consists of four related chapters that together describe the depositional and post-depositional history of the basal carbonate rocks of the Middle Ordovician sequence in East Tennessee. Each chapter covers a different aspect of this lithologically distinct stratigraphic sequence. Chapter 2 provides important background information about the overall tectonic setting and the regional and local stratigraphy. Chapter 3 consists of detailed descriptions of the sedimentary features of the rocks and fine-scale interpretations of the environments in which the strata were deposited, and concludes with the presentation of a model that depicts the depositional history of the sequence. Chapter 4 includes detailed descriptions of the diagenetic features of the rocks and an interpretation of the environments in which diagenesis occurred, and summarizes the post-depositional history of the sequence. Chapter 5 uses the depositional and diagenetic models to interpret the development of a regional erosional surface that occurs at the top of the sequence. Chapter 6 summarizes the conclusions of Chapters 2 through 5.

When proposed, the purpose of this dissertation was to examine and interpret the diagenetic history of the basal carbonate deposits of the Middle Ordovician sequence in East Tennessee. The initially highly porous nature of these peritidal deposits, as indicated by the large volume of pore-filling cements in the rocks, suggested that the rocks may have served for some time as an aquifer--a permeable conduit through which interstitial fluids with meteoric and burial affinities may have moved freely. The original intention was to treat the basal Middle Ordovician carbonates as a paleoaquifer and, through petrographic observations and geochemical investigations, to determine the evolution of

pore waters as they were transmitted, across strike from basin to shelf, through this permeable medium.

Initial observations of diagenetic features in these rocks, however, showed that much of the diagenetic alteration, including porosity occlusion, was completed very early in the history of the units. Indeed, most cement phases are truncated at an erosional surface that caps the peritidal sequence in most places. Thus, at least portions of the peritidal deposits were extensively lithified and their original high porosity effectively sealed prior to the deposition of the immediately overlying units. This observation led to the early conclusion that the peritidal carbonates at the base of the Middle Ordovician sequence probably did not serve as a medium for transmission of fluids other than the meteoric and marine waters that flushed through the sediments during and shortly after deposition. Recognition that the sequence probably became an aquiclude very early in its post-depositional history necessitated changing the focus of the study, with more emphasis placed on interpreting depositional environments and understanding the early depositional controls on diagenesis.

The final product of this research is a dissertation that answers three groups of questions:

1) What was the depositional history of the Middle Ordovician peritidal carbonate rocks that immediately overlie the Knox unconformity in the Valley and Ridge of East Tennessee?

   In what types of environments were these rocks deposited?

   What type of depositional regime is indicated by the vertical sequence of these rocks?

2) What was the post-depositional (diagenetic) history of these rocks?

   In what diagenetic environments did this post-depositional alteration occur?

What was the nature of the fluids involved in the diagenesis?

How does this diagenetic evolution compare or contrast with that of the overlying Middle Ordovician strata?

3) How did the erosional surface at the top of the tidal-flat facies form?

Can this surface be correlated with very similar surfaces that occur at the same lithostratigraphic level throughout the southern Appalachians?

What does this surface mean in terms of sequence stratigraphy?

The first set of questions regarding the depositional history of the sequence is addressed in Chapter 3. The environments in which these rocks were deposited are interpreted following the "comparative sedimentology" method outlined by Hardie and Shinn (1986). This requires a detailed description of each lithofacies observed, followed by a comparison of that lithofacies with published descriptions of an appropriate modern analogue. The interpretations that result from this comparative sedimentology analysis are assembled into an integrated depositional model that summarizes the depositional history of the sequence.

Chapter 4 answer the second set of questions regarding the diagenetic alteration of the sequence. Using the Middle Ordovician depositional model developed in Chapter 3 as a framework, an analysis is made of all post-depositional features observed in the rocks. These features are used to interpret the diagenetic processes that were responsible for the alteration of the rocks, the types of fluids that were involved in the alteration, the diagenetic environments in which the processes occurred, and the paragenetic sequence of these processes.

The third group of questions, regarding the erosional surface at the top of the peritidal units, is answered in Chapters 5. The focus of this chapter is on the processes that were responsible for the formation of the erosional surface.

This dissertation summarizes the entire geological history (depositional and diagenetic) of a thin, yet physically discrete, carbonate lithofacies. The study is significant because the understanding gained fills in gaps in the understanding of the depositional and diagenetic history of an otherwise well-studied sequence (the Middle Ordovician carbonate/shale sequence of East Tennessee). Also, despite the tremendous amount of research that has been conducted on modern and ancient carbonate tidal flats, this study is a significant addition to that body of knowledge because the basal Middle Ordovician tidal-flat sequence is a well-preserved ancient analogue of a non-cyclic, transgressive tidal flat--one that differs significantly from most documented ancient tidal flats, which are typically composed of stacked, progradational cycles.

Methods

Approximately 250 samples were collected from 13 outcrops. From these samples, 233 polished slabs were prepared and examined. Detailed petrographic analyses were carried out on 199 45 x 75 mm thin sections that were prepared by the author for this study, and on an additional 23 thin sections that were collected by Steve Ruppel. All thin sections were stained with a mixed stain composed of alizarin red S and potassium ferricyanide according to the procedure outlined by Dickson (1965) to differentiate calcite and dolomite and to identify ferroan phases. Conventional microscopy was conducted using a Nikon Optiphot POL binocular microscope. Selected polished thin sections were analyzed for cathodoluminescence using Nuclide ELM-2AVG luminoscope, under operating conditions of 12-14 kev and 45 to 60 μamp. Samples for stable isotope analyses were drilled from polished slabs using a microscope-mounted microdrill assembly. A total of 22 samples were analyzed for carbon and oxygen isotopes

at the University of Tennessee stable isotope laboratory in the Department of Geological Sciences, using Chihuahuan calcite (HOCC) as a laboratory standard.

Chapter 2

GEOLOGIC SETTING AND STRATIGRAPHY OF THE BASAL MIDDLE ORDOVICIAN CARBONATE SEQUENCE, EAST TENNESSEE

Geologic Setting

Tectonic Framework

The early Middle Ordovician Whiterockian stage (Ross et al., 1980) was a time of profound tectonic change in the southern Appalachians. During this time, tectonic rearrangement driven by the events that culminated in the Blountian Phase of the Taconic Orogeny (Rodgers, 1971), caused a transition in southeastern strike belts in the southern Appalachians from deposition of shallow water carbonate rocks on a passive margin to mixed carbonate/clastic deposition in a rapidly deepening foreland basin and on an adjacent carbonate platform. The exact time of this transition from passive margin to convergent margin is uncertain because deposits of earliest Middle Ordovician age are generally absent from the stratigraphic record in the southern Appalachians. This interval is typically marked by the post-Knox (or post-Beekmantown) unconformity, which represents an interval of time that ranges from a minimum of a few million years in southeasternmost strike belts (Mussman and Read, 1986) to a maximum of about 40 million years in some northwestern strike belts in the southernmost Appalachians (in the vicinity of Birmingham, Alabama) (Roberson, 1988). This long interval of exposure is marked by significant paleokarst relief on the upper surface of the Knox Group throughout the southern Appalachians (Mussman and Read, 1986; Mussman et al., 1988; Roberson, 1988; Shaw et al., 1990; Steinhauff and Roberson, 1989). Because the deposits beneath the unconformity (carbonates of the Knox and Beekmantown Groups) are classic passive-margin deposits, and those above the unconformity in

southeasternmost thrust sheets are dominated by tectonic basin fillings, it is generally held that the transition from passive- to convergent-margin deposition began during this time of non-representation (Rodgers, 1971). In fact, the development of the regional Knox/Beekmantown unconformity in the southern Appalachians has been related to the tectonic transition (Mussman and Read, 1986; Roberson, 1988; Roberson et al., 1988).

Throughout the southern Appalachians, the Middle Ordovician rocks that overlie the post-Knox unconformity record a transgressive sequence. Transgression was driven by tectonic transition in the region and simultaneous eustatic sea level rise (Sloss, 1963). The basal deposits of this transgressive sequence form a thin veneer of predominantly peritidal carbonate lithologies on the lithified Knox surface. Variations in the thicknesses of the basal Middle Ordovician units across the region indicate that depositional patterns during the early Middle Ordovician were influenced and to some extent controlled by paleokarst relief on the Knox surface (Haynes and Kesler, 1989; Roberson, 1988). The basal Middle Ordovician peritidal units are overlain by shelf carbonates deposited in shallow, open marine conditions as the transgession proceeded. During this time, differentiation of the shelf occurred, so that deposition on the northwestern portion of this shelf remained in shallow shelf settings, but the depositional setting to the southeast changed from shallow ramp to a rapidly deepening foreland basin (Benedict and Walker, 1978; Shanmugam and Walker, 1978, 1980; Shanmugam and Lash, 1982; Benson and Mink, 1983; Ruppel and Walker, 1984; Mussman and Read, 1986; Roberson et al., 1988; Walker et al., 1980). This study is focussed on the thin succession of peritidal limestones that immediately overlies the unconformity.

Study Area

The basal Middle Ordovician carbonate rocks examined in this study are exposed in several thrust sheets in the Valley and Ridge physiographic province of East Tennessee. These thrust sheets generally strike about N70E and dip to the southeast. The rocks in portions of the study area are also folded into broad anticlines and synclines, particularly in the northeastern part, which is known as the Bays Mountain Synclinorium (Rodgers, 1953).

The outcrops used in this study occur in five strike belts, as shown in Figure 2.1. Names for these belts are those used in published conodont biostratigraphic studies for this area (Bergstrom, 1973; Bergstrom and Carnes, 1976), and previous stratigrahic studies, especially Prouty (1946) and Neuman (1955). From northwest to southeast, these five belts are:

1) The St. Paul belt, or exposures northwest of the Copper Creek Fault. Outcrops used in this study include Bethel Valley and Raccoon Valley.

2) The Copper Creek belt, or sections southeast of the Copper Creek Fault but northwest of the Saltville Fault. Sections used in this study include Thorn Hill, Idol Mine, and Cedar Springs.

3) The Hawkins belt, in the Saltville thrust sheet, is represented by the Red House Branch section.

4) The Friendsville belt, or sections southeast of the Saltville Fault but northwest of the Dumplin Valley Fault. Sections used for this study include Baptist Hospital and John Sevier Highway.

5) The Tellico-Sevier belt (or Bays Mountain Synclinorium), or sections southeast of the Dumplin Valley Fault. Sections include Boyd's Creek Road, Deep Springs, Dandridge, Nina, and Fish Hatchery Road.

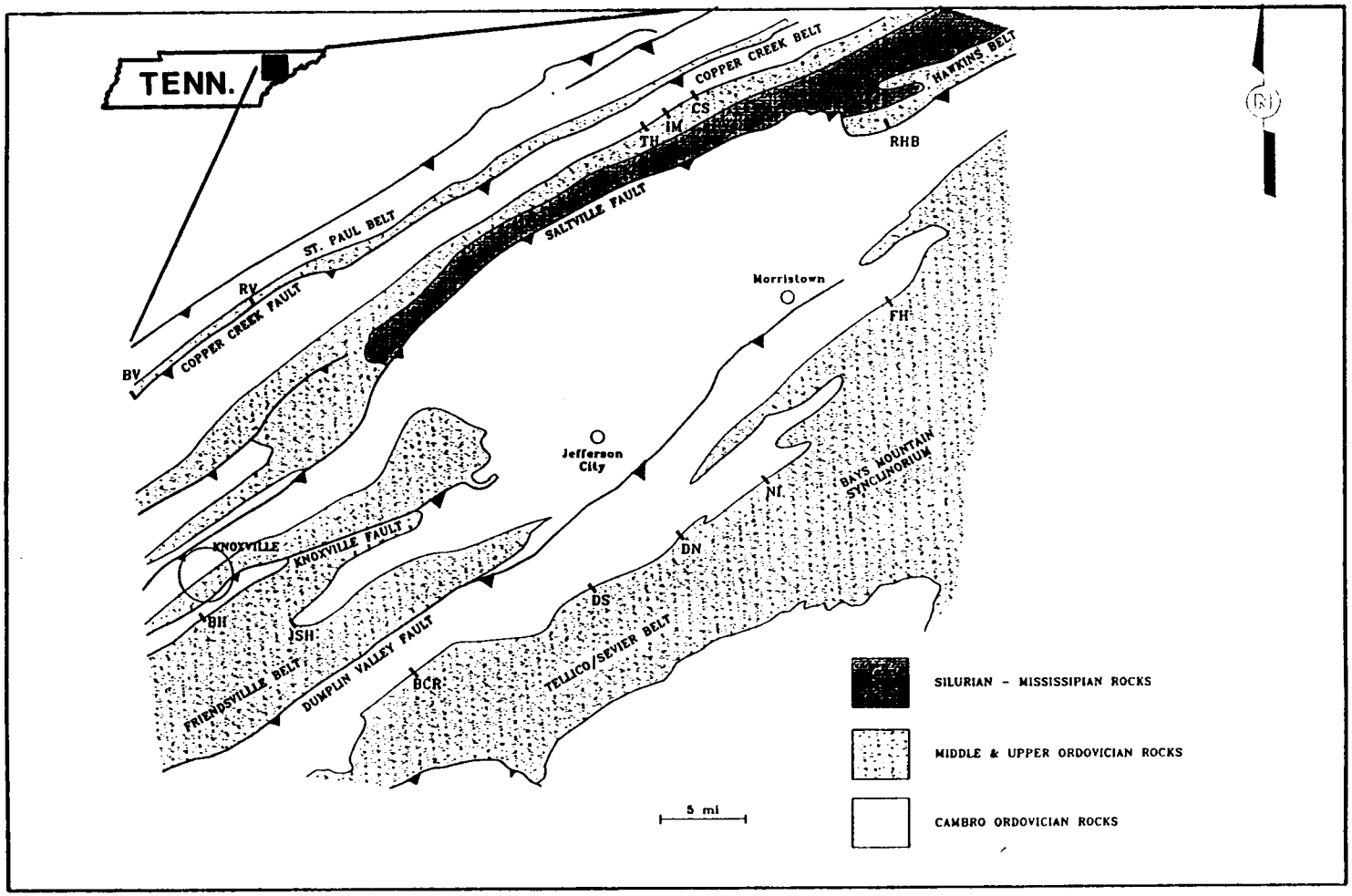


Figure 2.1. Location map of the study area, showing strike belts between major northwest-directed thrust faults and locations of outcrops used in the study. Abbreviations: BV - Bethel Valley, RV - Raccoon Valley, TH - Thorn Hill, IM - Idol Mine, CS - Cedar Springs, RHB - Red House Branch, BH - Baptist Hospital, JSH - John Sevier Highway, BCR - Boyd's Creek Road, DS - Deep Springs, DN - Dandridge, NI - Nina, FH - Fish Hatchery Road.

A total of twenty outcrops were examined in the field, but only the thirteen named above were used for collection of samples. Eleven of these locations were selected because of complete or near-complete exposure of the basal peritidal sections, and two (Baptist Hospital and John Sevier Highway) were selected because of very good exposure of critical stratigraphic intervals within the sequence (the upper and lower contacts, respectively).

Stratigraphy

Across-Strike Variations in Middle Ordovician Stratigraphy

The Middle Ordovician strata in eastern Tennessee are roughly divided by the Saltville Fault into two geographically discrete, yet approximately correlative, lithologic packages. Northwest of the Saltville Fault, the Middle Ordovician sequence consists primarily of shallow-water platform carbonates of the Chickamauga Group. Basin-filling, deep-water shales are absent from the Chickamauga Group. Lithofacies descriptions and interpretations of the depositional environments of the nine formations that comprise the group, as well as a discussion of the development of the Chickamauga platform, are published in Ruppel and Walker (1984). Southeast of the Saltville Fault, the Middle Ordovician sequence is considerably thicker and dominated by shale rather than limestone, although shallow platform carbonate units are present at the base of the sequence (Figure 2.2). In the southeastern belts, the Middle Ordovician sequence represents a succession from shallow shelf carbonates to deep basinal shales, and records the development and infilling of a foreland basin where a shallow platform existed previously (Shanmugam, 1977; Shanmugam and Walker, 1978, 1980; Shanmugam and Lash, 1982; Walker et al., 1980).

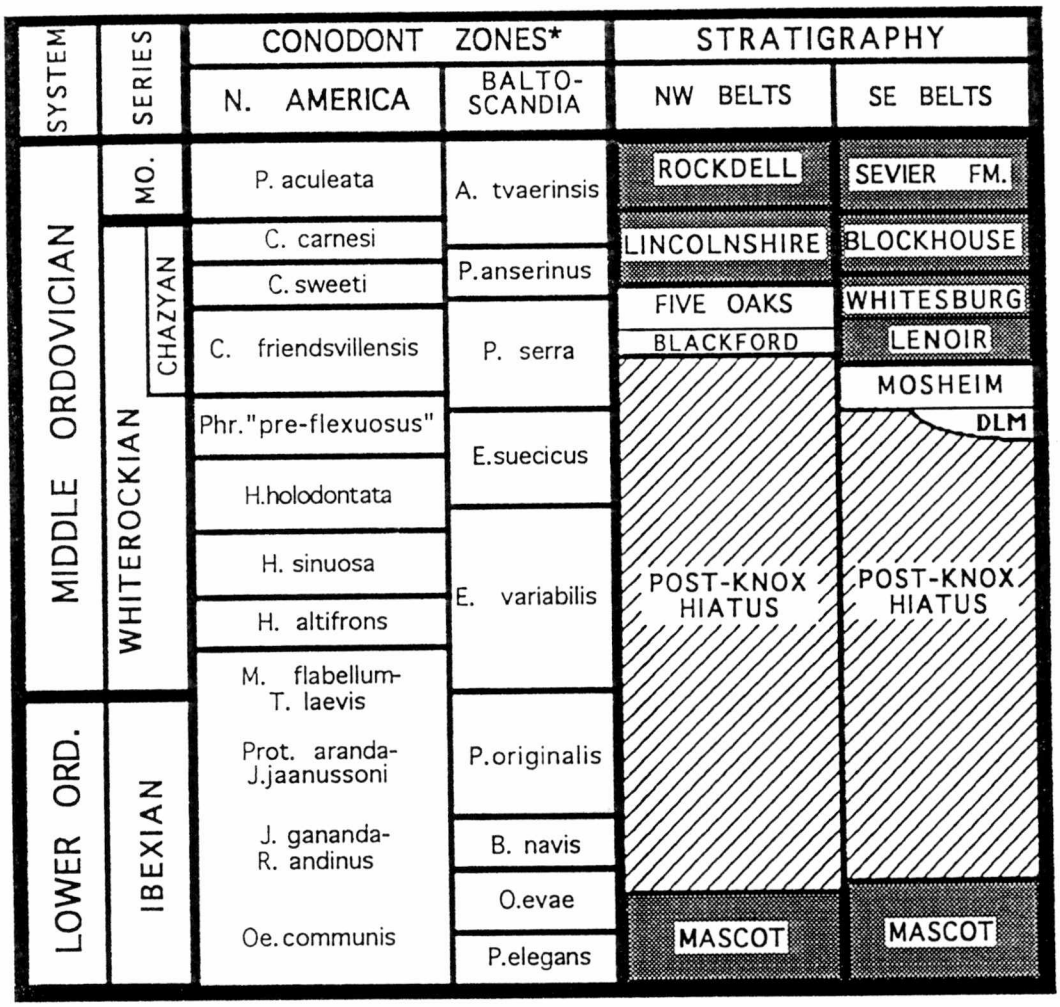


Figure 2.2. Basal Middle Ordovician stratigraphy of the study area. The peritidal units at the base of the Middle Ordovician sequence in strike belts northwest of the Saltville Fault include the Five Oaks Formation and its basal member, the Blackford Member. In southeastern strike belts the basal peritidal strata are assigned to the lower members of the Lenoir Formation--the Mosheim Member and the Douglas Lake Member (DLM). Although located northwest of the Saltville Fault, the basal Middle Ordovician stratigraphy of the Hawkins Belt is the same as in the southeastern belts. *Conodont zones are from Bergstrom (1973) and Bergstrom and Carnes (1976).

The focus of this study is on the lowermost carbonate deposits of the Middle Ordovician sequence, which are shown in stratigraphic position in Figure 2.2. The deposits discussed in this study include the basal members of the Lenoir Formation--the Douglas Lake and Mosheim Members--of the unnamed carbonate/shale group southeast of the Saltville Fault, and the Five Oaks Formation and its basal unit, the Blackford Member, of the Chickamauga Group northwest of the Saltville. These deposits invariably rest disconformably on the Knox surface; nowhere in the study area is there a gradational contact between the Lower and Middle Ordovician sequences, as has been previously speculated (Ruppel and Walker, 1984).

Ages of Basal Middle Ordovician Units

Typically, the basal Middle Ordovician peritidal deposits contain very restricted biotas, and are difficult to date precisely using biostratigraphic methods. Some stratigraphically important lithofacies, such as the basal conglomerates of the Douglas Lake Member, have yielded no fossils at all. The others, although yielding locally abundant conodonts, ostracodes, gastropods, and cephalopods, apparently contain no short-ranging, biostratigraphically diagnostic fossils. This is unfortunate, because these units signify the reinitiation of deposition following, or in some cases *during,* post-Knox exposure. As for the ages of these units, it can only be said that they are older than the basal beds of the overlying fossiliferous Lenoir and Lincolnshire facies, for which ages have been determined.

Conodont biostratigraphy has proven to be the most precise and reliable means of dating the basal Middle Ordovician units (Bergstrom, 1973; Bergstrom and Carnes, 1976; arris, 1982; Coffey, 1986). Perhaps the most striking result of these biostratigraphic studies is that the lowest datable unit of the Middle Ordovician section is considerably

younger in strike belts northwest of the Saltville Fault than in strike belts southeast of the fault. It should be pointed out, however, that the conodont assemblages in the Middle Ordovician rocks in the southeastern belts are affiliated with the Balto-Scandian conodont province, whereas the assemblages in the northwestern strike belts belong to the Mid-continent conodont province (Bergstrom, 1973). Correlation across the Saltville Fault is indirect because these two conodont provinces share no common elements. There appears to be little difference in the age of the basal units across the other faults. For example, the basal strata are of approximately the same age in the Copper Creek and St. Paul belts (Bergstrom and Carnes, 1976).

Southeast of the Saltville, ages of the basal Middle Ordovician units are best indicated by ages determined for the fossiliferous main body of the Lenoir Formation (Figure 2.2). The thickness of the Lenoir varies tremendously across the study area, and the amount of time represented by the unit varies accordingly. In the Bays Mountain Synclinorium, the Lenoir is very thin (less than ten meters), and was deposited during the earliest part of the *Pygodus serrus* conodont Zone, at most places during the *Eoplacognathus foliaceous* Subzone (Bergstrom, 1973; Harris, 1982). In the Friendsville belt, deposition of a much thicker Lenoir section (in places, exceeding 150 meters) began in the early part of the *P. serrus* Zone and continued to well within the *Pygodus anserinus* Zone (Bergstrom, 1973).

The Middle Ordovician peritidal units underlying the Lenoir facies (Mosheim and Douglas Lake members) are believed to be only slightly older than the Lenoir. This interpretation is based on depositional environment reconstructions (presented in Chapter 3), which indicate that deposition of the Mosheim and Douglas Lake members immediately preceded deposition of the Lenoir. Although the Lenoir at almost all outcrops in the study area is separated from these underlying units by an erosional surface or disconformity, the amount of time represented by this surface is thought to be minor; it

is certainly less than the duration of a conodont subzone, and perhaps as little as a few hundred or a few thousand years (see Chapter 5 for a discussion of this surface). Following this line of reasoning, the age of the Douglas Lake and Mosheim members is probably earliest Chazyan (*E. foliaceous* Subzone of the *P. serrus* Zone), or very latest Whiterockian (late *E. suecicus* Zone or *Phragmodus "pre-Flexuosus"* Zone) (Figure 2.2). This age is supported by correlations with similar units outside the study area (Shaw et al, 1990).

Northwest of the Saltville Fault, ages of the basal Middle Ordovician units must be approximated in a similar manner. In the Hawkins belt, the base of the Lenoir is probably no older than the *P. anserinus* Zone (Bergstrom and Carnes, 1976). At the Cuba locality, which is located near the Red House Branch section in the Hawkins belt, the base and top of the Mosheim fall within the *P. anserinus* Zone (A. Harris, personal communication, 1990). The Mosheim is probably of similar age at Red House Branch and other outcrops in the Hawkins belt.

In the Copper Creek belt, the basal units (Blackford Member and Five Oaks Formation) contain beds that have yielded abundant, if not diverse or short-ranging, conodont assemblages. At the Idol locality (Figure 2.1), a sample from two meters above the base of the Blackford and one from the basal bed of the Five Oaks indicate a rather imprecise age for the Blackford of somewhere within the *Cahabagnathus friendsvillensis* and *C. sweeti* Zones (Figure 2.2). A sample from immediately beneath the top of the Five Oaks at Idol indicates deposition during the *C. sweeti* Zone (A. Harris, personal communication, 1990). A sample from immediately above the base of the overlying Lincolnshire Formation at Idol, and samples from the lowermost four meters of the Lincolnshire at Cedar Springs (Figure 2.1) contain specimens of *C. carnesi* [*Polyplacognathus sweeti* (late form) of Harris (1982)], and indicate a very precise age for the basal Lincolnshire within the *C. carnesi* Zone of Bergstrom (1983) (Figure 2.2)

(A. Harris, personal communication, 1990). In light of typical tidal flat sedimentation rates, these and other samples suggest that the Five Oaks (and perhaps the Blackford as well) probably accumulated during the *C. sweeti* Zone.

Bergstrom and Carnes (1976) stated that the base of the Lincolnshire (their "Holston") Formation is roughly the same age in the St. Paul, Copper Creek, and Hawkins belts. In the absence of other data, there is no reason to speculate that the ages of the Five Oaks and Blackford units in the St. Paul belt differ significantly from those ages determined for the Copper Creek belt. It should be pointed out, however, that conodont age dating is imprecise; units determined to be the "same age" may in fact vary in age by 100,000 years or more (K. Walker, personal communication, 1991).

Correlation with Units Outside the Study Area

The Middle Ordovician of East Tennessee is part of a vast complex of carbonate and shale units that were deposited along the eastern margin of North America at various times during the Middle Ordovician (Rodgers, 1971). Consequently, the basal units of this sequence have litho-, bio-, and chronostratigraphic correlatives throughout the Appalachians, from Newfoundland to Alabama. A complete list of all the likely correlatives to these units will not be attempted here; however, a short discussion of possible correlatives in the southern Appalachians is offered below.

The lithofacies known in Tennessee as the Lenoir Formation and its basal peritidal member, the Mosheim limestone, extend essentially without interruption in southeastern strike belts from Virginia to the Coastal Plain onlap in central Alabama. Fortunately, the same names are applied throughout much of this area. In parts of Virginia, however, the name Lincolnshire is attached to limestones that appear to be more similar in lithology to the Lenoir of the southern Appalachians than to the Lincolnshire of Tennessee (Ruppel

and Walker, 1984). In the same areas, pure fenestral limestones at the base of the Middle Ordovician sequence, which are very similar to the Mosheim of Tennessee, are referred to as the New Market Formation (Read, 1980). There is little question that the New Market and Lincolnshire units of Virginia correlate with the Mosheim and Lenoir, respectively, of the present study area.

The oldest unit in southeastern strike belts, the Douglas Lake Member, has been correlated with a lithologically similar unit, the Cottingham Creek Member of the Lenoir Formation (Roberson, 1988), that fills paleosinkholes on the subaerial exposure surface at the top of the Knox Group southeast of the Helena Fault in Alabama (Shaw, et al., 1990). Unlike the Douglas Lake Member, the Cottingham Creek Member contains a biostratigraphically significant conodont assemblage that indicates deposition during the latest Whiterockian to earliest Chazyan (*Phragmodus "pre-Flexuosus"* Zone to early *Cahabagnathus friendsvillensis* Zone) (Shaw, et al., 1990). On the basis of lithostratigraphic correlation, a similar age is considered to be likely for the Douglas Lake Member.

Correlation of the basal Middle Ordovician peritidal units in northwestern strike belts (basal Chickamauga Group) is more difficult because of the large number of names that have been applied to the section. For example, the stratigraphic interval referred to in this study as the Five Oaks Formation (after Ruppel, 1979) is sometimes called Mosheim (Hall and Amick, 1934). In Virginia, limestones at the same stratigraphic position are called Tumbez, Blackford, or Elway (Read, 1980), and the Virginia names have been applied in Tennessee. Although each of these units is dominated by a different lithofacies, they all probably correlate roughly in age.

Different stratigraphic hierarchical levels for these units also have added confusion. For example, in the vicinity of Birmingham, Alabama, the Middle Ordovician section is very thin, and all strata are assigned to the Chickamauga Formation (Benson

and Mink, 1983). In northeastern Alabama, an attempt to elevate the Chickamauga to group status and subdivide it into the Stones River and Nashville Formations has been made (Drahovzal and Neathery, 1971), whereas in the Chickamauga type section in northwestern Georgia, the Chickamauga is given supergroup status and subdivided into the Stones River and Nashville Groups, each of which contains several formations (Milici and Smith, 1969). The application of the Stones River and Nashville names to these rocks is unfortunate, because the nomenclature has been transferred from Middle Ordovician limestones of central Tennessee, and applied to strata that correlate much better with the Chickamauga strata of the Valley and Ridge of eastern Tennessee. Nonetheless, the basal peritidal carbonates of the Chickamauga Group (or Formation or Supergroup, depending upon location) in the Valley and Ridge of Alabama and Georgia can be correlated, on the basis of lithology, and in many cases on the basis of age, with the Five Oaks Formation of this study area.

The Blackford Member of the Five Oaks seems to correlate well with the Attalla Chert Conglomerate Member of the Chickamauga Formation, which fills paleokarst depressions on the Knox surface northwest of the Helena Fault in Alabama (Roberson, 1988). The Attalla lacks fossils, but carbonate mudstones (Foster Mountain Member of Roberson, 1988) at the base of the Attalla near Foster Mountain in northeastern Jefferson County, Alabama have yielded conodonts that indicate an age of highest *Cahabagnathus sweeti* Zone to lowest *E. quadridactylus* Zone (Shaw et al., 1990). This age is generally younger than the age of the Blackford in East Tennessee, but the age of the base of the Chickamauga sequence gets younger to the southwest onto the Birmingham Anticlinorium (Hall et al., 1986; Roberson, 1988).

The Pond Springs Formation, the lowest unit of the Chickamauga Supergroup in northwest Georgia (Milici and Smith, 1969), appears to correlate, at least in part, with the Blackford as well. Conodonts collected from the Pond Springs suggest that it spans

the time period from lowest *C. friendsvillensis* Zone near its base to within the *P. aculeata* Zone at its top (Schmidt, 1982; Shaw et al. 1990). Although doubt has been expressed (Schmidt, 1982; Shaw et al. 1990) about the long time range indicated for the Pond Springs, at least the upper portion probably is coeval with, and represents similar depositional conditions as the Blackford. The lower portion of the Pond Springs may correlate with the Douglas Lake Member (Shaw et al., 1990).

Chapter 3

DEPOSITIONAL HISTORY OF THE BASAL MIDDLE ORDOVICIAN PERITIDAL CARBONATE ROCKS, EAST TENNESSEE: DEVELOPMENT AND MIGRATION OF AN ANDROS ISLAND-TYPE TIDAL FLAT WITHIN A TRANSGRESSIVE SEDIMENTARY SEQUENCE

Introduction

In this chapter, the depositional setting of the basal Middle Ordovician carbonate rocks is interpreted using a level of detail that has not been attempted previously for this part of the sequence. Previous investigations have interpreted the basal Middle Ordovician carbonates in the Southern Appalachians to represent tidal flat deposition (e.g., Stephenson et al., 1973), but there has been no apparent attempt to determine what specific type of tidal flat existed, or what subenvironments of the tidal flat have been preserved. The method of approach used here is the "comparative sedimentology" approach advocated by Hardie (1986), wherein depositional environments of ancient rocks are interpreted by comparing diagnostic sedimentary features preserved in the rocks with virtually identical features forming in analogous modern carbonate depositional environments. Hardie's approach differs from the conventional use of modern analogues only in the level of detail of the investigation. Hardie and other investigators have shown that exquisitely detailed reconstructions of depositional environments of ancient carbonate rocks can be made by focussing investigation on specific depositional subfacies, such as the supratidal marsh subfacies of a tidal flat deposit, rather than on the gross features of the tidal flat facies as a whole. It is this very detailed type of depositional environment reconstruction that has been conducted in this study.

A similar study was conducted on comparable tidal flat limestones of the Middle Ordovician St. Paul Group in the Central Appalachians by Mitchell (1981, 1985). It should be acknowledged that the approach taken in this study was largely patterned after Mitchell's study, and the success Mitchell achieved in reconstructing the depositional environments of the St. Paul Group tidal flat carbonates was also achieved in this study. The results of this investigation show that there are several similarities between the tidal flat deposits of the St. Paul Group and the basal Middle Ordovician tidal flat deposits of the Southern Appalachians, but that these two approximately coeval Middle Ordovician tidal flats differ greatly from most other carbonate tidal flats preserved in the rock record. There are, however, some important differences between the St. Paul Group tidal flat deposits and the rocks that were the focus of this study. The similarities and differences between these Middle Ordovician tidal flats and other ancient carbonate tidal flats are discussed in the conclusions of this report.

This chapter is written in two sections. The first section consists of detailed descriptions and photographs of the subfacies identified in this sedimentary sequence, and interpretations of these subfacies as ancient analogues of subenvironments of an analogous modern tidal flat. The second section of the paper is a summary of the interpreted depositional environments and depositional history of the sequence in the form of a comprehensive depositional model.

Geologic Setting

The geologic setting of the basal middle Ordovician tidal flat carbonate rocks was discussed in Chapter 2 of this dissertation. That chapter included a brief description of the overall tectonic setting for deposition of the rocks examined in this study, and a

discussion of the basal Middle Ordovician stratigraphy, both locally and regionally. A map of the study area is shown in Figure 2.1 and the stratigraphy is summarized in Figure 2.2.

Lithofacies Descriptions and Environmental Interpretations

In this section, the basal Middle Ordovician peritidal rocks are subdivided into discrete lithofacies, and the original depositional textures of each lithofacies are described in detail. On the basis of these descriptions, an attempt is made to interpret specific depositional environments that correspond to each recognized lithofacies, using the comparative sedimentology approach. In many cases, making such interpretations involves "reading through" diagenetic overprints such as dolomitization, dissolution textures, etc. In general, however, because most of the diagenetic alteration of these rocks occurred very early in the history of the rocks (in many cases, immediately following deposition), diagenetic alteration has largely preserved, rather than disguised, the diagnostic depositional features of the rocks, and actually facilitated interpretations of depositional environments. Diagenetic features interpreted to be syndepositional provide very useful information about the depositional environment, and are sometimes used in environmental interpretations. Diagenetic alteration of the peritidal facies is the topic of Chapter 4 of this dissertation.

The stratigraphic units that comprise the basal Middle Ordovician transgressive peritidal carbonate sequence in the study area were introduced in Chapter 2 and summarized in Figure 2.2. The lithofacies represented by these stratigraphic units are summarized on the following page. Within a given strike belt, the transgressive sequence consists of three primary lithofacies, arranged in the following vertical sequence: the terrestrial/ paralic lithofacies on bottom (where present), the tidal flat lithofacies

Basal Middle Ordovician Lithofacies

Nearshore Terrestrial/Paralic Lithofacies:

Douglas Lake Member of the Lenoir Formation
(outcrops southeast of the Saltville Fault), and

Blackford Member of the Five Oaks Formation
(outcrops northwest of the Saltville Fault)

Tidal Flat Lithofacies:

Mosheim Member of the Lenoir Formation
(outcrops southeast of the Saltville Fault), and

"main body" of the Five Oaks Formation
(outcrops northwest of the Saltville Fault)

Adjacent Offshore Marine Lithofacies:

"main body" of the Lenoir Formation
(outcrops southeast of the Saltville Fault), and

Lincolnshire Formation
(outcrops northwest of the Saltville Fault).

overlying the terrestrial/paralic units, and the adjacent offshore marine lithofacies overlying the tidal flat deposits. Each lithofacies is interpreted as representing a distinct depositional environment, and each lithofacies contains within it several distinct subfacies that represent subenvironments of the larger depositional environments. Descriptions of depositional features of the peritidal rocks and interpretations of corresponding depositional environments are made at the subfacies/subenvironment level to provide

maximum detail and enhance comparison with analogous modern depositional features and environments.

Nearshore Terrestrial / Paralic Lithofacies

The basal units of the Middle Ordovician sequence in the study area include the Douglas Lake Member of the Lenoir Formation and the Blackford Member of the Five Oaks Formation (Figure 2.2). These two members include a wide variety of lithologies that represent the initiation of deposition after, and in some cases, during exposure of the Cambro-Ordovician carbonate platform. These two units, and the subfacies within each, are discussed below.

Douglas Lake Member

Distribution

A variety of conspicuous lithologies restricted to paleokarst depressions on the Knox surface comprise the Douglas Lake Member of the Lenoir Formation, as named by Bridge (1955) for exposures on the northwest shoreline of Douglas Lake in Sevier and Jefferson Counties (Deep Springs and Dandridge outcrops of Figure 2.1). The name is restricted to such lithologies southeast of the Saltville Fault; similar rock types northwest of the Saltville are included in the Blackford Member of the Five Oaks Formation. The thickness of the unit is controlled by the depth of the Knox paleodolines in which the rocks are deposited, and varies greatly; at the outcrops examined in this study the thickness ranges from zero to about twelve meters. Laurence (1944) reported 37 meters of lithologies that would be assigned to the Douglas Lake Member filling a now-

submerged paleokarst depression that was exhumed during construction of Douglas Dam.

Lithofacies descriptions

The Douglas Lake Member is made up of three primary lithologic subfacies:

1. Dolomitic conglomerates
2. Detrital chert / quartz sandstones
3. Shaly dolomitic limestones

Of these lithologies, the coarse, dolomitic conglomerates are the most abundant and most characteristic. Volcanic ash has also been reported in the paleokarst depression at Douglas Dam (Laurence, 1944), but no volcanic ash was observed in the present study. The three subfacies listed above are described and interpreted below.

Dolomitic conglomerates

At the Deep Springs and Dandridge outcrops, irregular depressions (probably paleokarst sinkholes) on and immediately beneath the Knox surface are filled with coarse conglomerates (Figure 3.1A-D). The conglomerates are composed of unsorted, rounded to angular clasts of limestone, dolostone, and chert, in a matrix of finely-crystalline, detrital dolomite and abraded quartz and chert sand (Figures 3.1A-D, 3.2A). The clasts range from millimeter-sized granules to large blocks measuring 2 by 3 meters. The larger clasts are generally self-supporting, whereas the smaller clasts are matrix-supported. Lamination within many of the clasts shows that the clasts are randomly oriented with respect to the regional dip of the beds (Figure 3.1A-D), indicating that the clasts and matrix have simply fallen into depressions with essentially no reworking by currents.

Figure 3.1. Outcrop photographs of representative lithologies of the Douglas Lake Member. **A-D**. Basal dolomitic conglomerate subfacies. Photographs A-C were taken at the Dandridge outcrop, D was taken at the Deep Springs location. All photos show randomly-oriented, subrounded to angular blocks and cobbles of algally-laminated dolostone, limestone, and chert, which were derived through erosion of Knox Group carbonate rocks and redeposited in finely-crystalline, detrital dolomite matrix. Deposition occurred in paleotopographic depressions eroded on the Knox surface. Photos B and C show the conglomerates directly overlying the Knox unconformity surface (top of the Knox Group is at the base of the scale card in B, and at the top of the scale card in C). In D and F, the checkbook used for scale is 6 inches long. **E.** Detrital chert/quartz sandstone subfacies. Thin bed from near the top of the 3-m thick reddish-brown sandstone subfacies, which occurs only at the Dandridge location. The reddish color is due to an abundance of red clay that partially fills some of the pores in the subfacies. Note the high porosity of the unit, which is due in part to dissolution of carbonate clasts and cement. **F.** Shaly dolomitic limestone subfacies. Photo shows the Knox unconformity at the Deep Springs locality, which here separates light-colored Knox dolostone from overlying darker argillaceous dolomitic limestones of the Douglas Lake Member. At this portion of the Deep Springs outcrop, the basal conglomerate subfacies of the Douglas Lake Member is absent, and the shaly dolomitic limestone subfacies unconformably overlies the Knox Group. Several meters laterally from the point of this photo, the basal conglomerate subfacies occurs stratigraphically between the Knox and the shaly dolomitic subfacies.

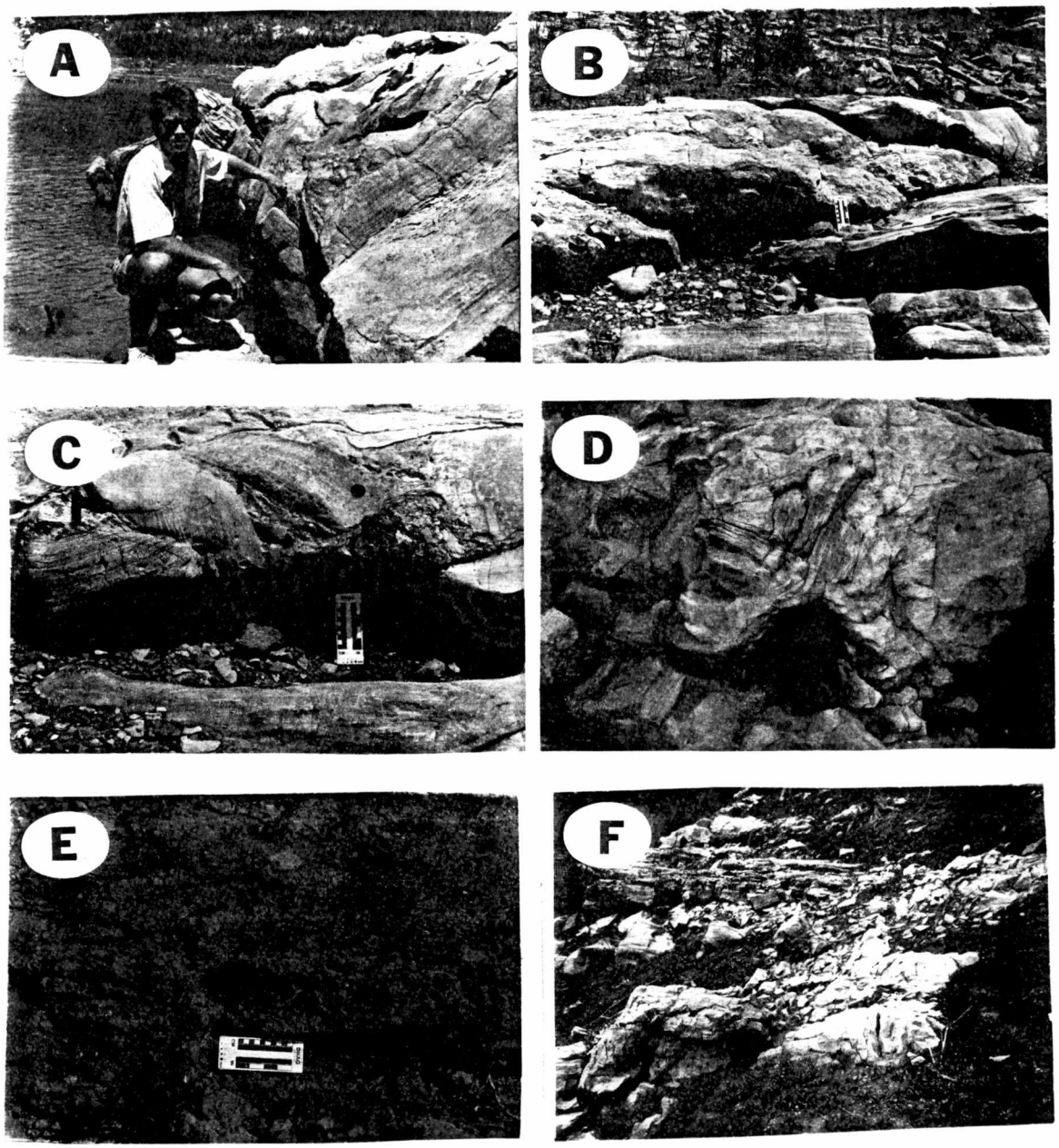
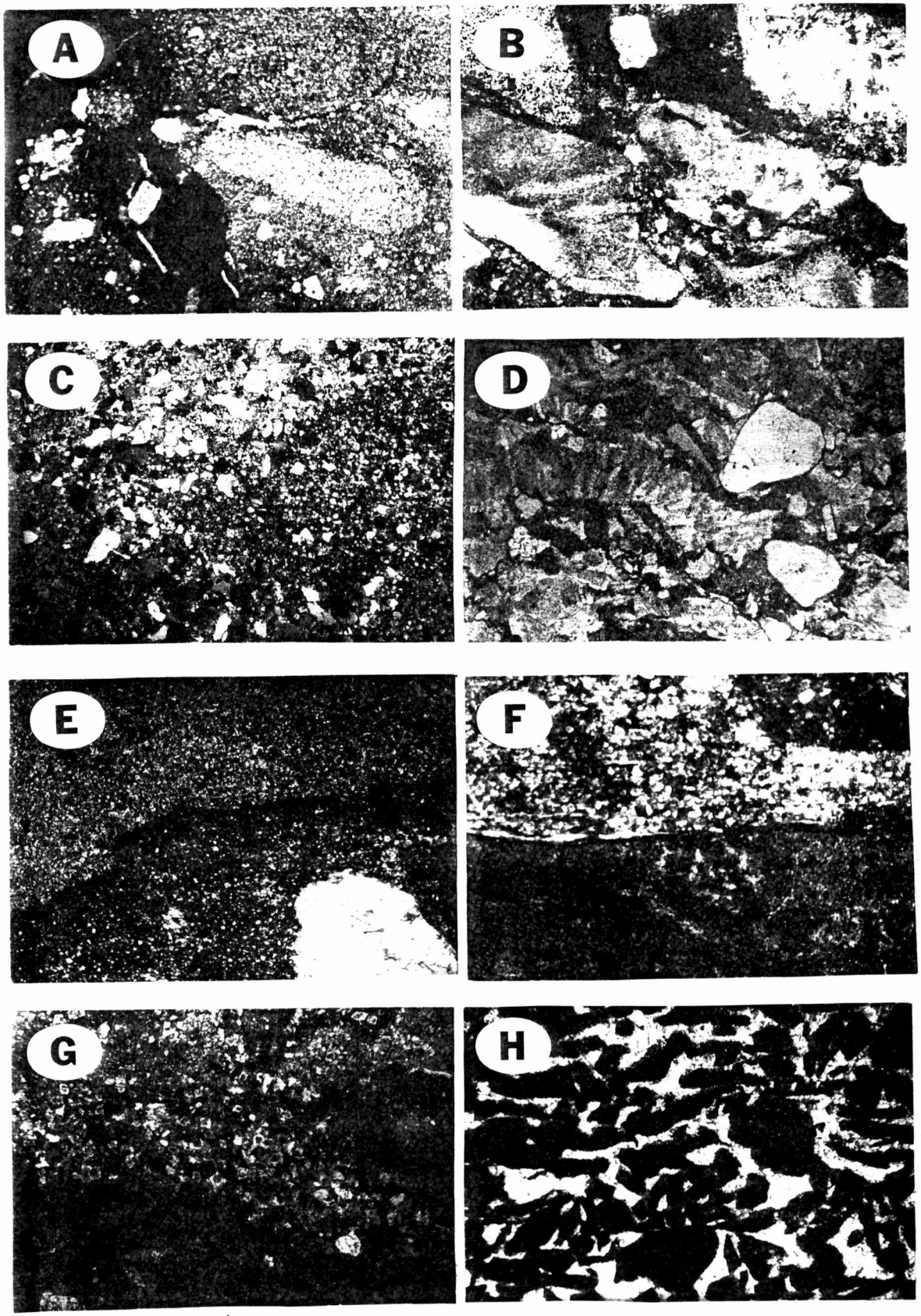

A
B
C
D
E
F

Figure 3.2. Thin-section photomicrographs of Douglas Lake and Blackford Member subfacies. C was taken under crossed nicols; all others were taken under plane-polarized light. The long axis field of view in all photomicrographs is 6.5 mm. **A.** Basal dolomitic conglomerate subfacies of the Douglas Lake Member, showing rounded clasts of limestone, dolostone, chert, and quartz sand in a matrix of finely crystalline, detrital dolomite, 0.5 m above the Knox unconformity (AKU), Dandridge outcrop. **B-D.** Basal conglomeratic dolostone and limestone subfacies of the Blackford Member. B shows clasts of chert in a dolomite matrix, 1 cm AKU, Idol section. C shows small clasts of limestone, dolostone, and chert in dolomite matrix, 0.4 m AKU, Idol section. D is a conglomeratic, intraclastic packstone with clasts of chert and dolostone, 1.9 m AKU, Idol section. Note the elongate void filled with fibrous cement. **E-F.** Photomicrographs of the Knox unconformity showing massive and conglomeratic dolostones of the Blackford overlying finely crystalline dolostone of the Mascot Formation (Knox Group). E is from the Idol section. Note the general similarity between the Blackford and Mascot dolostones. F is from the Bethel Valley section, where the basal Blackford dolostone consists of coarsely-crystalline, zoned dolomite rhombs. **G.** Massive, coarsely crystalline dolostone from a few cm AKU at the Idol section. Note the simple zonation within the dolostone rhombs, which consist of a dark central zone and a light outer zone. **H.** Intraclastic packstone/grainstone subfacies. This sample was collected from a 1-m thick bed of pale green dolomitic intraclastic grainstone, 6.1 m AKU at the Idol section. Note the elongate, angular shape of most of the clasts, which consist of dolomitized micrite. Also note the abundant intergranular micrite deposited on the tops of clasts and at points of contact between clasts. This intergranular mud is not dolomitized. Cements are all equant calcite.


A
B
C
D
E
F
G
H

The clasts are composed of lithologies typical of the underlying Jonesboro Formation (the uppermost formation of the Knox Group in this strike belt), and many clasts contain characteristic Knox features such as wavy stromatolitic lamination, multi-colored, banded chert nodules, and large, white, calcite-filled vugs that are identical to features in the Jonesboro. There is little doubt that the clasts and the detrital dolomite matrix that comprise these conglomerates were derived from the immediately underlying Knox carbonates.

The total absence of marine fossils and lime sediment in the matrix of the conglomerate subfacies suggests that the conglomerates are terrestrial deposits. Because the conglomerates lack any evidence of marine or fluvial current reworking and bear little evidence of tractive transport, they probably represent collapse breccias or accumulations of local clastic material in paleodolines. The Douglas Lake Member conglomerates probably represent deposition during subaerial exposure, *prior to* the marine inundation responsible for the deposition of the overlying Middle Ordovician marine carbonates.

Detrital chert / quartz sandstones

Approximately three meters of coarse, reddish-brown sandstone overlies the conglomerate subfacies at the Dandridge outcrop (Figure 3.1E). The sandstone is composed of subequal amounts of chert and quartz sand grains. Abundant dolomite matrix and a small amount of carbonate lithoclasts are present in the basal 0.5 meter of the sandstone subfacies, but the remainder of the sandstone lacks carbonate and contains abundant pore-filling red clay matrix. All sandstones in the Douglas Lake Member would be classified as lithic arenites using the system of Dott (1964). Clay content, chert:quartz ratio, and porosity increase upward in the sandstone subfacies. Porosity, which is as high

as 20% in some of the coarser-grained units, may be attributed to dissolution of carbonate grains and matrix.

Sandstone beds are up to 0.25 meter thick and interbedded with thin siltstone and shale layers. The thicker and coarser-grained beds contain trough cross-beds with amplitudes up to 0.25 meter. Vertical and horizontal burrows are very common throughout the sandstone, and probably represent traces left by soft-bodied marine organisms, but no body fossils have been observed. The upper meter of this subfacies is poorly exposed, but appears to be dominated by siltstone and shale. The upper contact of the sandstone with the overlying fossiliferous limestone of the Lenoir Formation is sharp and possibly erosional, but exposure is too poor to verify this interpretation. The Douglas Lake Member pinches out at both ends of this depression, and at these places fossiliferous limestone of the Lenoir Formation rests unconformably on the Knox Group.

Like the conglomerates, the sandstone subfacies of the Douglas Lake Member is also composed primarily of material derived from the Knox Group through subaerial erosion. The greater degree of rounding and sorting, the smaller average size, and the lower percentage of carbonate particles in the sandstone, relative to the conglomerates, however, suggests that the detrital material in the sandstone subfacies underwent more transportation and chemical breakdown than the carbonate-dominated clastic material that comprises the conglomerate subfacies. The sandstones probably represent terrigenous clastic material that was delivered by surface streams to the coastline, where it accumulated in a low-lying area that was already partially filled with the underlying dolomitic conglomerates. Some post-depositional reworking of this sediment during marine inundation is indicated by the network of burrows left by soft-bodied organisms and the trough cross-bedding. If marine reworking did occur, however, the current energy of the system was low enough to prevent the removal of clay material, which is abundant in the sediment. It is also possible that the clay matrix may have filtered into

the sediment after deposition, or that the clay is authigenic, derived from the breakdown of feldspar grains in the sediment.

In summary, the sandstone subfacies is interpreted as detrital material that was eroded from subaerially exposed Knox carbonates, transported to and deposited at the paleoshoreline, and reworked by tides during marine transgression.

Shaly dolomitic limestones

At the Deep Springs outcrop the sandstone subfacies is absent, and the dolomitic conglomerates are overlain by as much as seven meters of argillaceous, dolomitic limestone. Where the conglomerate subfacies pinches out laterally, the shaly dolomitic limestone subfacies rests sharply and unconformably on dolostones of the Knox Group (Figure 3.1F). This subfacies is characterized by nodular bedding and wispy argillaceous laminae with abundant thin shale interbeds, and is very similar in appearance to the main body of the Lenoir Formation. Dolomite content is much higher, and fossil content much lower than in the Lenoir, however. The shaly dolomitic limestone subfacies grades upward into about two meters of shale, and then into pure fenestral lime mudstones of the Mosheim Member. Deep Springs is the only outcrop where the shaly dolomitic limestones were observed, although Laurence (1944) reported several meters of this lithology at the now-inundated Douglas Dam locality, 3.2 kilometers west of Deep Springs.

The shaly dolomitic limestone subfacies of the Douglas Lake Member, unlike the conglomerate and sandstone subfacies, is composed primarily of material generated and deposited in the marine environment. Marine deposition is indicated by the types of sediment that comprise the lithofacies, and by the sparse marine fauna present in the rock. The sediment is a mixture of dark grey shale and lime mud that has been subsequently

dolomitized, and suggests deposition in a very quiet bay or lagoon environment isolated from wave or tide energy. The fauna is restricted to ostracodes, gastropods, and very rare cephalopods, and is essentially the same as that of the overlying tidal flat facies (the Mosheim Member), and indicates deposition in a severely restricted marine environment. The cause for the faunal restriction is uncertain, but it may be related to salinity. There is no evidence for hypersalinity, such as evaporite minerals or molds, however, so it is plausible that the waters were hyposaline or brackish. Such an interpretation is consistent with the coastal or paralic setting envisioned for the deposition of the subfacies. In summary, the shaly dolomitic limestones represent deposition in a quiet, brackish lagoon or bay physically restricted from the open ocean.

Blackford Member

Distribution

The Blackford Member of the Five Oaks Formation, as named by Butts (1940) for exposures in Russell County, Virginia, is the lowermost stratigraphic unit of the Chickamauga Group (Figure 2.2). Use of the name is restricted to strata northwest of the Saltville Fault. Like the Douglas Lake Member, the Blackford Member is comprised of several different lithofacies representative of deposition in a variety of paralic or coastal environments, some apparently terrestrial and some primarily marine. The stratigraphic position immediately above the post-Knox unconformity, the irregular distribution, and the suite of lithologies that make up the Blackford suggest that it, like the Douglas Lake Member, was deposited in paleokarst depressions on the Knox surface. Thickness of the Blackford varies greatly, from zero to as much as sixty meters in Hawkins County, Tennessee (Rodgers and Kent, 1948), and was probably controlled by the depth of the depressions in which the Blackford was deposited. In the study area, the

Blackford ranges from one to ten meters thick. The Blackford grades upward into the main body of the Five Oaks Formation.

Lithofacies descriptions

The Blackford Member is composed of a wide variety of rock types, including:

1. Conglomeratic dolostones and limestones
2. Massive and laminated dolostones
3. Red, gray, and green mottled lime mudstones
4. Intraclastic / skeletal packstones and grainstones
5. Reddish-brown shales

The stratigraphic position of the Blackford immediately overlying the post-Knox unconformity, and the presence of basal conglomerates and dolostones make the Blackford similar in those respects to the Douglas Lake Member. The other Blackford lithologies, however, have no counterparts east of the Saltville Fault. Also, unlike the Douglas Lake Member, there is no predictable stratification to the lithofacies in the Blackford. Dolostones are the most abundant lithology, but shale becomes increasingly more abundant northwest of the Copper Creek Fault (Ruppel, 1979).

Conglomeratic dolostones and limestones

Conglomerates typically mark the base of the Blackford, but also occur sporadically in several zones above the basal contact. As in the Douglas Lake Member, conglomerates typically consist of clasts of chert and dolostone derived from the underlying Knox Group embedded in a matrix of dolomite that is also probably reworked Knox detritus (Figure 3.2B, C). This is especially true of the conglomerates immediately above the Knox surface. However, the Blackford also includes conglomerates with an

intraclastic/skeletal lime matrix (Figure 3.2D). These slightly fossiliferous conglomeratic limestones, which generally occur several meters above the unconformity, contrast with the abiotic Douglas Lake conglomerates. The Blackford conglomerates also differ from those in the Douglas Lake in that the clasts are less angular, and the average clast size is much smaller in the Blackford. Clasts are typically no larger than 3 to 5 centimeters in diameter (Figure 3.2B). Also, chert constitutes a much higher portion of total clasts in the Blackford (Figure 3.2C). All these differences suggest that the Blackford clasts were transported greater distances before final deposition than their Douglas Lake counterparts.

The dolostone and chert clasts, and perhaps much or all of the dolomite matrix in the conglomerates, were probably derived through erosion of exposed Knox carbonates. Like the Douglas Lake Member conglomerates, the conglomeratic dolostones of the Blackford generally lack sedimentary structures, and lack evidence of tractive transport, and therefore probably do not record fluvial deposition. These abiotic conglomerates probably represent detrital material or regolith that was deposited, primarily as gravity flows, in paleokarstic depressions on the Knox surface. The conglomeratic limestones, however, contain fossil debris and peloids, which indicate that the sediment is of marine origin. It is possible that this marine sediment was blown onto land by storms and deposited, along with detrital material, in terrestrial depressions. Alternatively, the terrestrial detritus may have been delivered by streams to the shoreline, and deposited along with marine-generated sediment as a coastal marine deposit.

Massive and laminated dolostones

Greenish-gray to buff-colored dolostones are the dominant lithology in the Blackford, and are either massive or laminated. Laminated dolostones are of two varieties. In one type, the lamination is produced by alternations of dark, finely-crystalline dolomite and tan, medium-crystalline dolomite rhombs, whereas in the other variety, the lamination is produced by intercalations of mud layers with layers of laminoid fenestrae. Massive dolostones typically appear featureless in the field and in thin section (Figure 3.2E), but on polished slab surfaces many have a distinctive, "swirled" appearance. Other massive dolostones, especially in the St. Paul belt, are very coarsely-crystalline, "sucrosic" dolostones that consist of coarse, interlocking, zoned, anhedral dolomite crystals (Figure 3.2F, G). These rocks are often partially silicified, and contain large *in situ* nodules of maroon chert that is entirely different from the detrital chert clasts contained in the conglomerates. Silicification is most pronounced where these dolostones are interbedded with shales, as in the northwesternmost strike belt of the study area, and especially at the Bethel Valley location (Figure 2.1).

The depositional environments represented by these dolostones is uncertain. The laminar dolostones may represent penecontemporaneous dolomite deposited on supratidal portions of a tidal flat. It is also possible that the dolostones formed from deposition of reworked, detrital dolomite crystals in subtidal channels. The total lack of fossils and the presence of laminoid fenestrae (which are believed to indicate desiccation and subaerial exposure) in some of these dolostones suggest that the former interpretation is more likely. Another possibility is that the dolomite is not penecontemporaneous with deposition, but is a diagenetic replacement of original limestone. The position of the Blackford dolostones immediately overlying the

dolostones of the Knox Group (Figure 3.2E, F) would have made these strata susceptible to dolomitization by magnesium-rich fluids migrating along the Knox unconformity.

The fine-grained, massive dolostones with "swirled" internal fabric contain some small areas in which lamination is preserved. This suggests that the massive dolostones may have originally been laminated, and that the lamination was disrupted by subsequent bioturbation that produced the swirled fabric. If that is indeed the case, these dolostones were probably deposited in supratidal environments similar to those in which the laminated dolostones were deposited, and soon afterwards submerged beneath mean tide level into an environment in which the lamination was disrupted by burrowing organisms. The coarsely crystalline, sucrosic, chert-bearing dolostones are interpreted to be totally recrystallized, diagenetic dolostones for which sedimentary precursors and depositional environments cannot be determined. Again, the position of these dolostones above the Knox unconformity (Figure 3.2F) is consistent with extensive secondary dolomitization.

Mottled lime mudstones

Limestones in the Blackford Member, though not as abundant as dolostones, are interesting from a sedimentological standpoint. Two varieties exist: mottled mudstones, and skeletal/intraclastic packstones and grainstones. The mudstones are composed of peloids and small mud intraclasts in a nonlaminated mud matrix. A small amount of faunal debris, restricted to fragments of pelecypods, trilobites, ostracodes, calcareous algae, and rare bryozoans and echinoderms, is sometimes present. The mudstones generally are partly dolomitized, with burrows more dolomitic than the surrounding mud matrix.

The lime mudstones represent deposition of marine-generated calcium carbonate mud and peloids in quiet, restricted subtidal ponds that probably developed in depressions

on the Knox surface as marine transgression began. Extensive burrow-mottling and the presence of a fairly unrestricted, marine fossil assemblage indicate that the ponds were apparently open to circulation with sea water and inhabited by marine organisms.

Intraclastic / skeletal packstones and grainstones

The Blackford includes isolated occurrences of a packstone / grainstone subfacies that consists of coarse silt- to sand-sized fossil fragments, lime mud and dolomitized mud intraclasts, and reworked detritus derived from the Knox (dolostone and chert lithoclasts and quartz sand) (Figure 3.2H). Skeletal material is primarily abraded echinoderm grains and pelecypod shells, with lesser amounts of bryozoan, ostracode, calcareous algae, and inarticulate and articulate brachiopod debris. This material is deposited in cross-bedded layers up to one meter in thickness, which typically overlie scoured erosional surfaces developed on underlying dolostones. Similar packstones also occur in the overlying Five Oaks Formation.

The diversity of fossil fragments in the skeletal / intraclastic grainstones and packstones indicates deposition in well-circulated, normal marine water. The paucity of mud, abrasion of skeletal fragments, scoured bases, and the well-developed bidirectional cross-bedding indicates deposition in a fairly high-energy system characterized by bimodal currents. This evidence, and the lack of subaerial exposure indicators, indicates that this lithology represents a subtidal channel facies. These tidal channels served as conduits for transporting marine water and sediment landward onto the Knox surface during initial development of the tidal flat, and also allowed seaward transportation of detrital material eroded from exposed Knox carbonates.

Reddish-brown shales

The lower portion of the Chickamauga sequence in the St. Paul belt contains abundant reddish-brown shales in intervals that are up to three meters thick. These shale lithologies are generally assigned to the Tumbez Formation and the Fleenor and Eidson Members of the Lincolnshire, but in places occur interbedded with thinner, one- to two-meter thick intervals of dolostone and limestone in the Blackford Member. The abundance of the shales in these northwestern strike belts indicate that shale deposition exceeded carbonate deposition in this area at times during the early Middle Ordovician. The presence of the shales seems to mark the landward extent of migration of the Mosheim/Five Oaks tidal flat facies, as shale becomes increasingly abundant at the base of the Middle Ordovician section toward the northwest. These shales are entirely devoid of fossils, and perhaps represent concentrated accumulations of fine-grained insoluble residue derived through erosion of Knox Group carbonates. Shales collected from the lower third of the Raccoon Valley section are composed primarily of illite and kaolinite, and do not contain chlorite or feldspars (Metcalfe, 1974). The stratigraphically lowest occurrence of chlorite in the Raccoon Valley section is at approximately 260 meters above the Knox unconformity, and the lowest bentonite in the section is at 500 meters above the Knox (Metcalfe, 1974) . Metcalfe (1974) determined, on the basis of shale mineralogy, that the shales in the lower portion of the Raccoon Valley section were not related to the shales in the Sevier shale basin, and interpreted them to be derived from erosion of Knox bedrock. It is possible that these shales represent reworked terra rosa soils that developed on the exposed Knox surface.

Environmental Summary of Nearshore Terrestrial / Paralic Lithofacies

The Douglas Lake and Blackford Members are the lowermost deposits of the Middle Ordovician section in eastern Tennessee. The two units are lithologically similar, and consist of mixed carbonate and siliciclastic sediment that was deposited in a variety of terrestrial and marine coastal (paralic) environments during exposure of the Knox platform and at the onset of the Middle Ordovician marine transgression. Lithologic subfacies within each member represent deposition in different subenvironments of this coastal setting.

The Douglas Lake Member consists of dolomitic conglomerates, quartz / chert sandstones, and shaly dolomitic limestones. Conglomerates occur at the base of the unit, and are overlain either by the sandstone subfacies (at Dandridge), or by shaly dolomitic limestones (at Deep Springs). The conglomerates represent Knox regolith redeposited in terrestrial paleokarst depressions on and beneath the Knox surface during subaerial exposure. The sandstones are composed of detrital material eroded from Knox Group carbonates, transported by streams to the paleoshoreline, and there reworked by marine currents. The shaly dolomitic limestones represent marine sediment deposited in restricted subtidal conditions in low areas on the Knox surface during initial Middle Ordovician marine transgression.

The Blackford Member is similar to the Douglas Lake Member in that it represents deposition in depressions on the Knox surface during and immediately after post-Knox exposure. Some of the conglomerates, dolostones, and shales might represent terrestrial deposition, but most of the Blackford subfacies are limestones and dolostones that represent shallow marine deposition at the onset of Middle Ordovician transgression over the karstic Knox surface. Some of these lithologies (lime mudstones and laminated dolostones) appear to be of tidal flat origin, and probably represent the initial deposits of

the developing tidal flat represented by the overlying main body of the Five Oaks Formation.

By filling depressions on the Knox surface, the Douglas Lake and Blackford units reduced relief and provided a relatively flat surface upon which the overlying tidal flat developed. A modern analogue for this process exists in the Bahamas, where karst dolines that developed on exposed limestone during the Pleistocene sea level lowstand have been filled with detrital material during the Holocene sea level rise (Rasmussen and Neumann, 1988) .

Tidal Flat Lithofacies

Previous investigators of Middle Ordovician stratigraphy in the southern Appalachians (Stephenson et al., 1973; Bergstrom and Carnes, 1976; Shanmugam and Walker, 1978; Ruppel, 1979; Harris, 1982; Benson and Mink, 1983; Ruppel and Walker, 1984) have concluded that the Five Oaks Formation and the Mosheim Member of the Lenoir Formation represent parts of a large tidal flat that was deposited at the onset of Middle Ordovician transgression. This interpretation is based upon several observations: the predominance of low-energy, muddy and peloidal lithologies; the near-absence of high energy oolitic and skeletal sand deposits and wave- or current-worked sedimentary structures; the overwhelming abundance of fenestral lithologies; the extreme faunal restriction in the rocks; and the stratigraphic position of the sequence between a major subaerial exposure surface (the Knox unconformity) and shallow open marine facies (the Lenoir and Lincolnshire Formations). Although it has already been established by other workers that this basal Middle Ordovician sequence is of tidal flat origin, a detailed analysis of the conditions and subenvironments of tidal flat deposition has not previously been attempted.

The lithologies that comprise the Mosheim Member and the Five Oaks Formation are described in detail below. The suite of lithologies in these units are interpreted as subfacies of an ancient tidal flat, using the modern tidal flat on Andros Island, Bahamas, as described in Shinn et al. (1969), Hardie (1977), and Shinn (1986), as a modern analogue. Although other well-documented modern tidal flats could have served as an analogue for this sequence, such as the Persian Gulf (Purser, 1973) or Shark Bay, Australia (Logan et al., 1970), Andros Island is the most appropriate for several reasons.

First, Middle Ordovician tidal flat deposits in adjacent areas of the Appalachians have been interpreted as ancient Andros Island analogues. Grover and Read (1978, 1983) interpreted the fenestral limestones in the Middle Ordovician New Market Formation of Virginia to have formed in a humid tidal flat setting analogous to that on Andros Island. Mitchell (1981, 1985) interpreted the partly correlative Middle Ordovician tidal flats of the St. Paul Group of the central Appalachians to be an analogue of the humid, Andros Island-type tidal flat.

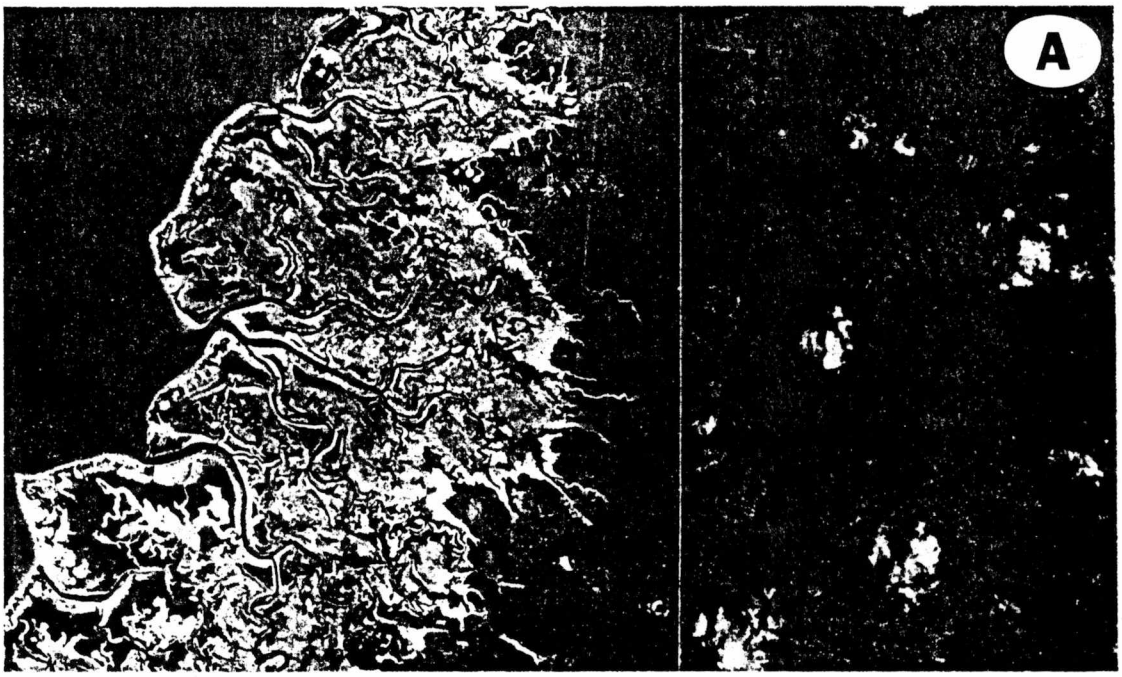
Second, the initial detailed examinations of samples collected from the Mosheim / Five Oaks facies for this study revealed that these samples generally lacked features such as evaporite minerals, mudcracks, prism cracks, tepee structures, primary dolomite crusts, and so forth, that would indicate intense evaporation, hypersalinity, or deposition in an arid environment. The paucity of such features indicated that an arid tidal flat, such as the Persian Gulf or Shark Bay, would not be an appropriate analogue.

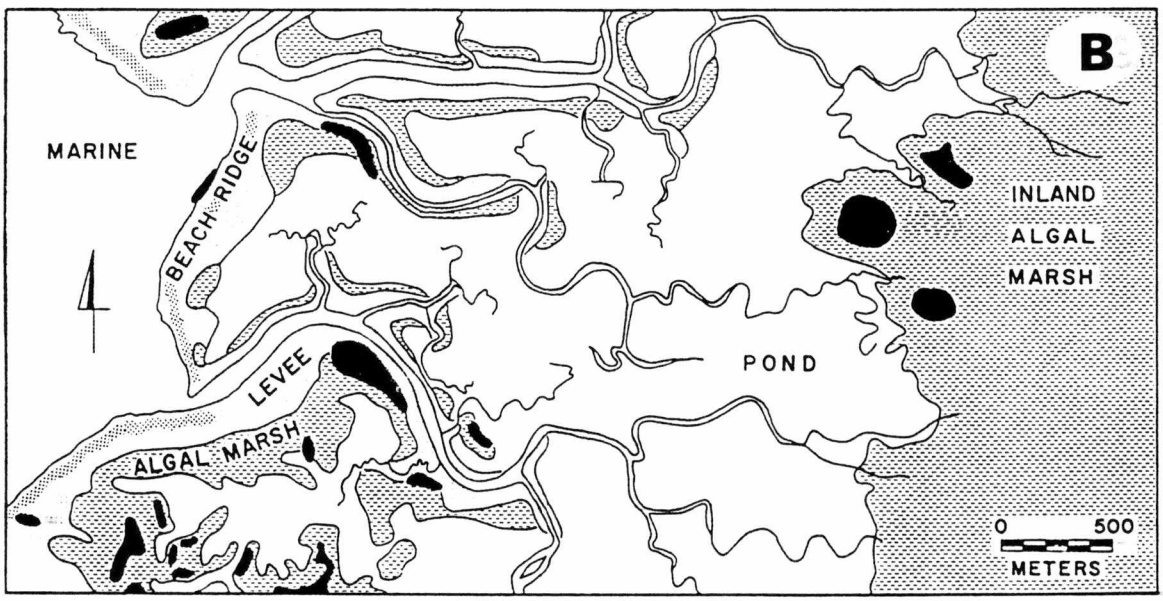
Third, as detailed analysis of the sedimentological features of the Mosheim / Five Oaks tidal flat facies progressed, it became clear that on all scales, from the most minute details to gross features of tidal flat morphology, the Mosheim / Five Oaks tidal flat was analogous to the Andros Island tidal flat. Recognizing and describing the similarities and differences between the two tidal flats became a primary goal of this study.

Characteristics of the Andros Island Tidal Flat

The general morphology and subenvironments of the Andros Island tidal flat, as documented by Hardie (1977) and Shinn (1983, 1986) are summarized diagrammatically in Figures 3.3 through 3.6. The Andros Island tidal flat consists of a supratidal inland "algal" marsh (the dark area that occupies the right half of the aerial photograph; Figure 3.3A) and a complex channeled belt (the white area in the photograph). The adjacent offshore shallow marine environment (the dark area in the upper left portion of the photograph) lies immediately seaward of the tidal flat, and is separated from the tidal flat by a low beach ridge (Figures 3.3B, 3.4, and 3.5). The channeled belt consists of many subenvironments, including ponds, channels, low "algal" marshes, high "algal" marshes, channel levees, and levee and beach ridge backslope environments (Figures 3.3B, 3.4, and 3.5). The position of these subenvironments relative to mean sea level (Figure 3.6) determines the amount of time each subenvironment is subaerially exposed, and the amount of subaerial exposure exerts influence over the types of sedimentary and early diagenetic structures that typify the deposits in each subenvironment (Hardie, 1977). The lamination types that characterize the various tidal flat subenvironments on the Andros Island tidal flat are summarized in Table 3.1. All of the lamination and bedding types documented on the Andros Island tidal flat (Hardie and Ginsburg, 1977) were recognized in the Mosheim/Five Oaks tidal flat facies in this study, and were used as modern analogues to interpret the depositional subfacies of the basal Middle Ordovician tidal flat.

Figure 3.3. **A**. Aerial photograph of the Three Creeks area, northwestern Andros Island tidal flat, Bahamas. From left to right, the photo clearly shows three major depositional environments: the adjacent offshore shallow marine environment, the channeled belt, and the inland algal marsh. Note the sharp boundaries between these zones. The boundary between the offshore marine environment and the channeled belt is the beach ridge. The dark color of the inland algal marsh (and the isolated algal marshes within the channeled belt) is due to dense algal cover. The boundary between the channeled belt and the inland algal marsh is the line where the algal marsh bounds tidal ponds, which lack algal cover due to the presence of algae-consuming organisms. **B.** Map of an enlarged portion of the photograph above. The channeled belt is a complex zone consisting of ponds, channels, algal marshes, and levees. The channeled belt is separated from the open ocean by the low beach ridge. The channels serve as pathways for the transport of seawater and sediment from the offshore marine environment to the interior ponds and the inland algal marsh, and for transport of freshwater from the inland algal marsh to the sea during rainy seasons. Up to 90% of the surface area of the channeled belt is occupied by shallow subtidal ponds. The photograph and the map are from Hardie and Garrett (1977).


A


B
MARINE
BEACH RIDGE
LEVEE
ALGAL MARSH
POND
INLAND
ALGAL
MARSH
0
500
METERS

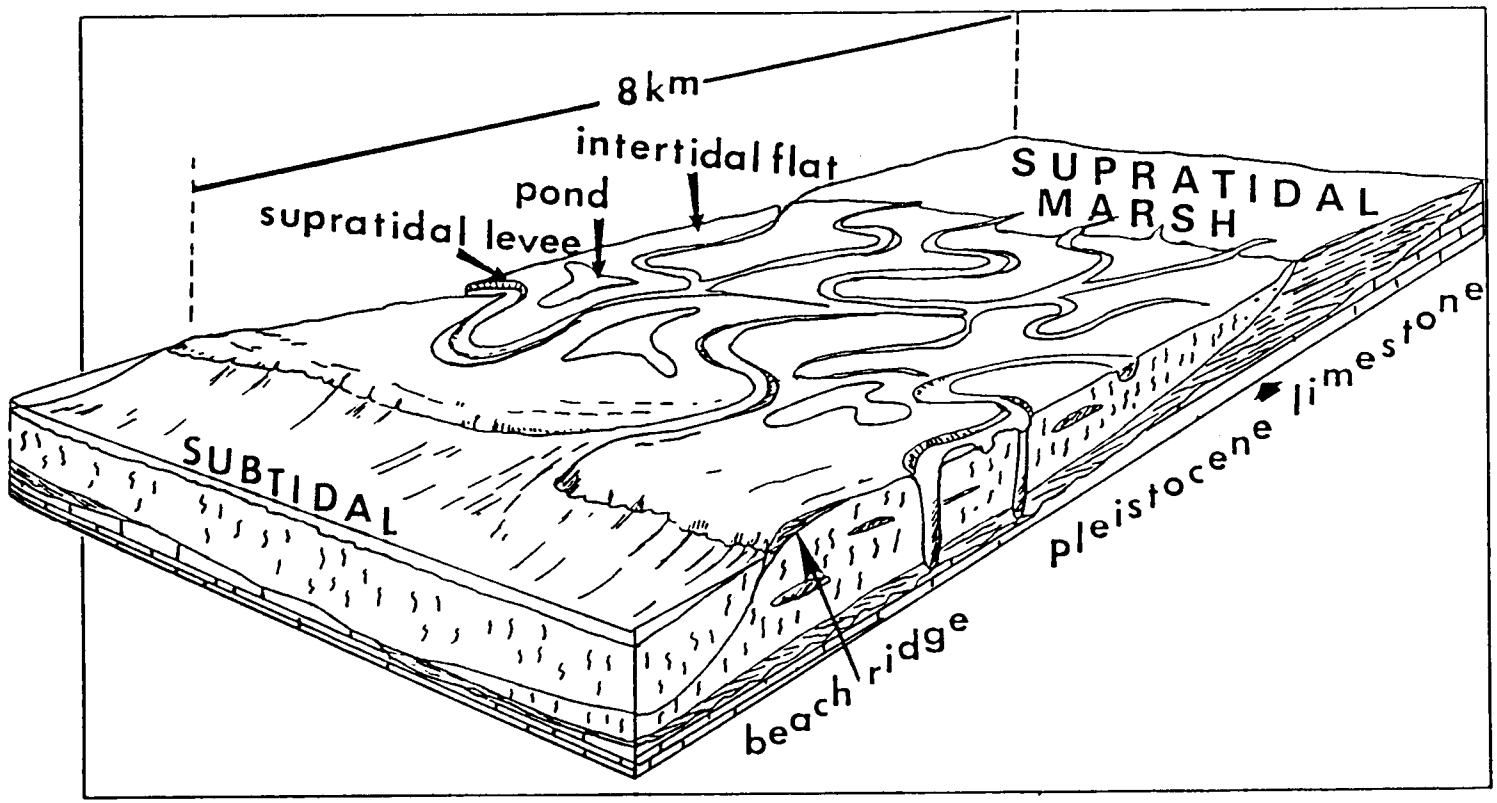


Figure 3.4. Block diagram showing the major depositional environments of the northwestern portion of the Andros Island tidal flat. Note the stratigraphic arrangement of the facies in this sedimentary package: the offshore subtidal marine facies overlies the channeled belt facies, the channeled belt facies overlies the inland supratidal algal marsh facies, which in turn overlies the Pleistocene limestone bedrock. This landward migration of marine environments (and marine facies) over coastal and terrestrial environments defines a transgressive, or onlap, sedimentary sequence, which is occurring in response to Holocene sea level rise. Erosion of tidal flat sediment occurs at the beach ridge as the subtidal marine environment migrates over the tidal flat. (From Shinn, 1986)

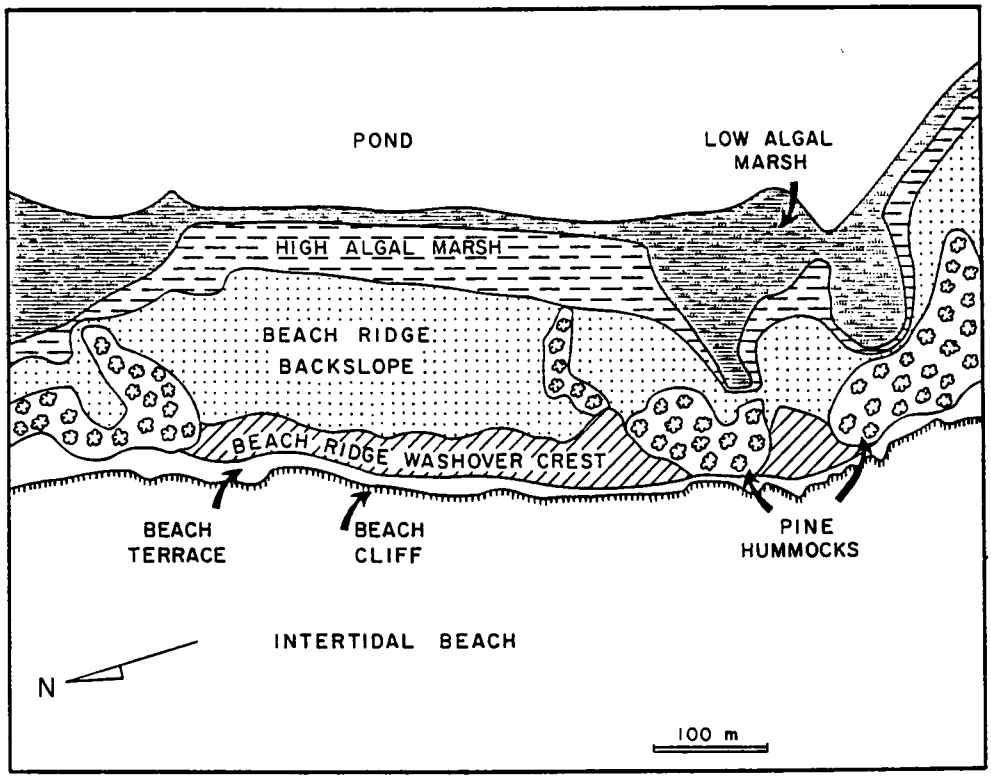


Figure 3.5. Detailed map showing subenvironments of the beach ridge and the algal marshes and ponds of the channeled belt that occur on the landward side of the beach ridge, Andros Island. The beach ridge slopes gradually landward from the beach ridge washover crest into the tidal pond. A cross-sectional profile across the beach ridge, from beach to pond, is shown in Figure 3.6. (From Hardie and Garrett, 1977)

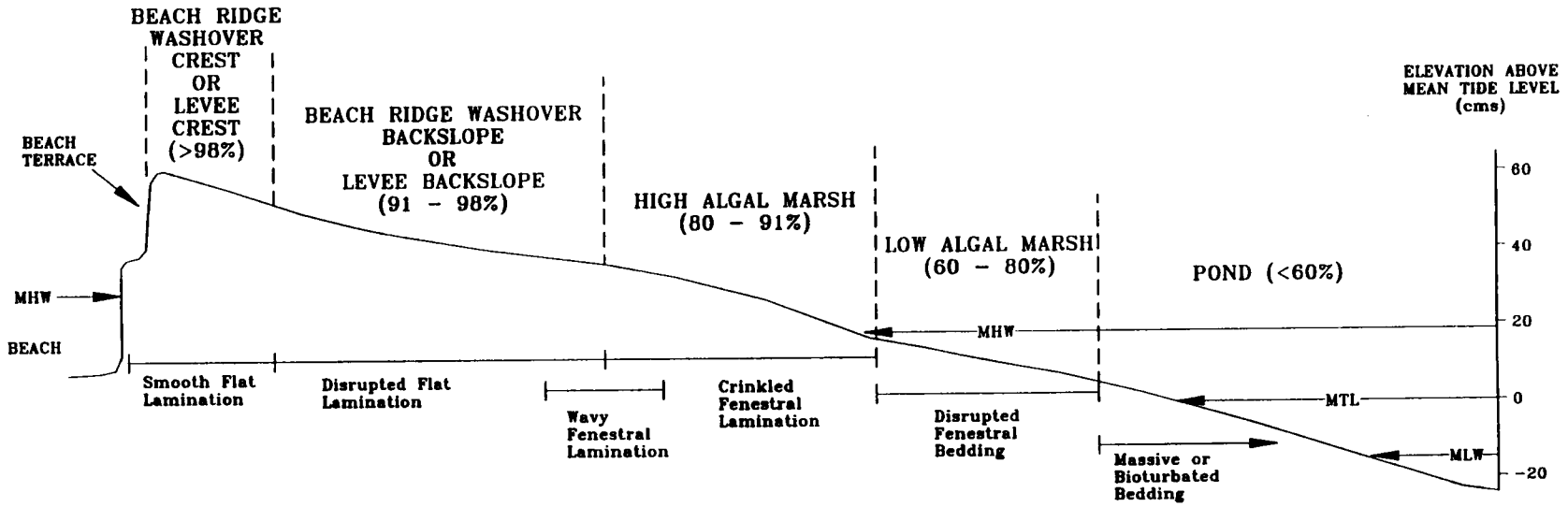


Figure 3.6. Profile across a portion of the Andros Island tidal flat, from beach ridge (or channel levee) to a tidal pond, showing the major depositional subenvironments relative to mean tide level (MTL), mean high water (MHW), and mean low water (MLW). Numbers in parentheses are the exposure indices (percent of time of subaerial exposure) for each subenvironment. Bars along the base of the drawing indicate the types of lamination or bedding associated with each subenvironment (see Table 3-1). (Modified from Hardie and Garrett, 1977)

Table 3.1: Lamination Types on the Andros Island Tidal Flat (a)

Lamination Type	Method of Development	Distinctive Features	Subenvironment	Exposure Index
Smooth flat lamination	Alternations of mud laminae with peloid sand laminae, with each lamina representing a discrete storm layer	Fenestrae are uncommon. Sandy laminae are discontinuous laterally (produced by migration of sand ripples). Laminae are not disrupted by mudcracks.	1) levee crest 2) beach ridge washover crest 3) beach terrace	>98% (highest supratidal)
Disrupted flat lamination	Alternations of mud laminae with peloid sand laminae	Similar to smooth flat lamination, but laminae are disrupted by mudcracks, sheetcracks, and burrows. Also contains abundant burrows. Also contains abundant laminoid and irregular fenestrae.	1) levee backslope 2) beach ridge backslope	91 to 98% (supratidal)
Wavy fenestral lamination	Consists of mud laminae draped over clots or lumps of mud or peloidal sediment.	Occurs in association with smooth flat or crinkled fenestral lamination. Irregular fenestrae occur within muddy sediment lumps, and laminoid fenestrae parallel wavy mud laminae.	1) levee or beach ridge backslope/high algal marsh boundary 2) beach terrace	85 to 95% (highest intertidal to supratidal)
Crinkled fenestral lamination	Alternation of mud or peloid sand layers with algal mats (or with rows of bed-parallel fenestrae after algal mat decay).	Fenestrae make up 5 to 50% of rock volume, and include abundant irregular and laminoid types. Lamination is well-developed where laminoid fenestrae are dominant, and vague to absent where irregular fenestrae dominate.	1) High algal marsh 2) Inland algal marsh	80 to 91% (high intertidal to supratidal)
Disrupted fenestral bedding (b)	Lacks distinct lamination, but consists of thin beds of coherent but unlithified muddy or peloidal sediment.	Randomly-oriented, irregular fenestrae are very abundant, and predominate over laminoid fenestrae. Develops in wet environments characterized by lush, tufted cyanobacterial mats.	1) Low algal marsh	60 to 80% (intertidal)

(a) Adapted from Hardie and Ginsburg (1977). Some of the lamination and layering types included in Hardie and Garrett's table have been deleted from this list because they are either unrecognized in the Mosheim/Five Oaks tidal flat facies, or they are not exclusively indicative of tidal flat deposition.

(b) Disrupted fenestral bedding is not a type of lamination, but is included in this table because it is the characteristic bedding type of low algal marsh deposits, and one of the most common layering types in the Mosheim/Five Oaks sequence.

Mosheim Member

Distribution

The Mosheim Member of the Lenoir Formation is generally the basal Middle Ordovician deposit in sequences southeast of the Saltville Fault. That is the case at all such outcrops in the study area, except at Deep Springs, where the Mosheim is underlain by the Douglas Lake Member, and at Dandridge, where the Mosheim is absent and the Douglas Lake Member underlies the main body of the Lenoir. Limestones identical to the Mosheim also occur at the base of the Middle Ordovician section northwest of the Saltville in the Hawkins belt, and are referred to as Mosheim in this report, although other workers have assigned those rocks to the Five Oaks Formation (e.g., Ruppel, 1979). Thickness of the Mosheim ranges from zero (at Dandridge) to 60 meters (in the American Limestone quarry adjacent to the John Sevier Highway outcrop), but 12 to 20 meters is typical. Thickness variations probably reflect relief on the Knox surface, with thicker sections accumulating in paleokarst depressions. This observation was made by Haynes and Kesler (1989), who determined that organic hydrocarbons accumulated preferentially in paleotopographic highs in the uppermost Knox Mascot Formation, and used the relative thickness of the Mosheim to identify highs and lows on the karsted Knox unconformity surface.

Lithofacies descriptions

In the field, the Mosheim Member appears to be a fairly monotonous section of medium to dark gray, pure lime mudstone, the majority of which exhibits a characteristic fenestral fabric. Although that generalization is basically true, closer inspection by means of polished slabs and thin sections reveals that the Mosheim includes several different

lithologies, listed below in order of decreasing abundance:

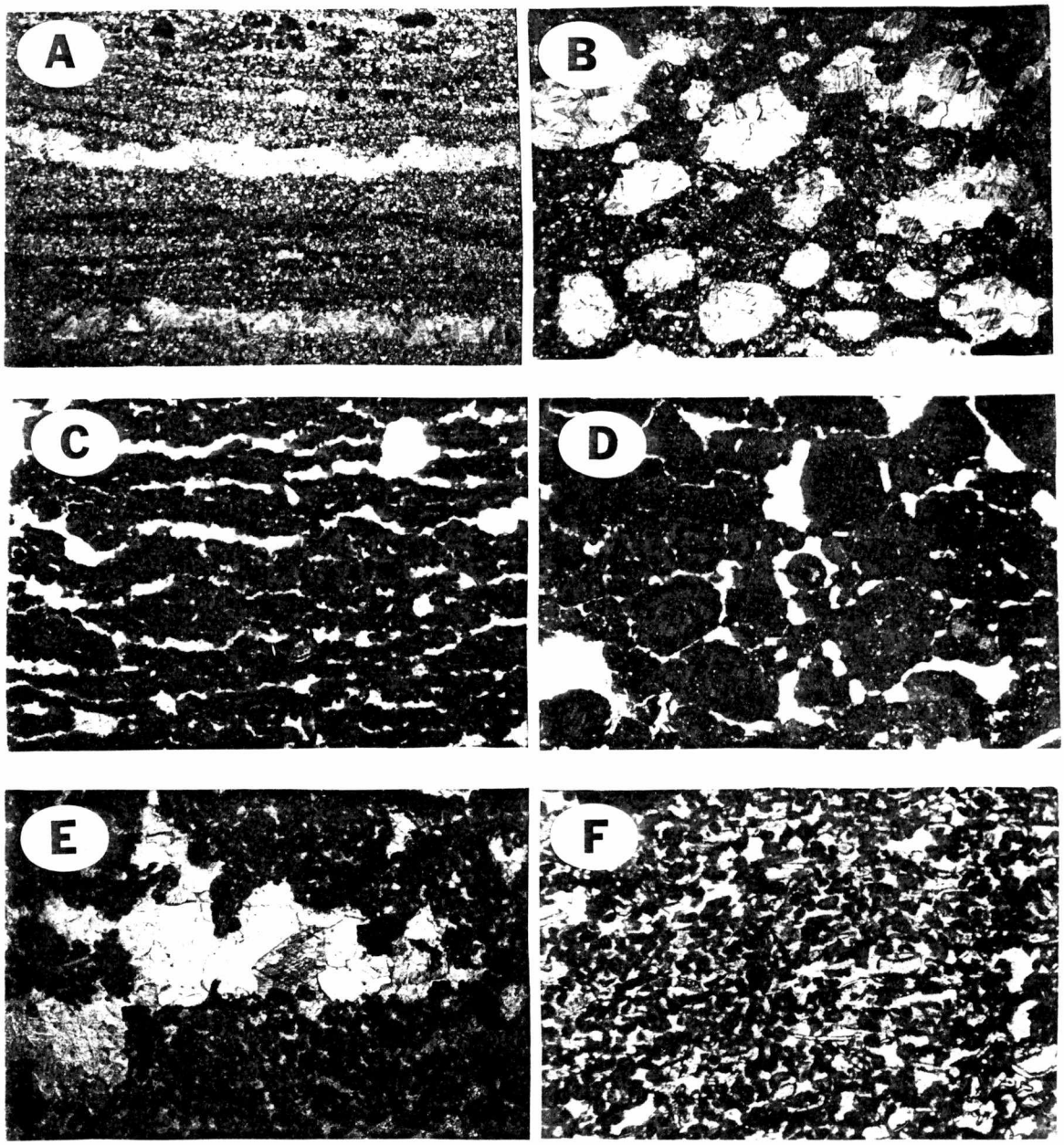
1) Fenestral mudstones
2) Fenestral peloidal / intraclastic grainstones and packstones
3) Non-fenestral mudstones
4) Peloidal / skeletal wackestones
5) Conglomeratic fenestral limestones

As a rule, there is no regular pattern, or cyclicity, in the occurrence or stratification of these primary lithologies within the Mosheim. Some exceptions to this are that the conglomerates, where present, are restricted to the basal meter of the unit; the peloidal/ intraclastic grainstones generally occur near the base and top of the Mosheim; and the non-fenestral mudstones and skeletal wackestones do not occur near the base of the unit. Most of the Mosheim (above the basal few meters and below the upper meter) is composed of a random stratigraphic arrangement of non-laminated fenestral and non-fenestral mudstones, and less commonly, skeletal wackestones. The Mosheim contains lithologies with high enough dolomite content to be called dolostone, but some lithologies in the basal meter of the unit were highly dolomitized (Figure 3.7A, B). The absence of dolostones in the Mosheim contrasts sharply with the dominance of dolostones in the tidal flat deposits of the underlying Knox Group.

Fenestral mudstones

Fenestral mudstone is by far the most abundant and most typical Mosheim lithology (Figure 3.7). This lithology consists of relatively pure (typically undolomitized and non-argillaceous) lime mud that is laced with a framework of fenestrae (Tebbutt et al., 1965) or birdseyes (Illing, 1959; Shinn, 1968). Fenestrae are defined as primary (synsedimentary) void spaces, typically larger than grain-supported, interparticle pores, that have no apparent means of support by the grain framework of the sediment (Tebbutt,

Figure 3.7. Lithologies of the Mosheim Member. A-F are thin section photomicrographs, taken under plane-polarized light. The long axis field of view in each photo is 6.5 mm. **A.** Disrupted flat lamination in highly dolomitized peloidal packstone, 0.4 m above the Knox unconformity (AKU), Boyd's Creek Road. This lamination type is produced by alternation of peloid layers with mud layers, but is accentuated by laminoid fenestrae which have coalesced into equant calcite-filled sheet cracks. **B.** Highly fenestral, dolomitized intraclastic mudstone, 5 cm AKU, Boyd's Creek Road. Contains abundant small (1 to 2 mm) irregular fenestrae and larger (2 to 5 mm), almost spherical "bubble" fenestrae. All fenestrae in this sample are filled with equant calcite cement, which occupies up to 45% of the rock volume in this and other samples of the basal Mosheim. **C.** Fenestral peloidal packstone, with abundant laminoid and less abundant irregular fenestrae, 0.6 m AKU, Boyd's Creek Road. Note the abundance of peloids and small mud intraclasts in the matrix. This sample is an example of the crinkled fenestral lamination that is characteristic of inland or high algal marsh sediment. Such lamination is produced by the predominant horizontal orientation of the laminoid fenestrae **D.** "Diagenetic grainstone/pisolite" fabric, from 7 m AKU at the Nina section. Muddy sediment has been altered by intense fenestral alteration in the vadose zone into discrete mud lumps (autoclasts) surrounded by curved laminoid fenestrae and larger irregular fenestrae, all of which are filled with equant calcite cement. Some of the lumps were concentrically coated with micritic rims and transformed into pisoids. This fabric appears to develop most commonly in highest intertidal to supratidal inland and high algal marsh environments, where subaerial exposure is prolonged. **E.** Irregular fenestrae in fenestral peloidal packstone. Matrix consists of discrete small clasts of depositional origin (peloids), rather than homogeneous lime mud. This lithology is most abundant in basal Mosheim sediments interpreted to represent deposition on the inland supratidal algal marsh. **F.** Intraclastic grainstone, with mostly very small irregular fenestrae. Matrix consists of small mud intraclasts and peloids and also contains fairly abundant abraded skeletal debris. This subfacies is rare in the Mosheim, but is fairly abundant in the Five Oaks.


A
B
C
D
E
F

et al., 1965). Fenestrae typically become filled shortly after their formation with sparry calcite cement or anhydrite, or less commonly, filled or floored with internal sediment (Tebbutt, et al., 1965; Shinn, 1968). According to Shinn (1968; 1983), fenestrae have two primary shapes, spherical (irregular) and planar (laminoid). Irregular fenestrae in the Mosheim have crudely spherical shapes and no particular orientation, and are 1 to 5 mm in diameter (Figure 3.7B-E), whereas the laminoid variety are elongate in a bed-parallel direction, and up to a few cm in length (Figure 3.7C). Many origins have been proposed for fenestrae (Illing, 1959; Shinn, 1968), but the most widely accepted are that the irregular voids are formed by air bubbles trapped in the sediment, or gas bubbles produced during the decomposition of organic matter, and the laminoid variety are formed by desiccation and shrinkage of muddy sediment during intermittent subaerial exposure (Fischer, 1964; Shinn, 1968). Similar spar-filled, vertically-elongate features have been called tubular fenestrae by some authors (e.g., Tebbutt, et al., 1965; Grover and Read, 1978), but since these features are generally interpreted to be either cement-filled animal burrows or root-tubes, they are more correctly referred to as burrows or root-tubes rather than a type of fenestra (Shinn, 1983).

Fenestrae are an almost ubiquitous feature of mudstones, grainstones, and dolostones deposited in modern intertidal and supratidal environments, and by association, have become widely accepted as indicators of peritidal, and especially supratidal, sedimentation. Shinn (1968) suggested that fenestrae might be useful as indicators of tidal flat deposition even when other reliable peritidal indicators are lacking. After the discovery of fenestra-like features in subtidal grainstones, Shinn (1983) constrained the interpretive value of fenestrae, by stating that fenestrae are most reliable as indicators of intertidal and supratidal deposition in mudstones and penecontemporaneous dolostones. Ideally, fenestrae should be associated with other

reliable supratidal or intertidal indicators, such as mudcracks, lamination, and algal structures, before such an interpretation is made (Shinn, 1983).

Hardie and Ginsburg (1977) showed that fenestrae, at least on Andros Island, are less common in the flat laminated sediments of the highest supratidal subenvironments such as levee and beach ridge crests and backslopes, than in the lower supratidal and high intertidal algal marshes (Table 3.1 and Figure 3.6). Fenestral fabrics in the Andros Island tidal flat sediments are most closely associated with the "crinkled fenestral lamination" that characterizes the supratidal high algal marshes and with the "disrupted fenestral bedding" that underlies the intertidal low algal marshes. Irregular fenestrae form by algal decay in sediments that infiltrate or drape lush growths of tufted cyanobacteria such as the modern *Scytonema,* which populate the pond-rimming "algal" marshes on Andros Island. Laminoid fenestrae form by the decay of algal mats that are interlayered with sediment laminae, or where desiccation causes the formation of large horizontal sheet cracks in the sediment. These desiccation cracks, ironically, do not form well in the highest supratidal subenvironments (levee and beach ridge crests) because of the tenacious binding of mucaceous cyanobacterial mats (*Schizothrix*), but instead form on the high algal marshes and the backslopes of levees and the beach ridge (Hardie and Ginsburg, 1977) (Table 3.1, Figure 3.6).

Both irregular and laminoid varieties of fenestrae are very common in the Mosheim. Beds containing irregular fenestrae occur interspersed with non-fenestral mudstone layers throughout the Mosheim, but irregular fenestrae are generally larger (commonly up to 5 mm) and most abundant near the base of the unit, where fenestrae-filling cement occupies as much as 45% of the rock volume (Figure 3.7B). Well-developed, laterally-persistent laminoid fenestrae, with few exceptions, are restricted to the lower one to three meters of the unit, where they occur in association with large irregular fenestrae (Figure 3.7C). Rarely, and only in the basal meter, laminoid fenestrae

have coalesced into larger, bed-parallel sheet cracks (Figure 3.7A). Shorter, curved laminoid fenestrae occur with irregular fenestrae throughout the Mosheim. Vertical, cement-filled burrows also occur, but are far less abundant than either variety of fenestra. The stratigraphic distribution and relative abundances of fenestral types are similar to those in the correlative Middle Ordovician New Market Limestone, as described by Grover and Read (1978), and indicate a complex overprinting of different fenestral fabrics.

As stated above, lamination is conspicuously rare in the Mosheim, but is preserved in some of the fenestral mudstones. Lamination is in some cases produced by alternations of organic-rich and organic-poor mud layers, but most often, lamination in the Mosheim is the result of separation of sediment layers by horizontal rows of laminoid fenestrae (Figure 3.7C). Lamination is best developed near the base of the Mosheim, and is almost always associated with laterally-coalesced, laminoid fenestrae. This type of lamination corresponds with the "crinkled fenestral lamination" on Andros Island (Hardie and Ginsburg, 1977) (Table 3-1). Fenestral mudstones in the Mosheim with well-developed fenestral lamination are interpreted as supratidal, high algal marsh sediments. Fenestral mudstones which lack well-defined crinkled fenestral lamination are analogous to the intertidal, low algal marsh sediments on Andros Island, which are characterized by the "disrupted fenestral bedding".

Another interesting lithology quite common in the Mosheim is the "diagenetic grainstone and pisolite" fabric described by Mazzullo and Birdwell (1989). This lithology (Figure 3.7) is included in this discussion with the fenestral mudstones, rather than with the fenestral peloidal grainstones, because the grainstone / pisolite fabric is interpreted to be an early, vadose diagenetic alteration of original fenestral mudstones, and is not a primary, depositional fabric. Production of diagenetic grainstones results from "the progressive development, enlargement, and coalescence of fenestrae in muddy carbonate

sediments" (Mazzullo and Birdwell, 1989), and involves redistribution and reorganization of lime mud from diffuse patches into discrete lumps. During this process, many of these lumps become coated by micrite envelopes and transformed into pisoids (Figure 3.7D) that provide further evidence of development under vadose conditions. The development of this diagenetic fabric is discussed further in Chapter 4 of this dissertation.

Fenestral peloidal/intraclastic grainstones and packstones

These fenestral limestones differ from the fenestral mudstones only in that the rock "matrix", rather than consisting of more or less homogeneous lime mud, is organized into discrete, muddy ovoid lumps of peloid and intraclast size (Figure 3.7E, F). Unlike the grains in the previously mentioned "diagenetic grainstones", these allochems are believed to be depositional particles, as indicated by the generally sharp edges of the grains, which suggests some degree of cohesiveness or lithification of the mud, and the rounded shape of the grains, which indicates at least some transportation or rolling of the particles prior to deposition.

Fenestral intraclastic grainstones typically occur at or within a few meters of the base of the Mosheim. Like the fenestral mudstones at the base of the unit, fenestral grainstones are often laminated due to the presence of well-defined laminoid fenestrae. Also, the fenestral peloidal packstones and grainstones are characterized by a very restricted biota, and are, in many cases, devoid of macrofossils. When fossils are present, the assemblage is typically restricted to gastropods and ostracodes. The extreme faunal restriction, the abundance of fenestrae, and the preservation of fenestral lamination indicates that the fenestral grainstones and packstones, like the fenestral mudstones, were deposited as supratidal, inland or high algal marsh sediments. Although it has been shown that special care must be taken in interpreting depositional environments of

fenestral grainstones because of the discovery of fenestra-like voids in subtidal grainstones (Shinn, 1983), the faunal restriction in the lithologies, the stratigraphic position relative to other features, and the association of these grainstones with other peritidal lithologies, suggest that a supratidal interpretation for these fenestral grainstones is valid.

Intraclastic grainstones containing minor amounts of highly abraded skeletal debris also are sometimes preserved immediately beneath the erosional surface at the top of the Mosheim (Figure 3.7F). In a few places, these upper grainstones contain "keystone vugs", or fenestrae that contain pendant fibrous cements that indicate marine vadose or "beachrock" cementation (Ginsburg, 1953). Similar grainstones at the top of the Mosheim in Alabama (the Lee Branch Member of Roberson, 1988) contain laminae that slope in a landward direction at up to 30 degrees. These upper, inclined bedded grainstones are interpreted as analogues of deposits on the supratidal, beach ridge "hammocks" on Andros Island (Hardie and Ginsburg, 1977) (Figure 3-5).

Non-fenestral mudstones and peloidal skeletal wackestones

Non-fenestral lithologies, though far less abundant than fenestral limestones, do occur in scattered horizons throughout the Mosheim, and are totally absent only from the basal meter or so. Non-fenestral lithologies include two main varieties: mudstones and peloidal skeletal wackestones. The mudstones are massive, non-laminated accumulations of essentially featureless lime mud. Vague mottling, probably produced by infaunal burrowing organisms, is sometimes present. Allochems of any kind are rare to absent. The wackestones are similar, but contain varying amounts of peloids and/or fossil debris. The faunal diversity in these wackestones also varies widely. The majority of the wackestones carry faunal assemblages that are limited to gastropods and ostracodes, but

some others, particularly those that occur in the upper few meters of the Mosheim at the Nina location (Figure 2.1), contain more open marine assemblages that include brachiopods, trilobites, bryozoans, and calcareous algae, in addition to gastropods and ostracodes.

The abundance of mud and evidence of burrowing, and the absence of laminations and exposure indicators such as fenestrae and mudcracks, indicate that the mudstones and wackestones accumulated in very low energy, shallow subtidal environments inhabited by infaunal burrowing organisms. These characteristics, and the stratigraphic and lateral association of these lithologies with fenestral intertidal and supratidal lithologies, suggests that the non-fenestral mudstones and wackestones were deposited in shallow subtidal ponds, such as those that dominate the channeled belt portion of the Andros Island tidal flat (Hardie and Garrett, 1977). Variations in the abundance and diversity of fossils suggest that some of the ponds were restricted from circulation of marine waters and could support only those organisms tolerant of harsh or fluctuating conditions, while others were relatively open, and inhabitated by stenotopic organisms. Because it is difficult to distinguish pond sediments from subtidal channel deposits (Hardie and Ginsburg, 1977), it is possible that some of the non-fenestral lithologies, especially the wackestones with diverse marine faunas, represent deposition in channels that carried seawater across the tidal flat.

Conglomeratic fenestral limestones

Conglomeratic limestones, as stated above, occur only at the base of the Mosheim, and generally do not persist more than a meter up into the unit. As in the conglomerates of the Douglas Lake and Blackford Members, the clasts include dolostone, limestone, and chert fragments derived from erosion of exposed Knox Group

carbonates. The Mosheim conglomerates are differentiated from those in the Douglas Lake Member, however, in that the lithoclasts in the basal Mosheim are redeposited in a matrix of fenestral mudstone or fenestral intraclastic grainstone that is otherwise identical to the previously described Mosheim lithologies. Douglas Lake conglomerates, on the other hand, have a non-fenestral matrix of detrital dolomite.

Because the matrix of the Mosheim conglomerates is not significantly different from the previously described fenestral mudstones and fenestral grainstones, and because the conglomeratic limestones commonly contain very well-developed fenestral lamination, a supratidal algal marsh depositional environment is also interpreted for the basal conglomerates. The only difference is that reworked Knox detritus has been incorporated along with marine-generated mud and intraclasts in the conglomerates.

Five Oaks Formation

Distribution

The Five Oaks Formation, named for exposures in southwestern Virginia, is the lowest formation of the Chickamauga Group. The previously described Blackford Member is the basal member of the Five Oaks Formation (Prouty, 1945). In this discussion, strata referred to as Five Oaks include only the "main body" of the Five Oaks Formation, or those strata that overlie the Blackford Member. The Five Oaks is present at all outcrops in the Copper Creek and St. Paul strike belts (Figure 2.1), with the exception of Bethel Valley, where shales of the basal Lincolnshire Formation (known as the Eidson or Fleenor Member, depending upon location; Cooper, 1956) overlie the Blackford. Fenestral limestones at the base of the Middle Ordovician section in the Hawkins belt are included with the Mosheim in this report, although some other authors have included those limestones with the Five Oaks (see Ruppel, 1979 for discussion of

this stratigraphic nomenclature problem). Thickness of the Five Oaks is generally 15 to 26 meters in the study area.

Lithofacies descriptions

The Five Oaks is lithologically quite similar to the Mosheim, and both units occupy a similar stratigraphic position at the base of the Middle Ordovician section. On the basis of lithostratigraphy, the two units are equivalent, but they do differ somewhat in age, as the Mosheim (at least in outcrop belts southeast of the Saltville Fault) is entirely older than the Five Oaks, due to the time-transgressive nature of the basal Middle Ordovician strata. This discussion emphasizes the lithologic similarities and differences between the two units.

All the lithofacies recognized in the Mosheim also occur in the Five Oaks. The relative abundances of the lithologies, however, differ between the two units. Also, the Five Oaks includes some lithologies that do not occur in the Mosheim. Lithofacies in the Five Oaks include the following groups:

Non-fenestral, non-laminated limestones

1. Mudstones
2. Peloidal / intraclastic / skeletal wackestones and packstones

Fenestral limestones

3. Fenestral mudstones
4. Fenestral intraclastic / peloidal packstones
5. Wavy-laminated, fenestral peloidal packstones

Non-fenestral, laminated limestones

6. Peloidal / mud laminites and disrupted laminites
7. Peloidal / intraclastic / skeletal grainstones
8. Arenaceous, intraclastic / skeletal packstones

In general, the Five Oaks shows more lithologic variability than the Mosheim. Of the lithologies listed above, lithologies 5, 6, 7, and 8, all of which contain laminations, do not occur in the Mosheim. Unlike the Mosheim, which is dominated by fenestral lithologies, the Five Oaks is composed predominantly of non-fenestral mudstones, wackestones, and packstones. With the exception of the Thorn Hill section, where fenestral mudstones are anomalously abundant, fenestral lithologies are essentially restricted to a one- to two-meter thick zone near the top of the Five Oaks. Another difference between the two units is that laminated lithologies are fairly common in the Five Oaks, whereas laminations of any type are rare in the Mosheim. The Five Oaks lithologies listed above are described and interpreted below.

Mudstones

Lime mudstones in the Five Oaks typically are non-fenestral and non-laminated, and extensively burrowed. These rocks either possess a mottled appearance produced by selective dolomitization of burrows, or contain abundant sediment- or sparry calcite cement-filled vertical burrows. The lack of lamination is probably the result of bioturbation. Mudstones sometimes contain small amounts of skeletal debris, which typically is limited to pelecypods, gastropods, and ostracodes. Mud intraclasts and peloids are also common.

The predominance of muddy lithologies, the lack of fenestrae, and evidence of extensive burrowing suggest that the mudstones were deposited in very quiet, shallow subtidal environments that did not experience periodic subaerial exposure. The general paucity of fossils indicates that these environments were not conducive to inhabitation by marine organisms; this is probably because the water was either hypersaline or diluted with fresh water, or because circulation of normal marine water was limited. Given the

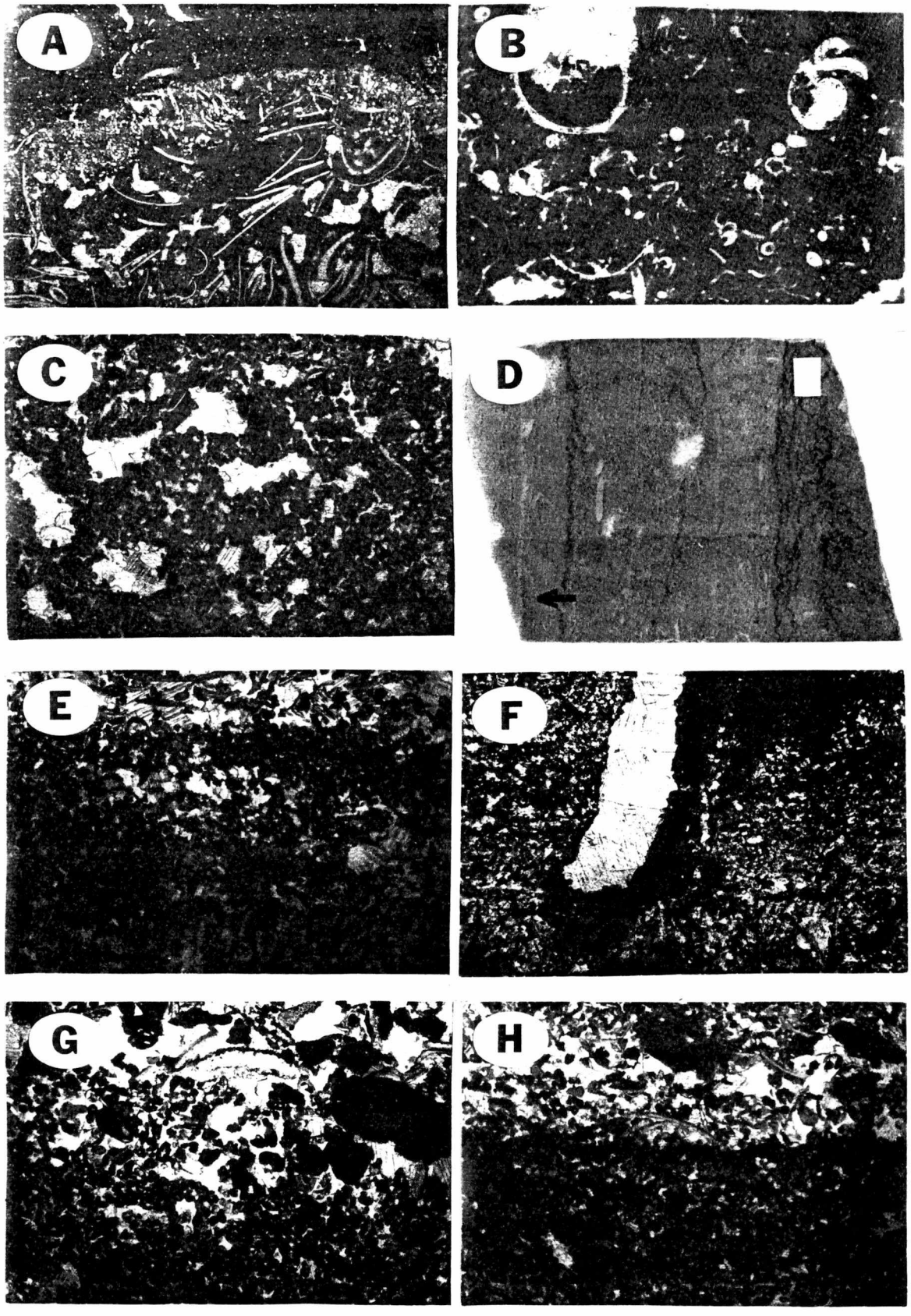
absence of evaporite minerals or molds, it is unlikely that the water was hypersaline. These characteristics, and the association of the mudstones with other tidal flat lithologies, suggest that the mudstones were deposited in brackish, shallow subtidal pond subenvironments.

Peloidal/intraclastic/skeletal wackestones and packstones

These lithologies, grouped together because of a great amount of overlap in constituent grain types, are the dominant rock type in the Five Oaks Formation. They are mud-dominated lithologies similar to the previously described mudstones, except that they contain significantly higher amounts (10 to 60% by volume) of peloids, intraclasts, and / or body fossils (Figure 3.8A, B). Like the mudstones, these rocks lack lamination, and typically show evidence of extensive bioturbation. Fossil assemblages are dominated by, and generally restricted to, pelecypods, gastropods, and ostracodes, but in some samples minor amounts of more stenotopic organisms such as red and green algae, sponges, bryozoans, trilobites, and echinoderms are present.

These rocks exhibit no evidence of subaerial exposure, and therefore are interpreted to be subtidal deposits. The dominance of mud-supported lithologies and the lack of current indicators indicates deposition in very quiet water, and the generally restricted, although in some cases abundant, biota indicates restricted communication with open marine water. Like the non-fenestral mudstones, these peloidal / intraclastic / skeletal limestones are interpreted to have been deposited in shallow, tidal flat ponds, like those described in Hardie and Garrett (1977). It is also very likely that some of these limestones, particularly those with more open marine faunas, represent deposition in tidal channels.

Figure 3.8. Lithologies of the Five Oaks Formation. A-C and E-H are thin section photomicrographs, taken under plane-polarized light. The long axis field of view in all photomicrographs is 6.5 mm. D is a photograph of a polished slab. **A.** Skeletal intraclastic wackestone, collected from the base of the Five Oaks, 10 m above the Knox unconformity (AKU), Idol Mine. Sample consists mostly of non-fenestral, non-laminated lime mud, but contains abundant intraclasts and broken pelecypod fragments and whole ostracodes. Also contains a 1 mm-thick bleached crust that extends across the thin section, that contains within it winding, calcified algal filaments. This lithology represents deposition on the boundary between the inland algal marsh and a subtidal pond. **B.** Biomoldic porosity (primarily leached gastropods) in skeletal wackestone from the subtidal pond subfacies, 12.7 m AKU, Thorn Hill. **C.** Irregular fenestrae in fenestral peloidal packstone lithology, 10.6 m AKU, Idol Mine. **D.** Fenestral peloidal/intraclastic packstone with well-developed wavy fenestral lamination, produced by coalescence of laminoid fenestrae, 25.9 m AKU, Idol Mine. Scale bar equals 1 cm. Note the sharp, but non-erosional surface near the base of the slab that separates the overlying wavy-laminated, fenestral peloidal packstone lithology from the underlying non-laminated, fenestral peloidal packstone. The large cement-filled void near the center of the sample is a solution-enlarged gastropod mold. **E.** Smooth flat lamination in peloidal packstone, 25.5 m AKU, Idol Mine. Sediment consists of peloids and small mud intraclasts, with minor amounts of highly broken and abraded skeletal debris, and little mud. The distinct lamination is produced by alternations between muddy peloid laminae and mud-free peloidal laminae. The mud-free laminae contain a higher percentage of skeletal debris and much more cement, which fills prior intergranular porosity. **F.** Cement-filled burrow that disrupts flat lamination in peloidal packstone, 22 m AKU, Thorn Hill. Lamination is vague, but very similar to the lamination in E, except that it has been disrupted by vertical burrows. Note that the burrow is floored with small fecal pellets. **G.** Smooth flat lamination in uppermost Five Oaks, 26 m AKU, Idol Mine. Very similar to the lamination illustrated above, but in this case the lamination is produced by alternation between skeletal intraclastic grainstone laminae and peloidal packstone laminae. The contact between the grainstone and packstone laminae is diffuse and gradational. **H.** Lamination as in G (from same thin section, different field of view), but in this case, the contact separating the skeletal intraclastic grainstone and peloidal packstone laminae is very sharp. The lower lithology was possibly cemented to some degree prior to deposition of the overlying lamina, but the surface between the laminae is non-erosional.


A
B
C
D
E
F
G
H

Fenestral mudstones and fenestral intraclastic / peloidal packstones

The scarcity of non-laminated, fenestral lithologies in the Five Oaks, relative to the Mosheim, has already been mentioned, and the significance of this difference will be discussed below. Where fenestral mudstones, diagenetic grainstones, and fenestral intraclastic / peloidal packstones do occur in the Five Oaks (Figure 3.8C), they are essentially identical to those in the Mosheim, and represent the same intertidal and supratidal algal marsh subenvironments.

Wavy-laminated, fenestral peloidal packstones

A 0.5 to 4.0 m-thick interval of fenestral peloidal packstones with a characteristic wavy lamination (Figure 3.8D) exists near the top of the Five Oaks Formation at the Thorn Hill, Idol, and Cedar Springs locations. Similar laminated fenestral packstones occur associated with other fenestral lithologies at various levels within the Five Oaks at Thorn Hill. These rocks are very similar to the previously described fenestral intraclastic / peloidal packstones in the Mosheim and Five Oaks, except these have an abundance of laterally-coalesced laminoid fenestrae that commonly arch over lumps of peloidal sediment, and impart a distinctive wavy fenestral lamination to the rock. This wavy lamination is essentially identical to that described and illustrated by Hardie and Ginsburg (1977) that forms on the supratidal beach terrace and the high algal marsh / beach ridge washover backslope boundary on the Andros Island tidal flat (Figure 3.5). The stratigraphic position of these wavy-laminated rocks very near the top of the Five Oaks suggests that they were deposited on a beach ridge that lay near the seaward margin of the tidal flat.

Peloidal / mud laminites and disrupted laminites

These non-fenestral rocks possess a characteristic millimeter-scale lamination produced by alternation of layers of mud-supported and mud-poor peloidal sediment (Figure 3.8E). Fossils are rare, and limited to fine ostracode and pelecypod debris that probably was transported along with peloids to the depositional site.

The lamination in these rocks, which occur only near the top of the Five Oaks, is identical to the smooth flat lamination characteristic of the highest supratidal subenvironments on Andros Island, the levee crests and beach ridge washover crests (Table 3.1 and Figure 3.6) (Hardie and Ginsburg, 1977). The lack of typical exposure features such as fenestrae and mudcracks in these driest subenvironments on Andros is the result of binding by thin, tough mats of the cyanobacterium *Schizothrix.* These laminites are formed solely by storm deposition, with each lamina recording a single storm (Hardie and Ginsburg, 1977). Because of their similarity to the Andros Island laminites, the laminites in the Five Oaks are interpreted as storm deposits on the supratidal beach ridge washover crest.

These laminites are associated with similar laminated rocks in the uppermost Five Oaks in which the primary storm laminations are disrupted by abundant vertical cement- and peloid-filled burrows and mudcracks (Figure 3.8F). These mudcracked flat laminites occur immediately beneath the undisrupted laminites, and are comparable to the "disrupted flat laminites" that are deposited on the supratidal beach ridge backslope on Andros Island (Table 3.1 and Figure 3.6) (Hardie and Ginsburg, 1977). Other disrupted laminites occur at various levels within the Five Oaks at Thorn Hill, and probably represent supratidal deposition on channel levee backslopes.

Peloidal / intraclastic / skeletal grainstones

The top of the Five Oaks Formation at all outcrops in the Copper Creek belt is marked by a thin (0.5 to 2.0 meter) interval of laminated, non-fenestral grainstone (Figure 3.8G, H). This lithology immediately overlies the wavy-laminated peloidal packstones and laminites previously described. The base of the grainstones is very sharp and slightly wavy, but is not erosional (Figure 3.8H). It is uncertain whether this lithology should be assigned to the uppermost Five Oaks or basal Lincolnshire, and is probably transitional between the two lithofacies. A similar layer of grainstone also occurs about 6.5 meters beneath the top of the unit in the Idol section.

These grainstones are composed primarily of small, discrete, dark peloids and lighter, diffuse peloids, but also contain minor amounts (generally 10 - 15 volume %) of highly abraded echinoderm, pelecypod, and ostracode debris and larger, ovoid mud intraclasts (Figure 3.8G, H). Laminations in the grainstones are generally flat or sometimes cross-bedded at very low angles, and are produced by millimeter-scale variations in peloid density. Laminations were preserved in these lithologies due to early cementation and the absence of burrowing animals. Laminoid fenestrae are not associated with these laminations. Fenestrae like those in other Five Oaks and Mosheim lithologies are absent from these rocks, but large (4 - 8 mm) voids filled with equant calcite cement do occur. The origin of these voids is uncertain, but they might be molds formed by leaching of aragonitic fossils, or the fenestra-like vugs sometimes found in shallow subtidal grainstones (Shinn, 1983).

Because of the lack of depositional mud, the moderate degree of sorting, and the rounding and abrasion of depositional grains, the intraclastic peloidal grainstones are interpreted to represent deposition in a fairly high-energy setting. The lack of evidence of exposure or desiccation indicates deposition in an environment generally covered by

seawater. The stratigraphic position of the grainstones above lithologies typical of tidal flat deposition and beneath open marine limestones of the Lincolnshire Formation indicates that this environment lay in a position intermediate between the tidal flat and the adjacent deeper subtidal marine environment. On the basis of this evidence, the intraclastic peloidal grainstones are interpreted as having been deposited on a moderately high-energy, shallow subtidal to intertidal beach immediately seaward of the tidal flat. The flat lamination of the sediment is consistent with this interpretation.

Arenaceous, intraclastic / skeletal packstones

A few isolated zones near the base of the Five Oaks and in the underlying Blackford Member contain cross-bedded, non-fenestral packstones composed of varying amounts of mud and dolomitic mud intraclasts, abraded skeletal fragments, and angular quartz sand. Those in the Blackford also contain abundant lithoclasts of detrital dolostone and chert derived from the Knox Group. These beds are up to one meter thick, and have sharp bases scoured into underlying lithologies. These cross-bedded packstones are described in the section on Blackford lithologies, and are interpreted to represent deposition on the floors of tidal channels which allowed bidirectional, tide-driven transportation of terrigenous and marine sediment during early development of the tidal flat.

Environmental Summary of the Tidal Flat Lithofacies

The suites of lithofacies in the Mosheim Member and the Five Oaks Formation are strikingly similar to those forming on the modern humid tidal flat on Andros Island, Bahamas. Through the process of comparative sedimentology (Hardie, 1986), each

lithofacies can be interpreted to represent a specific depositional subenvironment of an Andros Island-type tidal flat.

Lithofacies observed in the Mosheim / Five Oaks tidal flat sequence, and the depositional subenvironments they represent, include:

1) Basal conglomeratic fenestral limestones =
   supratidal inland algal marsh deposits

2) Fenestral mudstones and fenestral intraclastic / peloidal packstones and grainstones with fenestral lamination =
   supratidal inland and high algal marsh deposits
3) Fenestral mudstones and fenestral intraclastic / peloidal packstones and grainstones lacking fenestral lamination =
   supratidal high algal marsh and intertidal low algal marsh deposits

4) Non-fenestral, arenaceous, intraclast / skeletal packstones =
   subtidal channel deposits

5) Non-fenestral mudstones and peloidal / skeletal wackestones =
   subtidal pond and channel deposits

6) Peloidal / mud laminites and disrupted laminites =
   supratidal beach ridge washover crest, and beach ridge washover backslope deposits, respectively

7) Wavy-laminated fenestral peloidal packstones =
   supratidal beach ridge washover backslope or beach terrace deposits

8) Non-fenestral, peloidal / skeletal grainstones =
   intertidal beach deposits

Of these lithofacies, only 1, 2, 3, and 5 occur in the Mosheim. Thus, lithofacies in the Mosheim indicate that deposition occurred primarily in supratidal and intertidal algal marshes and subtidal ponds and channels. All of the above lithofacies, except 1, have been recognized in the Five Oaks, and indicate deposition occurred in subtidal ponds and channels, intertidal and supratidal algal marshes, and supratidal levee and beach ridge

subenvironments such as the washover crest, backslope, and terrace. Deposits at the top of the Five Oaks indicate deposition in a moderately high energy, intertidal beach setting.

The internal stratigraphic stacking of lithofacies in the Mosheim and Five Oaks, and the depositional history indicated by that stratigraphic succession, will be discussed below.

Adjacent Offshore Marine Lithofacies

The following offshore facies, though not truly part of the peritidal sequence, and not the focus of this study, are described briefly to emphasize their differences from the previously described terrestrial and tidal flat facies.

Lenoir Formation

Distribution

The main body of the Lenoir Formation sharply overlies the Mosheim Member at most outcrops southeast of the Saltville Fault, and it also occurs northwest of the Saltville in the Hawkins belt (Figure 2.1). At Dandridge, where the Mosheim is absent, the Lenoir overlies the Douglas Lake Member. Thickness of the Lenoir facies varies tremendously across strike, from a minimum of a few meters in the Bays Mountain Synclinorium and the Hawkins belt, to over 200 meters in the Friendsville belt.

Lithofacies description and environmental interpretation

The Lenoir is characterized by a dark, brownish-gray, nodular, argillaceous, skeletal wackestone / packstone lithofacies. Thin beds of grainstone also occur

irregularly in the unit, particularly near the base. The lower portion of the Lenoir contains a very diverse and abundant fauna dominated by brachiopods, bryozoans, trilobites, and gastropods. Sponges are also locally very abundant. Calcareous algae and *Girvanella* oncoids are abundant in the lower and upper parts of the unit. Other skeletonized green algae (e.g., *Contexta* and *Kazakhstanellia*) are abundant throughout much of the formation but absent in the middle of the unit. In general, biotic abundance decreases, and lime mud and terrigenous clay percentages increase, upward from the base to the middle of the unit, as packstones are replaced by shaly wackestones.

The character of the upper half of the Lenoir varies across strike. In the Tellico-Sevier Belt (Figure 2.1), algal and faunal abundance decrease upward in the unit, indicating that water depths increased gradually, but significantly, as the Lenoir grades upward into the overlying Whitesburg Formation. The abundance of lime mud and clay, and the general lack of bedforms indicate that current energy was low to moderate, and probably decreased as water depths increased. In the Friendsville belt, where the Lenoir grades upward into the Holston Formation, the uppermost part of the Lenoir contains a diverse biota including calcareous algae similar to the lower portion, indicating that water depths decrease upward. Overall, the abundance and diversity of the Lenoir's fauna indicate deposition in normal marine water and unrestricted circulation with the open ocean, whereas the abundance of algae in the lower half of the unit suggests that water depths were relatively shallow. The lower portion of the Lenoir is interpreted to represent deposition in a shallow subtidal, open marine shelf environment (Ruppel, 1979), that lay immediately seaward of the Mosheim tidal flat. However, the upper half of the Lenoir in the Friendsville Belt was deposited on the platform side (currently, to the northwest) of a developing platform margin, with the barrier facies represented by skeletal sands and reefs of the Holston Formation (Walker et al., 1980).

Lincolnshire Formation

The Lincolnshire Formation overlies the basal Middle Ordovician peritidal facies (usually the Five Oaks Formation) at all localities northwest of the Saltville Fault, except in the Hawkins belt. Thickness of the Lincolnshire is rather consistent, averaging about 100 meters throughout the study area (Ruppel and Walker, 1984).

Lithofacies descriptions and environmental interpretations

The Lincolnshire is comprised primarily of two lithofacies. At its type locality in southwestern Virginia (Cooper and Prouty, 1943), the Lincolnshire is a dark, argillaceous, nodular wackestone / packstone facies identical to shallow-water portions in the lower part of the Lenoir, as described above. Southwestward into East Tennessee, the Lincolnshire becomes coarser grained, less muddy, and more fossiliferous. In the study area, the Lincolnshire is dominated by a light gray or pinkish gray, medium- to coarse- grained, skeletal packstone / grainstone facies, although the nodular, Lenoir-like facies is also quite common (Ruppel and Walker, 1984). The skeletal packstone / grainstone facies is often cross-bedded. In exposures west of the Copper Creek Fault, the unit becomes very shaly, and has been subdivided into the Eidson and Hogskin Members (Cooper, 1956). To avoid confusion, that terminology is not employed in this dissertation.

Abraded echinoderm and bryozoan fragments are the dominant skeletal component in the Lincolnshire, but brachiopods, ostracodes, and trilobite fragments are also common. The facies also contains a noteworthy algal flora. Calcareous algae (*Solenopora, Hedstroemia*, and *Nuia*), are remarkably abundant, as are *Girvanella* oncoids (Moore, 1977). Skeletal grains often have algal coatings. Also, a prominent

stromatolitic zone marks the basal contact of the Lincolnshire at some outcrops (Ruppel and Walker, 1984).

As in the Lenoir Formation, the diverse and abundant biota of the Lincolnshire indicates deposition in well-circulated, normal marine water. The abundance of algae throughout the formation suggests that water depths remained relatively shallow throughout deposition of the unit. The stromatolites at the base of the unit point to low intertidal conditions at the beginning of Lincolnshire deposition, but the remainder is entirely subtidal. The Lincolnshire also contrasts with the Lenoir in its abundance of cross-bedding and the general paucity of mud, which indicate moderate to high current energy. Periods of current restriction are indicated by the intercalations of argillaceous wackestone. In summary, the Lincolnshire was deposited on a shallow subtidal, moderate to high energy, marine shelf open to circulation of ocean water (Ruppel and Walker, 1984).

Environmental Summary of the Adjacent Offshore Marine Lithofacies

The Lenoir and Lincolnshire Formations represent deposition in shallow subtidal, open marine shelf environments. These facies are analogous to the shallow shelf deposits of the Bahama Bank that lie immediately offshore from the Andros Island tidal flat. Deposition of this subtidal facies marks the end of tidal flat deposition at any given area as the Middle Ordovician transgression proceeded.

Nature of Tidal Flat Deposition

In the previous section, the detailed observations and descriptions of the sedimentary features of the basal Middle Ordovician peritidal carbonate rocks were used to differentiate between the different depositional subfacies, and to determine specific depositional environments for each subfacies recognized. In this section, attention is focussed on the tidal flat facies represented by the Mosheim Member and the Five Oaks Formation, in an attempt to determine exactly what type of tidal flat is represented by these units. From this point on, the Mosheim and Five Oaks limestones are considered as a single lithostratigraphic entity, as it was prior to late Paleozoic compressional deformation--a thin tidal flat facies that onlapped the North American continental platform edge in time-transgressive fashion as the basalmost part of the Middle Ordovician transgressive sequence. Salient features of this Middle Ordovician tidal flat are summarized, and interpretations are made about conditions that existed during deposition, such as paleoclimate and pore fluid chemistry. The summary of sedimentological features is followed by an analysis of the vertical arrangement of subfacies within the Mosheim / Five Oaks tidal flat facies, which facilitates recognition of parameters of tidal flat development such as the direction of relative sea level movement during deposition, and the direction and method of tidal flat accretion.

Summary of Sedimentological Features and Environmental Interpretations

To summarize the information presented in the preceding section, the Mosheim / Five Oaks tidal flat facies possesses the following sedimentological characteristics: it is dominated by mud-supported lithologies; it contains an abundance of well-developed fenestral fabrics; faunal abundance and diversity are restricted; preserved laminations are

relatively scarce; there is abundant evidence of very early freshwater alteration; and there is a lack of evidence for arid conditions during deposition. It should be noted that several features commonly associated with ancient and modern carbonate tidal flat lithologies are absent or very rare in the Mosheim / Five Oaks facies, and the absence or scarcity of these features is significant in determining the depositional setting for the Mosheim / Five Oaks tidal flat. Such features that occur only rarely in this sequence include mudcracks, prism cracks, sheet cracks, algal tufas, and incipient caliche crusts. Features that have not been observed in the Mosheim / Five Oaks facies include sabkha-type dolomite crusts, tepee structures, evaporite minerals, molds, and pseudomorphs, stromatolites and thrombolites, and root casts and molds. Root casts or any other evidence of land plants would not be expected in this sequence given that the age of the Mosheim/Five Oaks facies pre-dates land plants (Gensel and Andrews, 1987).

These characteristics of the Mosheim / Five Oaks tidal flat, and their implications with regard to interpretations of depositional environment, paleoclimate, relative sea level movement, and other ambient conditions, are discussed, point by point, below.

1. Dominance of mud-supported lithologies. The vast majority of lithologies within the tidal flat facies are mud-supported, and many consist entirely of lithified and cemented carbonate mud. The most abundant depositional grains comprising these lithologies--peloids and small intraclasts--are also composed of loosely bound carbonate mud. Grains indicative of moderate to high current energy, such as broken, abraded skeletal fragments or ooids, are uncommon and, like the peloids and carbonate mud, were transported to the tidal flat from higher-energy offshore environments. Grain-supported lithologies are rare, and are generally restricted to uppermost layers of the facies that have been interpreted as beach deposits. The ubiquitous presence of carbonate mud is typical of modern and ancient tidal flats, and indicates that deposition of the facies occurred in a low-energy

environment physically sheltered from the influence of tides and wave action. The overall vertical succession of lithologies in this tidal flat facies (discussed below) provides supporting evidence that this tidal restriction resulted from the presence of a low beach ridge that was positioned at the seaward edge of the tidal flat. The wide variety of mud-dominated lithologies within the facies indicates that deposition occurred in a mosaic of quiet, tidal flat subenvironments behind this barrier beach.

2. *Well-developed fenestral fabric.* Lithologies with well-developed fenestral fabric are very abundant in the Mosheim / Five Oaks tidal flat facies, especially in the Mosheim Member, where fenestral mudstones are the most characteristic lithology of the unit. Laminoid and irregular fenestral fabrics are both abundant, and are taken to indicate deposition in intertidal and supratidal subenvironments conducive to the growth of lush algal mats, analogous to the various algal marsh subenvironments of the modern Andros Island tidal flat (Hardie and Ginsburg, 1977). Fenestral lithologies predominate within the basalmost layers of the tidal flat facies, but also occur in abundance throughout the bulk of the facies, where fenestral lithologies interfinger laterally and vertically with non-laminated, non-fenestral subtidal lithologies. This random interfingering of shallow subtidal, intertidal, and supratidal lithologies throughout the main portion of the Mosheim / Five Oaks sequence indicates that a complex mosaic of ponds, channels, and levees, analogous to the Andros Island channeled belt, existed within the overall tidal flat facies, and apparently occupied the largest portion of the tidal flat.

3. *Faunal restriction.* The Mosheim / Five Oaks tidal flat facies, like most ancient tidal flat facies, is characterized by severely restricted faunal abundance and diversity. Many lithologies are entirely devoid of fossils, and those portions of the facies that do contain fossils typically contain only a few types of organisms that today are commonly tolerant

of abnormal or fluctuating water chemistry, such as ostracodes, gastropods, or pelecypods. In general, lithologies lacking fossils are characterized by sedimentologic features that indicate deposition in inter- or supratidal subenvironments, and those lithologies that contain some fossils typically lack exposure indicators and have been interpreted as subtidal pond or channel subfacies. By analogy with modern tidal flats, the organisms that inhabited the subtidal ponds and channels were probably infaunal, burrowing animals that completely bioturbated the sediment and obliterated all original depositional structures. The faunal restriction in the Mosheim / Five Oaks tidal flat facies is believed to be related not to hypersalinity, but to hyposalinity or brackish water chemistry resulting from the frequent mixing of sea water with fresh (meteoric) water. A more thorough discussion of paleoclimatic conditions during deposition of the Mosheim/Five Oaks sequence is presented later.

4. Scarcity of preserved laminations. Although most of the lamination and bedding types that are characteristic of intertidal and supratidal deposition on Andros have been recognized in the Mosheim / Five Oaks facies, none are particularly abundant. Of the four lamination types listed in Table 3-1, only one--crinkled fenestral lamination that is representative of supratidal and highest intertidal algal marsh subenvironments on Andros Island--has been observed in the Mosheim. All types of lamination described from Andros have been recognized in the Five Oaks, but laminated beds of all types combined make up less than 20% of the thickness of the Formation at any outcrop. The most abundant type of lamination in the facies is produced by horizontal orientation of laminoid fenestrae between layers of mud, and was preserved through early cementation in the fenestral voids. The scarcity of laminations in this ancient tidal flat facies is not surprising, for two reasons: 1) the vast majority of sediment on the Andros tidal flat is nonlaminated, bioturbated pond and channel sediment, and 2) many of the supratidal

sediments that are laminated when deposited at the surface of the Andros tidal flat will not be preserved in the geologic record as laminites because "almost all the uncemented sediment that gets buried below the water table in the channeled belt is soon homogenized by infaunal burrowers and its environmental record wiped out" (Hardie, 1977). Indeed, the limited occurrence of laminations in the Mosheim / Five Oaks sequence is what would be expected in an ancient Andros Island-type tidal flat, where early cementation is required for the preservation of original laminations, and where preservation is the exception, rather than the rule.

5. Evidence for early freshwater alteration. The diagenetic alteration of the Mosheim / Five Oaks tidal flat carbonate sediments is the topic of Chapter 4 of this dissertation, but will be briefly summarized here. The alteration of this carbonate sediment began very early, essentially during or immediately following deposition, and with relatively minor exceptions, was largely concluded prior to deposition of the overlying offshore facies. Thus, diagenetic alteration occurred, for the most part, in the depositional environment, and detailed study of the diagenetic features of the facies has provided invaluable information about the physical and hydrochemical conditions of the depositional environment. In general, the products of diagenetic alteration of the Mosheim / Five Oaks tidal flat facies carry the petrographic and geochemical signature of freshwater (meteoric) diagenesis. The dominant diagenetic features include alteration of the carbonate mud to micrite, precipitation of clear, equant calcite cements in virtually all pore spaces, and fairly abundant dissolution (microkarst) fabrics. Dolomitization is not pervasive and is common only in the basal meter of the facies; cements other than equant, low-magnesian calcite are rare (far less than one percent of the total cement volume); and evaporite mineralization is absent. Precipitation of calcite cements occurred predominantly in the meteoric phreatic zone, as indicated by cement morphologies, but

there is abundant evidence, in supra- and intertidal fenestral lithologies, of cementation and alteration in the vadose zone (vadose silt, pendant and meniscus cements, and vadose pisoids). Erosional truncation of fenestral cements at exposure surfaces within and at the top of the tidal flat facies indicates the very early timing of cement precipitation. All of these characteristics indicate that the dominant fluid passing through the facies, once the sediment had been transported from the offshore marine environment and deposited in the tidal flat regime, was freshwater. The supply of freshwater to this tidal flat was apparently abundant and continuous, and the lack of evidence of intense evaporation and desiccation of the sediment (discussed below) strongly suggests that the Mosheim / Five Oaks tidal flat was deposited under humid conditions.

6. Lack of evidence of arid conditions. Features considered to be indicative of arid conditions in many ancient tidal flat sequences are rare or missing from the Mosheim / Five Oaks tidal flat facies. Mudcracks have been observed in a few supratidal crusts, but these are uncommon and are generally only a few millimeters deep and less than a millimeter wide. Prism cracks and sheet cracks have been observed in disrupted supratidal crusts only in the basal meter of the Mosheim. There is no evidence that evaporite minerals, which would precipitate from marine pore fluids concentrated by intense evaporation, were ever precipitated in this tidal flat. Tepee structures, which are commonly found in arid, Persian Gulf-type tidal flats in association with evaporite minerals, have not been observed. Also, sabkha-type primary dolomite crusts and well-developed caliche crusts have not been observed in the facies. Some exposure surfaces within and especially at the top of the tidal flat facies contain caliche-type pisoids and have a chalky or micritic microtexture, but other features indicative of caliche development are lacking, and such crusts would have to be considered incipient caliche or incipient soil horizons, at best. In summary, there is no evidence of intense evaporation,

hypersalinity, or other factors that might indicate that arid conditions existed during deposition or early, post-depositional alteration of the sediment. On the contrary, there is abundant evidence that the tidal flat sediments were regularly flushed with fresh water, either in the form of groundwater or rain.

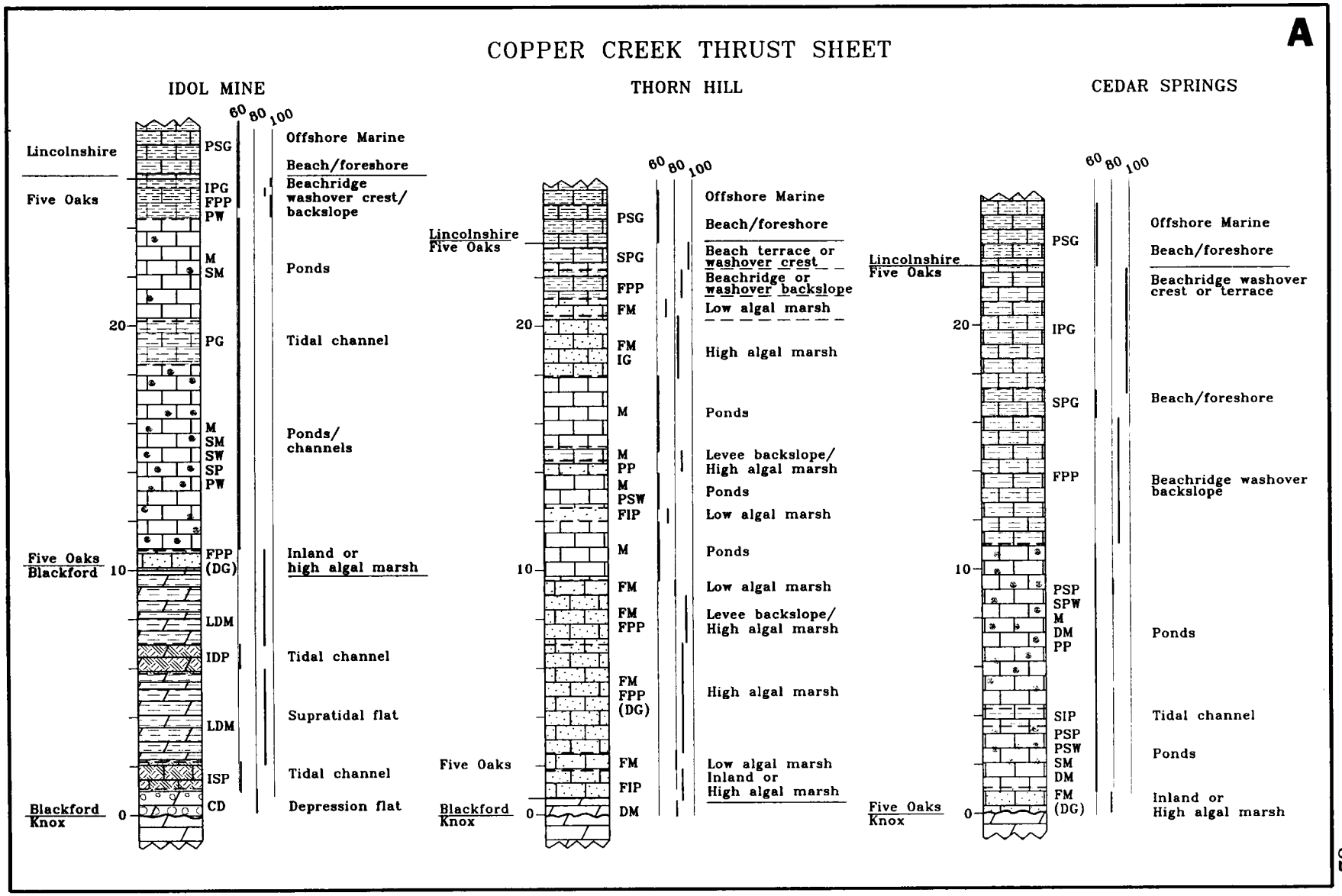
This summary of the salient characteristics of the Mosheim / Five Oaks tidal flat sequence demonstrates that this Middle Ordovician tidal flat possesses few of the characteristics of an arid, Persian Gulf-type tidal flat. The depositional and early diagenetic features summarized above clearly indicate that the sediments comprising the Mosheim / Five Oaks sequence were deposited under humid, rainy conditions on a tidal flat where the water that flooded subtidal portions of the flat and occupied the pores of the sediments were not hypersaline but a brackish mixture of seawater diluted by regular incursions of fresh water. Although Hardie (1986) stressed that "care must be taken not to try to force an ancient deposit to fit one of our few modern models", the Mosheim / Five Oaks tidal flat is closely analogous, in most ways, to the modern tidal flat on Andros Island. The detailed observations of the varied lithologies that comprise the Mosheim / Five Oaks tidal flat presented above show that the similarities between this Ordovician tidal flat and the Holocene Andros Island tidal flat are striking.

Vertical Arrangement of Subfacies Within the Tidal Flat Facies

The vertical succession of subfacies within the Mosheim / Five Oaks facies is shown for each outcrop location in Figure 3.9. This vertical succession, like the stratigraphic arrangement of the entire basal Middle Ordovician sequence in the study area (of which the tidal flat facies is but a very thin part), reflects a transgression of submarine environments over the previously exposed Knox surface. This transgression

Figure 3.9. Stratigraphic sections of basal Middle Ordovician strata at outcrops in the study area. Each section shows the vertical arrangement of lithologies at a given outcrop, along with interpretations of depositional subenvironment and exposure index. The vertical scale on all sections is in meters above the Knox unconformity. Lithologies are indicated by abbreviations, according to the following code. For the last letter of each abbreviation, M = mudstone, W = wackestone, P = packstone, and G = grainstone. D = dolostone. For letters that precede and modify the last letter, A = argillaceous, C = conglomeratic, D = dolomitic, F = fenestral, I = intraclastic, L = laminated, P = peloidal, and S = skeletal. The designation (DG) indicates "diagenetic grainstone". The exposure index is the percentage of time the depositional subenvironment for each lithology was subaerially exposed, following Hardie and Garrett (1977) and Ginsburg, et al. (1977). Vertical bars drawn along the 60% bar indicate the interpreted depositional subenvironment was exposed 60% of the time or less, and indicate shallow subtidal deposition. Vertical bars drawn in the zone between 60 and 85% indicate intertidal deposition. Vertical bars drawn between about 85 and 100% indicate supratidal deposition.

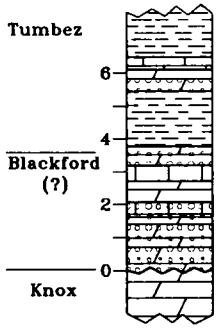
Figure 3.9A consists of three stratigraphic sections from the Copper Creek thrust sheet: the Thorn Hill, Idol Mine, and Cedar Springs sections. Figure 3.9B consists of two stratigraphic sections from the St. Paul strike belt (Raccoon Valley and Bethel Valley) and one section from the Hawkins strike belt (Red House Branch). Figure 3.9C consists of five stratigraphic sections from the Tellico-Sevier strike belt: the Boyd's Creek Road, Deep Springs, Dandridge, Nina, and Fish Hatchery Road sections.


A
COPPER CREEK THRUST SHEET
IDOL MINE
THORN HILL
CEDAR SPRINGS
60 80 100
Lincolnshire
Five Oaks
Five Oaks
Blackford
Blackford
Knox
20
10
0
PSG
IPG
FPP
PW
M
SM
PG
M
SM
SW
SP
PW
FPP
(DG)
LDM
IDP
LDM
ISP
CD
Offshore Marine
Beach/foreshore
Beachridge
washover crest/
backslope
Ponds
Tidal channel
Ponds/
channels
Inland or
high algal marsh
Tidal channel
Supratidal flat
Tidal channel
Depression flat
Lincolnshire
Five Oaks
Five Oaks
Blackford
Knox
PSG
SPG
FPP
FM
FM
IG
M
M
PP
M
PSW
FIP
M
FM
FM
FPP
FM
FPP
(DG)
FM
FIP
DM
Offshore Marine
Beach/foreshore
Beach terrace or
washover crest
Beachridge or
washover backslope
Low algal marsh
High algal marsh
Ponds
Levee backslope/
High algal marsh
Ponds
Low algal marsh
Ponds
Low algal marsh
Levee backslope/
High algal marsh
High algal marsh
Low algal marsh
Inland or
High algal marsh
Lincolnshire
Five Oaks
Five Oaks
Knox
PSG
IPG
SPG
FPP
PSP
SPW
M
DM
PP
SIP
PSP
PSW
SM
DM
FM
(DG)
Offshore Marine
Beach/foreshore
Beachridge washover
crest or terrace
Beach/foreshore
Beachridge washover
backslope
Ponds
Tidal channel
Ponds
Inland or
High algal marsh

B

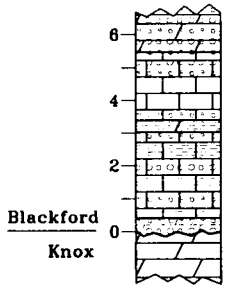
ST. PAUL THRUST SHEET

BETHEL VALLEY



Red Shale
Burgundy/gray peloidal skeletal packstone
Gray, sucrosic dolostone w/chert nodules
Red/brown shale
Gray, sucrosic dolostone
Burgundy/beige conglomeratic skeletal packstone
Gray, sucrosic dolostone
Burgundy, conglomerate, argillaceous limestone
Beige conglomeratic dolostone
Dolostone

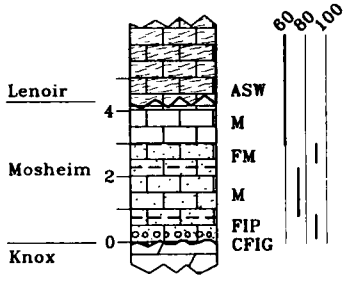
RACCOON VALLEY



Conglomeratic dolomudstone
Conglomeratic lime mudstone
Fenestral mudstone
Conglomeratic lime mudstone
Laminated dolomudstone
Conglomeratic skeletal
peloidal packstone
(laminated where not conglomeratic)
Conglomeratic dolomudstone
Dolostone

HAWKINS THRUST SHEET

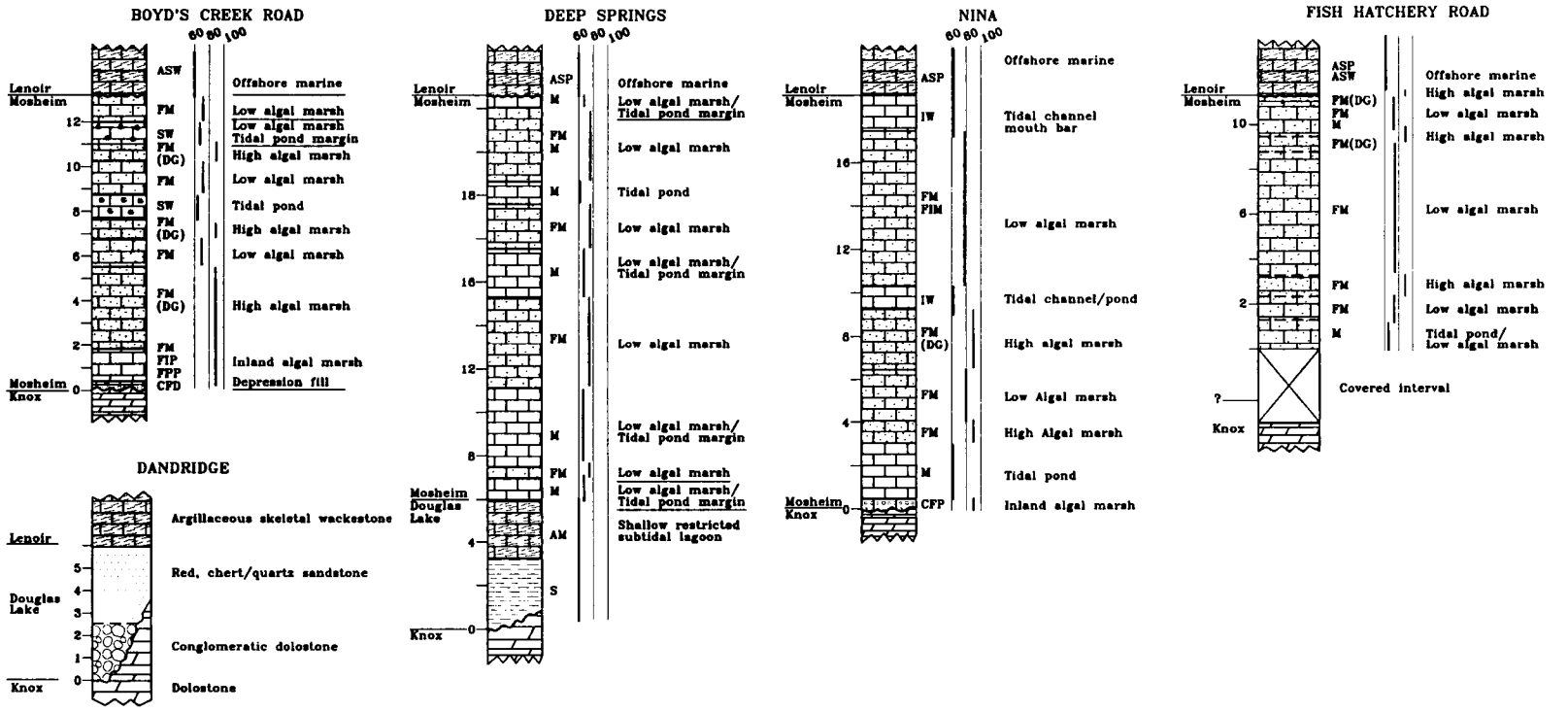
RED HOUSE BRANCH



Offshore Marine
Pond
High algal marsh
Low algal marsh
Inland or high
algal marsh

C

TELLICO – SEVIER THRUST SHEET



created the vertical sequence of subfacies recorded within the tidal flat facies, wherein each subfacies is deposited directly above the subfacies that lay immediately landward of it at any point in time (Figure 3-10). The vertical sequence of subfacies within the Mosheim / Five Oaks tidal flat, from top to bottom, and the lithologies that represent each subfacies, are as follows:

Tidal Flat Subfacies	*Representative lithologies*
Beach Ridge Subfacies	Upper laminated packstones/grainstones
Channeled Belt Subfacies (ponds, channels, and levees)	Bulk of Mosheim/Five Oaks (complex interfingering of subtidal, intertidal, and supratidal lithologies)
Inland Algal Marsh Subfacies	Basal supratidal fenestral lithologies

Each of these major tidal flat subfacies is characterized by distinctive sedimentological features that allow differentiation of one subfacies from another, and facilitate correlation of each subfacies from one outcrop to another. Each of the three subfacies is clearly analogous to the three major subenvironments of the Andros Island tidal flat (inland algal marsh, channeled belt, and beach ridge) shown in Figures 3.3, 3.4, and 3.5. The major features of each subfacies are discussed below.

Inland Algal Marsh Subfacies

The basal meter or so of the tidal flat facies is, in most places, marked by lithologies that contain overwhelming evidence of subaerial exposure and intense vadose alteration by meteoric pore fluids. Lithologies in this basal subfacies typically contain (1) the highest density of fenestrae and the greatest amounts of original fenestral porosity

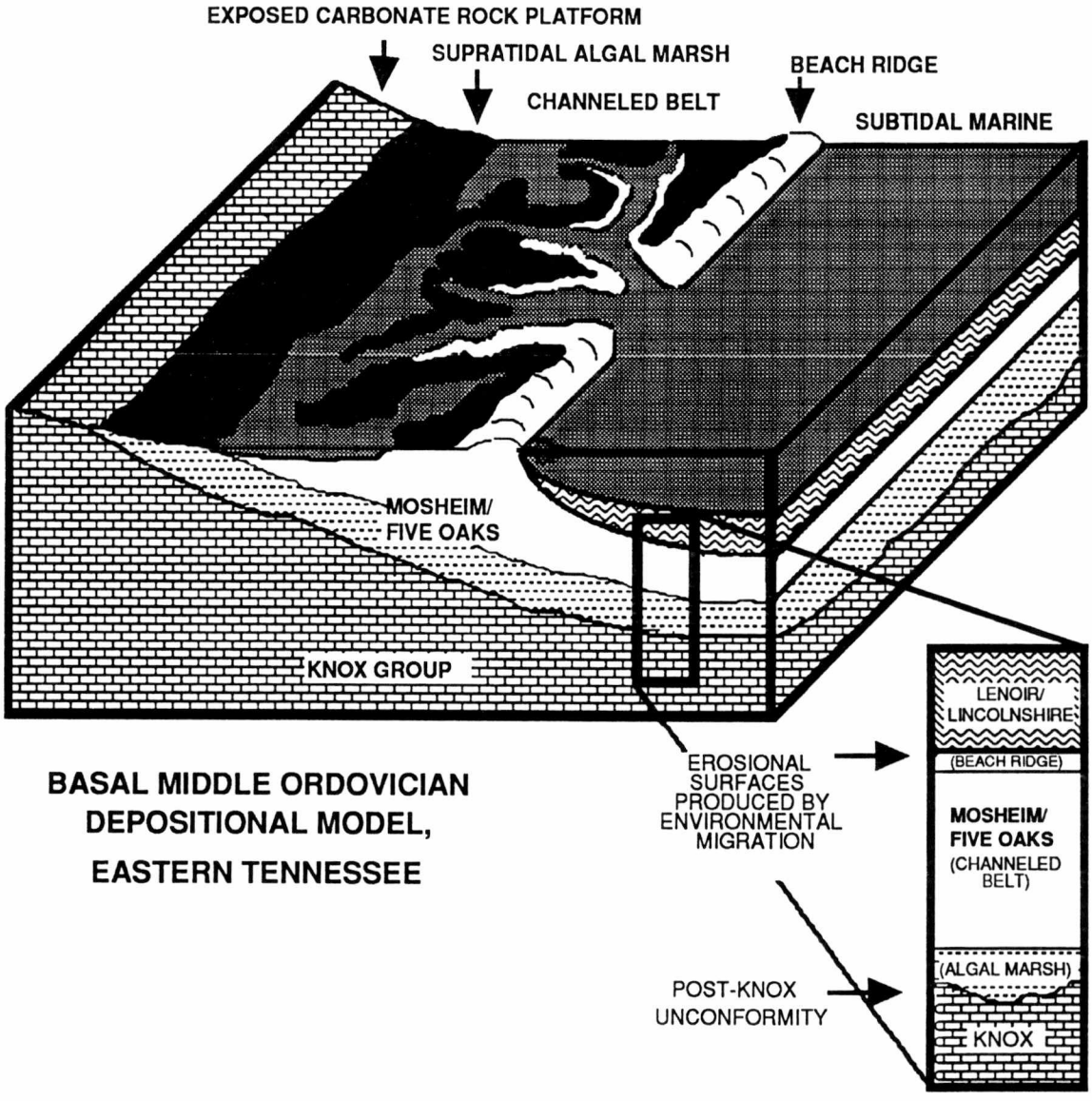


Figure 3.10. Depositional model for the basal Middle Ordovician peritidal strata in East Tennessee.

(now entirely cement-filled); (2) the best-developed lamination, produced by millimeter-scale alternation of sediment layers and laterally coalesced fenestrae; (3) the only observed occurrences of prism cracks, sheet cracks, and *in situ* flat pebble conglomerates formed by the break-up of supratidal crusts; (4) the highest concentrations of dolomite, and the only observed dolomite cements in the entire tidal flat facies (although the high dolomite content is probably diagenetic, and not primary) . These laminated, fenestral basal beds are clearly and entirely supratidal in origin, and unlike most supratidal lithologies that occur stratigraphically higher in the tidal flat facies, are not interbedded with intertidal or subtidal lithologies. The stratigraphic position of these lithologies at the base of the tidal flat, overlying depression-filling lithologies of the Douglas Lake / Blackford facies or directly overlying the Knox dolostones (Figures 3.9 and 3.10), indicates deposition in a supratidal environment at the landward edge of the developing tidal flat. This basal subfacies is interpreted to represent deposition in a subenvironment analogous to the supratidal inland algal marsh that lies landward of the channeled belt on the Andros Island tidal flat (Figures 3.3 and 3.4). The well-developed lamination in this subfacies probably was produced by episodic deposition of sediment on the land surface by discrete storm events, which punctuated periods of lush algal mat growth. Laminations were preferentially preserved in this environment because infaunal, burrowing organisms were absent and early cementation was facilitated by regular flushing of the sediment with meteoric groundwaters.

Channeled Belt

Stratigraphically above the basal inland algal marsh subfacies, the lithologies comprising the Mosheim / Five Oaks tidal flat facies consist of a complex and apparently random arrangement of non-laminated lithologies that represent deposition in a variety of

shallow subtidal, intertidal, and supratidal subenvironments including tidal ponds, channels, low algal marshes, high algal marshes, and levees. The specific internal arrangement of subfacies, laterally and stratigraphically, varies significantly from one outcrop to the next (Figure 3.9). This highly variable and complex package of subfacies, which occupies about 80 to 90 percent of the thickness of the Mosheim / Five Oaks tidal flat facies at any given outcrop, represents the package of subenvironments that collectively comprise the channeled belt on the Andros Island tidal flat (Figures 3.3 and 3.4). At any given time, the channeled belt is a complex mosaic of pond, channel, levee, and algal marsh subenvironments. Because of lateral migration of channels and other subenvironments through time, the sedimentary record left behind by deposition in the channeled belt would be a complex, laterally discontinuous package of interfingering subtidal, intertidal, and supratidal lithologies. The "main body" of the Mosheim / Five Oaks tidal flat is precisely such a package (Figure 3.10), and indicates that this tidal flat was composed of essentially the same physical elements as the Andros Island tidal flat.

Beach Ridge

The uppermost layers of the Five Oaks Formation, and the top of the Mosheim Member at several outcrops, differ significantly from the lower portions of the tidal flat facies. The upper meter or so of the tidal flat facies in many places consists of laminated, non-fenestral, grain-supported lithologies that are interpreted as having been deposited in supratidal beach ridge washover crest and beach ridge backslope subenvironments, and the intertidal beach subenvironment (Figures 3.4, 3.5, and 3.6). The position of the beach ridge was located at the interface between the channeled belt and the adjacent offshore marine environment and marked the seaward margin of the tidal flat; however, this interface migrated landward as the adjacent marine environment migrated over the tidal

flat during transgression (Figures 3.4 and 3.10). On the northwest side of Andros Island, where the tidal flats are migrating landward and onlapping the island, the beach ridge is retreating, and is being eroded at its seaward edge by the encroaching sea (Hardie and Garrett, 1977; Shinn, 1986). The upper surface of the Mosheim / Five Oaks tidal flat is also, in many places, a sharp erosional surface. The erosional surface at the top of the Mosheim, which marks the contact between the tidal flat facies and the adjacent offshore marine facies, is the topic of Chapter 5 of this dissertation.

The transgressive succession of these subfacies within the tidal flat facies reflects a continuation of the overall basal Middle Ordovician transgressive sequence, in that the inland algal marsh subfacies overlies the basalmost depression-filling deposits of the Douglas Lake / Blackford Facies (where present), and the beach ridge is overlain, via a sharp erosional surface, by the adjacent offshore marine facies (the Lenoir / Lincolnshire Facies). This continuous transgression is responsible for, and is in turn manifest by, the conspicuous absence of meter-scale, shallowing-upward, progradational cycles within the facies. The absence of such cycles is discussed further below.

Discussion: Absence of Progradational Cycles Within the Mosheim/Five Oaks Tidal Flat Facies

As stated above, lithologies representing deposition in the channeled belt make up the bulk of the Mosheim / Five Oaks tidal flat, which typically is 10 to 20 meters thick. At each outcrop, this portion of the tidal flat is a complex arrangement of subtidal, intertidal, and supratidal subfacies. However, *at no outcrop* are these subfacies arranged as a repetition of shallowing-upward, progradational, subtidal to supratidal cycles. There is no evidence that this tidal flat was built by a succession of progradational cycles. Apparently, the partly-correlative Middle Ordovician tidal flat contained within the St.

Paul Group carbonates in the Central Appalachians, which was also determined to be a close, ancient analogue of Andros Island (Mitchell, 1981; 1985), developed in a similar fashion. About the St. Paul Group tidal flats, Hardie (1986) wrote, "The complex arrangement of subfacies, both laterally and vertically, signifies that accretion was not by simple progradation of the tidal flats across a shelf-lagoon, but, instead, carbonate mud filled in a complex mosaic of shallow tidal-flat subenvironments separated from the open shelf-lagoon by some form of barrier bars or beach ridges." The same statement could be made for the Mosheim / Five Oaks tidal flat. However, Hardie (1986) points out that within the St. Paul Group tidal flats "it is possible to recognize within the complex succession of subfacies individual...shallowing upward sequences that record local progradation or vertical accretion..." Such cycles have not been observed in the Mosheim / Five Oaks tidal flat, although a considerable amount of effort was expended searching for evidence of them. From all indications, the Mosheim / Five Oaks tidal flat nucleated on the shoreline of the exposed Knox carbonate platform as the Middle Ordovician transgression in the southern Appalachians began, developed into an Andros Island-type tidal flat consisting of well-defined inland algal marsh, channeled belt, and beach ridge subenvironments, and then migrated westward as a transgressive package across the previously exposed Knox carbonate platform.

It is not known if another purely transgressive tidal flat has been recognized in the rock record. It is interesting to note that Shinn (1986) wrote, "In the rock record, transgressive sequences are thin and probably produce only thin sedimentary records." If this is true, a transgressive tidal flat should indeed be thin, with its thickness reflecting the width of the flat from its landward to seaward margins, not compounded by the stacking of progradational cycles. It may be significant that the thickness of the Mosheim / Five Oaks tidal flat, top to bottom, at the outcrops in the study area averages about 14 meters, and generally ranges from 10 to 25 meters. In comparison, most ancient tidal flats,

especially those characterized by stacked, shallowing-upward cycles, are many tens to hundreds of meters thick. That a fully-developed tidal flat like the Mosheim / Five Oaks sequence, which contained all the major physical elements of the Andros Island tidal flat, would leave such a thin sedimentary record is at least consistent with the conclusion that it was purely transgressive and lacks progradational cycles.

Is there a good modern analogue for a non-cyclic, transgressive tidal flat? The northwest portion of the Andros Island tidal flat, which has proved to be a remarkably useful modern analogue for the Mosheim / Five Oaks sequence so far, is probably more than adequate. Concerning the Andros Island tidal flat, Shinn (1986) made the following observations. The northwestern portion of the Andros Island tidal flat is currently experiencing transgression, which is characterized by retreat of the channeled belt in a landward direction over the marsh subenvironment, and active erosion of the beach ridge as the adjacent offshore shallow marine environment transgresses over the tidal flat. Coring has shown that this landward migration of the entire tidal flat is producing a transgressive vertical sequence of subfacies (Figure 3.4). The southwestern portion of the Andros Island tidal flat, however, is currently accreting or prograding seaward, and producing a regressive (offlap) vertical sequence. Coring in this part of the tidal flat has shown that there are several abandoned beach ridges preserved in the tidal flat complex landward of the present beach ridge location. Interestingly, transgression in the northwestern portion and regression in the southwestern portion of the Andros Island tidal flat are occurring simultaneously, in response to the same Holocene sea level rise. These diametrically opposed types of facies migration result from differences in prevailing wind direction, depth of the offshore marine environment (the Bahama Bank), wave size and intensity, and sediment supply. Southwestern Andros is prograding seaward because of abundant sediment supply and low wave intensity. Retreat of the northwestern portion

is driven by lower sediment supply, and erosion of the beach ridge in response to higher wave intensity (Shinn, 1986).

Another difference between the northwestern and southwestern portions of the Andros Island tidal flat is the nature of the channels and the channeled belt. On the northwestern, transgressive portion of the tidal flat, tidal channels are well developed and active, and serve as pathways to funnel water and sediment across the tidal flat to the more landward subenvironments such as the inland algal marsh (Figure 3.4). In this way, the tidal flat can extend landward while the beach ridge migrates landward in response to wave erosion (Shinn, 1986). The channeled belt is often largely flooded, with as much as 90 percent of the surface area occupied by subtidal ponds (Hardie and Garrett, 1977). On the southwestern, regressive portion of the tidal flat, channels are choked with sediment and inactive, and do not serve as conduits for transport of water or sediment across the tidal flat (Shinn, 1986). For this reason, sediment builds up at the seaward margin of the tidal flat, and causes the flat to prograde seaward.

Given that the vertical sequence of subfacies within the Mosheim / Five Oaks defines a transgressive trend, uninterrupted by meter-scale progradational cycles, and that the bulk of the tidal flat facies represents deposition in a well-developed, active channeled belt behind a beach ridge, it is clear that the transgressive, northwestern portion of the Andros Island tidal flat is the appropriate modern analogue for this Middle Ordovician tidal flat. The lack of progradational cycles from such a sequence is not surprising for two reasons: (1) the presence of a beach ridge could potentially isolate the channeled belt from the effects of very minor sea level fluctuations, so that shallowing upward cycles would not form as readily, and (2) the lateral migration of tidal channels and associated channeled belt subenvironments behind a beach ridge would tend to erase evidence of cycles before preservation, even if cycles did form. It is plausible, however, that the Mosheim / Five Oaks tidal flat was deposited during a continuous and relatively

rapid sea level rise upon which small-scale sea level falls or stillstands were not superimposed. Transgression proceeded at a rate and with a regularity that inhibited progradational cycles from forming. Cycles develop best on a stable carbonate platform when sedimentation exceeds subsidence during a period of relatively stable sea level. At the time the Moshiem / Five Oaks tidal flat was deposited in the study area, the Cambro-Ordovician platform had ceased to be stable, the Sevier foreland basin was forming to the east in response to the Blountian Phase of the Taconic Orogeny (Rodgers, 1953; 1971), and a well-documented eustatic sea level rise (Sloss, 1963) was in effect. Continuous, uninterrupted sea level rise could explain the nature of the Mosheim / Five Oaks tidal flat as a thin, entirely transgressive sequence that records a landward-directed, "single pass" of the tidal flat facies across the previously exposed Cambro-Ordovician carbonate platform.

Summary: Depositional Model

The basalmost Middle Ordovician carbonate units of eastern Tennessee were deposited in three general types of depositional environments that were positioned adjacent to one another along the eastern shoreline of the North American continent during the early Middle Ordovician period. The depositional environments represented by these units include: 1) a variety of isolated, nearshore terrestrial and paralic settings, 2) a humid carbonate tidal flat, and 3) the adjacent shallow marine environment that lay just offshore from the tidal flat. The limestones deposited in these adjacent environments became stacked vertically in a transgressive sequence as sea level rose and inundated the lithified carbonate rocks of the Knox Group. Figure 3.10 depicts the depositional environments and depositional history of this transgressive sequence.

The stratigraphically lowest of these units, the Douglas Lake and Blackford Members, represent nearshore terrestrial and restricted marine sediments that were deposited in isolated topographic depressions on the exposed Knox surface. These depression-filling units essentially prepared the topographically irregular, karsted Knox surface for tidal flat development.

The Mosheim Member of the Lenoir Formation and the main body of the Five Oaks Formation are composed of various subfacies representing subenvironments of the basal Middle Ordovician tidal flat that developed along the paleoshoreline, and overlie the depression-filling, terrestrial/paralic units (Douglas Lake / Blackford facies), or directly and unconformably overlie the Knox surface where the terrestrial/paralic units are absent.

The tidal flat facies is then overlain by the main body of the Lenoir Formation and the Lincolnshire Formation, which were deposited in the offshore shallow subtidal marine environment.

Conclusions

1. The stratigraphic sequence of basal Middle Ordovician strata indicates a transgression, as a terrestrial surface (the emergent Knox) was overlain unconformably by nearshore terrestrial and paralic deposits (the Douglas Lake / Blackford facies) or tidal flat deposits (Mosheim / Five Oaks facies), the upper surface of which is a sharp erosional surface. This surface is overlain by shallow marine deposits (Lenoir / Lincolnshire Formations).

2. The Mosheim / Five Oaks tidal flat was a remarkably close ancient analogue to the northwestern portion of the Holocene tidal flat on Andros Island.

3. The tidal flat facies is composed of three major subfacies, each of which is a direct analogue of a major subenvironment of the Andros Island tidal flat. The highly fenestral, laminated basal portion of the Mosheim / Five Oaks facies was deposited in a supratidal environment very similar to the inland algal marsh, the most landward portion of the Andros Island tidal flat complex. The majority of the Mosheim / Five Oaks sequence consists of a complicated arrangement of shallow subtidal, intertidal, and supratidal lithologies that represent deposition in a complex mosaic of ponds, channels, algal marshes, and levees. Taken together, this portion of the sequence represents a well-developed Andros Island-type channeled belt. The uppermost layers of the sequence represent supratidal and intertidal deposition in various subenvironments of a beach ridge that formed the seaward margin of the tidal flat.

4. The vertical succession of subfacies within the Mosheim / Five Oaks tidal flat facies defines a purely transgressive sequence that contains no evidence of progradational, shallowing-upward cycles. The lack of cycles within this tidal flat sequence, which would certainly be a sensitive recorder of even the most minute changes in sea level, suggests that this transgression occurred as a "single pass" of the vertical stack of facies across the Cambro-Ordovician carbonate platform as it was drowned by the Middle Ordovician sea level rise.

5. The upper surface of the tidal flat facies, which marks the contact between the Mosheim / Five Oaks tidal flat facies and the overlying Lenoir / Lincolnshire shallow subtidal marine facies, is sharp and in many places, erosional. The tidal flat facies and the overlying shallow subtidal marine facies do not interfinger, and the base of the Lenoir / Lincolnshire facies at any given location within the study area marks the final flooding of the tidal flat due to sea level rise and landward migration (transgression) of the offshore marine environment, and the end of peritidal deposition.

Chapter 4

EARLY DIAGENESIS OF A MIDDLE ORDOVICIAN CARBONATE TIDAL FLAT IN A FRESHWATER-DOMINATED COASTAL MIXING ZONE

Introduction

In this chapter, the diagenetic history of the basal Middle Ordovician tidal flat facies in eastern Tennessee is described and summarized. The chapter begins with an overview of the depositional history and depositional setting of the tidal flat facies and a brief summary of the burial history of the sequence. This is followed by detailed descriptions of the diagenetic features of the tidal flat facies and interpretations of the diagenetic processes that produced these features. That section is followed by a summary of the diagenetic history, which includes a brief discussion on the relationships that constrain the timing of diagenetic processes, and a summary of the paragenetic sequence and the diagenetic environments in which each process occurred. The chapter concludes with a paleohydrologic model that summarizes the early diagenetic alteration of the facies within the context of its deposition in a freshwater-dominated coastal mixing zone.

This chapter is a counterpart to Chapter 3 of this dissertation, in which the depositional setting and depositional history were discussed in detail. The diagenetic history of the sequence cannot be divorced from its depositional history, because most of the diagenetic alteration occurred soon after deposition, prior to deposition of the overlying subtidal marine sequence, while the sediments remained in the depositional setting.

Geologic Setting

The geologic setting of the basal middle Ordovician tidal flat carbonate rocks was discussed in Chapter 2 of this dissertation. That chapter included a brief description of the overall tectonic setting for deposition of the rocks examined in this study, and a discussion of the basal Middle Ordovician stratigraphy, both locally and regionally. A map of the study area is shown in Figure 2.1 and the stratigraphy is summarized in Figure 2.2.

Depositional History and Environments of Deposition

Chapter 3 of this dissertation included a detailed discussion of the depositional setting and depositional history of the basal Middle Ordovician tidal flat sequence in eastern Tennessee, which is represented in the rock record by the Mosheim/Five Oaks facies. A depositional model (Figure 3.10) presented at the end of that chapter interprets the Mosheim/Five Oaks facies as a carbonate tidal flat that had the following characteristics:

1. The tidal flat was a remarkably close ancient analogue to the northwestern portion of the Holocene tidal flat on Andros Island in the Bahamas, as described in detail by Shinn et al. (1969), Hardie and Garrett (1977), and Shinn (1986).

2. The tidal flat facies is composed of three major subfacies, each of which is a direct analogue of a major subenvironment of the Andros Island tidal flat. The highly fenestral, laminated basal portion of the Mosheim / Five Oaks facies was deposited in a supratidal environment very similar to the inland algal marsh, the most landward portion of the

Andros Island tidal flat complex. The majority of the Mosheim / Five Oaks sequence consists of a complicated arrangement of shallow subtidal, intertidal, and supratidal lithologies that represent deposition in a complex mosaic of ponds, channels, algal marshes, and levees. Taken together, this portion of the sequence represents a well-developed Andros Island-type channeled belt. The uppermost layers of the sequence represent supratidal and intertidal deposition in various subenvironments of a beach ridge that formed the seaward margin of the tidal flat.

3. The vertical succession of subfacies within the Mosheim / Five Oaks tidal flat facies defines a purely transgressive sequence that contains no evidence of progradational, shallowing-upward cycles. The tidal flat facies occurs within, and near the base of, the Middle Ordovician carbonate sequence, the lower portion of which is also entirely transgressive.

4. The upper surface of the tidal flat facies, which marks the contact between the Mosheim / Five Oaks tidal flat facies and the overlying Lenoir / Lincolnshire shallow subtidal marine facies, is sharp and in many places, erosional. The tidal flat facies and the overlying shallow subtidal marine facies do not interfinger, and the base of the Lenoir / Lincolnshire facies at any given location within the study area marks the final flooding of the tidal flat due to sea level rise and landward migration (transgression) of the offshore marine environment, and the end of peritidal deposition.

Burial History

Shortly after deposition of the basal Middle Ordovician carbonate rocks in the Tellico-Sevier Belt/Bays Mountain Synclinorium (Figure 2.1), these rocks were buried

beneath a thick section of Middle Ordovician hemipelagic clastic rocks and distal turbidites of the Sevier shale basin. In contrast, the basal Middle Ordovician carbonate rocks in the Knoxville area and northwest of the Saltville Fault were overlain by a much thinner section of younger Middle Ordovician platform limestones (the Chickamauga Group) (Ruppel and Walker, 1984; Shanmugam, 1977; Shanmugam and Walker, 1978, 1980; Shanmugam and Lash, 1982; Walker et al., 1980). This difference in burial history between the on-shelf and basinal sections is summarized in Figure 4.1. Largely because of the different burial histories of the on-shelf and basinal sections, there are significant differences in the late-stage, burial diagenesis of the Middle Ordovician carbonate rocks in the two areas (Johnson, 1988; Steinhauff, 1993; Steinhauff et al., 1989; Steinhauff and Walker, 1987; Steinhauff and Walker, in prep; Walker et al., 1986; Walker et al., 1987; Walker et al., 1992). Despite these paleogeographic differences in burial history and differences in the patterns of pore-filling cements in much of the Middle Ordovician carbonate sequence, there appears to be little difference in the diagenetic history of the basal Middle Ordovician peritidal carbonate rocks examined in this study, whether they were deposited in the area that became the Sevier shale basin or on the Chickamauga shelf. The reason for this is one of the main points of this chapter: most of the diagenetic alteration of the basal Middle Ordovician tidal flat carbonate rocks occurred very early, while the sediment remained in the tidal flat depositional environment. Differences in the burial history between on-shelf and basinal Middle Ordovician carbonates had essentially no effect on the basal tidal flat sequence, because virtually all pore spaces in the tidal flat lithofacies were already occluded by diagenetic materials (mostly equant calcite cement) before the shelf differentiation occurred.

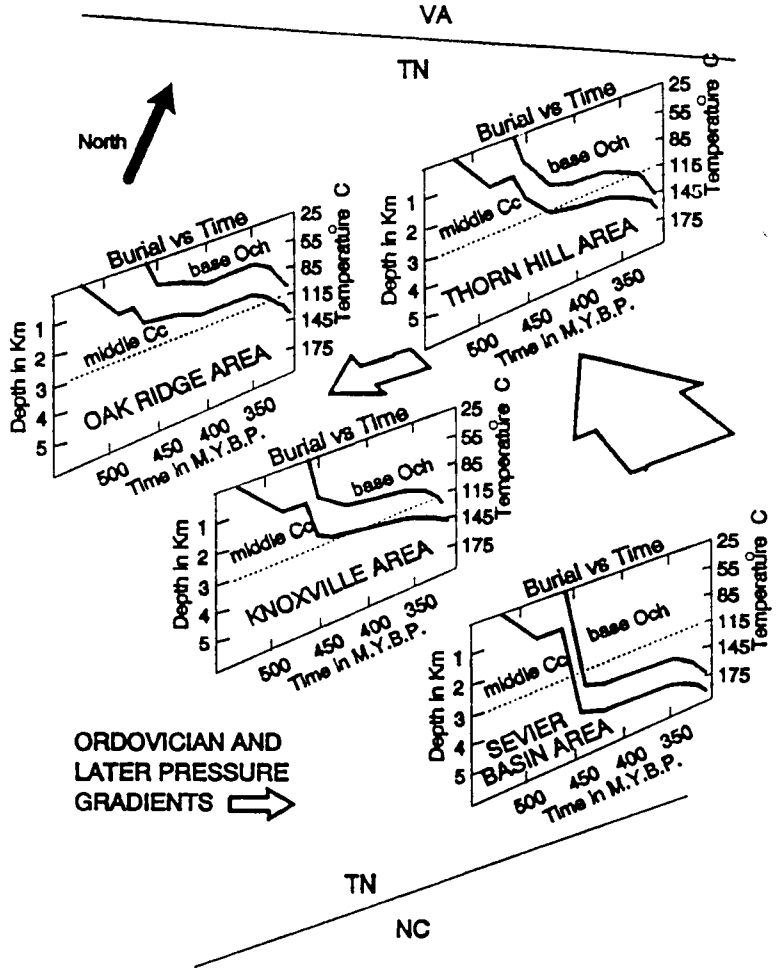


Figure 4.1. Burial history curves for the Middle Ordovician sequence of East Tennessee. The burial curves for the Oak Ridge and Thorn Hill areas represent the carbonate platform deposits of the Chickamauga Group, northwest of the Saltville Fault, with Oak Ridge area approximately equivalent to the St. Paul Belt, and Thorn Hill representing the Copper Creek Belt. The burial curve for the Knoxville area represents deposits near the Middle Ordovician shelf margin, and the burial curve for the Sevier shale basin represents sections in the Tellico-Sevier Belt, southeast of the Saltville Fault. The upper line for each area (labeled Och) represents the base of the Middle Ordovician section (the Knox unconformity). The curves are from Walker et al. (1992).

Diagenetic Features and Processes

In this section, all features produced by diagenetic (post-depositional) alteration of the tidal flat sediments of the Five Oaks Formation and the Mosheim Member of the Lenoir Formation are described in detail. Interpretations of the diagenetic processes that produced these features are made on the basis of these descriptions, and related processes and factors are also discussed. The features are grouped for discussion by the major type of diagenetic process by which they were produced. These types of processes include porosity development, porosity occlusion, matrix lithification, and post-lithification (burial) diagenesis.

Porosity Development

Porosity was very high in the early history of the basal Middle Ordovician tidal flat sediments, as evidenced by the large percentage of the rock volume now occupied by internal sediments and cements. The original porosity in the sediments upon deposition was quite high, but this amount was increased substantially by early meteoric diagenetic alteration, primarily through development of fenestral fabrics and desiccation voids and dissolution of unstable mineral phases. Maximum porosity was probably attained very shortly after deposition, while the sediments remained in their environments of deposition or after burial beneath a few centimeters of similar tidal flat sediment. The pores did not remain open long, however, as porosity occlusion by internal sediments and cements also began very shortly after deposition, while the sediments remained in the depositional environment.

Most of the porosity types described by Choquette and Pray (1970) existed, prior to occlusion, in the Mosheim/Five Oaks tidal flat facies. Porosity types included primary

pores, or those present in the sediment immediately after final deposition, and secondary pores, which were created by diagenetic processes after final deposition (Choquette and Pray, 1970). The types of primary porosity that have been observed in these rocks are briefly discussed, but the focus of this portion of this paper is on the development of secondary, diagenetic porosity. There is some stratigraphic variation in the relative abundances of porosity types within each unit. Stratigraphic variations in porosity type abundance are discussed below, and shown in Figure 4.2.

Primary porosity

Primary porosity, or porosity that was present in the Middle Ordovician peritidal carbonate rocks immediately after deposition, was mostly intergranular, but intragranular and shelter pores were also quite common in certain stratigraphic horizons. Primary intergranular porosity was undoubtedly very high throughout much of the muddy tidal flat strata, especially at the sub-microscopic scale between mud particles. Initial porosities of modern carbonate muds are typically on the order of 50 to 70 percent (Moshier, 1989b), and it is likely that original porosities of the Mosheim/Five Oaks tidal flat muds were in that range. Much of this initial interparticle porosity was probably reduced by compaction during the first few decimeters of burial. Larger, macro-scale intergranular porosity was greatest, or at least most apparent, in the basal conglomerates and in peloidal and intraclastic packstone and grainstone lithologies because pore sizes were larger in these lithologies. Intragranular porosity, or porosity within depositional grains, was largely limited to the chambers of gastropods and the interiors of articulated ostracode shells (Figure 4.3A), and was highest in subtidal pond and channel lithologies that contained significant amounts of fossils. Shelter porosity was most abundant beneath

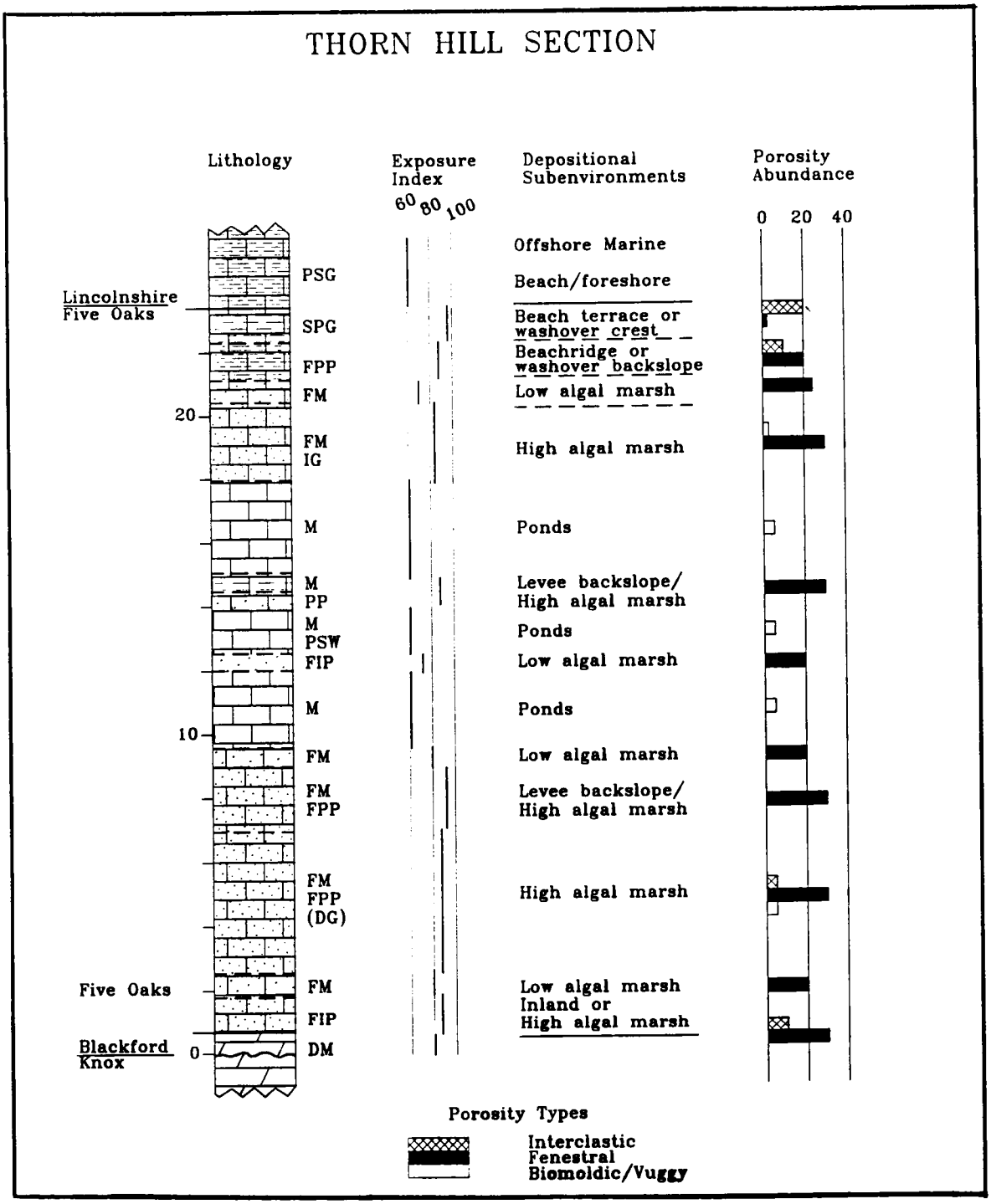
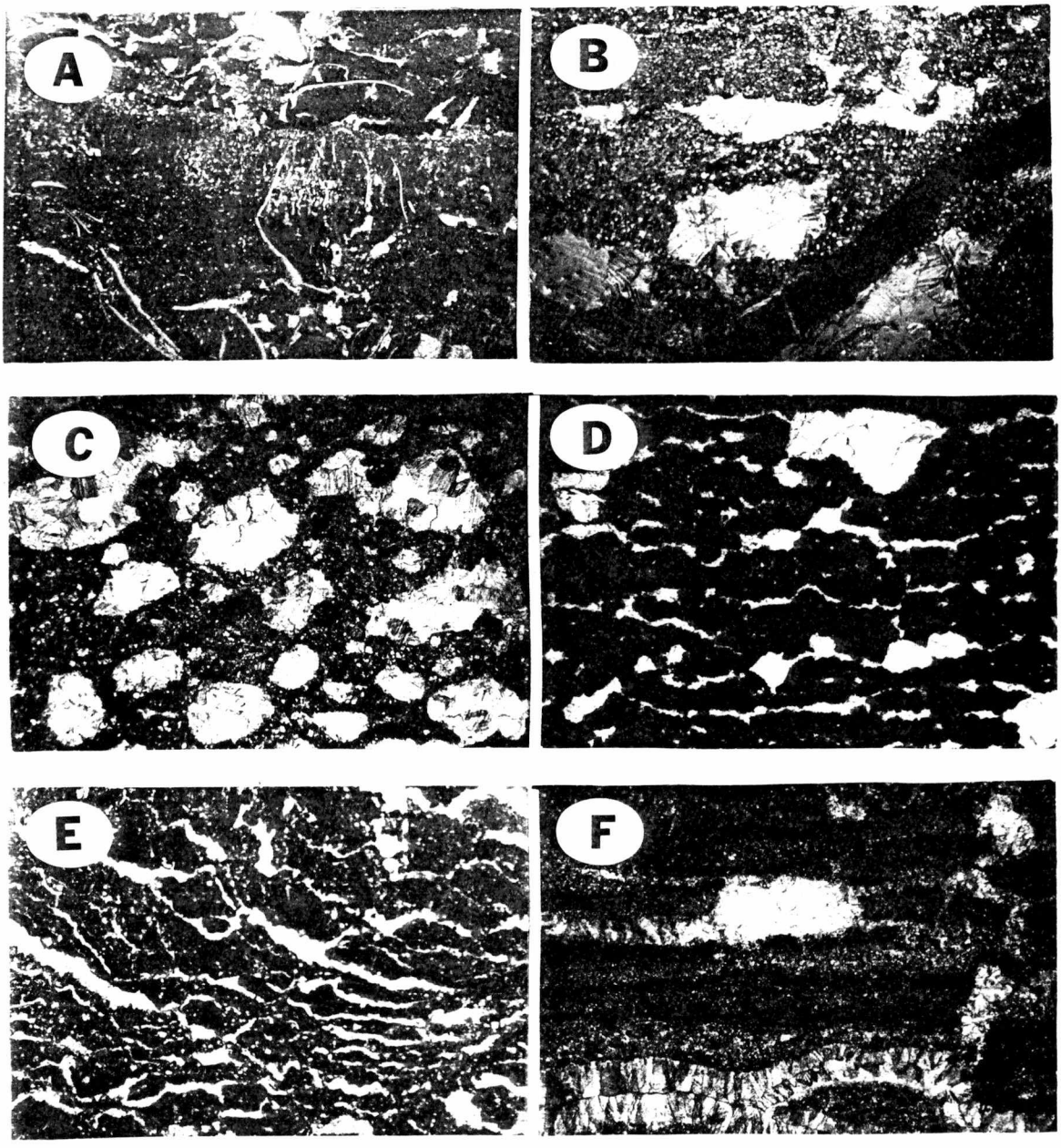


Figure 4.2. Stratigraphic variation in porosity-type abundance, Thorn Hill section. The relative abundance of pore types in a given sample is directly related to the depositional subenvironment of the lithology and the early diagenetic alteration associated with that subenvironment. Thus, stratigraphic variations in porosity type are tied to the vertical arrangement of depositional subfacies within a given stratigraphic section. Abbreviations for lithologies are the same as in Figure 3.9.

Figure 4.3. Primary and secondary porosity types in the Mosheim/Five Oaks sequence. The long axis field of view in all photomicrographs is 6.5 mm. A, B, D, and E were taken under plane-polarized light; C and F were taken under crossed nicols. A and B illustrate primary porosity types; C-F illustrate early secondary pore types. All pores are filled with calcite cement. **A.** Skeletal intraclastic wackestone, from the base of the Five Oaks, 10 m above the Knox unconformity (AKU), Idol Mine. Porosity is primarily biomoldic, after pelecypod fragments, but note also the primary intragranular porosity within whole, articulated ostracode shells. **B.** Primary shelter porosity beneath dolostone lithoclasts in basal Mosheim fenestral conglomeratic dolostone, 0.1 m AKU, Nina section. These shelter pores are difficult to differentiate from early secondary, irregular fenestrae that are also present in this lithology. **C.** Small (1 to 2 mm) irregular fenestrae and larger (2 to 5 mm), almost spherical "bubble" fenestrae in highly fenestral dolomitized intraclastic mudstone, basal Mosheim, 5 cm AKU, Boyd's Creek Road. Equant calcite cement occupies up to 45% of the rock volume in this and other samples of the basal Mosheim. **D.** Irregular and laminoid fenestrae from fenestral peloidal packstone, 3.0 m AKU, Thorn Hill section. Abundant, bed-parallel, laminoid fenestrae give this lithology "crinkled fenestral lamination" characteristic of inland or high algal marsh deposits. **E.** Arching laminoid fenestrae in lower Mosheim fenestral mudstone, 3.2 m AKU, Nina. This lithology contains "wavy fenestral lamination" typical of supratidal levee backslope or beach ridge backslope subenvironments. **F.** Bed-parallel sheet cracks and bed-normal mudcracks in highly dolomitized peloidal packstone, basal Mosheim, 0.4 m AKU, Boyd's Creek Road. "Smooth flat lamination" characteristic of the highest supratidal subenvironments is produced by alternation of peloid layers with mud layers, but has been altered in this sample to "disrupted flat lamination" by the sheet cracks and mudcracks, which have broken the laminated sediment into discrete dolomitic crusts (see Figure 4.8f). Sheetcracks and the fibrous cements filling them are very rare in the Mosheim/Five Oaks sequence.


A
B
C
D
E
F

large lithoclasts in the conglomeratic strata that immediately overlie the post-Knox unconformity at the base of the section (Figure 4.3B).

Secondary porosity

Secondary porosity, or porosity of diagenetic origin, greatly enhanced the amount of porosity in the basal Middle Ordovician peritidal carbonate sediments. Secondary porosity types observed in these rocks include the following:

Fenestrae
Shrinkage cracks
Fabric selective dissolution features (fossil molds)
Non-selective dissolution features (vugs)
Biogenic pores (burrows and borings)

The abundance of each of these porosity types within the tidal flat facies is largely controlled by lithology, and so is directly related to the subenvironment in which each subfacies was deposited (Figure 4.2). For this reason, the relative abundance of each secondary porosity type varies between the Mosheim Member and the Five Oaks Formation, due to differences in the proportions of different lithologies within each unit. For example, fenestral porosity is the dominant porosity type in the Mosheim, which contains abundant supratidal and high intertidal lithologies, whereas biomoldic porosity is the major porosity type in the Five Oaks, which includes considerably more subtidal pond lithologies.

Fenestrae

Fenestrae are defined by Tebbutt and others (1965) as primary (synsedimentary) void spaces, typically larger than grain-supported interparticle pores, that have no

apparent means of support by the grain framework of the sediment. Choquette and Pray (1970), however, classified fenestrae as a type of secondary porosity, because the fenestral pores form by processes that alter the sediment after deposition. Development of fenestral porosity begins so soon after deposition, however, that fenestrae are used widely and reliably as depositional environment indicators. In this paper, fenestrae are considered very early secondary pores that formed by diagenetic processes while the sediment remained in the environment of deposition. When reference is made to fenestrae in the Mosheim/Five Oaks sequence, it should be understood that the fenestrae are not open pores, but are original fenestral pores that are now filled with cement or internal sediment.

According to Shinn (1968; 1983), fenestrae have two basic morphologies, spherical (irregular) and planar (laminoid). Irregular fenestrae in the Mosheim/Five Oaks sequence have crudely spherical shapes and no particular orientation, and are 1 to 5 mm in diameter (Figure 4.3C,D), whereas the laminoid variety are elongate in a bed-parallel direction, and are up to a few cm in length (Figures 4.3D,E). Spar-filled, vertically oriented features with the same cross-sectional shape, but which are tube-like in three dimensions, have been called tubular fenestrae by some authors (e.g., Tebbutt, et al., 1965; Grover and Read, 1978). However, since these features are generally interpreted to be either cement-filled animal burrows or root tubes, they are more correctly referred to as burrows or root tubes rather than a type of fenestra (Shinn, 1983). The latter are discussed below under as biogenic pores.

Fenestrae are an almost ubiquitous feature of lime mudstones, grainstones, and dolostones deposited in modern intertidal and supratidal environments, and by association, have become widely accepted as indicators of peritidal, and especially supratidal, sedimentation in ancient carbonate rocks. Many origins have been proposed for fenestrae (Illing, 1959; Shinn, 1968), but the most widely accepted are that the

irregular voids are formed by air bubbles trapped in the sediment, or gas bubbles produced during the decomposition of organic matter, and the laminoid variety are formed by desiccation and shrinkage of muddy sediment during intermittent subaerial exposure (Fischer, 1964; Shinn, 1968). Hardie and Ginsburg (1977) observed that fenestrae, at least on Andros Island, are less common in the flat laminated sediments of the highest supratidal subenvironments, such as levee and beach ridge crests and backslopes, than in the lower supratidal and high intertidal algal marshes (see Table 3.1 in Chapter 3). Fenestral fabrics are most closely associated with the "crinkled fenestral lamination" that characterizes the supratidal high algal marshes and with the "disrupted fenestral bedding" that underlies the intertidal low algal marshes. Irregular fenestrae form by decay of cyanobacteria in sediments that infiltrate or drape lush growths of tufted cyanobacteria such as the modern *Scytonema,* that populates the pond-rimming marshes on the Andros Island tidal flat. Laminoid fenestrae form by the decay of cyanobacterial mats that are interlayered with sediment laminae, or where desiccation causes the formation of large horizontal sheet cracks in the sediment. These desiccation cracks, ironically, do not form well in the highest supratidal subenvironments (levee and beach ridge crests) because of the tenacious binding of mucaceous cyanobacterial mats (formed by *Schizothrix*), but instead form on the high "algal" marshes and the backslopes of levees and the beach ridge (Hardie and Ginsburg, 1977).

Both irregular and laminoid varieties of fenestrae are very common in the Mosheim, and combined, accounted for most of the porosity in the unit. Beds containing irregular fenestrae occur interspersed with non-fenestral mudstone layers throughout the Mosheim, but irregular fenestrae are generally larger (commonly up to 5 mm) and most abundant near the base of the unit, where cements that fill fenestral pores occupy as much as 45% of the rock volume. Well-developed, laterally-persistent laminoid fenestrae, with few exceptions, are restricted to the lower one to three meters of the Mosheim, where

they occur in association with large irregular fenestrae. Shorter, curved laminoid fenestrae occur with, and often wrap around, irregular fenestrae throughout the unit. The stratigraphic distribution and relative abundances of fenestral types in the Mosheim are similar to those in the correlative Middle Ordovician New Market Limestone, as described by Grover and Read (1978), and indicate a complex overprinting of different fenestral fabrics.

Fenestrae are less abundant in the Five Oaks than in the Mosheim, and are a common type of porosity only near the base and top of the unit. Irregular fenestrae are the dominant porosity type in the lower portion of the Five Oaks, and are especially abundant at the Thorn Hill outcrop. Laminoid fenestrae are prevalent in the supratidal beach ridge sediments near the top of the formation, and have imparted to these rocks the "wavy fenestral lamination" characteristic of levee and beach ridge backslope environments on Andros Island (Hardie and Ginsburg, 1977).

Shrinkage cracks

Shrinkage cracks are elongate pores, genetically related to laminoid fenestrae, that form in muddy sediment that is subjected to intermittent subaerial exposure. Shrinkage cracks include vertically-oriented mudcracks that form in response to lateral contraction of sediment due to evaporation of pore water during desiccation, and bed-parallel sheetcracks that form by vertical separation of sediment layers during desiccation. Mudcracks are often filled with sediment from the immediately overlying layer, but some escape sedimentation and become filled with cement. Sheetcracks are typically filled with internal sediment, cement, or both.

Both varieties of shrinkage cracks are rare in the Middle Ordovician tidal flat sediments, probably because of the inferred humid climate that prevailed during

deposition and early diagenesis. It is possible that shrinkage cracks simply did not form in abundance in these Middle Ordovician sediments because the climate remained wet, but it is also possible that shrinkage cracks formed during dry periods and then "healed" during insuing rainy periods. This process has been observed on Andros Island (Hardie and Garrett, 1977). In the Middle Ordovician peritidal strata, sheetcracks have been observed only in laminated, dolomitic supratidal sediments within 0.5 meter of the base of the Mosheim (Figure 4.3F). These sheetcracks are commonly several cm long and filled with fibrous cement, and resemble stromatactis structures that occur in the basal Mosheim in Alabama (Roberson and Foreman, 1989). These sheetcracks differ from stromatactis structures in that they are not laterally continuous over a significant distance (the stromatactis persists laterally for several meters), they generally are filled with a single generation of fibrous cement, and because they did not divide the sediment into elaborate, three-dimensional frameworks. Mudcracks are rare, but do occur in supratidal beach ridge backslope sediments near the top of the Five Oaks.

Fabric selective dissolution (biomoldic porosity)

Pores created through fabric-selective or mineral-specific dissolution were a fairly common type of porosity in the basal Middle Ordovician peritidal limestones. In these rocks, fabric-selective porosity was primarily biomoldic, and formed through dissolution of gastropod and pelecypod shells (Figure 4.3A), which were probably originally composed of aragonite (Horowitz and Potter, 1971). Fossil molds were particularly abundant in the non-fenestral, muddy lithologies deposited in subtidal ponds. Biomoldic porosity was very important in such lithologies, because these lithologies typically lacked most other porosity types, such as macroscopic intergranular pores, fenestrae, shrinkage features, and non-selective dissolution vugs. Because of the predominance of subtidal

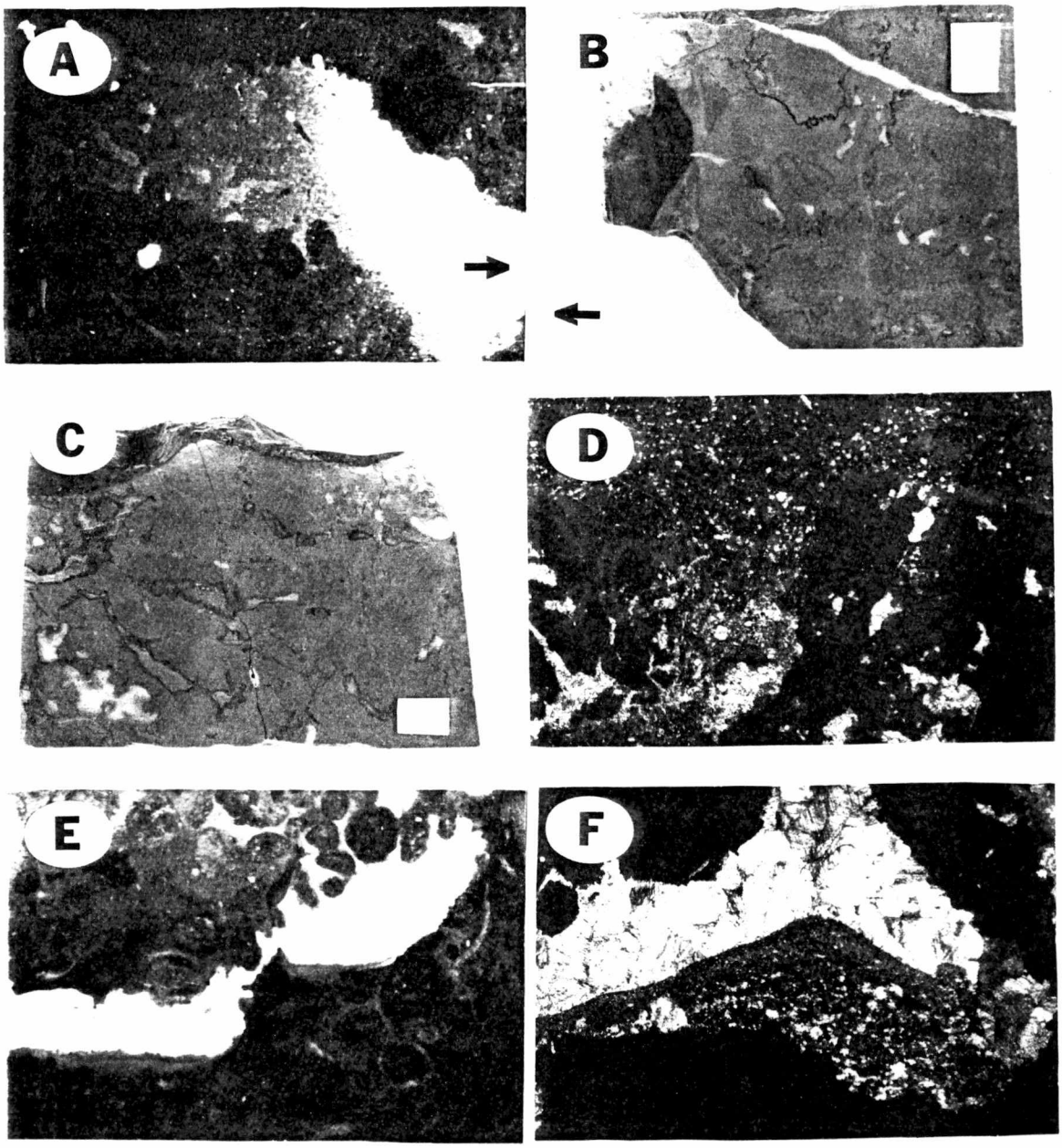
deposits in the Five Oaks Formation, biomoldic porosity was volumetrically the most important porosity type in that unit. Biomoldic porosity was far less abundant in the Mosheim because of the relative scarcity of fossiliferous subtidal deposits.

Non-selective dissolution (vuggy porosity)

Wholesale dissolution of carbonate material, regardless of fabric or specific mineralogy, was uncommon in the Mosheim, and was essentially non-existent in the Five Oaks. Vugs were common in the Mosheim only in the uppermost meter or so, and their development was probably related to the erosional surface that caps the unit (see Chapter 5 for a discussion of this surface). These vugs range in size from about 0.5 cm to 3 cm., and unlike other types of voids, are commonly floored or filled with sediment that differs significantly from the characteristic host micrite of the Mosheim (Figure 4.4B,C,F). These vug-filling sediments are discussed below in the section on internal sediments. Similar vugs and solution-enlarged fissures in Middle Ordovician tidal flat carbonates beneath a possibly correlative erosional surface in Quebec were reported by Desrochers and James (1988).

Other voids that are larger than fenestrae occur in scattered horizons throughout the Mosheim. These pores occur in all types of lithologies, including subtidal pond deposits, and probably represent non-selective dissolution caused by the passage of undersaturated groundwater through the tidal-flat facies in the meteoric phreatic zone during very shallow burial. These pores are thought to be vugs, but an unequivocal solutional origin for these voids was not demonstrated. These voids are typically filled with equant calcite, or floored with internal sediment that is similar to the Mosheim host sediment.

Figure 4.4. Secondary porosity types and internal sediments. A, D, E, and F are thin section photomicrographs taken under plane-polarized light. The long axis field of view in all photomicrographs is 6.5 mm. B and C are photographs of polished slabs. The scale bars in B and C equals 1 cm. Arrows indicate the up direction in A and B; all others are oriented so that the up direction is toward the top of the page. A. Vug in highly altered lime mudstone with abundant "caliche-type" pisoids, 5 cm beneath the top of the Mosheim, Baptist Hospital. Note that the internal sediment filling the vug has been burrowed by very small infaunal organisms. B. Vugs filled with reddish-brown, laminated internal sediment at the top of the Mosheim, Baptist Hospital. The sediment filling these vugs resembles the laminated sediment often found in "neptunian dikes", and does not resemble the matrix of either the Mosheim or the Lenoir. The host sediment of this sample (and in Figure 4.4C) has been altered to an incipient caliche. C. Vugs filled with multiple generations of equant calcite cement and internal sediments, from the top of the Mosheim, Baptist Hospital. This sample contains the scalloped, erosional contact between the Mosheim (the lower vuggy lithology) and the overlying Lenoir. The vugs contain an initial, pore-rimming generation of dark gray, equant calcite cement, followed by gray internal sediment, light beige vadose silt, or both. Vadose silt occupies the pore centers of many of the vugs. The remaining pore space (especially in the lower left and upper right portions of the sample) is filled by a second generation of white equant calcite that overlies internal sediment and vadose silt. Both generations of cement as well as the internal sediment and vadose silt are truncated at the erosional surface. D. Biogenic pore (boring) carved into semi-lithified lime mud, extending 2 mm downward from a bleached exposure surface in the Five Oaks, 24.3 m above the Knox unconformity (AKU), Idol Mine. The boring is filled with slightly dolomitized sediment from the overling layer. E. Enlarged fenestrae in pisoid-rich, incipient caliche, 10 cm beneath the top of the Mosheim, Baptist Hospital. The pores are floored with internal sediment that was probably eroded from a higher stratigraphic level within the Mosheim and transported to these pores through the open pore network. The sediment rests directly on the altered host sediment, and is not underlain by an initial cement generation. Note the size difference between this internal sediment and the crystal silt in the adjacent photograph (Figure 4.4F) (both photos are at the same scale). F. Large fenestra or vug in fenestral mudstone,13.2 m AKU, Nina. The pore contains a mound of internal crystal silt, larger detrital cement crystals, and very small intraclasts of the host mud matrix. The intraclasts and broken cement crystals are concentrated near the base of the mound, whereas the upper half of the mound consists mostly of vaguely laminated crystal silt. The morphology of the mound suggests that the material was deposited on the floor of the pore from the top of the pore.


A
B
C
D
E
F

Biogenic pores (burrows and borings)

The Mosheim/Five Oaks facies contains pores that formed after deposition by organisms that burrow through unconsolidated or semi-lithified sediment. These burrows typically have vertical to subvertical orientations, and commonly have very smooth walls that attest to at least partial consolidation of the host sediment prior to formation of the burrows (Figure 3.8F). Some burrows are backfilled with pellets that presumably were deposited by the organisms that created the voids, but more commonly they are filled with sediment from the overlying layer or equant calcite cement. These burrows have been referred to as "tubular fenestrae" (Tebbutt, et al., 1965; Grover and Read, 1978), but are not genetically related to fenestral pores, and should not be called fenestrae (Shinn, 1983). Similar vertical voids in younger rocks are formed by decay of plant roots, but because the Mosheim/Five Oaks sequence was deposited prior to the origin of land plants (Gensel and Andrews, 1987), that mode of formation is not possible for these voids.

Borings, or tube-shaped voids carved into lithified limestone, occur rarely in the Mosheim and Five Oaks. Their occurrence is restricted to the uppermost surface of the tidal flat facies, and to thin cemented crusts that exist at various stratigraphic horizons within the facies. These borings truncate cements, and clearly formed after thorough lithification of the sediment, and in this way are differentiated from the burrows described above. Outcrop photographs of such borings into Middle Ordovician exposure surfaces in Virginia and Quebec are presented in Grover and Read (1978) and Desrochers and James (1988), respectively. Borings extend downward from lithified surfaces, and are typically filled with sediment from the overlying bed (Figure 4.4D). They did not add significantly to the total porosity of the tidal flat facies.

Porosity Occlusion

Virtually all porosity in the basal Middle Ordovician peritidal carbonate rocks, regardless of type, has been occluded by pore-filling materials, so that the rocks now are essentially nonporous and impermeable. Porosity-occluding materials include several types of internal sediments and cements, which are discussed below. Most porosity occlusion occurred very early in the history of the peritidal rocks, and in places, precipitation of cements and emplacement of internal sediments predated deposition of the overlying lithologies. In particular, supratidal and intertidal lithologies, at several levels within the tidal flat facies, were cemented and lithified before deposition of overlying subfacies, as evidenced by erosional truncation of cements and development of microkarst surface features at exposure surfaces. The degree of early lithification of subtidal facies is not known because cross-cutting relationships (such as truncation of cements) are lacking, but phreatic alteration of subtidal sediments had probably begun prior to the deposition of the offshore shallow marine facies (the Lenoir and Lincolnshire formations) above the tidal flat facies. It is feasible that the tidal flat limestones assumed the characteristics of an aquitard, and acted as a barrier to the migration of porewaters, very shortly after deposition. The timing and paragenetic sequence of porosity occlusion are discussed later in the section entitled "Diagenetic History".

Internal sedimentation

Internal sediment is very abundant as a porosity-occluding material in the Middle Ordovician peritidal limestones. Internal sediment here includes any material that was mechanically deposited in secondary pores, and was thus deposited after the onset of diagenesis. This definition excludes sediment in primary pores, which typically cannot be

differentiated from original, depositional sediment (matrix), and excludes materials that were passively precipitated from solution (cements). Types of internal sediment include marine sediment, fecal pellets, and crystal silt. Internal sediments typically occur in geopetal positions on the floors of pores, and are overlain by cements that occlude the remaining pore space, but in some cases internal sediment fills entire pores. Internal sediments are most common in fenestrae and vugs, but also occur in burrows, sheet cracks, and fossil molds.

Marine sediments

Of the varieties of internal sediment listed above, sediment inferred to be of marine origin is by far the most abundant. Two basic types of internal marine sediment have been recognized in the peritidal limestones: 1) autochthonous gray lime mud that is essentially identical to the host micrite, and 2) allochthonous beige or brown muds that differ significantly from the peritidal host sediment. Of these, the first variety is most common, and occurs in all types of secondary pores throughout much of the peritidal carbonate sequence. This sediment generally consists of pure lime mud, but rarely contains peloids and/or rare ostracode shell fragments or whole, articulated ostracodes. Except for its position within secondary pores, this sediment is difficult to distinguish from the host micrite. When viewed in thin section in transmitted light, the internal micrite appears lighter-colored and less dense than the host micrite (Figure 4.4A,C,E), a difference that probably results from less compaction, because deposition of the internal sediment occurred in pores within a rock mass that had already undergone some degree of lithification. Under cathodoluminescence, the internal sediment has the same dull orange luminescence as the host micrite. Because this sediment is so similar to the host micrite, it is interpreted to be host sediment that was eroded from pore walls and

redeposited at slightly lower stratigraphic levels within the pore network of the peritidal limestone sequence by percolating or circulating ground waters. Interestingly, this type of internal sediment is most abundant in stratigraphic horizons that underlie zones where vadose alteration or dissolution was extensive. The position of this autochthonous sediment immediately adjacent to diffuse pore walls indicates that it generally predates all varieties of cements, and suggests that redeposition occurred before cement precipitation began. The presence of burrows within this type of internal sediment indicate that it was redeposited while the sediment remained in the depositional environment (Figure 4.4A).

The second type of internal marine sediment includes two varieties, skeletal argillaceous lime mud, and yellow or reddish-brown, laminated mud. Both varieties are restricted to vugs in the upper meter of the Mosheim that apparently were connected to the erosional surface that caps the unit. Some vugs contain fossiliferous sediment that is essentially identical to the matrix of the overlying Lenoir Formation, whereas others contain laminated, reddish-brown marine sediment, with abundant ostracodes, that is not characteristic of either the Mosheim or Lenoir (Figure 4.4B,C). Unlike the reworked peritidal host sediments, these sediments post-date initial cement generations, and are believed to be allochthonous shallow subtidal marine sediments that infiltrated the vugs from above during initial marine inundation.

Crystal silt

Crystal silt (also referred to as vadose silt or diagenetic silt) has been reported as a very abundant internal sediment type in secondary voids in correlative tidal flat limestones of the Middle Ordovician New Market Limestone in Virginia, where it reportedly occurs in 60% of the samples analyzed (Grover and Read, 1978). Although internal sediment is indeed very common in the Mosheim/Five Oaks, crystal silt, *sensu*

stricto, is actually quite rare. In this study, much care has been taken to differentiate between true crystal silt and internally redeposited host micrite, which was discussed above.

As interpreted by Dunham (1969a), crystal silt consists of silt-sized particles of calcite *cement* that have been mechanically removed from pore walls, transported through the pore network, and redeposited on pore floors by currents of meteoric water that flush through partially cemented limestone in the freshwater vadose zone. In contrast, internal marine sediment consists of particles of host sediment--*not cement*--that are eroded and redeposited in the same manner. Although the two are visually differentiated primarily by a difference in size, other differences are also important. Because it is composed of cement particles and not micrite, crystal silt typical has greater clarity. But a more striking and important difference is apparent when these internal sediment types are viewed under cathodoluminescence. Internally redeposited micrite has dull orange luminescence identical to the host micrite. In fact, host micrite usually cannot be differentiated from internal micrite under cathodoluminescence. In contrast, crystal silt has either the totally non-luminescent appearance characteristic of vadose cements, or consists of tiny black crystals separated by flecks of brightly luminescent, orange intercrystalline cement.

Because crystal silt consists of redeposited cement, deposition of crystal silt must, by necessity, occur after the onset of cementation. This is also indicated by the fact that crystal silt generally rests on an earlier precipitated generation of drusy cement (Dunham, 1969a). This is also the case where crystal silt occurs in the Middle Ordovician peritidal limestones (Figure 4.4F). Internally redeposited micrite, on the other hand, generally is not separated from the host micrite by cement (Figure 4.4A,E), and was thus deposited prior to initial cementation. Deposition of internal micrite therefore preceded deposition of crystal silt. Not surprisingly, when redeposited micrite and crystal silt occur in the

same pore, crystal silt always overlies the internal micrite. This relationship is illustrated by Grover and Read (1978, Figure 9B), although in the caption to that figure both layers are referred to as crystal silt. In the Mosheim/Five Oaks sequence of this study area, true crystal silt makes up only about ten percent of the internal sediment observed within pores, and that occurs primarily near the top of the facies. Crystal silt is also associated with diagenetic grainstone/pisolite fabrics and zones of incipient caliche, as discussed below.

Fecal pellets

Another type of internal sediment that is rarely observed in the peritidal carbonates are deposits of pellets of uniform size and shape that floor or backfill the smooth-walled vertical burrows discussed above (Figure 3.8F). Although peloidal mud occurs inside fenestrae and other pore types, the occurrence of these pellet deposits is typically restricted to burrows. The author interprets these small ovoid grains as true fecal pellets left behind by the animals that excavated the burrows. Similar pellet deposits are found in burrows made by worms in supratidal deposits on the Andros Island tidal flat (Hardie and Ginsburg, 1977).

Cementation

A limited variety of cements occurs in the basal Middle Ordovician peritidal carbonate sequence, including equant calcite, fibrous calcite, microcrystalline (micritic) calcite, and baroque dolomite. A few non-carbonate authigenic minerals such as pyrite, celestite, and quartz occur as pore-filling materials. Each of these cement types and authigenic materials is discussed below. However, it should be pointed out that while a

variety of cement types is present in the sequence, the abundances of these cements are not equal. In fact, *the combined total of all cement types other than equant calcite is far less than 1% of the volume of cement in the sequence*. In effect, the sequence is cemented by non-ferroan, equant calcite. This is in marked contrast to other overlying parts of the Middle Ordovician succession, in which fibrous calcite and ferroan equant calcite cements (interpreted to be of marine and burial origin, respectively) are much more abundant (Jernigan, 1987; Steinhauff and Walker, in press; Steinhauff et al., 1989; Walker et al., 1987). Although the other cement types in the Mosheim/Five Oaks sequence are volumetrically insignificant, their presence yields important information about the conditions and diagenetic environments in which cementation occurred.

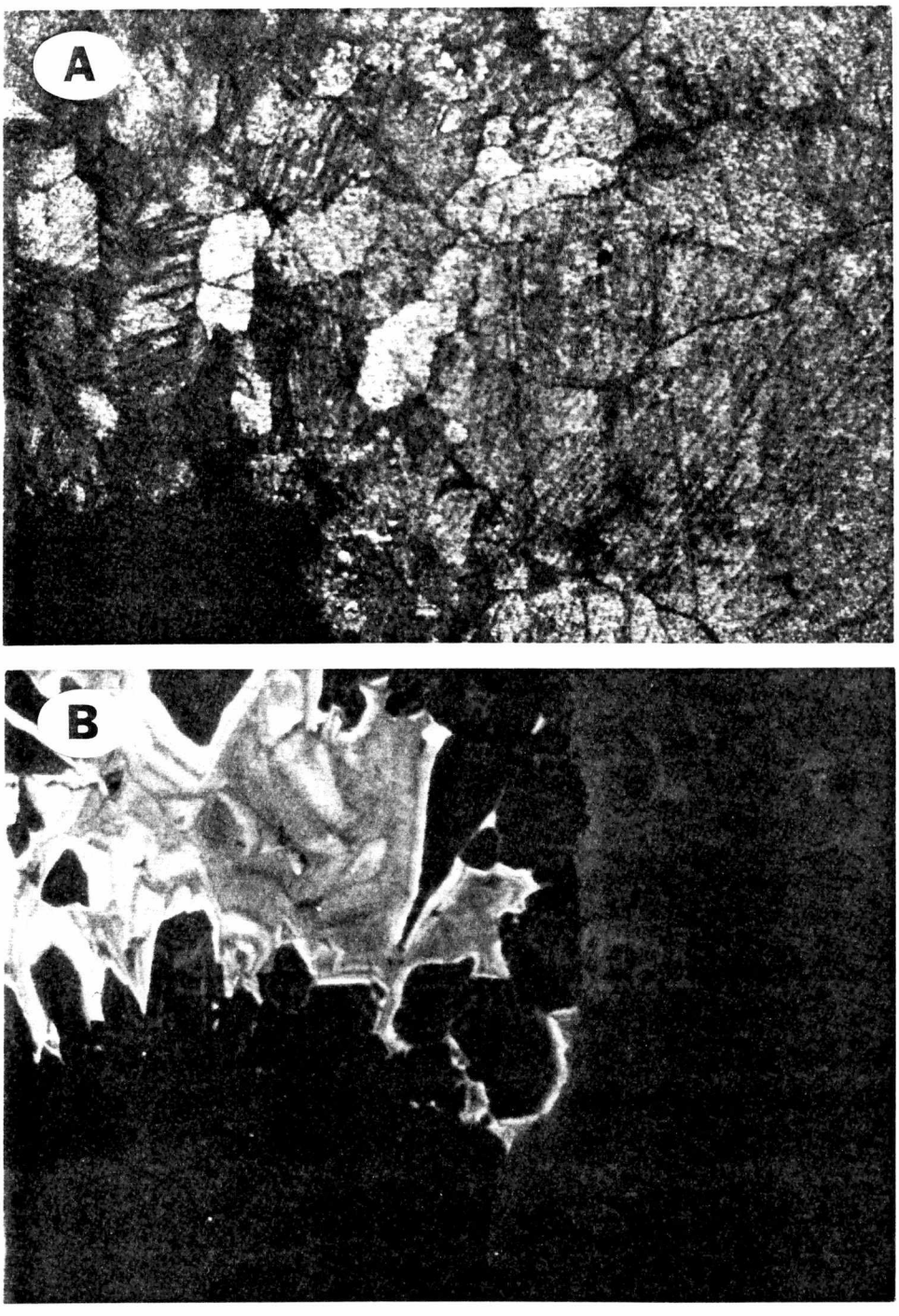
Equant calcite

Virtually all pores in the Mosheim / Five Oaks tidal flat sequence, with the exception of the localized or volumetrically insignificant cement types discussed below, is filled with low-Mg, equant, or blocky, calcite cement (Figures 4.3 and 4.4). This ubiquitous cement is the dominant cement in all types of pores, both on the macro-scale, such as fenestrae and intergranular void space, and on the micro-scale, such as the interparticle space within the micrite matrix. Equant calcite cement is typified by exceptional crystal clarity due to the lack of inclusions. These cement crystals are present in a spectrum of sizes, from tiny μm-sized crystallites that often line pore walls, to large single crystals up to 5 mm in diameter that totally fill large vugs or shelter voids. Typically, equant cements exhibit a drusy fabric, or an increase in crystal size toward pore centers, but there are exceptions. Commonly, fenestral pores in supratidal lithologies, especially those with evidence of vadose diagenetic alteration, are filled entirely with very small equant calcite crystals. Large equant crystals that fill entire pores are most

abundant in molds or vugs in non-fenestral, subtidal pond lithologies. Otherwise, there appears to be little paleogeographic, stratigraphic or depositional environmental control over the petrographic nature of the equant calcite.

Under cathodoluminescence, many of the equant cements show compositional zoning. In many cement-filled pores, cements show the characteristic zoning sequence of non-luminescence, bright luminescence, and dull luminescence from the outside to the center of the pore (Figure 4.5). Typically, the initial generation of equant calcite cement that lines pores is non-luminescent (black), and in many samples this first cement generation has a pendant distribution indicating precipitation in unsaturated (vadose) pores. These non-luminescent cement crystals are typically rimmed or outlined by one thin, brightly-luminescent cement band, or less commonly by a zone that consists of up to five thin bands of alternating brightly luminescent and non-luminescent cement. Finally, pore centers are typically occluded by dull-luminescent calcite cement, which sometimes is vaguely subzoned. This cement zonation sequence is commonly observed in carbonate rocks, and has been explained as representing a progressive change in redox conditions during cement precipitation, from initial precipitation in highly oxidizing environments (such as the vadose zone, the shallow marine environment, and the upper portion of the meteoric phreatic zone) to final precipitation under reducing conditions in the deep phreatic zone and the burial diagenetic environment (Fairchild, 1983; Frank et al., 1982; Grover and Read, 1983; Machel, 1985; Srinivasan et al., 1989). In the Mosheim/Five Oaks tidal flat sequence, this three-phase zonation is especially common in larger pores, such as large fenestrae, fossil molds, and vugs. Smaller intergranular and fenestral pores very commonly are filled entirely by a single generation of non-luminescent cement. In general, zoned cements appear to be more common in samples collected from near the

Figure 4.5. Photomicrograph pair showing a cement-filled fenestra (left side) that is truncated by a vein (right half of photo), from just beneath the top of the Mosheim, Baptist Hospital. The long axis field of view in both photomicrographs is 1.5 mm. **A.** Under transmitted light, the cements filling the fenestra appear to be petrographically very similar to the vein calcite, except that the vein cement is more coarsely crystalline. **B.** The same field of view under cathodoluminescence. The fenestra cement is composed of zoned cement: an initial zone of non-luminescent (black) cement that rims the pore wall, and a second zone that includes alternating bands of bright and non-luminescent cement and becomes more dull toward the pore center. In contrast, the vein calcite is entirely dull, with a luminescence that is intermediate between the dull pore-central fenestral cement and the non-luminescent cement initial generation cement.


A
B

top of the tidal flat sequence, although zoned cements have been observed throughout the sequence. An interesting exception to this is that most pores in samples from the basal meter or two of the tidal flat sequence (i.e., samples interpreted to represent deposition on the inland algal marsh) are entirely occluded by non-luminescent cement, regardless of pore size. Three-phase cement zonations, and brightly-luminescent cements in particular, are more common in the Mosheim Member than in the Five Oaks Formation, where most cements are either non-luminescent or dull-luminescent.

Equant calcite cements from fenestrae just beneath the top of the Mosheim at the Baptist Hospital location were sampled and analyzed for stable isotope ratios. The $\delta^{18}O$ values obtained depleted relative to SMOW (standard mean ocean water) by a mean value of -6.64 (the range of values was -5.56 to -7.53), and were the most depleted of all calcite samples analyzed (Table 4.1; Figure 4.6). The $\delta^{13}C$ ratios of the samples, relative to the PDB standard, were not depleted (the mean was +0.07, and the range was from -0.29 to +0.38) (Table 4.1; Figure 4.6).

Equant calcite cements are typically composed of low-Mg calcite, and are generally accepted as an indication of calcite precipitation from meteoric fluids saturated with respect to calcium carbonate (Bathurst, 1975; James and Choquette, 1984; Jernigan and Walker, 1989; Longman, 1980; Roberson, 1989). Given that the Mosheim/Five Oaks tidal flat was subaerially exposed much of the time, and susceptible to influx of meteoric groundwater and rainfall, a meteoric origin in inferred for the equant calcite cements in this sequence. The luminescence (Figure 4.5) and stable isotopic signature (Figure 4.6) of these cements is consistent with a meteoric origin.

Table 4.1
Stable Isotope Data*

Sample #	Sample Type	δ18O	δ13C
BH8-V1	Equant vein calcite	-6.16	-0.14
BH8-V2	Equant vein calcite	-5.36	+0.21
BH8-V3	Equant vein calcite	-6.33	-0.08
BH8-V4	Equant vein calcite	-7.16	-0.30
	(Mean)	-6.25	-0.08
BH8-F1	Equant fenestral calcite	-7.23	-0.18
BH8-F4	Equant fenestral calcite	-7.53	-0.29
BH8-F5	Equant fenestral calcite	-6.22	+0.37
BH8-F7	Equant fenestral calcite	-5.56	+0.38
	(Mean)	-6.64	+0.07
BH8-F3	Fibrous calcite (dark)	-5.60	+1.26
BH8-F6	Fibrous calcite (white)	-5.58	-0.04
	(Mean)	-5.59	+0.61
BH8-M1	Mosheim micrite	-6.19	+0.61
BH8-M3	Mosheim micrite	-6.20	+0.07
BH8-S1	Mosheim internal sediment	-6.04	+0.28
	(Mean)	-6.14	+0.32
BH8-L1	Lenoir matrix	-6.24	-0.50
BH8-L2	Lenoir matrix	-6.27	-0.24
	(Mean)	-6.26	-0.37

*Samples were collected from either side of the Mosheim/Lenoir contact, Baptist Hospital section.

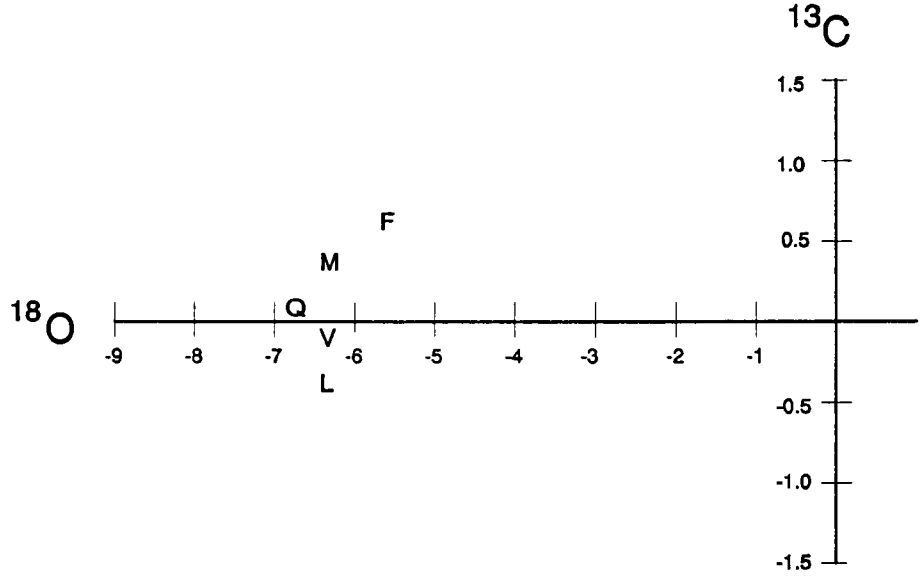


Figure 4.6. Stable isotope signatures of various diagenetic and depositional materials in the Mosheim. Abbreviations are as follows: F = fibrous calcite, L = Lenoir matrix, M = Mosheim matrix, Q = fenestral equant calcite, V = equant vein calcite.

Fibrous calcite

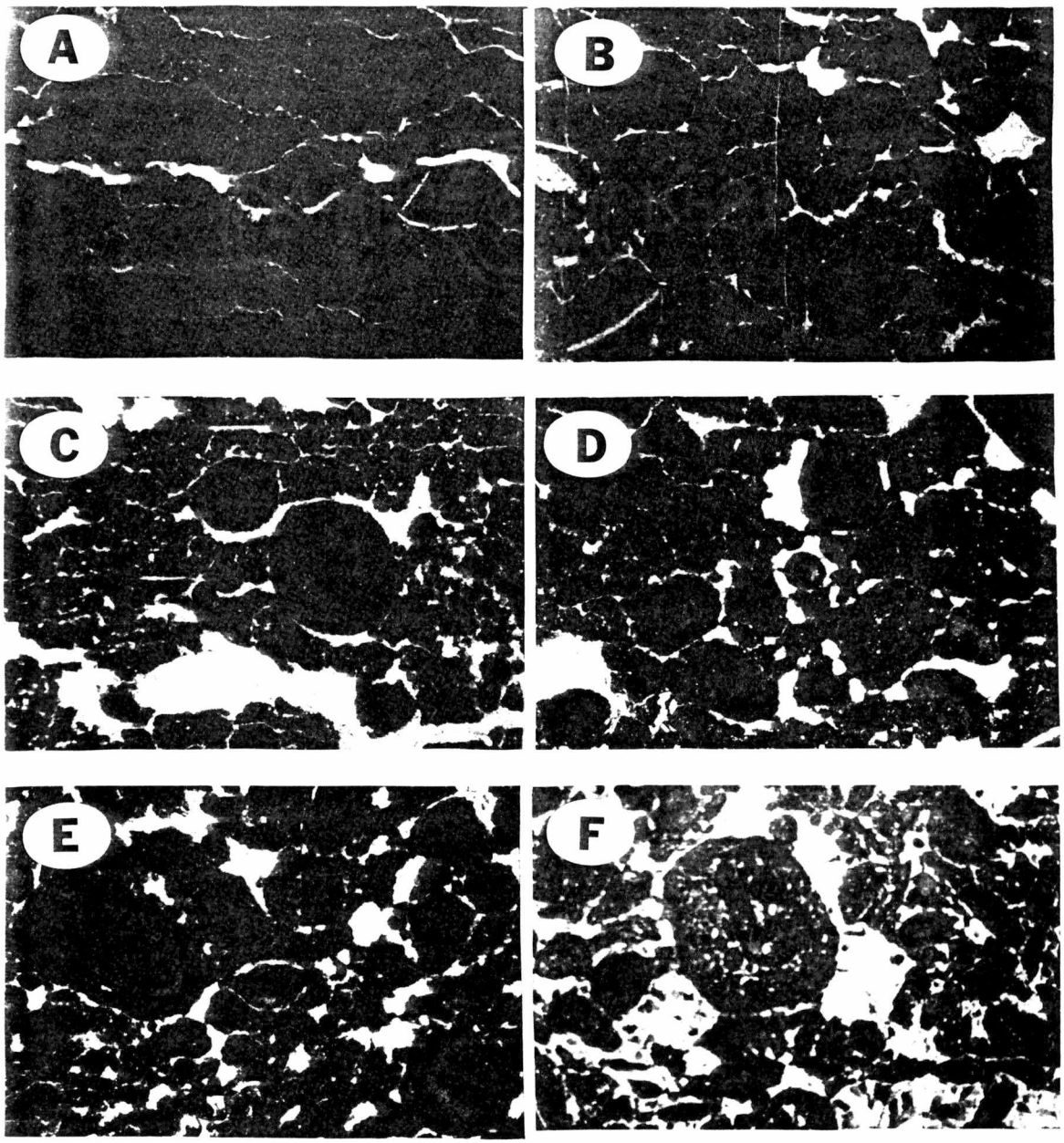
Fibrous calcite cement, characterized by crystals with a length to width ratio greater than 6:1 (Folk, 1965) is extremely scarce in the Mosheim, and has not been observed at all in the main body of the Five Oaks, although a minor amount is present in subtidal grainstones in the Blackford Member (see Figure 3.2D in Chapter 3). Fibrous calcite occurs in a few sheetcracks in brecciated, dolomitized supratidal crusts in the basal meter of the Mosheim, where it is the first (and in most cases, the only) generation of cement (Figure 4.3F). Near the top of the Mosheim, some large fenestrae and vugs that apparently connected to the erosional surface at the top of the unit also contain fibrous cement, but in these voids the fibrous cement was emplaced after initial precipitation of equant calcite.

Fibrous cement in this sequence has a brownish color in transmitted light, and is cloudy in appearance due to an abundance of inclusions. Under cathodoluminescence, the fibrous cements are black (nonluminescent), and stand out from the matrix, which is typically very dull orange. These cements are isotopically heavy (enriched in ^{18}O relative to the equant cements), and contrast with the equant cements (Table 4.2 and Figure 4.6). The nonluminescence and enrichment in heavy isotopes support the common interpretation that fibrous calcite cements probably precipitated from seawater (Bathurst, 1975; Davies, 1977; Folk, 1965; James and Choquette, 1983; James and Klappa, 1983; Jernigan and Walker, 1989; Kendall, 1985). These rare cements represent the only arguably marine cementation in the Mosheim/Five Oaks tidal flat sequence.

Micritic calcite

Unequivocal microcrystalline, or micritic, calcite cement in this sequence occurs only in limestones that exhibit well-developed diagenetic grainstone/pisolite texture. This diagenetic texture, which is discussed below under "Matrix alteration", is characteristic of intense vadose alteration of fenestral carbonates (Mazzullo and Birdwell, 1989). The diagenetic grainstone fabric occurs in several horizons in the Mosheim / Five Oaks sequence (Figure 4.7), but micritic cement has been observed only in zones that show the most advanced stages of this process (Figure 4.7D-F). In these highly altered limestones, the micritic cement occurs in meniscus positions, bridging gaps between adjacent pisoids and rounded mud lumps at their points of contact (Figure 4.7D,E). It is entirely likely that micritic cements occur elsewhere in the sequence, but because of their similarity with depositional micrite, they generally go undetected. One important difference between micrite and micritic cement has been observed, however. Under cathodoluminescence, micritic cements are strikingly non-luminescent, whereas the host micrite has a dull orange luminescence. The non-luminescent character of the micritic cement indicates that it probably precipitated either from marine water, or from highly oxidized meteoric water, such as exists in the vadose zone. The typical meniscus habit of the micritic cement and its association with the diagenetic grainstone / pisoid texture also support a vadose origin for the micritic cement, but do not resolve whether the cement precipitated from marine or meteoric fluids. Stable isotope analyses could provide this answer, but the cement areas are not large enough to be microsampled.

Figure 4.7. Progressive development of diagenetic grainstone/pisolite texture. A-F are thin section photomicrographs, taken under plane-polarized light. The long axis field of view in all photomicrographs is 6.5 mm. Samples are from various stratigraphic levels within the Mosheim Member at the Boyd's Creek Road and Nina sections. **A.** Initial formation of hairline laminoid fenestrae and segregation of mud into discrete mud lumps. **B.** Different area of the same thin section as A, showing more advanced redistribution of mud into lumps surrounded by thin, curved laminoid fenestrae (circumgranular cracks). Note the rounding and initial concentric lamination of some mud lumps (especially in the upper left quarter of the photo) as the lumps are transformed into pisoids. Also note the irregular fenestrae that had developed between some of the diagenetic "grains" in the upper right quarter of the slide. **C.** The same trends described in B are illustrated in this slide, but here the development of diagenetic grainstone texture and pisoids was arrested somewhat further along in the process. Note the well-developed spherical pisoid with multiple concentric laminations, just right of center, and the increased abundance of irregular fenestrae that had formed between grains. **D.** Similar to C, but with more pisoids and more even distribution of irregular fenestrae. Note that laminoid fenestrae are almost absent, having developed into irregular fenestrae as the mud lumps became more rounded. Also note the presence of micritic cements at the points of contact between the diagenetic grains. **E.** Well-developed diagenetic grainstone/pisolite texture, with very abundant "caliche-type" pisoids. The irregular fenestrae that had formed during early vadose diagenesis, simultaneously with the development of the diagenetic grainstone texture, are hardly recognizable as fenestrae, as they more closely resemble primary, intergranular pores. **F.** Very mature diagenetic grainstone texture, with essentially all original mud matrix reorganized and segregated into diagenetic grains and pisoids. Note the composite pisoid (composed of several smaller grains and pisoids) in the center of the slide. It should be pointed out that dolomite is virtually absent from these and all diagenetic grainstones observed in the Mosheim/Five Oaks sequence.


A
B
C
D
E
F

Baroque dolomite

White, megacrystalline dolomite (Morrow, 1982b), or baroque dolomite (Folk and Assereto, 1974), or saddle dolomite (Radke and Mathis, 1980), as it is often called, is present as a cement in fenestral and shelter pores in a few samples from one outcrop (John Sevier Highway). These cements possess the curved crystal faces and sweeping extinction characteristic of baroque dolomite, but are uncharacteristically non-ferroan, as indicated by staining with potassium ferricyanide. The samples that contain these cements were collected from immediately above the post-Knox unconformity, and the cements do not persist more than 5 cm above the unconformity. The close association of the baroque dolomite to the unconformity suggests that these cements may have precipitated from burial fluids that moved along the unconformity, and may be related to Mississippi Valley Type lead/zinc mineralization and dolomitization that is common in carbonate rocks along and beneath this unconformity in Tennessee and elsewhere (Bridge, 1956; Churnet, 1979; Harris, 1969, 1973; Hoagland et al., 1965; Kesler et al., 1989; Misra et al., 1989, 1992; Oder and Ricketts, 1961; Secrist, 1924; Wedow and Laurence, 1967). If burial fluids were the source of this dolomite, then the cements probably were precipitated during deep burial, or fairly late in the diagenetic history of the peritidal sequence. If that is the case, then the question remains as to how and why these few pores remained open well into burial, whereas virtually all other pores in the tidal flat sequence seem to have been occluded very early, prior to deposition of the immediately overlying limestones. That need not be the case, however. Instead of these pores remaining open, perhaps the baroque dolomite cement is a replacement of an earlier calcite phase. It is theoretically possible that the fluid from which the dolomite precipitated was simultaneously undersaturated with respect to calcite and saturated with respect to dolomite (Hanshaw et al., 1971; Badiozamani, 1973; Wigley and Plummer,

1976). Such a fluid could dissolve the first-generation calcite, and fill the ensuing void with dolomite cement. It is unknown why such a fluid would dissolve pore-filling calcite cements, but not dissolve the surrounding micrite matrix, unless this matrix was already dolomitized at the time. Another possibility is that this dolomite cement is not of burial origin, but instead precipitated from sulfate-rich seawater that locally collected and evaporated in an isolated, localized depression on the Knox surface as tidal flat deposition began. In summary, the origin of this very minor occurrence of baroque dolomite cement remains enigmatic.

Non-carbonate minerals

Authigenic minerals other than calcite and dolomite occur only rarely in isolated voids. These materials include pyrite, celestite, and silica. Though rare, pyrite has a fairly wide distribution throughout the sequence, and is certainly more common than fibrous calcite, micritic calcite, and dolomite cements. Pyrite generally occurs as subhedral, micrometer-sized framboids disseminated through the micrite matrix, but also occurs as a pore-filling "cement" in some of the smaller (<1 mm) fenestrae. When present as a cement, pyrite is usually associated with dull-luminescent, pore-central, equant calcite cement, and represents precipitation under reducing conditions. Celestite was observed partially filling a gastropod chamber in one sample in the Mosheim, and is associated in the same sample with the only observed occurrence of authigenic evaporite minerals (gypsum) in the tidal flat sequence. Silica is extremely rare as a pore-filling cement, but has been observed in a few fenestrae. Silica is slightly more common as a vein-filling mineral, but is most abundant in the sequence where certain strata in the northwesternmost strike belt have been pervasively silicified into chert. Silicification is discussed below in the section on matrix alteration.

Matrix Alteration

In addition to the diagenetic processes involved in the formation and occlusion of secondary porosity, diagenesis in the Moshiem / Five Oaks sequence involved several processes that altered the original lime mud matrix to rigid limestone. These processes operated concurrently with the development of porosity and early cementation, and included mineralogic stabilization and lithification of the matrix, development of diagenetic grainstone and pisolite fabrics, partial replacement of lime mud by dolomite, and very minor replacement by authigenic silica, pyrite, and negligible amounts of evaporite minerals. These diagenetic processes are discussed below.

Diagenetic grainstone / pisolite fabrics

Diagenetic grainstone texture

Highly fenestral supratidal beds in the Mosheim / Five Oaks tidal flat sequence commonly contain layers and/or lenses of a distinctive lithology that, according to the carbonate classification scheme of Dunham (1962), would be classified as grainstones. These limestones consist of discrete lumps of micrite, some almost perfectly spherical, that are surrounded and separated by irregular fenestrae and curved, laminoid fenestrae (in this case, the laminoid fenestrae are equivalent to circumgranular cracks in pedogenic carbonates; Wright and Tucker, 1991). Most fenestrae are filled with equant calcite cement (Figure 4.7), but some contain significant amounts of vadose silt. These rocks are essentially devoid of "loose" matrix; hence their classification as grainstones. However, there is no evidence, such as grading, lamination, or other sedimentary structures, to suggest that these lumps are depositional grains. On the contrary, it is

apparent that these grain-supported lithologies were formed *in situ* by diagenetic alteration. The process by which mudstones are converted into "diagenetic grainstones" is a type of textural inversion referred to as "grainification" by Wright and Tucker (1991). Grainification is commonly observed in subaerially exposed, pedogenic carbonates (calcretes) (Wright and Tucker, 1991). The formation of diagenetic grainstones from fenestral mudstones was discussed and demonstrated experimentally by Mazzullo and Birdwell (1989). It is apparent from Mazzullo and Birdwell (1989) that the formation of diagenetic grainstones is not necessarily a discrete, pedogenic process, but can also be a continuation of the development of fenestral porosity in the vadose environment. This appears to have been the case in the Mosheim/Five Oaks facies. Figure 4.7 illustrates several stages in the alteration of fenestral mudstones to diagenetic grainstones. Production of diagenetic grainstones results from "the progressive development, enlargement, and coalescence of fenestrae in muddy carbonate sediments" (Mazzullo and Birdwell, 1989), and involves redistribution and reorganization of lime mud from diffuse patches into discrete lumps. During this process, many of these lumps become coated by micrite envelopes and transformed into pisoids (Figure 4.7) that provide further evidence of development under vadose conditions (Peryt, 1983). The development of pisoids is discussed further in the following section.

Diagenetic grainstones in the Mosheim / Five Oaks occur at various levels within the sequence, but are always associated with supratidal sediments. Their development is concomitant with secondary porosity development, and may precede or occur simultaneously with the onset of cementation. The process is taken to indicate very early post-depositional alteration in the vadose zone. As pointed out by Mazzullo and Birdwell (1989), it is not clear what type of fluids are required for this vadose process. Diagenetic grainstones in the Permian Tansill Formation of New Mexico are associated with extensive dolomitization and evaporite precipitation (Mazzullo and Birdwell, 1989), yet

identical features in the Mosheim / Five Oaks contain neither dolomite nor evaporites. In fact, diagenetic grainstones contain the lowest dolomite content (essentially zero) of any lithology in the Mosheim / Five Oaks sequence. It is believed that supratidal sediments in the sequence underwent extensive leaching by unsaturated meteoric fluids (rain) in the vadose zone, as indicated by very low trace element (Mg, Mn, Fe, Sr) contents (Johnson, 1988). It is obvious, then, that the formation of diagenetic grainstones does not require hypersaline fluids, and at least in this case, appears to indicate freshwater diagenesis.

Pisoids and caliche

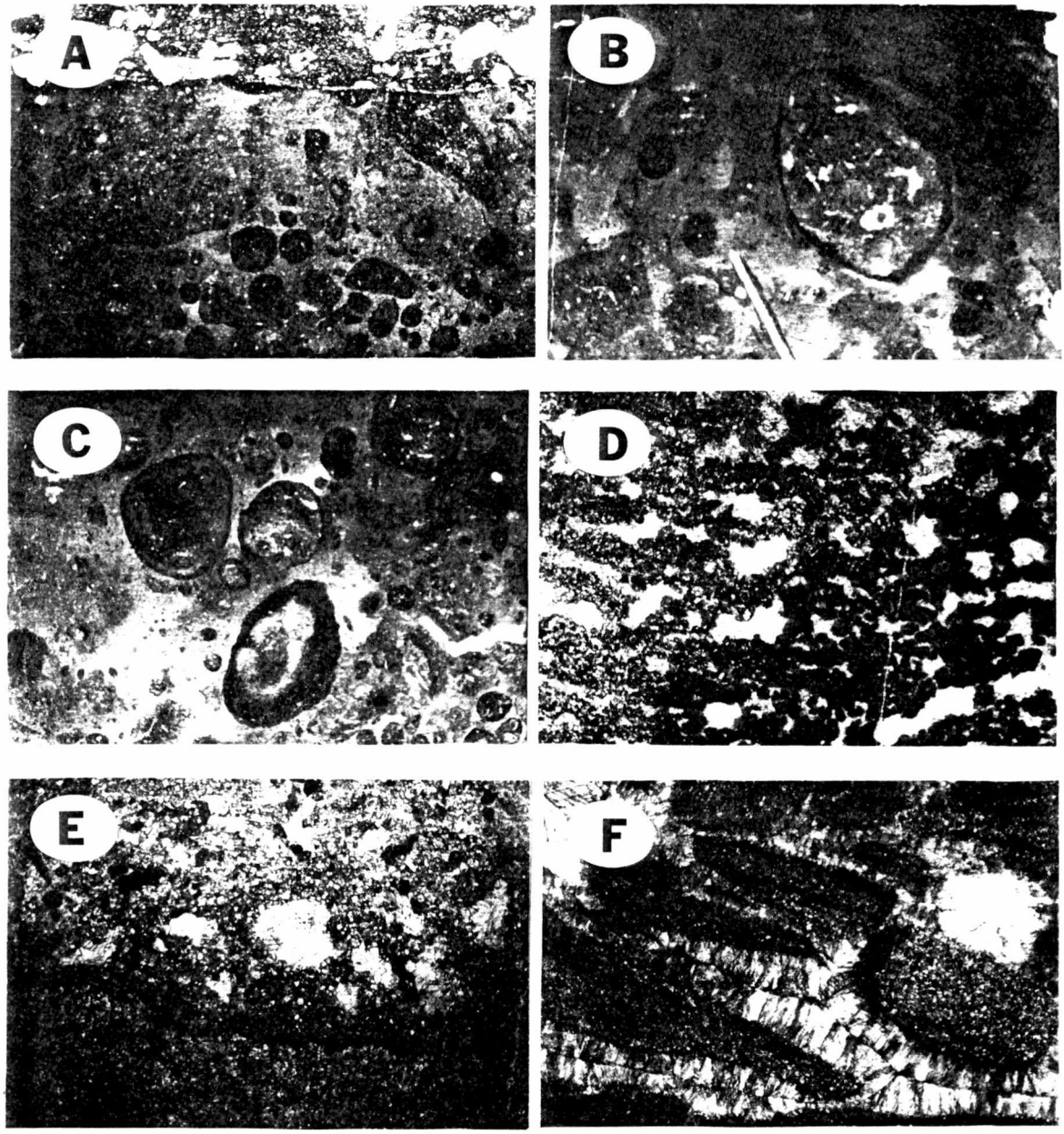
Many supratidal portions of the Mosheim / Five Oaks sequence, especially horizons where diagenetic grainstone texture is well-developed, contain abundant pisoids (Figures 4.7). Pisoids are $CaCO_3$-coated grains that, unlike oncoids and ooids, form not by depositional processes, but during vadose diagenesis (Peryt, 1983). Pisoids form in a variety of vadose settings, including caves, hypersaline tidal flats, and caliches. On the basis of characteristic physical features, Esteban (1976) differentiated between pisoids that form from freshwater ("caliche pisolite") and those that form from marine or hypersaline water ("vadose pisolite"). Esteban's classification, however, has been criticized as being overgeneralized (Chafetz and Butler, 1980; Peryt, 1983), because of much overlap between his two varieties. For example, Chafetz and Butler (1980) reported recent pisoids in the Cretaceous Edwards Formation of central Texas that are associated with spelean carbonates and apparently formed from meteoric fluids, yet more closely resemble the marine vadose pisoids of Esteban (1976) than typical caliche pisoids. For further evidence of the controversy over the origin of pisoids, note the different opinions published on the origin of the pisolite facies of the Permian Capitan Reef Complex of west Texas and New Mexico (Dunham, 1969b; Kendall, 1969; Scholle and

Kinsman, 1974; Esteban, 1976; Esteban and Pray, 1983). Because of the difficulty in determining specific origin, and because both freshwater and marine pisoids form in the vadose environment, Peryt (1983) proposed the term "vadoid" to include both varieties. Peryt (1983) suggested that the genesis of specific vadoids be determined not from the nature of the vadoids themselves, but through consideration of "the entire sedimentological and geological background setting" of the pisolite facies.

Pisoids in the Mosheim / Five Oaks sequence typically consist of a nucleus that is generally composed of a lump of micrite, surrounded by an envelope of micrite that in thin section appears darker than the nucleus (Figures 4.7 and 4.8A-C). Some pisoids, however, have as a nucleus a grapestone-like aggregrate of several micritic peloids (Figures 4.7F and 4.8B). The envelopes are entirely micritic and vaguely laminated if laminated at all, and show no evidence of alteration from radial fibrous crystal fabrics. Sizes of pisoids range from about 0.3 mm to 8 mm, but the typical size is about 1 mm. These pisoids are virtually identical to pisoids from caliche horizons illustrated by James (1972), Harrison and Steinen (1978), and Calvet and Julia (1983), and the "caliche pisoids" of Esteban (1976); they do not at all resemble the larger and more distinctly laminated "vadose pisoids" of the Permian Reef Complex, as illustrated in Dunham (1969), Esteban (1976), Esteban and Pray (1983), Peryt (1983), or the spelean-associated, concentrically-laminated pisoids from the Edwards Formation (Chafetz and Butler, 1980).

In the Mosheim/Five Oaks sequence, pisoids occur embedded in two types of matrix. Typically, pisoids occur as distinct spherical grains in highly fenestral lithologies, especially those in which the diagenetic grainstone texture is well developed. In these lithologies, the pisoids are surrounded by fenestral pores and lumps of micrite (Figure 4.7). These pisoids are undoubtedly products of the same matrix-altering process that produced the diagenetic grainstone texture, as discussed above. That is, they formed by

Figure 4.8. Matrix alteration in the Mosheim/Five Oaks tidal flat sequence. All photos are thin section photomicrographs taken under plane-polarized light. The long axis field of view in A, D, E, and F is 6.5 mm; in B and C the long axis field of view is 1.5 mm. A - C show incipient caliche and pisoids; D - F illustrate dolomitization in the basal portion of the sequence. **A.** The top of the Mosheim and its contact with the overlying Lenoir Formation, Baptist Hospital. Here the upper Mosheim was pervasively altered by vadose processes to an incipient caliche. The original lithology, which was probably a fenestral mudstone, on the basis of stratigraphic and lateral association with preserved fenestral lithologies, is not recognizable as such. Note how the abundant pisoids appear to "float" in a chalky, micritic, cryptocrystalline matrix. The erosional surface at the top of the Mosheim sharply truncates all of these early vadose diagenetic features, and indicates that the caliche texture had formed prior to the formation of the erosional surface and deposition of the overlying subtidal lithology. **B** and **C** are enlargements of different fields of view within the same thin section. **D.** Dolomitization front in fenestral intraclastic packstone, basal Mosheim, 0.6 m above the Knox unconformity (AKU), Boyd's Creek Road section. The lower right half of the photomicrograph consists of relatively undolomitized mud intraclasts and equant cement-filled fenestrae, whereas the upper left half consists of the same lithology after dolomitization. Note that even in the portion of the slide where the matrix is heavily dolomitized, fenestrae are filled with equant calcite cement. This suggests that occlusion of porosity by equant calcite cement preceded dolomitization. **E.** The Knox unconformity at the Nina section, with heavily dolomitized, fenestral intraclastic packstone of the basal Mosheim overlying dolostone of the Mascot Formation (Knox Group). The unconformity surface, though clearly visible in this thin section, had "healed" to some extent during the dolomitization of the basal Mascot. The unconformity appears much more sharp in hand sample and at the outcrop than in thin section. **F.** Laminated, dolomitic crusts broken up by shrinkage cracks into an *in situ* "flat-pebble conglomerate", 0.4 m AKU, Boyd's Creek Road.


A
B
C
D
E
F

redistribution and aggradation of micrite during meteoric vadose alteration of fenestral mudstones.

At one outcrop of the upper Mosheim (Baptist Hospital), however, pisoids occur in a different lithology. Here, in a few horizontally-elongate lens-shaped bodies only a few cm thick, pisoids are embedded in a chalky, micritic matrix similar to the cryptocrystalline matrix described by James (1972) and Calvet and Julia (1983), or appear to "float" in equant calcite cement or a mixture of cement and micrite (Figure 4.8A-C). In these lenses, the limestone has been so altered by diagenetic processes that the original lithology cannot be determined. The presence of fenestrae is not obvious; however, these lenses are laterally and stratigraphically associated with fenestral lithologies, and probably represent zones where the original fenestral fabric has been obscured during alteration. It is suggested that these pisolite lenses represent localized zones on the tidal flat where prolonged subaerial exposure and particularly intense vadose alteration led to incipient soil formation. The similarity of these zones to pisolitic horizons in modern and ancient caliches is striking (compare Figure 4.8A-C of this paper with Figure 9 of James, 1972; Figures 7a and 7b of Harrison and Steinen, 1978; and Figure 2f and 2g of Calvet and Julia, 1983), and suggests that the pervasively altered pisolite zones in the Mosheim are indeed of pedogenic origin, and represent thin accumulations of incipient caliche. It should be stressed, however, that this caliche is poorly developed, and lacks many of the features typically associated with caliche, such as laminated crusts (Multer and Hoffmeister, 1969; James, 1972; Harrison and Steinen, 1978), well-developed soil profiles (Esteban and Klappa, 1983), and *in situ* brecciation fabrics (Harrison and Steinen, 1978; Klappa, 1980; Ettensohn et al., 1988). The absence of such features may be related to environmental factors that inhibited, or were not conducive to, caliche formation. Given their formation on an active tidal flat, it is certainly possible that caliche development was arrested in infancy by resumed

sedimentation after a period of subaerial exposure. Deposition and early diagenesis in a climate which was too humid to promote caliche formation (Aristarain, 1970; Reeves, 1970; James, 1972) could have been responsible for the immature caliches. Yet another likely reason for the poorly developed caliches is their formation during the Middle Ordovician, prior to the appearance of land plants (Gensel and Andrews, 1987). Considering the critical role played by plant roots in the development of modern caliche profiles, pre-Devonian caliches would be expected to be different in ways difficult to predict (Esteban and Klappa, 1983).

In summary, the occurrence of pisoids in the Mosheim / Five Oaks sequence is clearly associated with highly fenestral, supratidal lithologies, and their origin was through diagenetic alteration of fenestral mudstones in the vadose environment. These pisoids are very similar to pisoids in many ancient and recent caliches, and are unlike pisoids whose formation has been attributed to marine or hypersaline vadose waters. In this regard, it is interesting that Esteban (1976) interpreted the hypersaline "vadose pisolite" facies as "a depositional facies closely related to the fenestral (keystone) grain-supported facies". The pisoids in the Mosheim / Five Oaks are obviously related to supratidal fenestral grainstones, yet their "caliche pisoid" textures suggests an origin related to incipient pedogenic processes in the freshwater vadose zone. There is little reason why soils should not be found in ancient tidal flat sequences like the Mosheim / Five Oaks, for soil development has been reported on supratidal hammocks on Andros Island (Hardie and Garrett, 1977) and on Eleuthera in the Bahamas (Foos, 1991). These subenvironments are subaerially exposed nearly 100% of the time (inundated only during hurricanes), and are essentially terrestrial islands within the tidal flat complex, complete with land plants and potable fresh water (Hardie and Garrett, 1977). The pisolite horizons within the Mosheim probably formed in analogous, meteoric-dominated, supratidal subenvironments of the basal Middle Ordovician tidal flat. This interpretation

is supported by the absence of features that indicate hypersalinity, and the association with an abundance of features indicative of meteoric diagenesis in the Middle Ordovician tidal flat sequence.

Matrix lithification and stabilization

Matrix lithification, or the diagenetic alteration of carbonate mud to micrite and / or microspar, is a complex process that has received much discussion (especially Folk, 1965, 1974; Bathurst, 1975; Steinen, 1978, 1982; Lasemi and Sandberg, 1984; and Moshier, 1987, 1989). Recent work, however, indicates that lime mud diagenesis can be viewed simply as micro-scale dissolution and reprecipitation, accompanied by compaction (Moshier, 1989), and in that regard, does not differ greatly from the well-known processes of porosity development and cementation, except in scale. During matrix lithification, a very porous mass of mud (initial porosities of 50 - 70%) is transformed into a nonporous, calcite crystal mosaic (porosities typically 5% or less) (Moshier, 1989). The decrease in porosity is accomplished primarily through precipitation of cements in micropores and an increase in average particle size (Lasemi and Sandberg, 1984; Moshier and McManus, 1986), but is facilitated by mechanical compaction during shallow burial and chemical compaction (pressure solution) during deep burial (Moshier, 1989). Porosity reduction is accompanied by a decrease in permeability as pore networks are disrupted and reorganized, and pore throats decrease in diameter or are blocked due to cementation and compaction (Moshier, 1989).

Porosity reduction in lime muds is accompanied by, and to a great extent, driven by mineralogic stabilization of aragonite or high-Mg calcite to low-Mg calcite, or the reorganization of crystals without mineralogic change in muds composed of original low-magnesium calcite. Regardless of original mineralogy, the micrite produced through lime

mud diagenesis will be composed of low-Mg calcite; textural parameters such as average grain size and the amount of intercrystalline porosity, however, are controlled by the original mineralogy of the mud, and the degree of rock / water interaction (Lasemi and Sandberg, 1984; Moshier, 1989). According to Lasemi and Sandberg (1984), micrites derived from calcite-dominated precursor muds will have fine equant texture because of the abundance and close spacing of calcite seed crystals, upon which cements will nucleate, whereas alteration of aragonite-dominated precursor muds results in coarser microspar textures that reflect precipitation on widely spaced calcite nuclei. Micrites of aragonite derivation should be characterized by elevated strontium content, relative to calcite-precursor micrites, or should contain relic aragonite inclusions (Sandberg, 1984; Moshier, 1989).

Textures of shelf and peritidal micrites from the Middle Ordovician of East Tennessee (including the Mosheim and Five Oaks units) were studied using SEM techniques by Johnson (1988). These micrites consist of equant to subequant calcite crystals that exhibit a bimodal grain size distribution, with a prominant mode at 4 - 6 μm and a minor one at 10 - 12 μm. Acid-etched grains of the dominant, smaller size mode have rough surfaces caused by very fine blebs of material (microdolomite inclusions?) that stand out in micro-relief from the groundmass of the grains, but lack pits and molds indicative of mineral-specific dissolution. Johnson (1988) interpreted these smaller grains to be slightly enlarged depositional mud particles. The less abundant, larger-sized grains are inclusion-poor and have smooth surfaces, and approximate the size range of low-Mg calcite microspar cements that fill micropores in Pleistocene carbonates (Steinen, 1978). Johnson (1988) interpreted these larger crystals as micropore-filling low-Mg calcite cements.

Because the Middle Ordovician micrites possess textures dominated by unpitted, "micrite"-sized (5 μm) particles, and lack abundant microspar-sized crystals, they closely

resemble micrites formed through alteration of calcite-dominated precursor muds (Lasemi and Sandberg, 1984). On the basis of this textural evidence, Johnson (1988) interpreted an original magnesian calcite mineralogy for the Middle Ordovician micrites. Johnson (1988) determined this calcitic mud to be of biotic, not physicochemical, origin. Inorganic precipitation of calcium carbonate generally requires hypersaline conditions in the depositional environment (Broecker and Takahashi, 1966), but evidence for hypersalinity, such as evaporite minerals or pseudomorphs, or high sodium content, is lacking from the basal Middle Ordovician sequence (Johnson, 1988).

Whole-rock trace element analyses on the Middle Ordovician micrites support an original magnesian calcite mud mineralogy. A cross-plot of magnesium versus strontium content in these shelf limestones defines a field that coincides with the idealized trend for equilibrium stabilization of magnesian calcite to calcite under meteoric diagenesis (Johnson, 1988). Even the most Sr-enriched samples (>500 ppm) plot closer to the Mg-calcite equilibration trend than the aragonite equilibration trend. Samples from across the shelf (peritidal, inner shelf, and outer shelf facies) show little variation from this trend, and all indicate an original magnesian calcite-dominated precursor mud (Johnson, 1988).

Peritidal facies (Mosheim and Five Oaks) have trace element compositions that are more depleted in Sr, Fe, and Mn than overlying Middle Ordovician shelf samples. Johnson (1988) interpreted the peritidal limestones to represent a facies (his Geochemical Facies II) that is geochemically distinct from other Middle Ordovician limestones. The more depleted trace element values (Table 4.2) indicate more complete alteration by meteoric fluids, and diagenesis in a system open to addition of undersaturated fluids. These interpretations are consistent with deposition and synsedimentary diagenesis in a humid tidal flat environment. Although samples from this facies show significant depletion in Sr, Fe, and Mn, their Mg concentrations are among the highest of the Middle Ordovician facies. The elevated magnesium content reflects the presence of significant

Table 4.2
Elemental Geochemistry of Tidal Flat Dolomicrites*
(from Johnson, 1988)

	Mg	Sr	Mn	Fe
Five Oaks Formation	5280	176	25	208
	5570	176	21	175
	7230	179	32	284
Mosheim Member	9870	257	34	626
	10500	254	34	586
	20100	287	27	673
	10700	292	24	454

*All concentrations are in parts per million (ppm)

amounts of dolomite in some (though not all) samples, particularly near the basal contact of the sequence with the underlying Knox dolostones. Possible origins for this dolomite are discussed below.

Dolomitization

Characteristics and distribution of dolomite

Dolomite is relatively uncommon in the basal Middle Ordovician peritidal sequence, particularly when compared with other ancient tidal flat sequences in the geologic record. Dolomite occurs predominantly in the form of finely to very finely crystalline, subhedral to euhedral rhombohedra that are disseminated throughout the matrix. The majority of this dolomite is not directly associated with stylolites, as is the case for much of the dolomite in the overlying Middle Ordovician units. On the basis of petrographic and SEM observations, this dolomite appears to be matrix-replacive (Johnson, 1988). Pore-filling dolomite cements occur, but are far less abundant than matrix-replacive dolomite. Dolomite content in the Moshiem/Five Oaks tidal-flat limestones is generally less than ten volume percent, and commonly on the order of 2 to 5%, as determined through visual estimates of stained thin sections. Some samples are totally devoid of dolomite rhombs large enough to be seen through conventional microscopy. Bulk-rock analyses of magnesium content (Johnson, 1988) support these petrographic observations. The overall paucity of dolomite is reflected in the fact that the Mosheim is extensively quarried throughout the southern Appalachians for industrial high-calcium lime, for which very low magnesium content is required (Butts, 1940; Puckett, et al., 1990). Supratidal dolomite crusts and pervasively recrystallized beds of dolostone are absent from the tidal flat facies (the Mosheim Member and the main body

of the Five Oaks Formation). Bedded dolostones are common, however, in the underlying, basalmost Middle Ordovician depression-filling deposits (the Douglas Lake and Blackford Members).

Dolomite occurs as widely disseminated rhombs throughout the tidal flat sequence, but as a rule, its abundance decreases upward. This decrease is not gradual; instead, there is a fairly abrupt decrease in dolomite abundance about a meter above the base of the sequence. In places, there are patches of more highly dolomitized matrix surrounded by less dolomitized matrix (Figure 4.8D). The most highly dolomitized strata in the tidal flat facies occur in the basal meter of the Mosheim, where samples typically contain 20 - 30% dolomite. In these basal samples, the micrite matrix is extensively dolomitized, but pores large enough to be observed through conventional petrography are typically filled with equant calcite cement (Figures 4.3B,C and 4.8D,E), or rarely, fibrous calcite cement (Figures 4.3F and 4.8F). Some basal supratidal lithologies consist of laminated dolomitic micrite that has been parted by sheet cracks (Figure 4.3F) or broken up into *in situ* breccias (Figure 4.8F). Some conglomeratic lithologies at the base of the sequence contain abundant, redeposited lithoclasts of Knox dolostone, and accordingly, have higher total dolomite content than samples that lack dolostone clasts. A few samples immediately above the post-Knox unconformity consist entirely of dolomite, with matrix totally replaced and all porosity filled by baroque dolomite cements. Above these basal beds, however, dolomite content is consistently quite low.

In addition to the matrix-replacive dolomite, a minor amount of pore-filling dolomite cement occurs in the sequence. Dolomite cements occur in two varieties. Rare, non-ferroan, baroque dolomite cements fill fenestrae in a few samples immediately above the base of the Mosheim (within 5 cm of the post-Knox unconformity). These have been discussed above in the section on cements. Scanning electron microscope (SEM) photos in Johnson (1988) also show amorphous mineral aggregations that fill interparticulate

microporosity in some dolomicrites. This material is more resistant to acid etching than the host micrite and connects to dolomite rhombohedra, and is therefore interpreted to be dolomite cement (Johnson, 1988). These micropore-filling cements are very similar to the "amoeba-shaped" dolomite cements described in Carballo et al. (1987). Like matrix-replacive dolomite, micropore-filling dolomite cements are most abundant near the base of the sequence.

Dolomite abundance also appears to be influenced by factors other than stratigraphic position, such as lithology and depositional environment. Interestingly, supratidal lithologies in the Mosheim / Five Oaks sequence (except those at the base of the sequence) typically contain the *least* dolomite, and are the lithologies most commonly devoid of dolomite. In this respect, this tidal flat differs significantly from most other ancient tidal flat sequences. The highest dolomite abundances through the bulk of the sequence generally occur in bioturbated subtidal pond lithologies, in which dolomite is preferentially concentrated in burrows where secondary permeabilities may have been higher.

Sources of magnesium ions for dolomitization

Morrow (1982a, b) states that three conditions are required for dolomitization: an adequate source of Mg^{++} ions, a mechanism for the delivery of Mg^{++} ions to the site of dolomitization, and suitable solution chemistry. The necessary solution chemistry for dolomitization is controlled by three parameters: the Mg/Ca ratio, the CO_3/Ca ratio, and the ionic strength or total salinity of the solution (Morrow, 1982a).

The distribution of dolomite within the Mosheim / Five Oaks tidal flat sequence offers many clues about possible sources for the magnesium ions necessary for dolomitization. Three likely Mg^{++} sources are discussed here: 1) seawater;

2) stabilization of original Mg-calcite to calcite; and 3) dissolution of pre-existing (Knox) dolostones. It is believed that none of these sources provided all the Mg^{++} used in dolomitization. Rather, it is more likely that each of these sources, and possibly others as well, contributed magnesium ions to the diagenetic system.

One very likely source of magnesium is the seawater circulated through the tidal flat system by tidal pumping. Seawater is often cited as a source of Mg^{++} ions for dolomitization (Morrow, 1982b; Hardie, 1987), and certainly must be considered as a possible source here. During deposition of the Mosheim / Five Oaks tidal flat sediments, sea water was funneled landward across the tidal flat into shallow subtidal ponds by a system of tidal channels analogous to those on the Andros Island tidal flat (Shinn, et al., 1969; Hardie and Garrett, 1977). Thus, during periods of normal high tides, subtidal and intertidal portions of the tidal flat were inundated by normal marine water. During storms, supratidal parts of the tidal flat were also inundated by seawater. Although this seawater was probably mixed with meteoric water that flowed through the sediments as groundwater or entered the sediments and ponds as rainfall, it still was an essentially constant provider of Mg^{++} ions to submerged surface sediments and to any sediments shallowly buried beneath the tidal flat surface. Thus, seawater was a likely source of Mg^{++} for the penecontemporaneous dolomitization of shallow subtidal pond lithologies, which, as stated above, generally contain the highest amounts of dolomite in the tidal flat sequence. Subaerially-exposed intertidal and supratidal lithologies would receive less Mg^{++} from seawater, and would be less susceptible to dolomitization in this manner. During extended dry periods, evaporative pumping could draw concentrated seawater into supratidal sediments and conceivably induce dolomitization in the manner described by Hsu and Siegenthalar (1969), McKenzie et al. (1980), and Carballo et al. (1987), but there is no evidence that this process occurred in this Middle Ordovician sequence. As

stated above, supratidal sediments typically contain the lowest dolomite abundances in the sequence.

An autogenic source of magnesium, favored by Johnson (1988), is provided by the exsolution of Mg^{++} ions from inferred high-Mg calcite precursor muds during stabilization to low-Mg calcite, a process referred to as autocannibalism (Machel and Mountjoy, 1986) or solution cannibalism (Goodell and Garman, 1969). This magnesium would be leached from magnesian calcite by meteoric waters percolating downward through the tidal flat muds, and reprecipitated as dolomite rhombohedra in stratigraphically lower portions of the sequence. This process is attractive for the following reasons. First, it explains the scarcity of dolomite in lithologies that bear evidence of extensive subaerial exposure, which would be subjected to the most extensive leaching by undersaturated meteoric waters in the vadose and uppermost phreatic zones. Second, the downward mobilization of Mg^{++} is at least consistent with the increase in dolomite (and total magnesium concentration) in the lower portions of the sequence.

A third possible source of Mg^{++} ions could be the release of Mg^{++} from pre-existing dolostone bodies during meteoric diagenesis. Some Mg^{++} could be derived from dolostone lithoclasts that are abundant in conglomeratic limestones near the base of the Mosheim and in the Blackford Member of the Five Oaks Formation. These clasts represent redeposited detritus from the Knox Group, and consist of a type of dolomite that is different from the authigenic dolomite in the surrounding micritic matrix. These clasts offer proof that the Knox Group was thoroughly dolomitized (and lithified) prior to Middle Ordovician deposition. An interesting, common feature of these dolostone clasts are dedolomite reaction rims. Magnesium ions exsolved from these clasts during dedolomitization could have been reprecipitated as authigenic dolomite in the surrounding matrix. It is difficult to envision a chemical environment in which dedolomitization and dolomitization could occur simultaneously; however, it is possible

that exsolved Mg^{++} ions were transported in solution to another area where the pore fluids were supersaturated with respect to dolomite, and there precipitated in the form of dolomite (Back et al., 1983). It is doubtful that dedolomitization of lithoclasts provided Mg^{++} to solution in quantities large enough to produce much dolomite. However, it is possible that a minor amount of Mg^{++} provided in this manner was responsible for some of the dolomite near the base of the section.

Wholesale dissolution of Knox dolostones by meteoric waters flowing downward and seaward along the post-Knox unconformity from recharge areas to the northwest could provide a much more abundant supply of Mg^{++} ions for dolomitization of the tidal flat sediments. Although dissolution of dolostone would provide Ca^{++} ions to solution at the same rate as Mg^{++} ions, this process could still increase the Mg/Ca ratio if the original solution was Mg-poor, as meteoric solutions generally are. It would also raise the CO_3/Ca ratio, and would elevate the total salinity of the solution, and could therefore provide favorable solution chemisty for dolomitization (Morrow, 1982a,b). If fluids supersaturated with respect to dolomite were moving along the post-Knox unconformity, and were indeed capable of dolomitization, the basal Middle Ordovician strata immediately overlying the unconformity would be the most susceptible to dolomitization. As stated above, these beds are the most highly dolomitized of all the Middle Ordovician peritidal lithologies.

It is also quite possible that Mg-rich fluids expelled from compacting Middle Ordovician basinal shales moved shelfward along the post-Knox unconformity during deep burial. Such fluids could be responsible for some of the dolomitization of the basal Middle Ordovician strata, especially in the more recrystallized dolomicrites overlying the unconformity. Fluid migration along this unconformity surface has been invoked to explain Mississippi Valley-type mineralization, which is associated with extensive dolomitization (Bridge, 1956; Churnet, 1979; Harris, 1969, 1973; Hoagland et al., 1965;

Kesler et al., 1989; Misra et al., 1989, 1992; Oder and Ricketts, 1961; Secrist, 1924; Wedow and Laurence, 1967). Mississippi Valley-type dolomites, however, are typically ferroan, and commonly occur as megacrystalline, baroque (saddle) dolomite, and therefore differ from the finely crystalline, non-ferroan dolomite that is most abundant in the Mosheim and Five Oaks. The minor amount of baroque dolomite cement at this stratigraphic level may have been precipitated from burial fluids.

In summary, there are several likely sources that could have furnished Mg^{++} ions for dolomitization in the Mosheim / Five Oaks sequence. Highly dolomitized limestones within the basal meter of the sequence could have received Mg^{++} from penecontemporaneous interaction with seawater, downward percolation of waters enriched in Mg^{++} derived from the stabilization of high-Mg calcites, and groundwaters saturated with ions derived through cannibalization of Knox dolostones. Slightly dolomitized subtidal limestones could have received Mg^{++} from tidal pumping of seawater, or from chemical equilibration of overlying, subaerially exposed, Mg-calcite sediments.

Given that there are several plausible sources of Mg^{++} ions for dolomitization of the Middle Ordovician peritidal sediments, it is perhaps surprising that dolomite is as uncommon as it is. The scarcity of dolomite, however, is consistent with, and indicative of, the meteoric-dominated hydrologic system inferred to be responsible for the diagenesis of these sediments. A model for this non-pervasive dolomitization is presented below.

Dolomitization model

A model for the dolomitization of the basal Middle Ordovician peritidal limestones must take into account the following features:

1) Dolomite is primarily in the form of finely to very finely crystalline rhombs scattered throughout the matrix. Coarse dolomite fabrics and pervasively dolomitized zones are essentially absent from the tidal-flat facies.

2) Dolomite is primarily matrix-replacive, although a very minor amount is pore-filling cement.

3) Dolomitization appears to be related to, and played an important role in, matrix lithification. Because matrix lithification occurred very early, most of the dolomite was probably early (pre-burial) as well.

4) Dolomite abundance is greatest in the basal meter of section, and decreases upward.

5) Supratidal lithologies generally lack dolomite. Dolomite abundance is greater in shallow subtidal lithologies.

6) Dolomite is not associated with evidence of hypersalinity. Evaporite minerals and evaporite molds are absent and Na+ contentis low.

7) Very little dolomite is directly associated with stylolites.

8) Possible sources of Mg^{++} include seawater, stabilization of original Mg-calcite muds, and dissolution of Knox dolostones.

Of the published dolomitization models reviewed by Morrow (1982b), Machel and Mountjoy (1986), and Hardie (1987), most are inappropriate for explaining the Mosheim/ Five Oaks dolomite. The seepage reflux model (Adams and Rhodes, 1960; Deffeyes et al., 1965) and its supratidal variant, the sabkha model (Illing et al., 1965;

Patterson and Kinsman, 1981, 1982), are not viable models for this sequence because both require hypersalinity and association with evaporite minerals. The theory whereby dolomitization occurs as a result of redistribution of Mg^{++} from Mg-calcite during pressure solution (Logan and Semeniuk, 1976; Wanless, 1979) can only explain the minor amounts of dolomite that are clearly associated with stylolites. Another problem with the pressure solution model is that most of the Mosheim / Five Oaks dolomite is believed to have formed before burial, and thus before the onset of pressure solution. The burial compaction model (Jodry, 1969; Mattes and Mountjoy, 1980; Morrow, 1982b), in which dolomitization results from Mg-rich fluids expulsed during compaction of shales, or from other sources (Machel and Mountjoy, 1986), could be used to explain some of the Mosheim / Five Oaks dolomite, particularly immediately above the post-Knox unconformity. The "shallow subtidal" model (Sass and Katz, 1982; Bein and Land, 1983) might provide a viable explanation for extensive penecontemporaneous dolomitization of some subtidal sequences by normal to slightly hypersaline seawater (Machel and Mountjoy, 1986). However, this model does not appear to apply to the Mosheim / Five Oaks dolomite because the tidal flat facies was not placed into subtidal conditions until deposition of the overlying Lenoir and Lincolnshire formations began, and it is believed that dolomitization in the tidal flat sediment was already underway or possibly completed by that time. Furthermore, the shallow subtidal model should result in dolomitization of the subtidal Lenoir and Lincolnshire facies, but these contain less dolomite than the Mosheim and Five Oaks (Johnson, 1988).

The Coorang model (Von der Borch and Lock, 1979; Muir et al., 1980) is attractive because it accounts for penecontemporaneous, non-evaporitic, finely-crystalline dolomites produced in a peritidal environment of mixed marine and freshwater. Coorang dolomites, however, are associated with a very specific environment (ephemeral coastal lakes), and sedimentary structures (Muir et al., 1980) that do not occur in the Mosheim /

Five Oaks sequence. The Coorang model is basically an environment-specific variant of the more general mixed water or dilution model (Morrow, 1982b), which appears to be more appropriate as a model for the Mosheim / Five Oaks dolomite.

The mixed water, or mixing zone, model has received extensive application and support (Morrow, 1982b), as well as harsh criticism (Machel and Mountjoy, 1986; Hardie, 1987) as a mechanism for dolomitization of carbonate sequences. The widespread use of the mixing zone model results from the common inappropriateness of other dolomitization models, and from the fact that a very large percentage of ancient dolomitic carbonate sequences, at one point or another in their diagenetic history, have been exposed to mixed fluids. Most of the criticism of the mixing zone model comes from disagreement over the correctness of its theoretical basis (see especially discussions in Machel and Mountjoy, 1986, and Hardie, 1987), and from the absence of pervasive dolomitization in modern mixing zones, where the dominant diagenetic processes are dissolution (either fabric-selective removal of unstable carbonate phases or wholesale dissolution) and/or precipitation of low-Mg calcite cement. Most modern mixing zones, in fact, have no dolomite at all (Steinen and Matthews, 1973; Plummer et al., 1976; Machel and Mountjoy, 1986). According to Machel and Mountjoy (1986), dolomite formation in Holocene seawater / freshwater mixing zones has been reported only by Land (1973) and Magaritz et al. (1980), and in these cases dolomitization is far from pervasive. It appears, therefore, that the mixing zone model does not provide an appropriate explanation for pervasively recrystallized dolostones (Machel and Mountjoy, 1986; Hardie, 1987).

On the other hand, the mixing zone model might be quite applicable for sequences where dolomitization is sparse or limited to a few horizons. The few examples of Quaternary dolomites for which a mixed meteoric / marine origin seems appropriate are characterized by relatively minor amounts of dolomite or alternating dolomite / calcite

cements, and only partial replacement by dolomite of lime mud matrix (Land, 1973; Gebelein et al., 1980; Sibley, 1980; Kaldi and Gidman, 1982; Ward and Halley, 1985; Humphrey, 1988). Older examples of similar, partially dolomitized carbonate sequences have been reported as products of mixed fluids by Choquette and Steinen (1980), Sears and Lucia (1980), and Kaldi and Gidman (1982).

The limited distribution of the Mosheim / Five Oaks dolomite, and its association with meteoric diagenetic features, indicates that it may be of mixed water origin. The Mosheim/Five Oaks tidal flat sequence, a humid tidal flat analogous to the Andros Island tidal flat, was deposited in a coastal mixing zone. Tidal flats are, by their very nature, zones of mixing between meteoric and marine waters. This is particularly true of the humid tidal flats, such as those on the coast of Belize, and on Andros and other Caribbean islands, where the large input of meteoric water insures brackish water chemistry. The question that remains is whether or not the dolomite in the sequence formed in this mixing zone.

The Mosheim/Five Oaks dolomite is similar in many ways to some Quaternary dolomites interpreted to be of coastal mixing zone origin (Land, 1973; Gebelein et al., 1980; Ward and Halley, 1985; Humphrey, 1988). The scattered distribution of small dolomite rhombs throughout the micrite matrix in the Pleistocene Hope Gate and Falmouth formations on Jamaica (Land, 1973) matches that of the Middle Ordovician dolomite. Those formations, however, also contain fairly abundant dolomite cements in primary pores and fossil molds, as do the coastal limestones on the Yucatan (Ward and Halley, 1985) and on Barbados (Humphrey, 1988). Macropore-filling dolomite cements are exceedingly rare in the Mosheim / Five Oaks sequence. Most similar to the Mosheim / Five Oaks are the partially dolomitized Holocene tidal flat sediments beneath supratidal hammocks and adjacent supratidal crusts on Andros Island (Gebelein et al., 1980). In this tidal flat mud, which resides in localized zones of mixed fresh and marine water,

dolomite is not abundant, nor has it pervasively replaced the original aragonite-dominated sediment. Instead, tiny (1 μm) rhombs of protodolomite, too widely scattered to contribute significantly to the lithification of the sediment, have grown as cements in previously existing pore spaces (Gebelein et al., 1980). This slightly dolomitized Holocene tidal flat sediment may be the closest modern analogue for the Mosheim / Five Oaks sequence.

In summary, the relatively minor amounts of dolomite in the Mosheim / Five Oaks tidal flat sequence probably formed penecontemporaneously with deposition in a coastal zone of mixing between meteoric and marine water. None of the other popular dolomitization models adequately explain the early, non-hypersaline, non-supratidal, matrix-replacive dolomite that occurs in this sequence. The primary shortcoming of the mixing zone model--its inability to pervasively dolomitize thick carbonate sequences (Machel and Mountjoy, 1986)--does not hinder its application to this sequence.

Other localized or minor alterations

Evaporite mineral growth

Evaporite minerals are exceedingly rare in the Middle Ordovician tidal flat sequence. A few mm-sized nodules of authigenic gypsum have been observed in one Mosheim sample. The same sample contains abundant pyrite crystals and a gastropod chamber that is partially filled with celestite cement. Rather than filling void space, the gypsum nodules appear to have grown displacively or replacively within the Mosheim mud matrix. This sample presumably represents a very localized accumulation of sulfur-rich sediment that was isolated from oxidizing fluids.

A few small anhydrite lithoclasts have been observed in two samples of basal Mosheim conglomerates. The association of these clasts with Knox-derived dolostone and limestone lithoclasts in the basal conglomerates suggests that the anhydrite clasts also represent reworked Knox detritus, and reflect the arid, evaporitive conditions under which Knox deposition took place. The preservation of such highly soluble clasts within the humid Mosheim tidal flat sediments, however, indicates that the clasts were probably not long exposed to meteoric fluids during subaerial exposure, transportation, and / or shallow burial.

Silicification

Wholesale replacement of peritidal carbonate matrix by silica (chert) has been observed only in the northwesternmost strike belt of the study area (St. Paul belt), in basal Chickamauga Group strata referred to as the Tumbez Formation. Authigenic chert occurs in the form of nodules and thin, bed-parallel layers within carbonate beds that are intercalated with shale. Petrographic observations reveal these nodules and thin layers to be thoroughly silicified, but "ghosts" of original carbonate textures (especially dolomite rhombs) are sometimes preserved. Silicification does not appear to be restricted to any particular original lithology, but instead is restricted to carbonate beds that occur beneath shale beds. This restriction, and the absence of chert in southeastern strike belts that lack shale, suggests that the silicification results from the mobilization of silica from shales within the sequence. Presumably, silica was leached from shales by downward percolating groundwaters, and reprecipitated as chert in a matrix-replacive process. However, since these shales are primarily illitic (Metcalfe, 1974), the exact chemical mechanism for the transfer of silica from the shales to the carbonates is uncertain. Other possible sources of the silica are volcanic ash dispersed through the carbonate sediment

(O. Kopp, personal communication, 1993) and silica provided by sponge spicules, which are abundant in several lithologies of the Chickamauga Group (Ruppel and Walker, 1984).

Burial Diagenesis

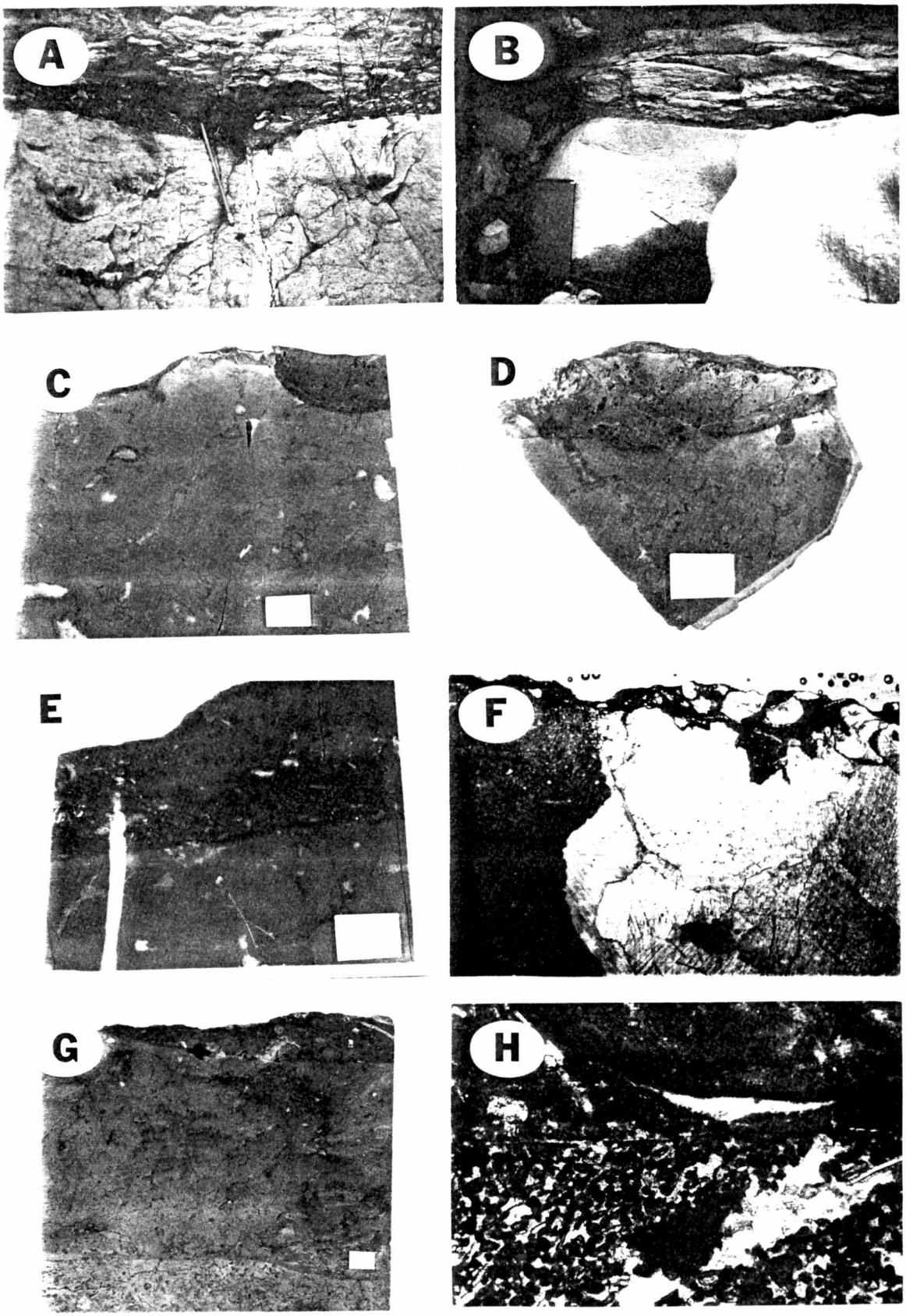
Pressure solution

Bed-parallel pressure solution seams (stylolites) form by dissolution of bulk carbonate material in response to lithostatic pressure placed on the rock by overlying strata (Wanless, 1979), and are accepted as a feature formed almost exclusively in the deep burial diagenetic environment (Longman, 1980). Stylolites are present in virtually all carbonate rocks that have been subjected to deep burial, and are fairly abundant within the Mosheim / Five Oaks tidal flat facies. In thin section, stylolites cut across all other features in the facies except cement-filled veins.

Fracturing and vein filling

Fractures are very common in the tidal flat facies of the Mosheim/Five Oaks sequence because of the brittle failure of this essentially pure limestone lithology. Fracture abundance has been observed to decrease significantly across the Mosheim/Lenoir contact, because the response to stress in the nodular, argillaceous limestones of the Lenoir is more ductile. Fractures have been observed to die abruptly at this contact (Figure 4.9A,F), or to propagate only a very short distance upward into the Lenoir before ending (Figure 4.9E). Fractures are especially abundant in the Mosheim at the Red House Branch section, which is located very close to the Saltville Fault, and at

Figure 4.9. The erosional surface at the top of the Mosheim Member. **A.** Outcrop photograph at the Baptist Hospital section, showing a large bed-normal vein that appears to be truncated at the Mosheim/Lenoir contact (pencil for scale). The cathodoluminescent character of vein cements is entirely different from all other pore-filling cements in the lithology (see Figure 4.5), and indicates that the fracture was filled by burial cements, despite the apparent truncation at this contact. **B.** The Mosheim/Lenoir contact at the Deep Springs outcrop (checkbook for scale). The Mosheim here is riddled with fractures, whereas the Lenoir is not. The difference in fracture abundance is due to the more brittle response to stress of the Mosheim, compared with the more ductile response of the argillaceous Lenoir. **C.** Polished slab photograph of the Mosheim/Lenoir contact, Baptist Hospital, showing the sharp, scalloped erosional surface produced by surface microkarst and wave scour action. The scale bar equals 1 cm. Note that the upper centimeter of the Mosheim is bleached, and that the scalloped area has cut down into the unbleached matrix. Also note the truncated vug just to the left of the bleached ridge: the vug is lined with an initial generation of equant calcite cement, but the central portion of the vug is filled with sediment from the overlying Lenoir, indicating that the vug was only partially cemented prior to deposition of the Lenoir. **D.** Polished slab photograph of the Mosheim/Lenoir contact, Baptist Hospital section. Scale bar equals 1 cm. This photo shows vugs truncated at the erosional surface. Note the bryozoan at the base of the Lenoir at the upper left of the sample; the bryozoan apparently used the semi-lithified Mosheim surface as a hardground upon which to attach itself following the initial marine inundation of the tidal flat. **E.** Polished slab photograph of the Mosheim/Lenoir contact, Deep Springs. Scale bar equals 1 cm. In this photograph the erosional surface is essentially planar, although there is up to 0.3 m relief on the surface at the outcrop. Note the small vein that cuts the Mosheim/Lenoir contact but dies out less than one cm into the Lenoir. **F.** Thin section photomicrograph of Mosheim/Lenoir contact, Baptist Hospital, taken under crossed nicols. Long axis field of view is 6.5 mm. The photomicrograph shows the top of a vertical fracture in the Mosheim that dies at the Mosheim/Lenoir contact, similar to the one shown in the outcrop photograph in Figure 4-10A. The contact here is modified by a stylolite that parallels the contact.


A
B
C
D
E
F
G
H

the Deep Springs outcrop. At these sections, portions of the Mosheim were shattered and subjected to *in situ* brecciation.

Regardless of the abundance or size of fractures, virtually all fractures in the sequence have been filled. By far the most abundant fracture-filling mineral in the Mosheim/Five Oaks sequence is coarsely crystalline, equant calcite. This cement typically appears milky-white to gray in hand sample, and contrasts with the more translucent, typically colorless cements that occlude fenestrae and other pores in the sequence. Under cathodoluminescence, all vein cements in the sequence are dull and unzoned, and clearly truncate (and therefore post-date) all other pore-filling cement phases (Figure 4.5). Fractures also cross-cut stylolites, indicating that formation of the fractures was a late-stage event, and that the fracture-filling vein cements are the latest diagenetic phase in the paragenetic sequence of the rocks.

Diagenetic History

Constraints on Timing of Diagenetic Events

Determining the timing and the temporal duration of the many diagenetic processes that have altered the Mosheim/Five Oaks tidal-flat facies is facilitated by the presence and wide stratigraphic distribution of physical features and cross-cutting relationships that constrain the sequence of events. Features that provide such constraints include (1) minor exposure surfaces at various stratigraphic levels within the tidal flat facies, (2) the major exposure / erosional surface at the top of the tidal flat sequence, and (3) abundant stylolites and cement-filled veins. The significance of each of these types of features in determining the paragenetic sequence of diagenetic processes is discussed below.

Exposure surfaces within the tidal flat sequence

At various stratigraphic levels within the tidal flat facies, intertidal and supratidal lithologies contain subaerial exposure surfaces. Some exhibit evidence of very minor (probably no more than a few millimeters) erosion. These surfaces commonly appear on outcrops as thin, slightly undulose, bed-parallel, bleached zones that are typically less than a cm thick and persist laterally for tens of centimeters to a few meters. These surfaces generally die out laterally at any given location, and certainly cannot be correlated from one outcrop to the next. They are overlain by a variety of shallow subtidal, intertidal, and supratidal lithologies, and even locally do not appear to cap shallowing-upward cycles. In thin section, some of these thin zones consist of chalky or clotted micritic mud that suggests very immature soil development (Esteban and Klappa, 1983). Their upper surfaces are sharp and truncate equant calcite fenestral cements. A few of these surfaces located near the base of the facies (in lithologies interpreted to represent deposition on the inland supratidal algal marsh) contain small, vertically oriented tubules that resemble algal tufa (Figure 3.8A of Chapter 3). A few others contain small borings that extend down into the bleached zone from the upper surface (Figure 4.4D).

Given the association of these localized surfaces with intertidal and supratidal lithologies, it is very likely that the surfaces are the result of subaerial exposure. The incipient soil-like characteristics of these surfaces suggests that they may have formed during slightly protracted periods of exposure, presumably on small, elevated "islands" within the channeled belt complex that escaped sedimentation for some time.

These surfaces within the tidal flat facies provide the following temporal constraints on diagenetic alteration: 1) The truncation of fenestra-filling cements at these surfaces indicates that the process of cementation, at least at the sediment surface,

was well underway before deposition of the overlying sedimentary layer, while the tidal flat was still being built; and 2) The presence of borings excavated into the altered exposure surface indicates that various submicroscopic matrix-altering processes, such as lithification of lime mud to rigid limestone and incipient soil development, occurred during relatively brief periods of subaerial exposure.

Exposure surface at the top of the tidal flat sequence

The upper surface of the tidal flat facies is a sharp contact between the tidal flat and the overlying shallow subtidal marine facies (Figure 4.9). More thorough discussion of this surface, and a model for its development, are presented in Chapter 5 of this dissertation. A concise description of this surface, and information relevant to a determination of the timing of diagenetic events, are presented here.

Several lines of evidence demonstrate that the erosion surface was at one time a subaerial exposure surface. The presence of low-relief karst forms (especially rillenkarren, rundkarren, and kamenitzas [Sweeting, 1973]) (Figure 4.9C) on the surface indicates not only thorough early lithification but surface exposure to undersaturated fluids as well. The limestones immediately beneath this erosion surface include abundant petrographic features that indicate meteoric diagenesis. These features include: (1) dissolution features such as fossil molds (Figure 3.8A,B in Chapter 3) and solution-enlarged molds and vugs (Figures 4.4 and 4.9C,D); (2) vadose features such as pendant and meniscus cement distributions (Figures 4.7), geopetal crystal and pellet silt in fenestrae and vugs (Figure 4.4), alteration of fenestral fabric to diagenetic grainstones and pisolites (Figures 4.7 and 4.8A-C), and incipient caliche development (Figure 4.8A-C); and (3) features suggestive of meteoric phreatic diagenesis such as stabilization of

marine mud to micrite and the ubiquitous presence of clear, non-ferroan, compositionally-zoned, equant calcite cements and microspar (Figures 4.3, 4.4, 4.5, and 4.7), some of which are truncated at the erosional surface (Figures 4.4C and 4.9C,D).

There is abundant evidence that the tidal flat limestones immediately beneath the erosion surface were significantly lithified prior to the deposition of the overlying sediments. Early lithification of the upper tidal flat surface is indicated by 1) the presence of paleokarst features on the erosion surface (Figure 4.4C and 4.9C); 2) borings and fissures extending downward from the erosion surface; 3) encrustation of the surface by calcareous marine organisms (Figure 4.9D); and 4) erosional truncation of cements as well as depositional material in the fenestral mudstones (Figures 4.4C and 4.9C,D).

Burial features (stylolites and veins)

Stylolites within the tidal flat facies cut across all other features except cement-filled veins, and indicate that cementation and virtually all phases of diagenetic alteration were complete prior to deep burial. Veins and fractures generally cut across, and in some places offset, stylolites, and indicate that brittle fracturing of the Mosheim and Five Oaks limestone units occurred after deep burial, and probably during late Paleozoic Alleghenian compressional deformation and thrusting. Veins also cut across the contact at the upper surface of the tidal flat facies, indicating that fracturing occurred after burial of the tidal flat facies by overlying units (Figure 4.9E). In some places, veins appear to be truncated at the erosional surface that caps the tidal flat facies (Figure 4.9A,F). In this situation, post-depositional fracturing apparently stopped at the interface between the brittle, pure limestone of the Mosheim/Five Oaks facies and the ductile, argillaceous Lenoir/ Lincolnshire facies. The equant calcite cements that fill most of the veins in the Mosheim / Five Oaks rocks closely resemble other early equant cements in the sequence,

such as those that fill fenestrae (Figure 4.5A). Under cathodoluminescence, however, it is clear that the vein cements are a different generation of cement than the fenestra-filling cements. The vein cements truncate the fenestral cements (Figure 4.5B), indicating that the fracturing and precipitation of vein calcite occurred after lithification of the facies. The vein cements also have different isotopic signatures than the fenestral cements, as indicated in Figure 4.6 and Table 4.1. The exact timing of vein cementation is uncertain, but it likely occurred during deep burial, and post-dated virtually all other diagenetic events.

Paragenetic Sequence

The diagenetic processes that altered the Mosheim/Five Oaks tidal flat sequence occurred in the depositional environment, in the shallow burial (phreatic) diagenetic environment, and to a lesser extent, in the deep burial environment. The paragenetic sequence, or relative timing, of all diagenetic processes that affected the facies is shown diagrammatically in Figure 4.10.

Diagenetic Environments

Information summarized in the preceding discussion on the diagenetic history of the Mosheim / Five Oaks tidal flat facies demonstrates that most of the diagenetic alteration of the tidal flat sediments occurred very early after deposition, and much of it occurred in the tidal flat depositional environment. Several of the diagenetic processes are clearly associated with a specific diagenetic environment, while other processes began in one environment and continued as the diagenetic environment changed due to burial beneath younger sediments. The complete diagenetic history of the basal Middle

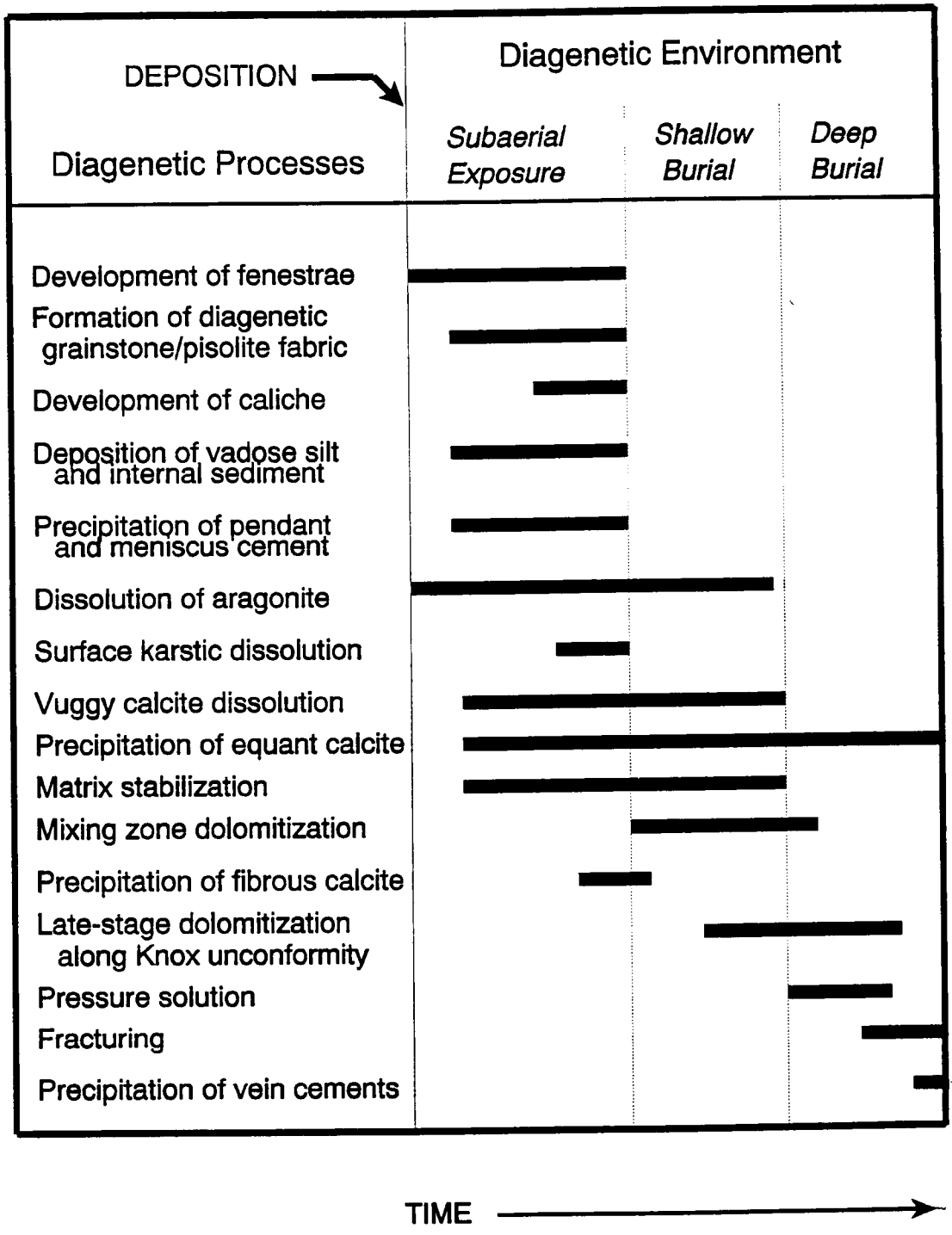


Figure 4.10. Paragenetic sequence of diagenetic processes in the Mosheim/Five Oaks tidal flat facies.

Ordovician tidal flat facies, and the diagenetic environments in which the various phases of diagenesis took place, is summarized in Table 4.3.

Relationship Between Diagenesis of the Basal Peritidal Limestones and the Overlying Middle Ordovician Strata

Although the contact that separates the basal Middle Ordovician tidal flat sequence (Mosheim Member and Five Oaks Formation) from the overlying subtidal shelf facies (Lenoir and Lincolnshire Formations) is in most places sharp and erosional, it does not represent a depositional sequence boundary (Roberson and Walker, 1990, and Chapter 5 of this dissertation). Biostratigraphic evidence indicates that this exposure surface represents little time (probably only a few hundred to a few thousand years, and certainly less than one conodont subZone), and also indicates that deposition of the tidal flat units was concomitant with seaward deposition of the shelf facies. The tidal flat sequence is therefore a facies of the Middle Ordovician onlap sequence, and not a discrete depositional sequence.

Diagenesis of the tidal flat facies, however, is largely distinct from the post-depositional alteration of the overlying shelf, slope, and basinal facies. The reasons for this are quite simple. First, deposition and early diagenesis of the tidal flat facies occurred primarily in a diagenetic environment (the meteoric vadose environment) to which the overlying facies were only rarely exposed. Second, because the tidal flat sequence was substantially lithified before transgression of the subtidal facies over the tidal flat facies occurred, the peritidal deposits were not as susceptible to further alteration in the shallow subsurface and deep burial diagenetic environments as the less-altered, overlying facies.

Table 4.3
Summary of Mosheim / Five Oaks Tidal Flat Diagenesis

Meteoric vadose diagenesis
These events occurred during subaerial exposure in the supra- and intertidal depositional environments above sea level and above the local fresh water table.

Development of fenestral fabrics
Evolution of diagenetic grainstone/pisolite fabrics
Development of incipient caliche
Deposition of internal sediment and vadose silt
Precipitation of pendant and meniscus calcite cements
Mineral-specific (aragonite) dissolution
Non- selective (vuggy) dissolution

Meteoric phreatic diagenesis
These events occurred or continued beneath subaerially exposed sediment in the zone saturated with fresh water.

Mineralogic stabilization of Mg-calcite mud to micrite
Mineral-specific (aragonite) dissolution
Non- selective (vuggy) dissolution
Precipitation of equant calcite cement

Mixed meteoric phreatic / marine diagenesis
These events occurred in the zone saturated with mixed meteoric/marine water.

Penecontemporaneous dolomitization
Non-specific (vuggy) dissolution

Marine diagenesis
These events occurred after marine inundation of the tidal flat.

Deposition of marine sediment in vugs and fissures (neptunian dikes)
Precipitation of fibrous cements

Burial diagenesis
These events occurred after deposition of overlying carbonate and shale units.

Pressure solution (stylolitization)
Late-stage dolomitization along Knox unconformity
Fracturing and filling of veins with ferroan equant calcite cement

Paleohydrologic Model

As discussed above, most of the diagenetic alteration of the Mosheim/Five Oaks tidal-flat sequence occurred very shortly after deposition, while the sediment remained in the tidal-flat depositional environment. The overwhelming abundance of products of freshwater diagenesis indicates that this diagenetic alteration was driven by the passage of meteoric fluids through the carbonate sediment. Therefore, any model designed to explain the diagenesis of the Mosheim/Five Oaks sequence must provide for frequent flushing of meteoric water through the tidal-flat facies. The simplest, and most likely hydrologic system in which early, near-surface, freshwater alteration of tidal-flat sediment would occur is a humid, coastal aquifer system, as depicted in Figure 4.11. Given the position that a tidal flat occupies at the interface between land and sea, it must be expected that subtidal and intertidal portions of the tidal-flat sediment will be covered (and saturated) at times by sea water, at other times by freshwater, and perhaps most commonly, by a brackish mixture of marine and meteoric fluids. This is especially true if the tidal flat has a well-developed network of channels that provides fairly open communication between the inland ponds and marshes and the sea. Such is the case on the Andros Island tidal flat, where during high tides, and especially during and after strong storms that blow seawater landward across the tidal flat, the tidal ponds, channels, and cyanobacterial marshes become filled with water with a chemistry that approaches that of normal seawater (Hardie and Garrett, 1977). During periods of prolonged or heavy rainfall, the saline water occupying the ponds and channels of the channeled belt is flushed out and replaced by essentially fresh water. On a normal, daily basis, the ponds and channels are filled with a mixture of marine and freshwater (Hardie and Garrett, 1977). Thus, in terms of hydrology, the portion of the Andros Island tidal flat that resides below mean sea level is an unconfined coastal aquifer saturated with water whose

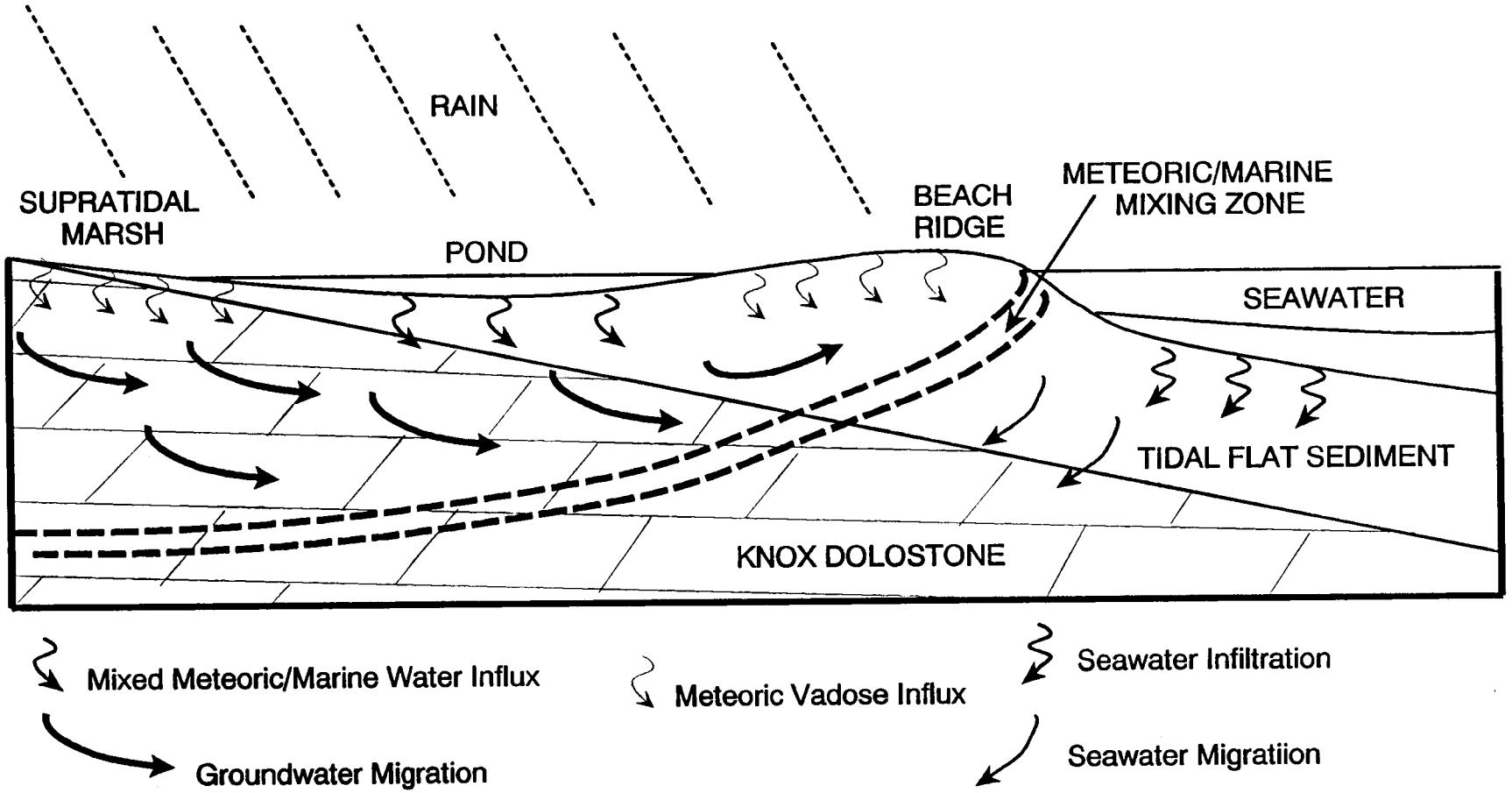


Figure 4.11. Paleohydrologic model for diagenetic alteration of the Mosheim/Five Oaks tidal flat facies.

chemistry fluctuates between freshwater and seawater end members. Intertidal and supratidal portions of the tidal flat are a vadose zone that is flushed periodically by downward-percolating rainfall or rarely, seawater.

Precisely such a system is envisioned as the environment in which most of the Mosheim/Five Oaks diagenetic alteration occurred (Figure 4.11). Although the tidal flat was regularly inundated and saturated by seawater or mixed fresh/marine water, the overwhelming imprint of meteoric diagenesis (and the paucity of features indicative of marine or mixed fluid diagenesis) within the Mosheim/Five Oaks facies requires that the system must have been strongly dominated by meteoric water. Thus, a humid, rainy climate comparable to, or perhaps even more humid than the modern Bahaman climate is inferred for the paleoclimate that prevailed during deposition of the Mosheim/Five Oaks tidal flat.

Sources and Travel Pathways of Fluids

The sources of fluids that entered the tidal flat/coastal aquifer system, and the travel pathways along which fluids migrated through the tidal-flat sediment are depicted in Figure 4.11. Fresh water probably entered the system from two sources: rainfall on the tidal flat surface, and shallow groundwater passing into the tidal-flat sediments from the underlying Knox dolostone. Seawater was provided to the system at the surface through the network of tidal channels and ponds, and probably also infiltrated downward through shallow subtidal marine sediment (the Lenoir/Lincolnshire facies) into the underlyuing, shallowly buried tidal-flat sediment. Rain falling directly on marshes and ponds, or entering ponds as surface runoff from the exposed Knox surface, mixed with seawater in the ponds and entered the sediment mass beneath the ponds as a mixed (but probably meteoric-dominated) fluid. Unmixed rain water falling on subaerially exposed supratidal

and intertidal marshes, channel levees, and the beach ridge percolated downward through unsaturated sediment to the saturated zone. Beneath the fresh water table (which was probably roughly equivalent to, or only slightly above mean sea level), migration through the tidal-flat sediment was probably primarily lateral.

Zones of Diagenetic Alteration

Because most of the diagenesis in the Mosheim/Five Oaks sequence occurred very early in the depositional environment, the type of diagenesis that characterizes a specific lithology can be directly related to the specific tidal-flat subenvironments in which the lithlolgy was deposited. Diagenesis in the unsaturated, supratidal portions of the tidal flat (beach ridge, channel levees, and high algal marshes) was accomplished almost exclusively by meteoric fluids (primarily rainfall) percolating downward through the vadose zone. Unequivocal supratidal lithologies in the Mosheim/Five Oaks sequence typically contain only non-luminescent or zoned, equant calcite cements, and with the exception of supratidal deposits immediately overlying the Knox unconformity, generally are devoid of dolomite. Freshwater diagenesis also was predominant beneath the inland cyanobacterial marsh because the fluids occupying the pores were dominantly of terrestrial or meteoric origin. (Inland marsh deposits in the Mosheim/Five Oaks sequence, however, are highly dolomitized because of their stratigraphic position overlying the Knox unconformity.) Intertidal, and especially subtidal, portions of the system deposited in ponds and channels were most likely to be saturated by fluids of mixed marine/meteoric composition, and it is these lithologies that typically show the most evidence of mixed water diagenesis, such as non-selective, vuggy dissolution, and contain the highest concentrations of dolomite within the sequence, except for lithologies

immediately above the Knox unconformity, which were probably dolomitized later by migration of magnesium-rich fluids along the unconformity.

Controls on Later Fluid Migration and Economic Implications

The case has been made above that much of the porosity in the Mosheim/Five Oaks tidal-flat facies was occluded very early after deposition by calcite cements precipitated from meteoric-dominated waters that passed through the sediment in the tidal flat depositional environment. If this is true, then by the time the Mosheim/Five Oaks sequence was buried beneath the overlying limestones or shales, it had probably already assumed the role of an aquiclude, or a barrier to the migration of fluids. Thus, since Middle Ordovician time, the basal Middle Ordovician tidal flat facies, where it is present, may have hindered the migration of fluids from the overlying shale basin into the Knox Group, or it may have acted as a stratigraphic trap, impeding the migration of fluids from the Knox Group upward into Middle Ordovician rocks. The presence of a thin, but relatively impermeable, veneer across the top of the Knox Group would control the migration of fluids along the Knox unconformity. Therefore, the early diagenesis of the Mosheim/Five Oaks facies could account for the accumulation of organic hydrocarbons and other economic minerals, such as lead and zinc, at or along the Knox unconformity (Bridge, 1956; Churnet, 1979; Harris, 1969, 1973; Haynes and Kesler, 1989; Hoagland et al., 1965; Kesler et al., 1989; Misra et al., 1989, 1992; Oder and Ricketts, 1961; Secrist, 1924; Wedow and Laurence, 1967).

Conclusions

1. Diagenetic alteration of the tidal flat facies is overwhelmingly dominated by features that indicate alteration by meteoric water. Meteoric diagenesis occurred above and below the water table in unsaturated (vadose) and saturated (phreatic) zones. Subaerial exposure and vadose zone alteration is indicated by several features, including: (1) abundant fenestral fabrics and less commonly, desiccation features such as mudcracks and sheet cracks; (2) alteration of fenestral fabric to diagenetic grainstones and pisolites; (3) thin bleached zones within and at the top of the supratidal and intertidal lithologies; (4) localized zones of incipient caliche development, typically just below exposure surfaces; (5) pendant and meniscus cement distributions; and (6) geopetal crystal silt in fenestrae and vugs. Additional evidence of meteoric diagenesis (which may have begun in the vadose zone and continued into the phreatic realm) includes dissolution features such as fossil molds and solution-enlarged molds and vugs; stabilization of marine mud to micrite; and the ubiquitous presence of clear, non-ferroan, compositionally-zoned, equant calcite cement and microspar. Virtually all porosity is occluded by equant calcite cement, and other types of cement are volumetrically negligible.

2. The majority of diagenetic alteration occurred very early, beginning immediately upon deposition of the tidal flat sediment and being largely concluded before deep burial. Most diagenesis occurred while the sediment remained in the tidal flat depositional environment. At least the uppermost surface of the tidal flat facies, and likely other subaerially exposed supratidal and intertidal horizons within the facies as well, underwent extensive lithification prior to deposition of the overlying strata. Evidence for early diagenetic alteration and lithification of intertidal and supratidal lithologies occurs in the form of 1) the presence of paleokarst features on the upper erosion surface; 2) erosional

truncation of cements as well as depositional material in lithologies underlying erosional surfaces; 3) borings and vugs extending downward from the erosion surface; and 4) encrustation of the upper erosion surface by calcareous marine organisms after marine inundation. The timing of diagenetic alteration of subtidal lithologies is less well constrained, but it probably was largely completed during shallow burial in the phreatic environment.

3. Dolomite within the tidal flat sequence occurs as single rhombs disseminated widely through the muddy matrix. Primary, supratidal dolomite crusts are absent, and the only pervasively dolomitized lithologies occur within a meter of the base of the tidal flat facies, where magnesium was available from several sources, including exsolution from the underlying Knox dolostones and movement of burial fluids along the Knox unconformity. Above this basal meter, i.e. in the channeled belt subfacies, dolomite abundance is related to depositional subenvironment, and is most abundant in burrowed, subtidal lithologies and least abundant in supratidal fenestral lithologies. Dolomitization of subtidal pond lithologies may have occurred by alteration of sediment by mixed meteoric / marine fluids in the coastal mixing zone. In general, dolomite abundance decreases upward, and dolomite is very rare in the uppermost beach ridge lithologies.

4. Hydrologically, this setting in which deposition and early diagenesis occurred was a zone of mixing of seawater and freshwater in an unconfined coastal aquifer. The fluids that covered this tidal flat and filled the sedimentary pores beneath the water table probably fluctuated between meteoric and normal marine end members, but the diagenetic features and geochemical data indicate that the predominant water chemistry was probably very dilute and closer to freshwater than seawater.

5. The tidal flat facies probably assumed the role of a barrier to groundwater migration (an aquitard) very early, because virtually all porosity was occluded before deep burial. The effects of deep burial diagenesis are minimal (limited to pressure solution and occlusion of late fractures by calcite and silica cements), probably because fluids did not readily move through the facies, except along fractures.

Chapter 5

A REGIONAL APPALACHIAN EROSIONAL SURFACE PRODUCED SOLELY BY ENVIRONMENTAL MIGRATION WITHIN A MIDDLE ORDOVICIAN TRANSGRESSIVE SEDIMENTARY SEQUENCE

Introduction

The purpose of this chapter is to discuss an example of a regionally widespread erosional surface that was produced *within* a Middle Ordovician sedimentary sequence simply by transgressive migration of depositional environments. The surface is one of sharp lithologic contrast between two adjacent facies, is accompanied by abundant evidence of subaerial and tidal erosion, and could easily be misinterpreted as a major unconformity or depositional sequence boundary. In sequence stratigraphic terminology, the surface is both an exposure surface and a submarine flooding surface, but it does not disrupt the predicted vertical stacking of facies in a transgressive sequence, and is therefore *not* a depositional sequence boundary.

This erosional surface formed during marine transgression when the shallow subtidal, offshore marine environment onlapped over early-lithified carbonate sediment that was deposited behind a low beach ridge on an Andros Island-type tidal flat. The erosional surface is, therefore, the carbonate equivalent of the *ravinement surface* described in terrigenous clastic transgressive sequences by Nummedal and Swift (1987) and Demerest and Kraft (1987). A modern analogue of this type of erosional surface is currently forming in a carbonate sequence on the transgressive northwestern portion of the Andros Island tidal flat (Hardie, 1977; Shinn, 1986). Sea level fall (eustatic or relative) is not involved in the formation of the Holocene erosion surface on Andros Island, and by analogy, was not required for the formation of this Middle Ordovician erosion surface.

Description of the Erosional Surface

Distribution and Stratigraphic Position

Scalloped and planar erosional surfaces have been reported within the basal portion of the Middle Ordovician carbonate sequence in the Valley and Ridge of Virginia by Read and Grover (1977). The sharp erosional surfaces discussed by Read and Grover (1977) occur both within and at the top of the thin (usually <20 meter thick) veneer of fenestral carbonate mudstones of tidal-flat origin (New Market Limestone) that immediately overlies the regional Knox/Beekmantown unconformity and forms the basal facies of the Middle Ordovician depositional sequence. Read and Grover (1977) make little genetic distinction between the erosional surfaces within the tidal flat facies and the erosional surface that forms the contact between the tidal flat limestones and the overlying shallow subtidal wackestones and grainstones of the Lincolnshire Limestone.

In this paper, discussion is focussed primarily on the erosional surface that caps the basal Middle Ordovician tidal flat facies. Despite physical similarities, it is believed that this surface formed by a different process than the erosional surfaces within the tidal flat facies, and unlike those surfaces, serves as an important stratigraphic marker because of its position between two markedly different lithofacies.

An initial point to be made is that this erosional surface is not limited to Virginia, but is regional in extent, and occurs at precisely the same lithostratigraphic position throughout the southern Appalachians from northern Virginia to the Coastal Plain overlap in central Alabama, a distance of at least 1000 kilometers (Figure 5.1). Throughout this area, this erosional surface is best developed in southeasternmost strike belts (typically southeast of the Saltville Fault in Virginia and Tennessee, the Rome Fault in northwest Georgia, and the Helena Fault in Alabama), where it forms the contact

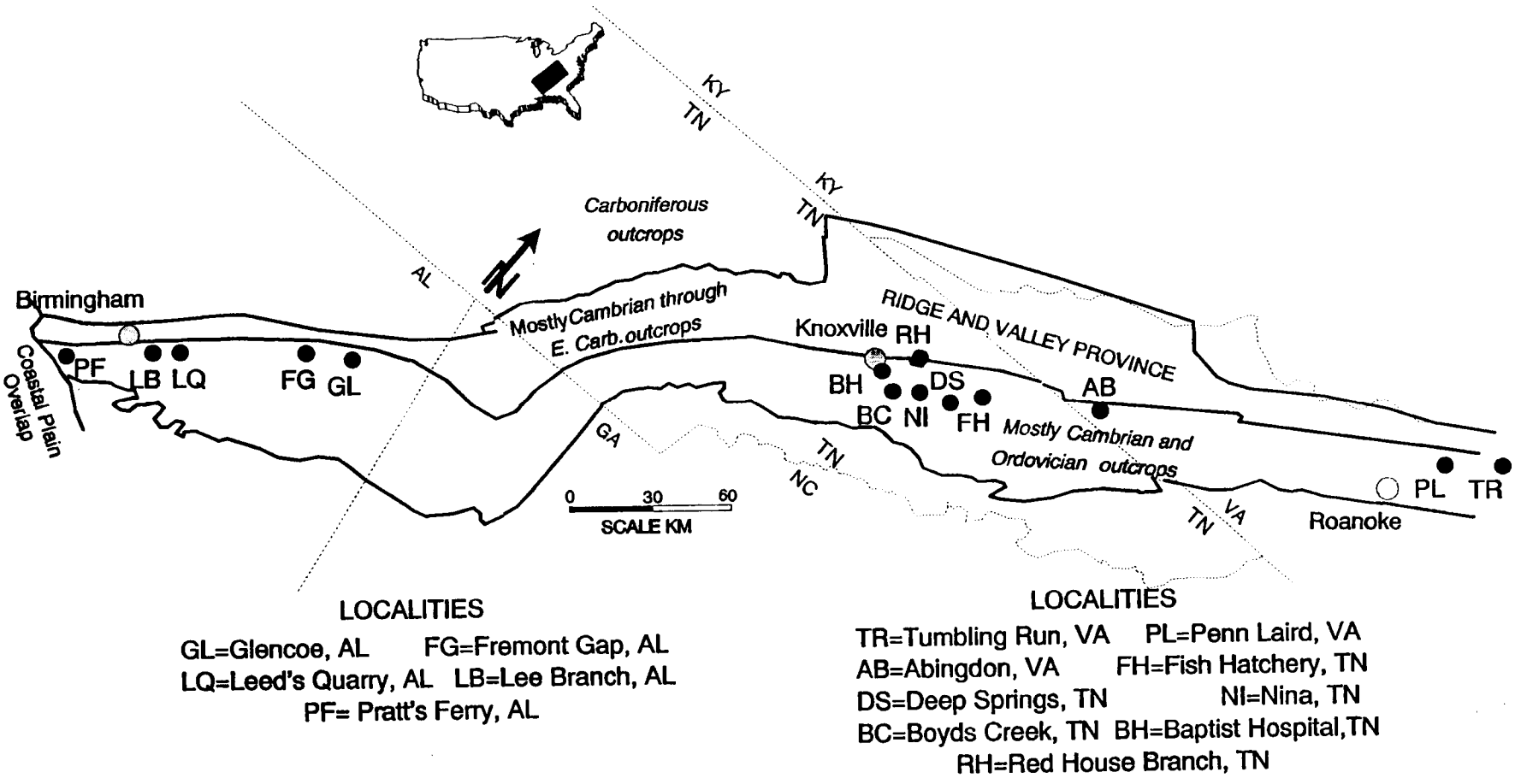


Figure 5.1. Location map of the southern Appalachian Valley and Ridge Province, showing noted exposures of the erosional disconformity between the basal Middle Ordovician tidal flat facies and the overlying shallow subtidal marine facies.

between tidal flat limestones (the New Market Limestone and the Mosheim Member of the LenoirFormation), and the overlying argillaceous lagoonal facies (the Lenoir and Lincolnshire formations) (Figure 2.2 of Chapter 2). Ulrich (1911) recognized this surface at Mosheim, Tennessee, and interpreted it to be a regional unconformity that represented a major gap in the depositional sequence. In strike belts northwest of the aforementioned thrust faults the contact between these facies is sharp due to lithologic contrast, but the amount of erosional relief is minimal (often one centimeter or less) in most places.

An erosional contact at precisely the same stratigraphic interval has been reported from the northern Appalachians as well. Desrochers and James (1988) discussed an erosional disconformity within the Mingan Formation exposed on the Mingan Islands of Quebec that separates tidal flat limestones of the Fantome Member from overlying shallow subtidal limestones of the Grande Pointe Member. This entire stratigraphic sequence is remarkably similar to the Middle Ordovician of the southern Appalachians, and the erosional surface bears many of the same features as the surface described herein. The erosional surface within the Mingan Formation, however, has local relief of as much as 20 meters (compared with 30 centimeters in the southern Appalachians), and therefore requires a different explanation for its development. This difference will be discussed toward the end of this paper.

Classification and Terminology

A point that should be considered here is whether the surface represents a significant period of non-deposition, and is thus a disconformity, or represents only a brief interruption of deposition and is thus more appropriately referred to as a diastem. Since the surface bears clear evidence of erosion (Figure 4.9 of Chapter 4), there is little doubt that there has been some removal of material at the surface. Thus, according to

the definitions put forth by Krumbein and Sloss (1963), this erosional surface could be considered an unconformity, and more specifically a disconformity since it separates essentially parallel strata. Also, the regionally widespread geographic extent of this erosional surface would seem to suggest that it is a significant, regionally correlatable disconformity, and not a diastem, which is typically a minor break in sedimentation of local extent. More recent definitions, however, stress that clear distinction be made between unconformities and diastems with regard to the period of time they represent. According to Bates and Jackson (1980), "an unconformity is a substantial break or gap in the geologic record where a rock unit is overlain by another that is not next in stratigraphic succession", whereas "a diastem is a relatively short interruption in sedimentation involving only a brief interval of time." However, most bedding planes are considered to be the result of brief interruptions in sedimentation, and are therefore diastems. With abundant evidence of surface karst development and erosional truncation of diagenetic as well as depositional components (discussed below), this surface appears to represent a more profound break in sedimentation than the average bedding plane. And yet the amount of time required for the development of this surface is small. A depositional model for the the basal Middle Ordovician peritidal sequence (Figure 3.10 of Chapter 3) constructed from detailed environmental interpretations (Chapter 3) and based on the Holocene Andros Island tidal flat indicates that the lithofacies beneath and above the erosional contact do indeed occur in the predicted stratigraphic succession for a transgressive sequence, and therefore, despite the evidence of erosion, this surface does not fit the Bates and Jackson (1980) definition of an unconformity. Because the surface is more significant than a diastem, but is not truly a disconformity, it will be referred to as an erosional surface in this chapter, its geographically widespread occurrence notwithstanding.

Biostratigraphic data (Figure 5.2) generally indicate that the amount of time missing at the erosional surface is small, but because of the severely restricted fauna of the tidal flat limestones beneath the surface (Mosheim, New Market, and Five Oaks units), biostratigraphic data generally do not have the resolution to allow an accurate determination of the hiatus. However, at one location (the Idol Mine section in Grainger County, Tennessee, Figure 5.1), a sample of a slightly fossiliferous peloidal grainstone at the top of the Five Oaks Formation immediately beneath the erosional surface yielded a biostratigraphically useful conodont assemblage (A. Harris, personal communication, 1990). This sample indicated deposition during the *Cahabagnathus sweeti* Zone (*A. kielcensis* Subzone of the *Pygodus anserinus* Zone) (Figure 5.2). A sample from the basal Lincolnshire Formation immediately above the erosional surface indicated deposition during the *C. carnesi* Zone (*A. inaequalis* to *B. variabilis* Subzones) (Figure 5.2). The presence of *C. sweeti* is restricted to the Five Oaks, whereas its descendant, *C. carnesi,* occurs only in the Lincolnshire above the erosional surface. The interval of overlap for this ancestor-descendant couplet appears to be missing at the erosional contact (A. Harris, personal communication, 1990). If the hiatus represented by the erosional surface at this location is limited to this interval of overlap, then the hiatus is likely very short. On the other hand, the segregation of *C. sweeti* and *C. carnesi* might be ecologic, reflecting the different environments of deposition of the Five Oaks and Lincolnshire facies, and not chronostratigraphic (A. Harris, personal communication, 1990). In any case, there is no conclusive paleontologic evidence from any of the locations suggestive of a major break in deposition at the erosional surface; the best available data indicate that the hiatus was of brief duration, and certainly less than the duration of one conodont subZone.

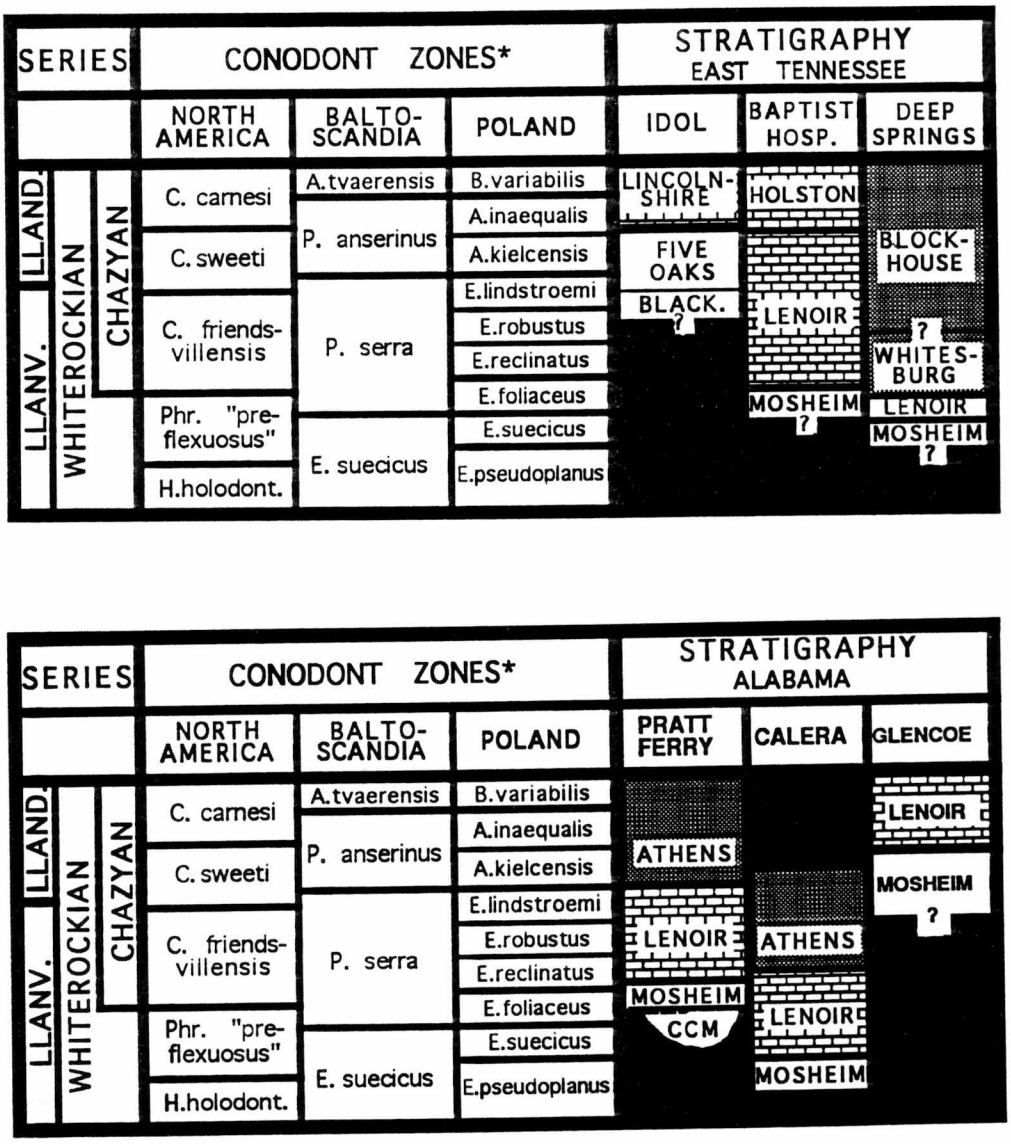


Figure 5.2. Biostratigraphic correlation of basal Middle Ordovician peritidal facies in Alabama and East Tennessee, based on conodont biostratigraphy. The age of the erosional surface that separates the tidal flat facies from the overlying subtidal facies varies considerably from outcrop to outcrop, and illustrates that the erosional surface is not a isochronous feature, and could not have been the result of a eustatic sea level rise. *Conodont zones are from Bergstrom (1973) and Bergstrom and Carnes (1976).

Physical Description

Environmental interpretations of sub-diastem lithologies

The Middle Ordovician erosion surface described herein is a surface of distinct lithologic contrast, as it separates fenestral limestones of tidal flat origin (Mosheim and New Market Limestones), from overlying fossiliferous, nodular limestones deposited in a subtidal marine setting (Lenoir and Lincolnshire Formations) (Figure 4.9). The erosion surface is developed upon lithologies that represent several subenvironments near the seaward margin of a humid transgressive tidal flat analogous to the northwestern portion of Andros Island (Hardie and Garrett, 1977). These lithologies are primarily fenestral mudstones, but non-fenestral mudstones and peloidal grainstones also occur. The fenestral mudstones beneath the erosion surface generally are not distinctly laminated, but do contain enough sedimentologic informaton to allow detailed interpretations of depositional environments (see Chapter 3). The Mosheim and New Market fenestral lithologies represent deposition in intertidal and supratidal subenvironments analogous to the low and high algal marshes, levee crests and backslopes, and beach ridge washover backslopes on the Andros Island tidal flat, as described by Hardie and Garrett (1977).

Less commonly, mudstones that generally lack fenestrae and lamination but sometimes contain a minor amount of fossil material occur immediately beneath the diastem. These mudstones represent deposition in subtidal pond subenvironments such as those that that make up the majority of the channeled belt that lies landward of the beach ridge on the Andros Island tidal flat. Subtidal pond sediments are, in some places, exhumed and exposed by wave erosion of the the landward-migrating Andros beach ridge (see Figure 23A in Hardie and Garrett, 1977). It is significant that this erosion and

exposure of subtidal pond sediment occurs due to beach erosion without any drop in sea level.

In some places, the erosional surface is developed upon flat- or wavy-laminated, grain-supported lithologies. These lithologies are essentially identical to sediments deposited in supratidal subenvironments of the beach ridge that lies at the seaward margin of the Andros Island tidal flat, and are interpreted as analogous, beach ridge deposits. At a few outcrops in central Alabama (Pratt Ferry and Lee Branch), the erosional surface truncates peloidal/intraclastic grainstones characterized by flat or gently undulose laminae that slope approximately 30 degrees in the landward direction (Figure 4.9G,H). These grainstones contain marine and meteoric vadose "beach rock" cements, and are analogues of the sandy, supratidal beach ridge "hammocks" on the Andros Island beach ridge (see Figure 15 in Shinn, et al, 1969; and Hardie and Garrett, 1977). This set of laminated lithologies provide compelling evidence that a supratidal beach ridge was present at the seaward edge of the Middle Ordovician tidal flat, and formed the interface between the channeled tidal flat and the shallow subtidal offshore marine environment.

More thorough discussions of the comparative sedimentology of the Middle Ordovician tidal flat in the southern and central Appalachians can be found in Grover and Read (1978), Hardie (1986), Mitchell (1981, 1985), and in Chapter 3 of this dissertation.

Evidence for early lithification

There is abundant evidence that the tidal flat limestones immediately beneath the erosion surface were significantly lithified prior to the deposition of the overlying sediments. Early lithification of the upper tidal flat surface is indicated by 1) the presence of paleokarst features on the erosion surface (Figure 4.4C and 4.10C); 2) borings and fissures extending downward from the erosion surface (Figure 4.4B); 3) encrustation of

the surface by calcareous marine organisms (Figure 4.9D); and 4) erosional truncation of cements as well as depositional material in the fenestral mudstones (Figures 4.4C and 4.9B, D). Read and Grover (1977) and Desrochers and James (1988) also interpreted early lithification on the basis of the same features observed in tidal flat facies beneath the erosional surfaces in Virginia and Quebec, respectively.

It is not known if the entire tidal flat facies was lithified prior to deposition of the overlying limestones, or if induration was limited to the strata immediately beneath the erosion surface. It is possible that the uppermost layer of tidal flat sediment was an indurated crust that "floated" on semi-rigid or unlithified carbonate mud. Such is the case for the Andros Island tidal flat (Hardie and Garrett, 1977). Another possibility is that lithification was heterogeneous throughout the tidal-flat facies, with the degree of lithification dependent upon the amount of subaerial exposure, and thus on the subenvironment of deposition within the tidal flat complex. In this scenario, supratidal and high intertidal portions of the tidal flat would exist as lithified lenses embedded in a partially indurated body of subtidal and lower intertidal carbonate mud. A third possibility is that the entire tidal flat facies was extensively lithified prior to deposition of the overlying subtidal facies. The second proposal is favored here, because minor erosion surfaces of only local extent, which exhibit many of the same features indicative of lithification as the upper erosional surface, exist at several levels within the tidal flat facies, particularly at the top of supratidal lithologies.

Evidence for subaerial exposure

Several lines of evidence demonstrate that the erosion surface was at one time a subaerial exposure surface. The presence of low-relief karst forms (especially rillenkarren, rundkarren, and kamenitzas [Sweeting, 1973]) on the surface indicates not

only thorough early lithification but surface exposure to undersaturated fluids as well. Subaerial exposure of high intertidal and supratidal portions of the tidal flat began immediately upon deposition of the sediment. Considering the frequency of subaerial exposure in the subenvironments in which these sediments were deposited, and the abundant evidence of freshwater diagenesis in a humid climate, it is a logical inference that early diagenetic alteration and lithification resulted from the passage of meteoric waters through the sediments. Petrographic data provide overwhelming support for this interpretation.

The limestones immediately beneath the erosion surface include abundant petrographic features that indicate meteoric diagenesis (Table 5.1). The combination of these features, and the scarcity of reliable indicators of other diagenetic environments, point convincingly to freshwater as the primary agent in the diagenesis of this Middle Ordovician tidal flat facies. Marine diagenesis played a minor role in the lithification, as indicated by rare fibrous cements in grainstones truncated beneath the exposure surface (Read and Grover, 1977; Roberson and Walker, 1990). Marine cementation followed freshwater diagenesis, occurring after the lithified tidal flat was inundated by onlap of the offshore marine environment.

Evidence for tidal scour and submarine inundation

Although there is considerable evidence for subaerial exposure and freshwater alteration of the tidal flat carbonates immediately beneath the erosion surface, it is also apparent that subaerial exposure was followed by a period of tidal scour as the marine transgression continued (Read and Grover, 1977). One of the dominant effects of tidal scour was the planation of the exposure surface (Figure 4.10A,E) and the inferred

Table 5.1
Features Indicative of Meteoric Diagenesis

Dissolution by undersaturated fluids
Fossil molds, enlarged fossil molds, and vugs (Figures 4.4C and 4.9C,D)
Vadose alteration
Caliche-type pisoids and incipient caliche (Figure 4.8A-C)
Geopetal crystal silt in fenestrae and vugs (Figure 4.4C,F)
Pendant and meniscus cement distributions (Figure 4.7D-F)
Alteration of fenestral fabrics to diagenetic grainstone fabrics (Figure 4.7)
Meteoric phreatic diagenesis
Stabilization of marine mud to micrite
Precipitation of non-ferroan, equant calcite cement that predates erosion along the exposure surface (Figures 4.4C and 4.9D)

removal of many paleokarst relief features (and doubtless other evidence of subaerial exposure) from the erosion surface. Tidal scour followed subaerial exposure, as scours can be seen to truncate subaerial exposure features such as the bleached surface crust in Figure 4.9C. In terms of the rate and amount of sediment removed, tidal scour may have been more important than freshwater dissolution in the formation of the erosional surface (Read and Grover, 1977).

The period of tidal or wave erosion was followed by submarine inundation, as evidenced by:

1) encrustation of the lithified surface by marine organisms such as bryozoans and calcareous algae (Figure 4.9D);

2) the filling of vugs, molds, and fissures connected to the surface with fibrous calcite cement precipitated from seawater and marine sediment (Figure 4.9C,D); and

3) burial of the erosion surface by subtidal marine carbonates of the Lenoir and Lincolnshire Formations.

Model for the Development of the Erosional Surface

Development of the erosional diastem at the top of the Mosheim tidal flat limestones can be explained through the use of a depositional model constructed from detailed interpretations of depositional environments (Figure 3.10 of Chapter 3). This model was developed by analogy with the environmental interpretation presented for the northwest portion of the Andros Island tidal flat by Shinn and others (1969), Hardie and Garrett (1977), and Shinn (1986). The depositional model for the basalmost Middle Ordovician tidal flat sequence in Tennessee and its similarities with the Holocene Andros Island tidal flat are discussed in greater detail in Chapter 3.

On the basis of the physical evidence presented above, this author concurs with Read and Grover (1977), and interpret the erosional surface to be the result of karstification of supra- and intertidal portions of the tidal flat during subaerial exposure, followed by wave scour as the adjacent subtidal marine environment migrated over the tidal flat during transgression. Read and Grover (1977), however, call on progradation of the tidal flats (and implicit relative sea level fall or standstill) as the driving mechanism for the production of these surfaces, whereas this author attributes development of the erosional surface to transgressive, landward migration of the peritidal facies (as opposed to progradation) during continued sea level rise.

The basal Middle Ordovician stratigraphic sequence in the southern Appalachians is essentially identical to the Holocene depositional sequence currently being produced by transgression on the northwest side of Andros Island (Shinn, et al., 1969; Hardie and Garrett, 1977; Shinn, 1986) (compare Figure 3.10 of Chapter 3 with Figure 22 in Shinn, 1986). In both cases, a lithified, karsted, seaward-dipping, carbonate rock platform (the Knox dolostones for the Ordovician sequence, and the Pleistocene limestones for Andros Island) is overlain unconformably by tidal flat sediments, which are in turn overlain by shallow subtidal marine sediments. In both cases, not only is the sequence of depositional facies identical, but the nature of the contact between the tidal flat facies and the overlying subtidal marine facies is the same. A sharp erosional surface analogous to that at the top of the Mosheim/New Market is currently forming at the seaward margin of the tidal flat beach ridge on northwest Andros Island (see Figure 24 in Hardie and Garrett, 1977), where the subtidal marine environment is migrating landward over the tidal flat. This Holocene beach ridge erosion is entirely the result of transgressive environmental migration and landward retreat of the beach ridge, and is thus a ravinement surface, as defined by Demerest and Kraft (1987) and Nummedal and Swift (1987). The Middle Ordovician erosional surface was produced in precisely the same manner, although the

process covered a much larger area and continued over a longer period of time than in the Andros Island analogue.

Is the Middle Ordovician sequence truly analogous to Andros Island?

The transgressive tidal flat sequence on the northwest side of Andros Island and the Middle Ordovician sequence in the southern Appalachians are remarkably similar in terms of the subenvironments represented in each case, and the overall stratigraphic arrangement of those subenvironments. The mechanism responsible for the depositional sequence on Andros and for the erosional surface within that sequence appears to serve well as a modern analogue for the Middle Ordovician. However, there is one major difference that needs to be addressed.

The Middle Ordovician tidal flat sediments, at least those immediately beneath the erosional surface, were largely lithified prior to deposition of the overlying subtidal marine sediments. The degree of lithification is uncertain, but is believed to have been quite thorough. Lithification of the tidal flat sediment on Andros, on the other hand, is significantly less advanced. Some cementation has occurred, as indicated by the accumulations of intraclasts at the base of the low, wave-cut cliff that marks the seaward edge of the beach ridge, and the intraclasts that are strewn about on the surface of the beach ridge terrace and washover crest (see Figures 24, 25, and 26 of Hardie and Garrett, 1977). These intraclasts are derived from erosion and break-up of "cemented crusts" within the tidal flat and beach ridge sediment (Hardie and Garrett, 1977). Cementation on Andros appears to be limited to these crusts.

What conditions were different in the Middle Ordovician that allowed the tidal flat to undergo such thorough cementation? Extensive early lithification would seem to require either a longer period of subaerial exposure than the Andros tidal flat has

experienced, or more intense diagenetic alteration during a comparable period of exposure. It is quite possible that one or both of these conditions were met. Greater lithification of the Middle Ordovician sequence relative to the Andros tidal flat could simply reflect the youth of the Andros sediments. Hardie and Garrett (1977) have determined that the entire body of tidal flat sediment on Andros has accumulated with the last 5000 years, so the uppermost portions have certainly been exposed for a much shorter period of time than that. Given sufficient time, cementation on Andros might become comparable to the Ordovician tidal flat. Another possibility is that the Middle Ordovician transgression proceeded at a rate which was much slower than the Holocene transgression, or that the Ordovician tidal flat sediments accumulated at a slower rate, and thus allowed exposed portions of the tidal flat more time to become cemented.

Longer exposure might not be necessary if the rate of Middle Ordovician diagenesis (primarily cementation) was more rapid. It is possible that the climate in which the Middle Ordovician tidal flats of the the southern and central Appalachians were deposited was even more humid and rainy than the current Bahamian climate. If so, freshwater alteration might have proceeded more rapidly and more thoroughly lithified the tidal flat sediments prior to transgression of the overlying offshore marine facies. In any case, given the other striking similarities, the greater degree of lithification of the Middle Ordovician tidal flat facies does not invalidate the use of Andros Island as a modern analogue for the formation of the erosion surface.

Was sea level fall required for the formation of the erosion surface?

Extensive lithification, whether the result of prolonged subaerial exposure, or more rapid diagenetic alteration, or both, would certainly be facilitated by a temporary interruption of the sea level rise that drove the Middle Ordovician transgression. It is

possible that a minor (4th or 5th order) sea level fall or stillstand was superimposed on the larger scale early Middle Ordovician sea level rise, and that interruption of the sea level rise provided the time and isolation required for lithification of portions of the tidal flat. Sea level fall would also have facilitated meteoric diagenesis by deepening the fresh water lens and extending it seaward, therefore allowing more of the sediment to come in contact with meteoric fluids.

Sea level fall or stillstand would not be necessary for lithification to occur, however. Prolonged periods of subaerial exposure are the norm for large portions of tidal flats, and subaerial exposure surfaces showing evidence of early lithification are abundant in modern and ancient tidal flat sequences (Shinn, 1983; Hardie and Shinn, 1986). Given that much of a tidal flat is deposited above mean sea level, sea level fall need not be invoked to explain such exposure. Another factor that would enhance lithification at the seaward margin of a tidal flat is the presence of a well-developed channel network, such as exists on the transgressive portion of the Andros Island tidal flat (Shinn et al, 1969; Hardie and Garrett, 1977). Tidal channels funnel storm tides and sediment-laden seawater toward the landward margin of the tidal flat, and allow the elevated beach ridge and supratidal levees near the seaward edge of the flat to escape inundation and sedimentation. On Andros Island, the beach ridge is inundated only by the strongest storms (hurricanes) and is only rarely blanketed by new sediment (Hardie and Garrett, 1977). Because it experiences the most subaerial exposure, the beach ridge is the most susceptible of all tidal flat subenvironments to freshwater alteration. Shinn (1986) suggests, by analogy with Andros Island, that transgressive tidal flats in the geologic record should possess well-developed channeled belts landward of a beach ridge. Evidence exists for both beach ridge and channeled belt subfacies in the Middle Ordovician tidal flats (Mitchell, 1985; Chapter 3 of this dissertation).

If sea level fall had been a factor in the formation of the Middle Ordovician erosional surface, one would expect to see evidence of progradation of the tidal flat and the development of an offlap stratigraphic sequence, but the signature of regression is lacking from the stratigraphic record of the Mosheim/Five Oaks/New Market tidal flat. The basal Middle Ordovician stratigraphic package in the southern Appalachians is entirely transgressive, and records only a single pass of peritidal environments during deposition of the transgressive sequence that unconformably overlies the Knox Group. Beginning at the base (the Knox unconformity), this stratigraphic package consists of the supratidal algal marsh, the channeled belt complex (ponds, channels, levees, etc.), the beach ridge (sometimes removed by erosion), erosion surface, and the adjacent subtidal marine facies. This package, which would be the vertical arrangement predicted by uninterrupted transgression, is shown in Figure 3.10. The repetitive stacking of meter-scale, shallowing-upward (progradational) cycles that is typical of many ancient tidal flat sequences (Hardie, 1986) does not occur in the Middle Ordovician peritidal sequence in the southern Appalachians.

If significant sea level fall had occurred, evidence of subaerial exposure in shallow subtidal sediments should also exist, but unequivocal evidence of such has not been observed in the Middle Ordovician tidal flat facies. Subtidal limestones in many places within the tidal flat facies contain dissolution fabrics, but this dissolution could have occurred many meters beneath an exposure surface when fresh water or mixed meteoric / marine fluids passed through the pore system of the sediment. The timing of dissolution and freshwater alteration in subtidal lithologies is not well-constrained by cross-cutting relations, such as erosional truncation of cements, so the alteration could have occurred at any depth or time following deposition. For this reason, vugs in shallow subtidal limestones are not regarded as indicators of early subaerial exposure of those sediments.

Reliable indicators of vadose alteration are restricted to inter- and supratidal portions of the tidal flat sequence.

The minimal amount of relief on the erosional surface (no more than 30 centimeters has been observed in the southern Appalachians) could have developed due to a combination of surface dissolution and tidal scour of supratidal zones, and does not require any drop in sea level.

Also, if a single sea level fall were responsible for the erosion surface, the surface should be correlatable from location to location, and that is not the case, as indicated by paleontologic information (Figure 5.2). Time of formation of the erosional surface is discussed in the following section.

It should be pointed out that sea level fall is not presently occurring on the Great Bahama Bank (Shinn, 1986), and is not a factor in the production of the erosional surface at the seaward margin of the Andros Island tidal flat, and therefore was not necessary as an agent in the development of the Middle Ordovician diastem. This shows that subaerial erosion surfaces in the stratigraphic record, especially in paralic environments such as tidal flats, are not always indicative of sea level fall, and do not always coincide with depositional sequence boundaries.

Is the erosion surface isochronous throughout the southern Appalachians?

Given that the erosion surface under discussion always forms the contact between the basal Middle Ordovician tidal flat and the overlying marine deposits, and as such serves as an important stratigraphic marker, it might seem that the surface at all places represents a stratigraphically important, one-time event, such as a regional flooding event or major sea level fluctuation. Detailed biostratigraphic work done to determine the timing of other events in the southern Appalachians (Bergstrom, 1973; Bergstrom and

Carnes, 1976; Finney, 1984; Coffey, 1986; Hall, et al., 1986; A. Harris, personal communication, 1986, 1990; Shaw et al., 1990), however, clearly shows that the erosional surface formed at different times at different places, and is time-transgressive from southeast to northwest across the depocenter. Figure 5.2 shows the approximate time of development of the diastem at various locations in Alabama and Tennessee where conodont biostratigraphic analyses have been made. This figure illustrates two important points: (1) the erosional surface is of brief duration (too short to be accurately resolved by conodont biostratigraphy but definitely shorter than the duration of a single conodont zone), and (2) the erosional surface cannot be correlated chronostratigraphically from one location to another, and clearly did not form simultaneously throughout the region. At any given location, the erosional surface formed when the marine transgression caused the offshore marine environment to onlap over the tidal flat in that area. Such erosion and inundation was time-transgressive across the region, and therefore strengthens an interpretation that the surface is a ravinement diastem, as defined by Nummedal and Swift (1987).

Conclusions

1. Middle Ordovician scalloped and planar erosion surfaces, as described by Read and Grover (1977) for the Virginia Appalachians, occur in the same stratigraphic position, at the top of the basal Middle Ordovician tidal flat facies, throughout the southern Appalachians, from Central Alabama to northern Virginia. A comparable erosion surface has also been reported in a very similar carbonate sequence of the same general age from as far north as Quebec (Desrochers and James, 1988).

2. These surfaces exhibit abundant evidence of subaerial exposure, early lithification, and wave scour, and, as suggested by Read and Grover (1977), probably formed through a combination of subaerial karstification and tidal erosion.

3. Despite evidence of subaerial exposure and erosion, paleontologic data indicate that this surface represents a relatively brief break in deposition (probably no more than a few hundred to a few thousand years), and is therefore considered a diastem and not a major disconformity. The vertical sequence of facies predicted by Walther's Law for transgressive migration of peritidal facies is not disrupted by this erosion surface.

4. The regionally widespread distribution of this erosional surface would normally suggest that the surface formed in response to a eustatic sea level drop superimposed on the well-documented overall Middle Ordovician (Chazyan) sea level rise. However, conodont biostratigraphic analyses show that the surface is diachronous, and time-transgressive from southeast to northwest. The surface therefore cannot be the result of eustatic sea level fall.

5. This surface is an erosional feature within a transgressive sedimentary sequence, and is not a depositional sequence boundary. The surface is thus the carbonate equivalent of the ravinement diastem, as defined for clastic transgressive sequences by Nummedal and Swift (1987) and Demerest and Kraft (1987). An analogous erosional surface is presently forming without sea level fall in a very similar stratigraphic setting on the northwest side of Andros Island as a result of transgressive migration of peritidal environments. It is suggested here that the Middle Ordovician erosional surface was produced by precisely the same process.

Chapter 6

CONCLUSIONS

Chapters 2 through 5 of this dissertation provided information regarding the stratigraphy, depositional history, and diagenetic alteration of the basal middle Ordovician carbonate rocks. The conclusions from those chapters are summarized below.

1. The lithologic units that comprise the basal portion of the Middle Ordovician sequence and overlie the post-Knox unconformity in the Valley and Ridge province of eastern Tennessee signify the resumption of deposition following a major Early - Middle Ordovician regression that resulted in exposure of a large portion of the Cambro-Ordovician platform in the Southern Appalachians. Different stratigraphic nomenclature is used on either side of the Saltville Fault to describe these units. On the southeast side of the fault, the basal Middle Ordovician stratigraphic units include the Lenoir Formation and its basal members, the Douglas Lake Member and the Mosheim Member. On the northwest side of the fault, the sequence is represented by the Lincolnshire Formation, the Five Oaks Formation and its basal member, the Blackford Member.

2. The basal Middle Ordovician carbonate units were deposited in three adjacent depositional environments that were positioned parallel to the eastern shoreline of the North American continent. The Douglas Lake and Blackford Members are the stratigraphically lowest of these units, and were deposited in isolated topographic depressions on the exposed Knox surface in a variety of isolated nearshore terrestrial and paralic environments. The Mosheim Member of the Lenoir Formation and the main body of the Five Oaks Formation comprise the basal Middle Ordovician carbonate tidal flat,

and overlie the Douglas Lake / Blackford facies, or directly overlie the Knox surface where the terrestrial/paralic units are absent. The main body of the Lenoir Formation and the Lincolnshire Formation overlie the tidal flat facies, and represent deposition in the shallow subtidal marine environment that lay just offshore from the tidal flat.

3. The vertical succession of these three facies defines a deepening-upward, transgressive sequence that resulted from the landward migration of the package of peritidal environments. Transgression was driven by the Middle Ordovician sea level rise and the foundering of the Cambro-Ordovician platform and development of the Sevier foreland basin.

4. The tidal flat represented by the Mosheim / Five Oaks facies is a remarkably close ancient analogue to the northwestern portion of the Holocene tidal flat on Andros Island in the Bahamas, as described in detail by Shinn et al. (1969), Hardie and Garrett (1977), and Shinn (1986). Most features commonly associated with arid, Persian Gulf-type tidal flats are extremely rare or absent in this tidal flat facies.

5. The Mosheim / Five Oaks tidal flat facies is composed of three major subfacies, each of which is a direct analogue of a major subenvironment of the Andros Island tidal flat. The highly fenestral, laminated basal portion of the Mosheim / Five Oaks facies was deposited in a supratidal environment very similar to the inland algal marsh, the most landward portion of the Andros Island tidal flat complex. The majority of the Mosheim / Five Oaks sequence consists of a complicated arrangement of shallow subtidal, intertidal, and supratidal lithologies that represent deposition in a complex mosaic of ponds, channels, algal marshes, and levees. Taken together, this portion of the sequence represents a well-developed Andros Island-type channeled belt. The uppermost layers of

the sequence represent supratidal and intertidal deposition in various subenvironments of a beach ridge that formed the seaward margin of the tidal flat.

6. The vertical succession of subfacies within the Mosheim / Five Oaks tidal flat facies defines a purely transgressive sequence that contains no evidence of progradational, shallowing-upward cycles. The tidal flat facies occurs within, and near the base of, the Middle Ordovician carbonate sequence, the lower portion of which is also entirely transgressive.

7. The upper surface of the tidal flat facies, which marks the contact between the Mosheim / Five Oaks tidal flat facies and the overlying Lenoir / Lincolnshire shallow subtidal marine facies, is sharp and in many places, erosional. The tidal flat facies and the overlying shallow subtidal marine facies do not interfinger, and the base of the Lenoir / Lincolnshire facies at any given location within the study area marks the final flooding of the tidal flat due to sea level rise and landward migration (transgression) of the offshore marine environment, and the end of peritidal deposition.

8. Diagenetic alteration of the tidal flat facies is dominated by features that indicate alteration by meteoric water. Meteoric diagenesis occurred above and below the water table in unsaturated (vadose) and saturated (phreatic) zones. Subaerial exposure and vadose zone alteration is indicated by several features, including: (1) abundant fenestral fabrics and less commonly, desiccation features such as mudcracks and sheet cracks; (2) alteration of fenestral fabric to diagenetic grainstones and pisolites; (3) thin bleached zones within and at the top of the supratidal and intertidal lithologies; (4) localized zones of incipient caliche development, typically just below exposure surfaces; (5) pendant and meniscus cement distributions; and (6) geopetal crystal silt in fenestrae and vugs.

Additional evidence of meteoric diagenesis (which may have begun in the vadose zone and continued into the phreatic realm) includes dissolution features such as fossil molds and solution-enlarged molds and vugs; stabilization of marine mud to micrite; and the ubiquitous presence of clear, non-ferroan, compositionally-zoned, equant calcite cement and microspar. Virtually all porosity is occluded by equant calcite cement, and other types of cement are volumetrically negligible.

9. The majority of diagenetic alteration occurred very early, beginning immediately upon deposition of the tidal flat sediment and being largely concluded before deep burial. Most diagenesis occurred while the sediment remained in the tidal flat depositional environment. At least the uppermost surface of the tidal flat facies, and likely other subaerially exposed supratidal and intertidal horizons within the facies as well, underwent extensive lithification prior to deposition of the overlying strata. Evidence for early diagenetic alteration and lithification of intertidal and supratidal lithologies occurs in the form of 1) the presence of paleokarst features on the upper erosion surface; 2) erosional truncation of cements as well as depositional material in lithologies underlying erosional surfaces; 3) borings and vugs extending downward from the erosion surface; and 4) encrustation of the upper erosion surface after flooding by calcareous marine organisms. The timing of diagenetic alteration of subtidal lithologies is less well constrained, but it probably was largely completed during shallow burial in the phreatic environment.

10. Hydrologically, the setting in which deposition and early diagenesis occurred was a zone of mixing of seawater and freshwater in an unconfined coastal aquifer. The fluids that covered this tidal flat and filled the sedimentary pores beneath the water table probably fluctuated between meteoric and normal marine end members, but the

diagenetic features and geochemical data indicate that the nature of the water was probably very dilute and closer to freshwater than seawater.

11. Dolomite within the tidal flat sequence occurs as single rhombs disseminated widely through the muddy matrix. Primary, supratidal dolomite crusts are absent, and the only pervasively dolomitized lithologies occur within a meter of the base of the tidal flat facies, where magnesium was available from several sources, including exsolution from the underlying Knox dolostones and movement of burial fluids along the Knox unconformity. Above this basal meter, i.e. in the channeled belt subfacies, dolomite abundance is related to depositional subenvironment, and is most abundant in burrowed, subtidal lithologies and least abundant in supratidal fenestral lithologies. Dolomitization of subtidal pond lithologies may have occurred by alteration of sediment by mixed meteoric / marine fluids in the coastal mixing zone. In general, dolomite abundance decreases upward, and dolomite is very rare in the uppermost beach ridge lithologies.

12. The tidal flat facies probably assumed the role of a barrier to groundwater migration (an aquitard) very early, because virtually all porosity was occluded before deep burial. The effects of deep burial diagenesis are minimal (limited to pressure solution and occlusion of late fractures by calcite and silica cements), probably because fluids did not readily move through the facies, except along fractures. Because of its relative impermeability, the tidal flat facies probably played a significant role in controlling fluid flow (and associated mineralization) along the Knox unconformity.

13. The surface at the top of the tidal flat facies exhibits abundant evidence of subaerial exposure, early lithification, and wave scour, and probably formed through a combination of subaerial karstification and tidal erosion. Despite the extensive vadose alteration and

erosion, paleontologic data indicate that this surface represents a very brief break in deposition, and is not a major disconformity. The vertical sequence of facies predicted by Walther's Law for transgressive migration of peritidal facies is not disrupted by this erosion surface.

14. The erosional surface at the top of the tidal flat facies occurs in the same lithostratigraphic position throughout the southern Appalachians, from central Alabama to northern Virginia. The regionally-widespread distribution of this erosional surface would normally suggest that the surface formed in response to a eustatic sea level drop superimposed on the well-documented overall Middle Ordovician sea level rise. However, conodont biostratigraphic analyses show that the formation of the surface was diachronous along regional strike throughout the southern Appalachians, and time-transgressive from southeast to northwest. The surface therefore cannot be the result of eustatic sea level fall.

15. This erosional surface occurs within a transgressive sedimentary sequence, and is not a depositional sequence boundary. The surface is thus the carbonate equivalent of the ravinement diastem, as defined for clastic transgressive sequences by Nummedal and Swift (1987) and Demerest and Kraft (1987). An analogous erosional surface is presently forming without sea level fall in a very similar stratigraphic setting on the northwest side of Andros Island as a result of transgressive migration of peritidal environments. It is suggested here that the Middle Ordovician erosional surface formed in precisely the same manner.

REFERENCES

REFERENCES

Adams, J.E., and Rhodes, M.G., 1960, Dolomitization by seepage refluxion: American Association of Petroleum Geologists Bulletin, v. 44, p. 1912-1920.

Aristarain, L.F., 1970, Chemical analysis of caliche profiles from the High Plains, New Mexico: Journal of Geology, v. 78, p. 201-213.

Back, W., Hanshaw, B.B., Plummer, L.N., Rahn, P.H., Rightmire, C.T., and Rubin, M., 1983, Process and rate of dedolomitization: mass transfer and 14C dating in a regional carbonate aquifer: Geological Society of America Bulletin, v. 94, p. 1415-1429.

Badiozamani, K., 1973, The Dorag dolomitization model-application to the Middle Ordovician of Wisconsin: Journal of Sedimentary Petrology, v. 43, p. 965-984.

Bates, R.L., and Jackson, J.A., 1980, Glossary of Geology: American Geological Institute, 751 p.

Bathurst, R.G.C., 1975, Carbonate Sediments and Their Diagenesis, Second edition, Developments in Sedimentology 12, Amsterdam, Elsevier, 658 p.

Bein, A., and Land, L.S., 1983, Carbonate sedimentation and diagenesis associated with Mg-Ca-Chloride brines: The Permian San Andres Formation in the Texas Panhandle: Journal of Sedimentary Petrology, v. 53, p. 243-260.

Benedict, G.L., and Walker, K.R., 1978, Paleobathymetric analysis in Paleozoic sequences and its geodynamic significance: American Journal of Science, v. 278, p. 579-607.

Benson, D.J., and Mink, R.M., 1983, Depositional history and petroleum potential of the Middle and Upper Ordovician of the Alabama Appalachians: Gulf Coast Association of Geological Societies, Transactions, vol. 33, p. 13-21.

Bergstrom, S.M., 1973, Biostratigraphy and facies relations in the lower Middle Ordovician of easternmost Tennessee: American Journal of Science, v. 273, p. 261-293.

Bergstrom, S.M., and Carnes, J.B., 1976, Conodont biostratigraphy and paleoecology of the Holston Formation (Middle Ordovician) and associated strata in eastern Tennessee, *in* Barnes, C.R., ed., Conodont paleoecology: Geological Association of Canada Special Publication 15, p. 27-58.

Bridge, J.A., 1955, Disconformity between Lower and Middle Ordovician Series at Douglas Lake, Tennessee: Geological Society of America Bulletin, v. 66, p. 725-730.

Bridge, J.A., 1956, Stratigraphy of the Mascot-Jefferson City zinc district, Tennessee: U.S. Geological Survey Professional Paper 277, 76 p.

Broecker, W.S., and Takahashi, T., 1966, Calcium carbonate precipitation on the Bahama Banks: Journal of Geophysical Research, v. 71, p. 1575-1602.

Butts, C., 1940, Geology of the Appalachian Valley in Virginia: Virginia Geological Survey Bulletin, v. 52, part 1, 568 p.

Calvet, F., and Julia, R., 1983, Pisoids in the caliche profiles of Tarragona (N.E. Spain), *in* Peryt, T., ed., Coated Grains: Berlin, Springer-Verlag, p. 456-473.

Carballo, J.D., Land, L.S., and Miser, D.E., 1987, Holocene dolomitization of supratidal sediments by active tidal pumping, Sugarloaf Key, Florida: Journal of Sedimentary Petrology, v. 57, p. 153-165.

Chafetz, H.S., and Butler, J.C., 1980, Petrology of recent caliche pisolites, spherulites, and speleothem deposits from central Texas: Sedimentology, v. 27, p. 497-518.

Choquette, P.W., and Pray, L.C., 1970, Geological nomenclature and classification of porosity in sedimentary carbonates: American Association of Petroleum Geologists Bulletin, V. 54, p. 207-250.

Choquette, P.W., and Steinen, R.P.,1980, Mississippian non-supratidal dolomite, Ste. Genevieve Limestone, Illinois Basin: evidence for mixed-water dolomitization, *in* Zenger, D.H., Dunham, J.B., and Ethington, R.L., eds., Concepts and Models of Dolomitization: Society of Economic Paleontologists and Mineralogists Special Publication No. 23, p. 163-196.

Churnet, H.G., 1979, The relationships between dolomitization and sphalerite mineralization in the Lower Ordovician upper Knox carbonate rocks of the Copper Ridge District, east Tennessee (unpublished Ph.D. dissertation): Knoxville, University of Tennessee, 237 p.

Coffey, M.L., 1986, Paleoecology and biostratigraphy of the Fetzer Formation, Middle Ordovician, of eastern Tennessee (unpublished M.S. thesis): Knoxville, Univ. of Tennessee, 140 p.

Cooper, G.A., 1956, Chazyan and related brachiopods: Smithsonian Miscellaneous Collection, v. 127, part 1, 1024 p.

Cooper, G.A., and Prouty, C.E., 1943, Stratigraphy of the lower Middle Ordovician of Tazewell County, Virginia: Geological Society of America Bulletin, V. 43, p. 819-886.

Davies, G.R., 1977, Former magnesian calcite and aragonite submarine cements in upper Paleozoic reefs of the Canadian Arctic: a summary: Geology, v. 5, p. 11-15.

Deffeyes, K.S., Lucia, F.J., and Weyl, P.K., 1965, Dolomitization of recent and Plio-Pleistocene sediments by marine evaporite waters on Bonaire, Netherlands Antilles, *in* Pray, A.C., and Murray, R.C., eds., Dolomitization and Limestone Diagenesis: Society of Economic Paleontologists and Mineralogists Special Publication 13, p. 71-88.

Demerest, J.M., II, and Kraft, J.C., 1987, Stratigraphic record of Quaternary sea levels: implications for more ancient strata: Journal of Sedimentary Petrology, v. 57, p. 223-239.

Desrochers, A., and James, N.P., 1988, Early Paleozoic surface and subsurface paleokarst: Middle Ordovician carbonates, Mingan Islands, Quebec, *in* James, N.P., and Choquette, P.W., eds., Paleokarst: New York, Springer-Verlag, p. 183-210.

Dott, R.L., Jr., 1964, Wacke, graywacke, and matrix--what approach to immature sandstone classification?: Journal of Sedimentary Petrology, v. 34, p. 625-632.

Drahovzal, J.A., and Neathery, T.L., 1971, Middle and Upper Ordovician stratigraphy of the Alabama Appalachians, *in* Drahovzal, J.A., and Neathery, T.L., eds., The Middle and Upper Ordovician of the Alabama Appalachians: Alabama Gelolgical Society, Ninth Annual Field Trip Guidebook, p. 1-62.

Dunham, R.J., 1969a, Early vadose silt in Townsend mound (reef), New Mexico, in Friedman, G.M., ed., Depositional Environments in Carbonate Rocks: Society of Economic Paleontologists and Mineralogists Special Publication 14, p. 139-181.

Dunham, R.J., 1969b, Vadose pisolites in the Capitan reef (Permian), New Mexico and Texas, in Depositional Environments in Carbonate Rocks: Society of Economic Paleontologists and Mineralogists Special Publication 14, p. 182-191.

Dunham, R.J., 1962, Classification of carbonate rocks according to depositional texture: American Association of Petroleum Geologists Memoir 1, p. 108-121.

Esteban, M., 1976, Vadose pisolites and caliche: American Association of Petroleum Geologists Bulletin, v. 60, p. 2048-2057.

Esteban, M., and Pray, L.C., 1983, Pisoids and pisolite facies (Permian) , Guadalupe Mountains, New Mexico and west Texas, *in* Peryt, T., ed., Coated Grains: Berlin, Springer-Verlag, p. 503-537.

Esteban, M. , and Klappa, C.F., 1983, Subaerial exposure environment, *in* Scholle, P.A., Bebout, D.G., and Moore, C.H., eds., Carbonate Depositional Environments: American Association of Petroleum Geologists, Memoir 33, p. 1-54.

Ettensohn, F.R., Dever, G.R., Jr., and Grow, J.S., 1988, A paleosol interpretation for profiles exhibiting subaerial exposure "crusts" from the Missisippian of the Appalachian Basin, Geological Society of America, Special Paper 216, p. 49-79.

Fairchild, J.J., 1983, Chemical controls on cathodoluminescence of natural calcite and dolomites: new data and review: Sedimentology, v. 30, p. 579-583.

Finney, S.C., 1984, Biogeography of Ordovician graptolites in the southern Appalachians, in Bruton, D.L., ed., Aspects of the Ordovician System: Palaeontological Contributions from the University of Oslo, no. 295, p. 167-176.

Fischer, A.G., 1964, The Lofer cyclothems of the Alpine Triassic, in Merriam, D.R., ed., Symposium on Cyclic Sedimentation: State Geological Survey of Kansas, Bulletin 169, v. 1, p. 107-149.

Fischer, A.G., 1975, Tidal deposits, Dachstein Limestone of the North-Alpine Triassic, in Ginsburg, ed., Tidal Deposits: Springer-Verlag, New York, p. 235-242.

Folk, R.L., 1965, Some aspects of recrystallization in ancient limestones, *in* Pray, A.C., and Murray, R.C., eds., Dolomitization and Limestone Diagenesis: Society of Economic Paleontologists and Mineralogists Special Publication 13, p. 14-48.

Folk, R.L., 1974, Natural history of crystalline calcium carbonate: effect of magnesium content and salinity: Journal of Sedimentary Petrology, v. 44, p. 40-53.

Folk, R.L., and Asseretto, R., 1974, Great aragonite rays and baroque white dolomite in tepee fillings, Triassic of Lombardy, Italy (abstract): American Association of Petroleum Geologists, Abstracts with Program, p. 34-39.

Foos, A.M., 1991, Aluminous lateritic soils, Eleuthera, Bahamas: a modern analog to carbonate paleosols: Journal of Sedimentary Petrology, v. 61, p. 340-348.

Frank, J.R., Carpenter, A.B., and Oglesby, T.W., 1982, Cathodoluminescence and composition of calcite cement in the Taum Sauk limestone (Upper Cambrian), southeast Missouri: Journal of Sedimentary Petrology, v. 52, p. 631-638.

Gebelein, C.D., Steinen, R.P., Garrett, P. Hoffman, E.J., Queen, J.M., and Plummer, L.N., 1980, Subsurface dolomitization beneath the tidal flats of central west Andros Island, Bahamas, *in* Zenger, D.H., Dunham, J.B., and Ethington, R.L., eds., Concepts and Models of Dolomitization: Society of Economic Paleontologists and Mineralogists Special Publication No. 23, p. 163-196.

Gensel, P.G., and Andrews, H.N., 1987, The evolution of early land plants: American Scientist, v. 75, p. 478-489.

Ginsburg, R.N., 1953, Beachrock in South Florida: Journal of Sedimentary Petrology, v. 23, p. 85-92.

Ginsburg, R.N., Hardie, L.A., Bricker, O.P., Garrett, P., and Wanless, H.R., 1977, Exposure index: A quantitative approach to defining position within the tidal zone, *in* Hardie, L.A., ed., Sedimentation on the modern carbonate tidal flats of northwest Andros Island, Bahamas: Baltimore, Johns Hopkins.University Press, p. 7-11.

Goodell, H.G., and Garman, R.K., 1969, Carbonate geochemistry of Superior deep test well, Andros island, Bahamas: Association of Petroleum Geologists Bulletin, v. 53, p. 513-536.

Grover, G.A., Jr., and Read, J.F., 1978, Fenestral and associated vadose diagenetic fabrics of tidal flat carbonates, Middle Ordovician New Market Limestone, southwestern Virginia: Journal of Sedimentary Petrology, v. 48, p. 453-473.

Grover, G.A., Jr., and Read, J.F., 1983, Paleoaquifer and deep burial related cements defined by regional cathodoluminescent patterns, Middle Ordovician carbonates, Virginia: American Association of Petroleum Geologists Bulletin, v. 67, p. 1275-1303.

Hall, G.M., and Amick, H.C., 1934, The section on the west side of Clinch Mountain, Tennessee: Tennessee Academy of Sciences Journal, v. 9, p. 157-168 and 195-220.

Hall, J.C., Bergstrom, S.M., and Schmidt, M.A., 1986, Conodont biostratigraphy of the Middle Ordovician Chickamauga Group and related strata of the Alabama Appalachians, *in* Benson, D.J., and Stock, C.W., eds., Depositional History of the Middle Ordovician of the Alabama Appalachians: Alabama Geological Society, Guidebook, 23rd Annual Field Trip, p. 61-80.

Hanshaw, B.B., Back, W. and Deike, R.G. 1971, A geochemical hypothesis for dolomitization by groundwater: Economic Geology, v. 66, p. 710-724.

Hardie, L.A.(ed.), 1977, Sedimentation on the modern carbonate tidal flats of northwest Andros Island, Bahamas: Baltimore, Johns Hopkins University Press, 202 p.

Hardie, L.A., 1977, Distinctive features of a rainy, low-energy, tropical carbonate tidal flat: a summary: *in* Hardie, L.A., ed., Sedimentation on the modern carbonate tidal flats of northwest Andros Island, Bahamas: Baltimore, Johns Hopkins.University Press, p. 178-183.

Hardie, L.A., 1986, Stratigraphic models for carbonate tidal-flat deposition, *in* Carbonate Depositional Environments, Modern and Ancient 3, Tidal Flats: Colorado School of Mines Quarterly, v. 81, 74 p.

Hardie, L.A., 1987, Dolomitization: A critical view of some current views: Journal of Sedimentary Petrology, v. 57, p. 166-183.

Hardie, L.A., 1989, Cyclic platform carbonates in the Cambro-Ordovician of the central Appalachians, *in* Walker, K.R., Read, J.F., and Hardie, L.A., eds., Cambro-Ordovician Carbonate Banks and Siliciclastic Basins of the United States Appalachians: 28th International Geological Congress, Field Trip Guidebook T161, p. 51-81.

Hardie, L.A., and Garrett, P., 1977, General environmental setting, *in* Hardie, L.A., ed., Sedimentation on the modern carbonate tidal flats of northwest Andros Island, Bahamas: Baltimore, Johns Hopkins University Press, p. 12-49.

Hardie, L.A., and Ginsburg, R.N., 1977, Layering: the origin and environmental significance of lamination and thin bedding: *in* Hardie, L.A., ed., Sedimentation on the modern carbonate tidal flats of northwest Andros Island, Bahamas: Baltimore, Johns Hopkins University Press, p. 50-123.

Hardie, L.A., and Shinn, E.A., 1986, Carbonate depositional environments, modern and ancient 3, Tidal flats: Colorado School of Mines Quarterly, v. 81, 74 p.

Harris, C.S., 1982, Biostratigraphy and environmental distribution of conodonts from the lowermost Middle Ordovician in east Tennessee (unpublished M.S. thesis): Knoxville, University of Tennessee, 160 p.

Harris, L.D., 1969, Kingsport Formation and Mascot Dolomite (Lower Ordovician) of east Tennessee, *in* Papers on the Stratigraphy and Mine Geology of the Kingsport and Mascot Formations (Lower Ordovician) of East Tennessee: Tennessee Division of Geology, Report of Investigation 23, p. 1-39.

Harris, L.D., 1973, Dolomitization model for Upper Cambrian and Lower Ordovician carbonate rocks in the eastern United States: U.S. Geological Survey, Journal of Research, v. 1, p. 63-78.

Harrison, R.S. and Steinen, R.P., 1978, Subaerial crusts, caliche profiles, and breccia horizons: comparison of some Holocene and Mississippian exposure surfaces, Barbados and Kentucky: Geological Society of America Bulletin, v. 89, p. 385-396.

Haynes, F.M., and Kesler, S.E., 1989, Pre-Alleghenian (Pennsylvanian-Permian) hydrocarbon emplacement along Ordovician Knox unconformity, Eastern Tennessee: American Association of Petroleum Geologists Bulletin, v. 73, p. 289-297.

Hoagland, A.D., Hill, W.T., and Fulweiler, R.E., 1965, Genesis of the Ordovician zinc deposits in East Tennessee: Economic Geology, v. 60, p. 693-714.

Horowitz, A.S., and Potter, P.E., 1971, Introduction to the Petrography of Fossils: New York, Springer-Verlag, 592 p.

Hsu, K.J., and Siegenthalar, C., 1969, Preliminary experiments on hydrodynamic movement induced by evaporation and their bearing on the dolomite problem: Sedimentology, v. 12, p. 11-25.

Humphrey, J.D., 1988, Late Pleistocene mixing zone dolomitization, southeastern Barbados, West Indies: Sedimentology, v. 35, p. 327-348.

Illing, L.V., 1959, Deposition and diagenesis of some upper Paleozoic carbonate sediments in western Canada: Fifth World Petroleum Congress Proceedings, Section 1, Paper 2, p. 23-50.

Illing, L.V., Wells, A.J., and Taylor, C.M., 1965, Penecontemporary dolomite in the Persian Gulf, *in* Pray, A.C., and Murray, R.C., eds., Dolomitization and Limestone Diagenesis: Society of Economic Paleontologists and Mineralogists Special Publication 13, p. 89-111.

James, N.P., 1972, Holocene and Pleistocene calcareous crust (caliche) profiles: criteria for subaerial exposure: Journal of Sedimentary Petrology, v. 42, p. 817-836.

James, N.P., and Choquette, P.W., 1983, Diagenesis 6 -- limestones -- the seafloor diagenetic environment: Geosciences Canada, v. 10, p. 162-179.

James, N.P., and Choquette, P.W., 1984, Diagenesis 9 -- limestones -- the meteoric diagenetic environment: Geosciences Canada, v. 11, p. 161-194.

James, N.P., and Klappa, C.F., 1983, Petrogenesis of Early Cambrian reef limestones, Labrador, Canada: Journal of Sedimentary Petrology, v. 53, p. 1051-1096.

Jernigan, D.G., 1987, Comparative diagenetic histories of the Holston and Rockdell Formations, Middle Ordovician of Northeastern Tennessee (unpublished M.S. thesis): Knoxville, University of Tennessee, 234 p.

Jernigan, D.G., and Walker, K.R., 1989, Carbonate cementation environments and products: an overview, *in* Walker, K.R., ed., The Fabric of Cements in Paleozoic Limestones: University of Tennessee Studies in Geology 20, p. 11-18.

Jodry, R.L., 1969, Growth and dolomitization of Silurian reefs, St. Clair County, Michigan: American Association of Petroleum Geologists Bulletin, v. 52, p. 957-981.

Johnson, R.E., 1988, Petrogenesis of carbonate lithofacies along an evolving Paleozoic shelf, Lower Chickamauga Group and equivalents (Middle Ordovician), northeastern Tennessee (unpublished doctoral dissertation): Knoxville, University of Tennessee, 420 p.

Kaldi, J., and Gidman, J., 1982, Early diagenetic dolomite cements: examples from the Permian Lower Magnesian Limestone of England and the Pleistocene carbonates of the Bahamas: Journal of Sedimentary Petrology, v. 52, p. 1073-1085.

Kendall, C.G.St.G., 1969, An environmental reinterpretation of the Permian evaporite carbonate shelf sediments of the Guadalupe Mountains: Geological Society of America Bulletin, v. 80, p. 2503-2526.

Kendall, A.C., 1985, Radiaxial fibrous calcite: a reappraisal, in Schneidermann, N., and Harris, P.M., eds., Carbonate Cements: Society of Economic Paleontologists and Mineralogists Special Publication 36, p. 59-77.

Kesler, S.E., Gesnik, J.A., and Haynes, F.M., 1989, Evolution of mineralizing brines in the East Tennessee Mississippi Valley-type ore field: Geology, v. 17, p. 466-469.

Klappa, C.F., 1980, Brecciation textures and tepee structures in Quaternary calcrete (caliche) profiles from easten Spain: The plant factor in their formation: Geological Journal, v. 15, p. 81-89.

Krumbein, W.C., and Sloss, L.L., 1963, Stratigraphy and Sedimentation: San Francisco, W.H. Freeman, 660 p.

Land, L.S., 1973, Holocene meteoric dolomitization of Pleistocene limestones, North Jamaica: Sedimentology, v. 20, p. 411-424.

Lasemi, Z., and Sandburg, P.A., 1984, Transformation of aragonite-dominated lime muds into microcrystalline limestones: Geology, v. 12, p. 420-423.

Laurence, R.A., 1944, An Early Ordovician sinkhole deposit of volcanic ash and fossiliferous sediments in East Tennessee: Journal of Geology, v. 52, p. 235-249.

Logan, B.W., Davies, G.R., Read, J.F., and Cebulski, D.E., 1970, Carbonate sedimentation and environments, Shark Bay, Western Sustralia: American Association of Petroleum Geologists Bulletin, Memoir 13, p. 1-223.

Logan, B.W., and Semeniuk, V., 1976, Dynamic metamorphism: processes and products in Devonian carbonate rocks, Canning Basin, Western Australia: Geological Society of Australia Special Paper 6, p. 138.

Longman, M.W., 1980, Carbonate diagenetic textures from nearsurface diagenetic environments: American Association of Petroleum Geologists Bulletin, v. 64, p. 461-487.

Machel, H.-G., 1985, Cathodoluminescence in calcite and dolomite and its chemical interpretation: Geosciences Canada, v. 12, p. 139-147.

Machel, H.-G., and Mountjoy, E.W., 1986, Chemistry and environments of dolomitization--a reappraisal: Earth Sciences Review, v. 23, p. 175-222.

Magaritz, M., Goldenberg, L., Kafri, U., and Arad, A., 1980, Dolomite formation in the seawater-freshwater interface: Nature, v. 287, p. 622-624.

Mattes, B.W., and Mountjoy, E.W., 1980, Burial dolomitization of the Upper Devonian Miette Buildup, Jasper National Park, Alberta, *in* Zenger, D.H., Dunham, J.B., and Ethington, R.L., eds., Concepts and Models of Dolomitization: Society of Economic Paleontologists and Mineralogists Special Publication No. 28, p. 259-297.

Mazzullo, S.J., and Birdwell, B.A., 1989, Syngenetic formation of grainstones and pisolites from fenestral carbonates in peritidal settings: Journal of Sedimentary Petrology, v. 59, p. 605-611.

McKenzie, J.A., Hsu, K.J., and Schneider, J.F., 1980, Movement of subsurface waters under the sabkha, Abu Dhabi, United Arab Emirates, and its relation to evaporative dolomite genesis, *in* Zenger, D.H., Dunham, J.B., and Ethington, R.L., eds., Concepts and Models of Dolomitization: Society of Economic Paleontologists and Mineralogists Special Publication No. 28, p. 11-30.

Metcalfe, S.J., 1974, Acid-insoluble residues in Chickamauga equivalents (Middle Ordovician) in East Tennessee--an aid to paleogeographic reconstruction (unpublished M.S. thesis): Knoxville, University of Tennessee, 64 p.

Milici, R.C. and Smith, J.W., 1969, Stratigraphy of the Chickamauga Supergroup in its type locality: Georgia Geological Survey, Bulletin 57, 128 p.

Misra, K.C., Kopp, O.C., Paris, T.A., and Linkous, M.A., 1989, Mississippi Valley-type fluorite-barite-sphalerite mineralization in the Sweetwater district, Tennessee: Carbonates and Evaporites, v. 4, no. 2, p. 211-230.

Misra, K.C., Fulweiler, R.E., and Walker, K.R., eds., Zinc Deposits in East Tennessee: Society of Economic Geologists, Field Conference Guidebook, v. 14, p. 66-76.

Mitchell, R.W., 1981, Comparative sedimentology of the Bahamian-type shelf carbonates of the Middle Ordovician St. Paul Group of the central Appalachians (unpublished Ph.D. dissertation): Baltimore, The Johns Hopkins University, 495 p.

Mitchell, R.W., 1985, Comparative sedimentology of shelf carbonates of the Middle Ordovician St. Paul Group, Central Appalachians: Sedimentary Geology, v. 43, p. 1-41.

Morrow, D.W., 1982a, Diagenesis I. Dolomite--part I: The chemistry of dolomitization and dolomite precipitation: Geosciences Canada, v. 9, p. 5-13.

Morrow, D.W., 1982b, Diagenesis II. Dolomite--part II: Dolomitization models and ancient dolostones: Geosciences Canada, v. 9, p. 95-107.

Mosheir, S.O., 1987, On the nature and origin of microporosity in micritic limestones (unpublished Ph.D. dissertation): Louisiana State University, Baton Rouge, 291 p.

Mosheir, S.O., 1989, Lime mud diagenesis and microcrystalline cements, *in* Walker, K.R., ed., The Fabric of Cements in Paleozoic Limestones: University of Tennessee Studies in Geology 20, p. 78-90.

Moshier, S.O., and McManus, K.M., 1986, Textural evolution during lime mud diagenesis (abstract): American Association of Petroleum Geologists Bulletin, v. 70, p. 623-624.

Muir, M., Lock, D., and Von der Borch, C., 1980, The Coorang model for penecontemporaneous dolomite formation in the Middle Proterozoic McArthur Group, Northern Territory, Australia, *in* Zenger, D.H., Dunham, J.B., and Ethington, R.L., eds., Concepts and Models of Dolomitization: Society of Economic Paleontologists and Mineralogists Special Publication No. 23, p. 51-68.

Multer, H.G., and Hoffmeister, 1968, Subaerial laminated crusts of the Florida Keys: Geological Society of America Bulletin, v. 79, p. 183-192.

Mussman, W.J., and Read, J.F., 1986, Sedimentology and development of a passive- to convergent-margin unconformity--Middle Ordovician Knox unconformity, Virginia Appalachians: Geological Society of America Bulletin, v. 97, p. 282-295.

Mussman, W.J., Montanez, I.P., and Read, J.F., 1988, Ordovician Knox paleokarst unconformity, Appalachians, *in* James, N.P., and Choquette, P.W., eds., Paleokarst: New York, Springer-Verlag, p. 211-228.

Neuman, R.B., 1956, Middle Ordovician rocks of the Tellico-Sevier Belt, eastern Tennessee: U.S. Geological Survey Professional Paper 274f, p. 114-178.

Nowlan, G.S., 1981, Stratigraphy and conodont faunas of the Lower and Middle Ordovician Romaine and Mingan Formations, Mingan Islands, Quebec (abstract): Maritime Sediments and Atlantic Geology, v. 17, p. 67.

Nummedal, D., and Swift, D.J.P., 1987, Transgressive stratigraphy at sequence-bounding unconformities: some principles derived from Holocene and Cretaceous examples: Journal of Sedimentary Petrology, v. 57, p. 241-260.

Oder, C.R.L., and Ricketts, J.E., 1961, Geology of the Mascot-Jefferson City zinc district, Tennessee: Tennessee Division of Geology Report of Investigation 12, 29.

Patterson, R.J., and Kinsman, D.J.J., 1981, Hydrologic framework of a sabkha along the Arabian Gulf: American Association of Petroleum Geologists Bulletin, v. 65, p. 1457-1475.

Patterson, R.J., and Kinsman, D.J.J., 1982, Formation of diagenetic dolomite in a coastal sabkha along the Arabian (Persian) Gulf: American Association of Petroleum Geologists Bulletin, v. 66, p. 28-43.

Peryt, T., 1983, Vadoids, *in* Peryt, T., ed., Coated Grains: Berlin, Springer-Verlag, p. 437-439.

Plummer, L.N., 1975, Mixing of seawater with calcium carbonate groundwater: Geological Society of America Memoir, v. 142, p. 219-236.

Plummer, L.N., Vacher, H.L., MacKenzie, F.T., Bricker, O.P., and Land, L.S., 1976, Hydrogeochemistry of Bermuda: a case history of ground-water diagenesis of biocalcarenites: Geological Society of America Bulletin, v. 87, p. 1301-1316.

Prezbindowski, D.R., and Tapp, J.B., 1989, Asymmetric dissolution textures as evidence of subaerial exposure: Journal of Sedimentary Petrology, v. 59, p. 835-838.

Prouty, C.E., 1946, Lower Middle Ordovician of southwestern Virginia and northeast Tennessee: American Association of Petroleum Geologists Bulletin, v. 30, p. 1140-1191.

Puckett, T.M., Roberson, K.E., and Tew, B.H., 1990, High calcium deposits in the Newala Limestone: Geological Survey of Alabama, Circular 149, 29 p.

Radke, B.M., and Mathis, R.L., 1980, On the formation and occurrence of saddle dolomite: Journal of Sedimentary Petrology, v. 50, p. 1149-1168.

Rasmussen, K.A., and Neumann, A.C., 1988, Holocene overprints of Pleistocene paleokarst, Bight of Abaco, Bahamas, *in* James, N.P., and Choquette, P.W., eds., Paleokarst: New York, Springer-Verlag, p. 132-148.

Read, J.F., 1975, Tidal-flat facies in carbonate cycles, Pillara Formation (Devonian) Canning Basin, Western Australia, *in* Ginsburg, R.N., ed., Tidal Deposits: New York, Springer-Verlag, p. 251-256.

Read, J.F., 1980, Carbonate ramp-to-basin transition and foreland basin evolution, Middle Ordovician, Virginia Appalachians: American Association of Petroleum Geologists Bulletin, v. 64, p. 1575-1612.

Read, J.F., and Grover, G.A., Jr., 1977, Scalloped and planar erosion surfaces, Middle Ordovician limestones, Virginia: Analogues of Holocene exposed karst or tidal rock platforms: Journal of Sedimentary Petrology, v. 47, p. 956-972.

Reeves, C.C., Jr., 1970, Origin, classification, and geologic history of caliche on the southern high plains, Texas, and eastern new Mexico: Journal of Geology, v. 78, p. 352-362.

Roberson, K.E., 1988, The post-Knox unconformity and its relationship to bounding stratigraphy (unpublished M.S. thesis): Tuscaloosa, University of Alabama, 148 p.

Roberson, K.E., 1989, Meteoric cements, *in* Walker, K.R., ed., The Fabric of Cements in Paleozoic Limestones: University of Tennessee Studies in Geology 20, p. 54-65.

Roberson, K.E., Benson, D.J., and Walker, K.R., 1988, Stratigraphic evidence for late Early Ordovician shelf deformation in the Alabama Appalachians (abstract): Geological Society of America, Abstracts with Program, v. 20, no. 4, p. 311.

Roberson, K.E., and Foreman, J.L., 1989, Sedimentology and diagenesis of tidal flat stromatactis, Middle Ordovician, Alabama, *in* Walker, K.R., ed., The Fabric of Cements in Paleozoic Limestones: University of Tennessee Studies in Geology 20, p. 105-117.

Roberson, K.E., and Walker, K.R., 1990, Regional Appalachian disconformity produced solely by environmental migration within a Chazyan (Middle Ordovician) transgressive sedimentary sequence (abstract): Geological Society of America, Abstracts with Program, v. 22, p. 334.

Rodgers, J., 1971, The Taconic Orogeny: Geological Society of America Bulletin, v. 82, p. 1141-1178.

Rodgers, J., 1953, Geologic map of east Tennessee with explanatory text: Tennessee Division of Geology Bulletin 58, part II, 168 p.

Rodgers, J., and Kent, D.F., 1948, Stratigraphic section at Lee Valley, Hawkins County, tennessee: Tennessee Division of Geology Bulletin, v. 55, 47 p.

Ross, R.J., Jr., et al, 1982, The Ordovician System in the United States: International Union of Geological Sciences, Publication 12, 73 p.

Ruppel, S.C., 1979, The stratigraphy, carbonate petrology, and depositional environments of the Chickamauga Group (Middle Ordovician) of Northern East Tennessee (unpublished Ph.D. dissertation): Knoxville, University of Tennessee, 231 p.

Ruppel, S.C. and Walker, K.R., 1984, Petrology and depositional history of a Middle Ordovician carbonate platform: Chickamauga Group, northeastern Tennessee: Geological Society of America Bulletin, v. 95, p. 568-583.

Sass, E., and Katz, A., 1982. The origin of platform dolomites: American Journal of Science, v. 282, p. 1184-1213.

Schmidt, M.A., 1982, Conodont biostratigraphy and facies relations of the Chickamauga Limestone (Middle Ordovician) of the southern Appalachians, Alabama and Georgia (unpublished M.S. thesis): Columbus, The Ohio State University, 270 p.

Scholle, P.A., and Kinsman, D.J.J., 1974, Aragonitic and high-Mg calcite caliche from the Persian Gulf - a modern analog for the Permian of Texas and New Mexico: Journal of Sedimentary Petrology, v. 44, p. 904-916.

Sears, S.O., and Lucia, F.J., 1980, Dolomitization of Northern Michigan Niagara reefs by brine refluxion and freshwater/seawater mixing, *in* Zenger, D.H., Dunham, J.B., and Ethington, R.L., eds., Concepts and Models of Dolomitization: Society of Economic Paleontologists and Mineralogists Special Publication No. 23, p. 215-235.

Secrist, M.H., 1924, Zinc deposits of East Tennessee: Tennessee Division of Geology Bulletin 31, p. 37-52.

Semeniuk, V., 1971, Subaerial leaching in the limestones of the Bowan Park Group (Ordovician) of central western New South Wales: Journal of Sedimentary Petrology, v. 41, p. 939-950.

Semeniuk, V., and Johnson, D.P., 1985, Modern and Pleistocene rocky shore sequences along carbonate coastlines, southwestern Australia: Sedimentary Geology, v. 44, p. 225-285.

Shanmugam, G., 1977, Shelf to basinal sequences at Boyd's Creek, Tennessee, *in* Ruppel, S.C., and Walker, K.R., eds., The ecostratigraphy of the Middle Ordovician of the Southern Appalachians (Kentucky, Tennessee, and Virginia), U.S.A.: A field excursion: Univ. of Tennessee Studies in Geology No. 77-1, p. 106-115.

Shanmugam, G., 1978, The stratigraphy, sedimentology, and tectonics of the Middle Ordovician Sevier Shale basin in East Tennessee (unpublished Ph.D. dissertation): Knoxville, University of Tennessee, 222 p.

Shanmugam, G., and Lash, G.C., 1982, Analogous tectonic evolution of the Ordovician foredeeps, southern and central Appalachians: Geology, v. 10, p. 562-566.

Shanmugam, G., and Walker, K.R., 1978, Tectonic significance of distal turbidites in the Middle Ordovician Blockhouse and lower Sevier formations in east Tennessee: American Journal of Science, v. 278, p. 551-578.

Shanmugam, G., and Walker, K.R., 1980, Sedimentation, subsidence, and evolution of a foredeep basin in the Middle Ordovician, Southern Appalachians: American Journal of Science, v. 280, p. 479-496.

Shaw, T.H., Roberson, K.E., and Harris, A.G., 1990, Lithostratigraphy and conodont biostratigraphy across the Lower-Middle Ordovician disconformity (Early to Middle Whiterockian) at Pratt Ferry, Central Alabama, U.S. Geological Society Bulletin 1895, Shorter Contributions to Paleontology and Stratigraphy, p. C1-C15.

Shinn, E.A., 1986, Modern carbonate tidal flats: their diagnostic features, *in* Carbonate Depositional Environments, Modern and Ancient 3, Tidal Flats: Colorado School of Mines Quarterly, v. 81, p. 12-35.

Shinn, E.A., 1983, Tidal flat environment, in Scholle, P.A., Bebout, D.G., and Moore, C.H., eds.,Carbonate Depositional Environments: American Association of Petroleum Geologists, Memoir 33, p. 172-210.

Shinn, E.A., Lloyd, R.M., and Ginsburg, R.N., 1969, Anatomy of a modern carbonate tidal flat, Andros Island, Bahamas: Journal of Sedimentary Petrology, v. 39, p. 1202-1228.

Shinn, E.A., 1968, Practical significance of birdseye structures in carbonate rocks: Journal of Sedimentary Petrology, v. 38, p. 215-223.

Shinn, E.A., 1983, Birdseyes, fenestrae, shrinkage pores, and loferites: a reevaluation: Journal of Sedimentary Petrology, v. 53, p. 619-628.

Sibley, D.F., 1980, Climatic control of dolomitization, Seroe Domi Formation (Pliocene), Bonaire, N.A., *in* Zenger, D.H., Dunham, J.B., and Ethington, R.L., eds., Concepts and Models of Dolomitization: Society of Economic Paleontologists and Mineralogists Special Publication No. 23, p. 247-258.

Sloss, L.L., 1963, Sequences in the cratonic interior of North America: Geological Society of America Bulletin, v. 74, p. 93-113.

Steinen, R.P., 1974, Phreatic and vadose diagenetic modification of Pleistocene limestone: petrographic observations from subsurface of Barbados, West Indies: American Association of Petroleum Geologists Bulletin, v. 58, p. 1008-1024.

Srinivasan, K., Foreman, J.L., Johnson, R.E., Walker, K.R., and Steinhauff, D.M., 1989, A brief review of staining, luminescence microscopy, and geochemical methods in the study of carbonate cements, *in* Walker, K.R., ed., The Fabric of Cements in Paleozoic Limestones: University of Tennessee Studies in Geology 20, p. 19-36.

Steinhauff, D.M., 1993, Sequence stratigraphy and comparative diagenesis of Middle Ordovician shelf to shelf-edge limestones, the Copper Creek Allochthon, East Tennessee (unpublished Ph.D. dissertation): Knoxville, University of Tennessee, 460 p.

Steinhauff, D.M., and Walker, K.R., 1987, Carbonate cement sequences in the Middle Ordovician Five Oaks, Lincolnshire, and Rockdell Formations (Chickamauga Group), East Tennessee (abstract): Geological Society of America Abstracts with Programs, v. 19, no. 2, p. 131.

Steinhauff, D.M., and Walker, K.R., in press, Comparative diagenesis of Middle Ordovician shelf to shelf-edge limestones, the Copper Creek allochthon, East Tennessee, manuscript submitted to Geological Society of America Special Paper, 17 p. 21 figs., 2 tables.

Steinhauff, D.M., Jernigan, D.G., and Walker, K.R., 1989, Stratigraphic patterns of cementation in the Middle Ordovician Holston and Rockdell formations, East Tennessee, *in* Walker, K.R., ed., The Fabric of Cements in Paleozoic Limestones: University of Tennessee Studies in Geology 20, p. 118-138.

Steinhauff, D.M., and Roberson, K.E., 1989, Uppermost Knox Group, the Knox unconformity, and the Middle Ordovician transition between shallow shelf and deeper basin near Dandridge, Tennessee, *in* Walker, K.R., Read, J.F., and Hardie, L.A., eds., Cambro-Ordovician Carbonate Banks and Siliciclastic Basins of the United States Appalachians: 28th International Geological Congress, Field Trip Guidebook T161, p. 51-81.

Stephenson, J.P., Walker, K.R., and Moore, N.K., 1973, The Mosheim Member of the Lenoir Formation--supratidal and intertidal mudflats, *in* Milici, R.C., ed., Geology of Knox County, Tennessee: Tennessee Division of Geology Bulletin 70, p. 127-131.

Sweeting, 1973, Karst Landforms: London, MacMillan, 362 p.

Tebbutt, G.E., Conley, C.D., and Boyd, D.W., 1965, Lithogenesis of a distinctive carbonate rock fabric: Univ. Wyoming Contributions to Geology, v. 4., p. 1-13.

Ulrich, E.O., 1911, Revision of the Paleozoic Systems: Geological Society of America Bulletin, v. 22, p. 281-680.

Von der Borch, C., and Lock, D.E., 1979, Geological significance of Coorong dolomites: Sedimentology, v. 26, p. 813-824.

Walker, K.R., Broadhead, T.W., and Keller, F.B., eds., 1980, Middle Ordovician Carbonate Shelf to Deep Water Basin Deposition in the Southern Appalachians: University of Tennessee Studies in Geology, Number 4, 120 p.

Walker, K.R., Jernigan, D.G., and Steinhauff, D.M., 1986, Analysis of pore histories in Paleozoic rocks: an example from the Middle Ordovician of the Southern Appalachians: Appalachian Basin Industrial Associates, v. 12, p. 101-116.

Walker, K.R., Jernigan, D.G., and Steinhauff, D.M., 1987, Fluid flow timing and pathway prediction across carbonate shelf margins: the lower Paleozoic of the Southern Appalachians as a natural laboratory, *in* Rifts, Ramps, Reefs, and Royalties: West Virginia Geological and Economic Survey, Circular C-40, p. 105-118.

Walker, K.R., Steinhauff, D.M., and Roberson, K.E., 1992, Uppermost Knox Group, the Knox unconformity, the Middle Ordovician transition from shallow shelf to deeper basin near Dandridge, Tennessee, and a possible source for mineralizing fluids, *in* Misra, K.C., Fulweiler, R.E., and Walker, K.R., eds., Zinc Deposits in East Tennessee: Society of Economic Geologists, Field Conference Guidebook, v. 14, p. 66-76.

Walls, R.A., Harris, W.B., and Nunan, W.E., 1975, Calcareous crust (caliche) profiles and early subaerial exposure of Carboniferous carbonates, northeastern Kentucky: Sedimentology, v. 22, p. 417-440.

Wanless, H.R., 1979, Limestone response to stress: Pressure solution and dolomitization: Journal of Sedimentary Petrology, v. 49, p. 437-462.

Ward, W.C., and Halley, R.B., 1985, Dolomitization in a mixing zone of near-seawater composition, Late Pleistocene, northeastern Yucatan Peninsula: Journal of Sedimentary Petrology, v. 55, p. 407-420.

Wedow, H., Jr., and Laurence, R.A., 1967, The post-Knox unconformity and its relationship to zinc mineralization in the Douglas Lake area, Tennessee: Guidebook for the 1967 Field Trip, Geology and Geography Section, Tennessee Academy of Science, 17 p.

Wigley, T.M.L., and Plummer, L.N., 1976, Mixing of carbonate waters: Geochemica and Cosmochemica Acta, v. 40, p. 989-995.

Wright, V.P., and Tucker, M.E., 1991, Calcretes: an introduction, *in* Wright, V.P., and Tucker, M.E., eds., Calcretes: International Association of Sedimentologists, Reprint Series Volume 2, p. 1-22.

APPENDIX

SAMPLE DESCRIPTIONS

SAMPLE DESCRIPTIONS

This appendix consists of detailed descriptions of all the thin sections and polished slabs analyzed for this study. For each sample, the description comes primarily from petrographic analysis of the thin section, if one was prepared. If a thin section was not prepared for a given sample, the description was made from the polished slab. A total of 233 polished slabs and 222 45 x 75 mm thin sections were utilized in the study. The descriptions below include the sample number, the stratigraphic position of the sample in meters above the Knox unconformity (in parenthesis beneath the sample number), the carbonate lithology classification (after Dunham, 1962), and the interpreted depositional subenvironment (based on characteristic features representative of sedimentation and early diagenesis in the various subenvironments of the Andros Island tidal flat, as described by Hardie and Ginsburg, 1977). The descriptions include information on color (as appropriate), clast and matrix types, lamination types, early diagenetic features, luminescence characteristics of cements (when determined), fracture density (as appropriate), and any other petrographic features deemed important to an interpretation of the depositional and diagenetic history of the sample. Methods used are described in Chapter 1.

Measured sections for the basal Middle Ordovician strata are not provided in the customary fashion; instead, the vertical sequence of lithologies for each locality sampled is summarized diagrammatically in Figure 3.9 of Chapter 3.

Idol Mine Section

The Idol Mine (or "Idol") stratigraphic section is located along the road leading from State Route 131 to the Union Zinc Co "Idol" mine in Grainger County, Tennessee in the NE1/4, NE1/4, NW1/4 of the Avondale 7.5' topographic quadrangle. The intersection of State Route 131 with the road leading to the Idol Mine is located about 1.8 km (1.1 mi.) northeast of Thorn Hill. About 340 meters of Chickamauga Group strata are exposed in the road cut, in adjacent fields, and along Joe Mill Creek. The section has been sampled by Steve Ruppel and Mark Steinhauff. The basal, peritidal portion of the Chickamauga Group, including the Blackford Member, the Five Oaks Formation, and the lowermost Lincolnshire Formation, is exposed in its entirety directly across from the entrance to the Idol Mine. The sharp, unconformable contact between the Chickamauga Group and the underlying Mascot Dolostone of the Knox Group is also well-exposed at this outcrop. The lower portion of the section was sampled at approximately 1 m. intervals. Twenty-nine samples were collected, beginning at the base of the section (the Knox unconformity); the samples are labeled ISR 1 - 29. Polished slabs were prepared from all of the samples, and 22 thin sections were made.

Sample # (Position)	Carbonate Rock Classification	Depositional Subenvironment

Lincolnshire Formation

ISR 29 (28.6)	Peloidal skeletal grainstone	Tidal flat beach/foreshore (subtidal)

Composed of wide variety of abraded and rounded skeletal fragments, with abundant peloids, and peloidal and micritic intraclasts. The sample is completely free of depositional mud. The lithology is distinctly crossbedded at the outcrop, indicating a high-energy depositional setting.

ISR 28 (27.4)	Peloidal skeletal grainstone	Tidal flat beach/foreshore (subtidal)

Identical to ISR 29. (no thin section)

ISR 27 (26.5)	Skeletal peloidal grainstone	Tidal flat beach/foreshore (subtidal)

From base of Lincolnshire. Dominated by well-sorted, dense peloids with discrete margins; skeletal debris of open marine fauna is also very abundant. Contains well-rounded intraclasts composed primarily of indurated peloidal packstone (presumably derived from tidal flat). Some peloids and intraclasts have micritic coatings (oncoids). Crudely laminated, with alternations of dark zones composed of closely packed peloids and light zones which consist of larger skeletal grains (mostly echinoderms with clear syntaxial cement overgrowths. All cements are equant. No evidence of dissolution.

Five Oaks Formation

ISR 26 (26.0)	Intraclastic peloidal grainstone/ Fenestral peloidal packstone	Beach ridge washover crest (supratidal) Beach ridge washover backslope or beach terrace (supratidal)

This sample consists of two lithologies separated by a sharp but apparently non-erosive surface. Upper lithology is the base of a 0.5 m thick grainstone, and contains "smooth flat lamination" typical of the highest supratidal environments on Andros Island (beach terrace or beach ridge washover crest). This grainstone is dominated by small, dark, dense peloids with sharp margins, but light peloids with diffuse margins are also common. Peloids lack micritic coatings. Intraclasts are both ovoid and elongate with rounded edges, and are composed of muddy peloidal sediment. Broken shell material is fairly abundant, but limited to pelecypods, ostracodes, and gastropods. All cements are equant calcite. Lower packstone is composed of similar grains as above, but with less skeletal debris. Abundant laminoid fenestrae give the rock "wavy fenestral lamination" (more visible in hand sample than in thin section).

ISR 25 (25.9)	Fenestral peloidal packstone	Beach ridge washover backslope (high intertidal to supratidal)

Identical to lower part of ISR 26. Skeletal debris consists of pelcypods, inarticulate brachiopods, ostracodes, and echinoderms. Minor amount of mud in the sample may be derived through compaction of soft peloids. Many "peloids" have micritic rims and translucent centers, and may be micritized echinoderm grains. Contains "wavy fenestral lamination" as in ISR 26. There is no evidence of dissolution or vadose alteration. All cements are clear equant calcite.

ISR 24 (25.5)	Peloidal wackestone	Beach ridge washover crest or levee crest (supratidal)

Lacks fenestrae, but contains "smooth flat lamination" produced by alternations of muddy and peloidal layers. Contains a few vertical burrows.

ISR 23 (24.3)	Peloidal wackestone/ Burrowed mudstone	Low algal marsh/pond margin (low intertidal)

Sample consists of two lithologies separated by a sharp surface. Upper lithology consists of mud-supported peloidal sediment with minor amounts of skeletal debris (primarily pelecypods). Contains vague lamination produced by vertical alternations in the amount of mud vs. cement. Lower lithology is a mudstone disrupted by vertical burrows and/or vertically oriented fenestrae, vaguely similar to the "disrupted fenestral bedding" on Andros Island. Lower mudstone lacks peloids, except lining some burrows. Both lithologies lack fossils. The surface separating the lithologies is sharp and contains possible borings that extend as much as 5 mm down into the lower mudstone. The "borings" are filled partly with peloidal sediment from the upper lithology and partly with crystal silt. The upper 1 - 2 mm of the lower mudstone are bleached beneath the surface. This surface probably formed during brief subaerial exposure of the lower mudstone.

ISR 22 (21.2)	Skeletal mudstone	Tidal pond (subtidal)

Consists of bioturbated mud with common fossils (mostly whole pelecypod valves). Contains one cement-filled burrow. (No thin section)

ISR 21 (19.3)	Peloidal grainstone	Beach or tidal channel (subtidal)

From a 1.8 m thick bed of flat-laminated, moderately high energy grainstone. Dominated by small dense peloids, but contains approximately 15% abraded skeletal debris (mostly pelecypods, echinoderms, and ostracodes) and 5% angular fine quartz sand.

ISR 20 (18.8)	Peloidal grainstone	Beach or tidal channel (subtidal)

Identical to ISR 21.

ISR 19 (18.3)	Skeletal wackestone	Tidal pond (subtidal)

Non-fenestral, bioturbated mud with abundant gastropods and pelecypods. Burrows are filled with peloids. (No thin section)

ISR 18 (16.2) — Mudstone/skeletal packstone — Tidal pond or channel (subtidal)

Thick-bedded, layered limestone consisting of cm-scale alternations of mudstone and peloidal skeletal packstone. Mudstone appears to contain sponge spicules(?). Packstone consists of mud-supported fossils, primarily whole pelecypods, large ostracodes, and gastropod molds. Fenestrae and non-selective dissolution fabrics are absent. All pores are filled with large, clear, equant calcite crystals.

ISR 17 (14.4) — Mudstone — Tidal pond (subtidal)

Flaggy, "ribbon" limestone consisting of dark gray mudstone and brown, dolomitized, bioturbated zones.

ISR 16 (12.6) — Peloidal wackestone — Tidal pond or channel (subtidal)

Very similar to ISR 18. Consists mostly of bioturbated mud, but contains winnowed patches of peloids surrounded by equant cement. Micritic intraclasts are common. Contains several molds of fossil (pelecypod?) shells filled with equant cement. Also contains several relatively large (1.5 mm diameter) burrows filled with fecal pellets and cement.

ISR 15 (10.9) — Mudstone — Tidal pond (subtidal)

Mostly featureless carbonate mud. Lacks fenestrae, peloids, and lamination. Contains burrows and gastropod molds, some of which appear to be enlarged by dissolution. Some voids are filled with internal sediment, but no vadose silt was observed.

ISR 14 (10.6) — Fenestral peloidal packstone — High algal marsh (high intertidal)

Consists primarily of poorly-sorted, very small (0.1 mm) peloids in muddy matrix. Also contains small amount (5%) of broken (but unabraded) ostracode shell fragments, but no other fauna. Contains "crinkled fenestral lamination" produced by small irregular fenestrae and some thin muddy laminae. Lamination is disrupted in places by burrows. In addition to abundant fenestrae, contains intergranular pores and pelecypod molds. All porosity is now filled with small, equant, clear calcite cement crystals. Similar to ISR 25, but all grains and pores in this sample are much smaller, and "loose" mud portion is higher. More dolomitized than overlying samples.

ISR 13 (10.3) — Fenestral mudstone (altered to diagenetic grainstone) — Inland or high algal marsh (high intertidal to supratidal)

Fenestral mudstone with "crinkled fenestral lamination", more similar to Mosheim than typical Five Oaks. Has very well-developed "diagenetic grainstone" texture caused by intense fenestral alteration of original muddy sediment. Portions of this sample consist of mud lumps that fit together in jigsaw puzzle fashion, separated by thin, curving hairline fenestrae (shrinkage or desiccation cracks). In other areas, the lumps are more rounded and separated, and some micrite lumps have concentric micritic coatings that are more dense than the nucleus ("caliche pisoids"). The diagenetic grainstone texture and abundance of pisoids attests to vadose alteration during extended subaerial exposure. Fenestrae are typically large and irregular and filled with drusy, equant

calcite cements. Also contains a few vertical burrows. Contains essentially no fossil debris.

ISR 12 (10.2)	Fenestral intraclastic packstone	Inland or high algal marsh (high intertidal to supratidal)

Similar to overlying sample (ISR 13), but contains more intraclasts, which may be of diagenetic or depositional origin (or both). Sample is buff-colored in hand sample, but is not very dolomitic. Contains disrupted flat lamination that is produced by alternations of muddy and intraclastic laminae. Fenestrae are mostly very small, and many are curvilinear voids that wrap around mud lumps and suggest formation by shrinkage of sediment during desiccation. There is no evidence of dissolution, and all cements are equant calcite.

ISR 11 (10.0)	Skeletal intraclastic wackestone	Inland algal marsh (supratidal or intertidal)

This gray limestone sample was collected from immediately above strikingly different buff-colored dolostones, and is interpreted as the base of the main body of the Five Oaks. The lithology consists mostly of mud with abundant intraclasts and skeletal material. Intraclasts are micritic, with smooth, sharp edges that suggest near complete induration before redeposition. Skeletal fragments are mostly disarticulated but unbroken ostracodes and gastropods (leached). Also contains some pieces of red algae. Sediment probably represents storm deposition onto the surface of the underlying Blackford dolostones. Contains a bleached, indurated crust 1 mm thick that contains within it winding (but primarily vertical) calcified algal filaments and vertically-oriented ostracode valves. This crust is very similar to the "paper crusts" that occur in the supratidal inland algal marsh on Andros Island (Hardie and Garrett, 1977), or could be a poorly-developed algal tufa layer. Matrix in the sample is mostly mud that is only slightly dolomitized, but in places the mud has been winnowed out, leaving an intraclastic grainstone lithology cemented with equant calcite. Most void space is interparticle and gastropod molds; fenestrae are uncommon.

Blackford Member

ISR 10 (7.3)	Laminated dolomudstone	High algal marsh/levee backslope (supratidal to high intertidal)

Sample was collected near the base of a 3 m thick bed of buff-colored, pervasively dolomitized mudstone that forms the top of the Blackford Member at the Idol section. Much of the rock is laminated, with laminations the result of alternation of horizontally-oriented laminoid fenestrae with muddy layers. In places the lamination is disrupted by bioturbation, which results in a "swirled" appearance.

ISR 9 (6.1)	Intraclastic packstone	Tidal channel (subtidal)

Collected from a 1 m thick bed of pale green-colored, grain-supported dolostone. The lithology consists entirely of intraclasts embedded in equant calcite cement, although a small amount of depositional interparticle mud is present in places. The intraclasts are all composed of dolomitized micrite, but the interparticle mud is not dolomitized, suggesting that the intraclasts were ripped up from an already-dolomitized lithology.

The rock contains no fenestrae, no lamination, and no features indicative of subaerial exposure or dissolution.

ISR 8 (5.7)	Dolomudstone	Tidal flat (subenvironment not determined)

Pervasively-dolomitized micrite with clasts of dolomite and chert. Contains thin (1-1/2 cm) beds that alternate between mud layers and intraclastic layers. Most macropores are filled with calcite cements. (No thin section)

ISR 7 (4.7)	Dolomudstone	Levee crest (?)(supratidal)

Laminated, dolomitized micrite with large (up to 1 cm) angular chert clasts probably derived from erosion of underlying Knox group dolostones. Lamination is produced by alternating layers of dense mud with less dense mud; each lamina likely represents a discrete storm event. (No thin section)

ISR 6 (3.4)	Dolomudstone	Tidal flat (subenvironment not determined)

Consists of laminated dolostone, with lamination produced by alternations of finely-crystalline, dark dolomite layers (dark brown color results from organic residue) with light-colored layers of medium-crystalline dolomite. Contains some pyrite or dead hydrocarbons, a small amount of fine-grained chert, and some echinoderm debris with calcite syntaxial overgrowths.

ISR 5 (3.1)	Dolomudstone	Tidal flat (subenvironment not determined)

Consists of greenish-gray dolomitized micrite with occasional patches of black organic matter. (No thin section)

ISR 4 (1.9)	Intraclastic skeletal packstone	Tidal channel or beach (subtidal)

Sample collected from a 1 m-thick cross-bedded limestone layer that overlies a sharp, erosional surface. Consists primarily of echinoderm grains with syntaxial calcite overgrowths, but also contains some phosphatic inarticulate brachiopods and a minor amount of bryozoan fragments. The sample also contains a significant amount of dolomitic lithoclasts and some round to subangular, unsorted quartz sand and chert (derived from Knox?). Some large (1 mm), strikingly-zoned dolomite rhombs are also present, but the lithology is largely undolomitized, especially when compared with the bulk of the Blackford.

ISR 3 (0.9)	Conglomeratic dolostone	Depression fill

Consists primarily of light-colored (pinkish in hand sample), medium-crystalline dolostone lithoclasts derived from erosion of the underlying Mascot Formation embedded in a dark, finely-crystalline dolomite matrix. The entire rock is dolomite, with the exception of some chert fragments and a minor amount of inarticulate brachiopod debris. Very similar to the conglomeratic dolostones of the Douglas Lake Member.

ISR 2 (0.4)	Conglomeratic dolostone	Depression fill

Very similar to ISR 3, except that lithoclast size is smaller. (No thin section)

Post-Knox Unconformity

ISR 1 (0.0)	Dolostone	Depression fill

Sample contains the post-Knox unconformity, which separates light-colored, medium-crystalline dolomite with chert and dolostone lithoclasts (basal Blackford Member) from dark gray, finely-crystalline, intraclastic, bioturbated dolomudstone of the Mascot Formation. The unconformity is very sharp and slightly undulose.

Thorn Hill Section

The "old" Thorn Hill section is exposed in a road cut along the eastern and western portions of old U.S. Route 25E at Thron Hill community, Grainger County, Tennessee. The area is in the NE 1/4, NW 1/4, NE 1/4 of the Avondale 7.5 minute topographic quadrangle. The Knox unconformity is located within and adjacent to an old quarry located on the east side of the old highway, about 750 meters north of intersection of State Route 131 and the old highway in Thorn Hill. Thirty-four samples were collected for this study, and thin sections were prepared from 25 of those (three thin sections were made for sample TH 23.6). The samples were numbered based on their position (in meters) above the inferred position of the Knox unconformity, which proved to be 1.4 meters lower than initially thought. The lower four samples turned out to be from the upper Mascot Formation (Knox Group).

Sample # (Position)	Carbonate Rock Classification	Depositional Subenvironment

Five Oaks Formation

TH 24.6 (23.2)	Skeletal peloidal grainstone	Tidal flat beach/foreshore (low intertidal/subtidal)

Beige/brown, grain-supported limestone with vague flat lamination and no fenestrae. Collected from near the top of a 1 m-thick peloidal grainstone that represents a transition from typical Five Oaks tidal flat fenestral mudstones to Lincolnshire shallow subtidal skeletal grainstones. Interpreted to be the top of the Five Oaks Formation. Very similar to ISR 20, ISR 21, ISR 26, and CS 22, CS 23, and CS 24. Overlying grainstones are more similar to ISR 27 and ISR 29. See description of TH 23.8 thin section for more thorough description. (No thin section)

TH 23.8 (22.4)	Skeletal peloidal grainstone	Tidal flat beach/foreshore (low intertidal/subtidal)

Beige/brown grainstone with no fenestrae. Collected from 0.2 m above the base of the 1 m-thick grainstone bed from which TH 24.6 was also collected. This grainstone is separated from the underlying fenestral mudstones by a sharp scalloped surface. Contains "smooth flat lamination" produced by variations in the density of grains. Grains are predominantly small peloids, but intraclasts composed of carbonate mud and highly-abraded fossil fragments are also abundant. Fossils are mostly echinoderms with syntaxial overgrowths, but broken and abraded pelecypod, ostracode, inarticulate brachiopod, and green algae fragments are common. Lack of mud and abrasion of allochems indicates that this is a moderately-high to high-energy deposit, and probably represents the tidal flat beach that formed the interface between the Five Oaks tidal flat and the adjacent Lincolnshire offshore marine environment. All cements are clear, equant calcite. There is essentially no dolomite in this lithology.

TH 23.6 (22.2)	Fenestral peloidal packstone	Beach ridge washover backslope or beach terrace (high intertidal to supratidal)

Packstone consisting almost entirely of peloids and equant calcite cement with a minor amount of mud. Fossils are virtually absent, although a minor amount of very small ostracode shell fragments may be present. Contains some original lamination produced by alternations of peloidal and mud layers. Laminae are sometimes separated by laminoid fenestrae. Laminae arch and undulate, and give the appearance of cryptalgal origin, and are probably analogous to the "wavy fenestral lamination" described from Andros Island (Hardie and Garrett, 1977). Lamination is disrupted by common large, discrete, vertically-elongate, cement-filled burrows. Some of these burrows are backfilled with almost perfectly spehrical fecal pellets. The smooth walls of the burrows indicate at least some consolidation of the sediment prior to burrowing, but burrows do not appear to truncate cements. (Three thin sections-- TH 23.6A,B,C)

TH 23.4 (22.0)	Fenestral peloidal packstone	Beach ridge washover backslope or beach terrace (high intertidal to supratidal)

Identical to the overlying sample (TH 23.6).

TH 22.6 (21.2)	Fenestral mudstone	Low algal marsh/tidal pond margin (low intertidal)

Dove-gray mudstone with relatively uncommon small, irregular fenestrae. Also contains some patches of peloidal packstone. Some of the small cement-filled voids may actually be fossil molds, but fossils are very rare. There is also some cement-filled intergranular void space between peloids. There are vertically-oriented cement and sediment-filled burrows. All cements are equant calcite.

TH 21.4 (20.0)	Fenestral mudstone	High algal marsh (high intertidal to supratidal)

Dove-gray mudstone with abundant irregular fenestrae and hairline laminoid fenestrae. Bed-parallel orientation of fenestrae gives the rock a vague "crinkled fenestral

lamination". Fossils are rare, and limited to ostracodes. There is a minor amount of calcite cement-filled moldic porosity (after pelecypods ?). Very similar to the fenestral mudstones and fenestral peloidal packstones near the base of the Five Oaks at this location, especially TH 5.7.

TH 20.2 (18.8)	Intraclastic packstone/grainstone Fenestral mudstone	High algal marsh (high intertidal to supratidal)

Sample consists of two limestone lithologies separated by a rather vague, non-erosional surface. The upper lithology is a packstone/grainstone which consists of quite large (up to 0.5 cm) intraclasts, most of which are mudlumps, but some are grapestone aggregates and some resemble pisoids with distinct concentric layering. Fossils are rare but include red algae, inarticulate brachiopods, and ostracodes. The lower lithology is a fenestral mudstone with abundant small, irreguoar fenestrae. Contains isolated peloidal patches with intergranular pores (all pore space is filled with cement). The mudstone contains vague "disrupted fenestral bedding", as described from Andros Island (Hardie and Garrett, 1977). Fossil fragments are limited to ostracodes, but there is a minor amount of moldic porosity after pelecypod fragments. The mudstone portion of the sample contains a fairly high percentage of dolomite. A small portion of void space is filled with silica cements, but the vast majority of cement is equant calcite.

TH 19.2 (17.8)	Mudstone	Tidal pond (subtidal)

Light gray, dense mudstone lacking fenestrae. Contains rare vugs filled with clear equant calcite cement or greenish clay-like depositional material. (No thin section)

TH 17.9 (16.5)	Mudstone	Tidal pond (subtidal)

Medium-gray mudstone with rare vertically-oriented fenestrae or burrows, filled with equant calcite cement or internal sediment. (No thin section)

TH 17.8 (16.4)	Mudstone	Tidal pond (subtidal)

Medium-gray mudstone with rare fenestrae. Contains swarms of "horsetail" stylolites (very abundant). (No thin section)

TH 16.3 (14.9)	Mudstone	Tidal pond (subtidal)

Non-laminated mudstone with rare, but large, rounded fenestrae with very sharp borders. No laminoid fenestrae. Contains abundant vertically-oriented, cement-filled burrows. Some former pores are floored with internal sediment and/or crystal silt, and all remaining pore space is filled with equant calcite cement. Contains no fossils whatsoever, although there is some evidence of bioturbation.

TH 16.0 (14.6)	Mudstone/peloidal packstone	Levee backslope or high algal marsh (high intertidal to supratidal)

Distinctly laminated limestone, with lamination produced by alternations of mud layers and peloidal layers. Layers are in many places separated by abundant, bed-parallel, laminoid and irregular fenestrae. Mud layers contain mudcracks that do not penetrate down into underlying peloidal sediment. Lamination is most similar to the "wavy

fenestral lamination" described from Andros Island, but is disrupted by mudcracks in the manner of "disrupted flat lamination". Lamination is not flat, however, but distinctly undulose.

TH 15.0 (13.6) — Lithoclastic skeletal wackestone — Tidal pond (subtidal)

Non-fenestral, mud-supported limestone with abundant fossils and lithoclasts. Fossils include red algae, ostracodes, trilobites, pelecypods, and micrite-rimmed gastropod molds. Lithoclasts are composed of limestone, dolostone, and chert. Mud matrix is very dolomitic. Lithology was once quite porous, with abundant moldic, interparticle, and shelter pores that are now filled primarily with microspar or very small equant calcite cement crystals. Molds are predominantly from pelecypods and gastropods. Some voids contain an unusual green depositional clay-like material that in places is horizontally layered. There are also several dissolution vugs, indicating exposure of this subtidal lithology to meteoric groundwaters (probably in the phreatic zone, since there is no evidence of subaerial exposure).

TH 14.4 (13.0) — Mudstone — Tidal pond (subtidal)

Beige and gray, mottled mudstone. Contains small elongate vugs filled with equant calcite cement. Has very abundant stylolites. (No thin section)

TH 14.1 (12.7) — Peloidal, intraclastic skeletal wackestone — Tidal pond (subtidal)

Sample is very similar to TH 15.0, but contains much more skeletal debris. Fossil types are the same as above, with a few echinoderm grains. Like TH 15.0, this sample contains no fenestrae or other indicators of subaerial exposure. Porosity is primarily moldic, after gastropods and pelecypods, but shelter porosity beneath clasts is also abundant. All pores are now filled with microspar and finely-crystalline, equant calcite cement. Many shells and gastropod shell molds have micritic envelopes. Intraclasts are limestone and dolostone, but no chert. Matrix is extensively dolomitized.

TH 14.0 (12.6) — Peloidal, lithoclastic skeletal wackestone — Tidal pond (subtidal)

Sample is very similar to TH 15.0 and 14.1, but contains less fossil material than TH 14.1. Like those samples, the matrix is extensively dolomitized. Contains abundant chert, dolostone, and limestone lithoclasts.

TH 13.7 (12.3) — Fenestral intraclastic wackestone — Tidal pond/low algal marsh (subtidal to low intertidal)

Sample is similar in overall appearance to TH 14.0, but lacks chert lithoclasts and contains fairly abundant fenestrae. Also contains abundant wispy green clay laminae along stylolites. (No thin section)

TH 13.2 (11.8) — Mudstone — Tidal pond (subtidal)

Non-fenestral, non-laminated mudstone. Contains some cement-filled interparticle voids, burrows, and gastropod and pelecypod molds. Contains a few pelecypods and ostracode fragments. No evidence of subaerial exposure.

TH 12.0 (10.6)	Mudstone	Tidal pond (subtidal)

Mottled, slightly peloidal mudstone. Contains no hint of lamination and no fenestrae. Voids resembling fenestrae are large and irregular in shape and appear to be fossil molds and not true fenestrae. Other vertically-oriented voids are probably burrows, some of which are filled with fecal pellets. Some pores are floored with "grungy" material that resembles crystal silt, which is then overlain by a layered green mineral that resembles anhydrite in thin section. Similar greenish material was observed in samples TH 19.2 and TH15.0. All other void space is filled with equant calcite cement. Fossils are fairly abundant, but are limited to pelecypods and articulated ostracodes.

TH 10.8 (9.4)	Fenestral mudstone	Low to high algal marsh (high intertidal to supratidal)

Medium-gray fenestral mudstone, very similar to typical Mosheim lithology. Fenestrae are irregular and very abundant. Stylolites are also abundant. (No thin section)

TH 10.4 (9.0)	<u>Fenestral mudstone</u> Fenestral peloidal packstone	<u>Low to high algal marsh</u> Levee backslope (high intertidal to supratidal)

Sample consists of two similar lithologies, with the lower lithology transitioning upward into the upper lithology (not separated by a sharp surface). The upper lithology is a mottled mudstone with far fewer fenestrae than the lower lithology. Contains a few voids from leached gastropod shells and some shelter pores beneath pelecypod shells. Overall, however, fossils are rare in the upper mudstone. The lower lithology is a distinctly laminated packstone composed of alternations of peloidal muddy layers and peloidal packstone layers. Laminae are flat to gently undulating and resemble algal laminations (possibly representing storm deposition on algal mats). The lower lithology contains no fossil fragments at all. The sample contains no dolomite.

TH 9.4 (8.0)	Fenestral mudstone	High algal marsh/levee backslope boundary (highest intertidal/supratidal)

Distinctly laminated mudstone, with laminae produced by alternations of mud crusts (1 to 3 mm thick) separated by horizontally-oriented trains of almost spherical fenestrae. Fenestrae are very discrete with sharp, smooth borders. Laminae are disrupted by vertical mudcracks, but more closely fit the description of the "crinkled flat lamination" than the "disrupted flat lamination" described from Andros Island (Hardie and Garrett, 1977). Contains some pelecypods but no other fossils. All voids are filled with very small equant calcite cements.

TH 8.1 (6.7)	Fenestral mudstone	High algal marsh (high intertidal to supratidal)

Yellow and gray, highly fenestral mudstone. Fenestrae are mostly horizontally-oriented and irregular in shaped. Looks just like typical Mosheim fenestral mudstone except for the yellow color. (No thin section)

TH 7.4 (6.0)	Fenestral mudstone (altered to diagenetic packstone)	High algal marsh (highest intertidal/supratidal)

Highly fenestral mudstone, with most of the mud reorganized diagenetically by intense fenestral alteration into discrete, rounded grains surrounded by fenestral pores. Many of these grains have pisoid-like concentric micritic laminations. Also, the points of contact between adjacent grains are connected by meniscus micritic cements. Fenestrae are mostly irregular, with some connected laterally, imparting to the rock a "crinkled fenestral lamination". Fossils are very rare, and limited to inarticulate brachiopods and ostracodes.

TH6.8 (5.4)	Fenestral intraclastic peloidal packstone	Low algal marsh (intertidal)

Peloidal packstone with abundant muddy intraclasts and fenestrae. Fenestrae are irregular and large (commonly 2 to 3 mm) with rare laminoid fenestrae. Sample is not laminated, but probably could be described as analogous to the disrupted fenestral bedding characteristic of the low algal marsh on Andros Island (Hardie and Garrett, 1977). Contains very little dolomite.

TH 5.7 (4.3)	Fenestral mudstone	High algal marsh (highest intertidal/supratidal)

Highly fenestral mudstone, with the muddy matrix separated by intense fenestral alteration into discrete lumps that fit together in "jigsaw" fashion. Fenestral alteration has not proceeded as far in this sample as in TH 7.4, but still indicates extensive subaerial exposure and desiccation. Sample does not contain depositional mud particles such as intraclasts or peloids. Fenestrae are mostly large and irregular in shape, but the mudlumps are separated by hairline cracks (not laminoid fenestrae). Contains no fossils and no dolomite.

TH 4.4 (3.0)	Fenestral peloidal packstone	High algal marsh (highest intertidal/supratidal)

Peloidal packstone with very abundant, small (<0.5 mm), laminoid fenestrae and less abundant, larger (0.5 to 2 mm) irregular fenestrae. Alternation of layers of horizontally-oriented fenestrae with peloid layers gives the rock a distinct "crinkled fenestral lamination" characteristic of the high algal marsh on Andros Island (Hardie and Garrett, 1977). Contains some intraclasts composed of peloids and a few dolostone lithoclasts. The matrix contains very little dolomite, however. Fossils are very rare and limited to ostracodes.

TH 3.4 (2.0)	Fenestral mudstone	Low algal marsh (intertidal)

Beige/gray mottled fenestral mudstone, with fenestrae less common than in the overlying 6 samples. (No thin section)

TH 3.0 (1.6)	Fenestral intraclastic packstone	High algal marsh (highest intertidal/supratidal)

Packstone composed primarily of intraclasts, which in places appear to "float" in equant calcite cement. Other zones within the sample are more muddy. Laminoid and

irregular fenestrae are both abundant, and coalescense of fenestrae into bed-parallel layers gives the rock a distinctly laminated appearance, which most closely resembles "crinkled fenestral lamination". Despite abundant fenestrae, the sample contains no other indicators of vadose alteration. Contains almost no trace of fossils, but is more highly dolomitized than most fenestral limestones in the Five Oaks sequence.

TH 2.4 (1.0)	Fenestral peloidal packstone	Inland or high algal marsh (highest intertidal/supratidal)

Medium-gray fenestral limestone collected from 0.4 meters above the base of the fenestral limestone (limestone is underlain by dolostone at 0.6 m above the contact with the Knox Group). Sample contains extremely abundant irregular fenestrae as well as smaller intergranular pores. Very rare fossils are limited to ostracodes. Contains very little dolomite, and no other indicators of vadose alteration. The rock is only vaguely laminated because the fenestrae have no particular orientation.

Blackford Member

TH 1.8 (0.4) Beige, chalky, finely-crystalline dolostone. Sample was collected from 0.4 above the base of a 0.6 m-thick dolostone bed that is taken to represent the Blackford at this outcrop. Very similar to basal dolostone at Raccoon Valley (RV 0.7).

Mascot Formation (Knox Group)

TH 1.1 (-0.3) Mottled, medium-gray/beige dolomitic limestone. Beige areas appear to be dolomitized burrows. Many of these beige areas contain large vugs filled with white or clear equant calcite cement. This lithology is very similar to the uppermost Knox strata (Mascot Formation) at Raccoon Valley (RV 0.5A) and the Idol Mine section (ISR 0).

TH 0.9 (-0.5) Mottled, medium-gray/beige dolomitic limestone. Same as TH 1.1, but with fewer vugs.

TH 0.3 (-1.1) Beige dolostone with layers of cross-dipping darker detrital dolostone. Darker layer contains dark brown metallic minerals (?).

TH 0.0 (-1.4) Laminated, beige dolostone.

Cedar Springs Section

The Cedar Springs section lies in the Copper Creek Belt approximately 2 miles to the northeast of the Idol Mine section. The section is exposed along Cedar Springs Creek, which flows next to Cedar Springs Church Road. The basal part of the section and the Knox unconformity are exposed in the creek bed where the road crosses the creek beside the church. The section occurs in the SW 1/4, SW 1/4, SW 1/4 of the Swan Island 7.5 minute topographic quadrangle map. This section was sampled by Steve Ruppel as part of his Ph.D dissertation. The thin sections described below are from Ruppel's collection. Twenty-four samples were collected from the Five Oaks Formation at this outcrop, and

thin sections exist for 23 of these. Ruppel's samples are labeled CS 1 - 24, beginning near the base of the section.

Sample # (Position)	Carbonate Rock Classification	Depositional Subenvironment
Five Oaks Formation		
CS 24 (22.0)	Intraclastic peloidal grainstone	Tidal flat beach/foreshore (low intertidal/subtidal)
	Beige/brown grainstone with no fenestrae. Essentially identical to TH 23.8 but contains slightly fewer fossil fragments. Also very similar to the upper portion of ISR 26. Contains "smooth flat lamination" produced by variations in the density of grains. Grains are predominantly small peloids, but intraclasts composed of carbonate mud and highly-abraded fossil fragments are also abundant. Fossils are mostly echinoderm grains with syntaxial overgrowths, but broken and abraded pelecypod and ostracod fragments are common. Lack of mud and abrasion of allochems indicates that this is a moderately-high to high-energy deposit, and probably represents the tidal flat beach that formed the interface between the Five Oaks tidal flat and the adjacent Lincolnshire offshore marine environment. All cements are clear, equant calcite. There is essentially no dolomite in this lithology.	
CS 23 (20.0)	Intraclastic peloidal grainstone	Tidal flat beach/foreshore (low intertidal/subtidal)
	Same as CS 24.	
CS 22 (18.0)	Intraclastic peloidal grainstone	Tidal flat beach/foreshore (low intertidal/subtidal)
	Same as CS 23 and CS 24.	
CS 21 (16.3)	Skeletal peloidal grainstone	Tidal flat beach/foreshore (subtidal)
	Very similar to the overlying samples, but contains a higher portion of skeletal fragments, and skeletal fragments are generally larger and less abraded and more open marine organisms are included. The fossils mentioned above (echinoderms, pelecypods, and ostracodes) predominate, but brachiopods, bryozoans, and trilobites are also present. This sample contains some large fenestra-like void spaces that may be analogous to the features Shinn (1983) described from subtidal grainstones. This sample is more similar to ISR 27, 28, and 29 than the three overlying samples (CS 22 through CS 24), and is more like the basal Lincolnshire than the upper Five Oaks. This six meters of grainstone (CS 21 through CS 24) probably represents a transition from typical Five Oaks tidal flat deposition to Lincolnshire-type shallow subtidal, open marine deposition.	
CS 20 (16.0)	Fenestral peloidal packstone	Beach ridge washover backslope or beach terrace (high intertidal to supratidal)
	Virtually identical identical to TH 23.4, 23.6, and very similar to ISR 25, 26. This lithology is a packstone consisting almost entirely of peloids and equant calcite cement	

with intercalated mud laminae. Fossils are rare and limited to a minor amount of very small, highly abraded ostracode shell fragments. Contains lamination produced by alternations of peloidal and mud layers. Laminae are sometimes separated by laminoid fenestrae. Laminae arch and undulate, and give the appearance of cryptalgal origin, and are probably analogous to the "wavy fenestral lamination" described from Andros Island (Hardie and Garrett, 1977). Contains essentially no dolomite.

CS 19 (14.5) — Fenestral peloidal packstone — Beach ridge washover backslope (high intertidal to supratidal)

Identical to CS 20. Contains vertically-oriented burrows, and mudcracks that disrupt the bed-parallel laminae. Irregular fenestrae are abundant.

CS 18 (13.3) — Fenestral peloidal packstone — Beach ridge washover backslope (high intertidal to supratidal)

Identical to CS 19 and CS 20.

CS 17 (11.5) — Fenestral peloidal packstone — Beach ridge washover backslope (high intertidal to supratidal)

Identical to CS 18, 19 and 20.

CS 16 (10.6) — Peloidal packstone — Tidal pond (subtidal)

Mud-supported, peloid-rich limestone with some vertical burrows. Similar to overlying samples, but lacks fenestrae and fenestral lamination. Mud distribution is more homogeneous, probably due to bioturbation. Also, skeletal fragments are more abundant, and include bryozoans, inarticulate brachiopods, pelecypods, and ostracodes. Gastropod molds are also present, and filled with clear equant calcite.

CS 15 (8.9) — Dolomitic mudstone — Tidal pond (subtidal)

Sample consists mostly of mud, but contains some peloids and rare ostracodes and pelecypods. Relatively high dolomite content dispersed within mud matrix.

CS 14 (7.8) — Mudstone — Tidal pond (subtidal)

Non-laminated mudstone with rare, but large, rounded fenestrae with very sharp borders. No laminoid fenestrae. Contains abundant vertically-oriented, cement-filled burrows. Some former pores are floored with internal sediment and/or crystal silt, and all remaining pore space is filled with equant calcite cement. Fossils are very rare and limited to ostracodes. Virtually identical to TH 16.3 and similar to ISR 15.

CS 13 (7.3) — Mudstone — Tidal pond (subtidal)

Consists entirely of slightly dolomitized carbonate mud, with very rare skeletal fragments.

CS 11 (6.7) — Skeletal peloidal wackestone — Tidal pond (subtidal)

Mud-supported lithology very similar to CS 16, but more muddy. Trilobite, pelecypod, and gastropod fragments are fairly common (15%). Most skeletal grains have been leached and replaced with equant calcite cement.

CS 10 (6.3) — Skeletal peloidal wackestone — Tidal pond (subtidal)

Identical to CS 11.

CS 9 (6.0) — Peloidal, intraclastic skeletal wackestone — Tidal pond (subtidal)

Sample is identical to TH 14.1. The lithology is mud-supported, but contains abundant skeletal debris. Fossil types include red algae, ostracodes, trilobites, pelecypods, and micrite-rimmed gastropod molds, along with a few echinoderm grains. Like TH 14.1, this sample contains no fenestrae or other indicators of subaerial exposure. Porosity is primarily moldic, after gastropods and pelecypods, but shelter porosity beneath clasts is also abundant. All pores are now filled with microspar and finely-crystalline, equant calcite cement. Many shells and gastropod shell molds have micritic envelopes. Intraclasts are limestone and dolostone, but no chert. Matrix is extensively dolomitized.

CS 8 (5.5) — Peloidal skeletal wackestone/packstone — Tidal pond (subtidal)

Sample consists of alternating layers of skeletal wackestone and packstone. Individual layers are 1 to 5 cm thick. Fauna in both types of layers includes very abundant pelecypods, gastropods, and bryozoans, and rare ostracodes. All mollusc shells are leached and replaced with calcite cement. Peloids are of very uniform small size and shape, and may be mollusc fecal pellets. Sample is very similar to ISR 16 and ISR 18.

CS 7 (4.5) — Peloidal skeletal packstone — Tidal pond (subtidal)

Very similar to CS 9, but contains fewer intraclasts. Fauna is dominated by pelecypods and gastropods, but also includes some bryozoans, ostracodes, algae, and rare inarticulate brachiopods. Muddy matrix is highly dolomitized.

CS 6 (4.0) — Arenaceous, skeletal intraclastic packstone — Tidal channel (subtidal)

Moderately high-energy deposit very similar to ISR 4, but contains lower percentage of echinoderm grains. Contains very abundant inarticulate brachiopods, trilobites, red algae, and pelecypods. Intraclasts are rounded and consist almost entirely of lime mud. Unlike ISR 4, does not contain dolostone and chert lithoclasts. Contains very abundant angular quartz sand grains (more than ISR 4).

CS 5 (3.0) — Peloidal skeletal wackestone/packstone — Tidal pond (subtidal)

Layered lithology identical to CS 8.

CS 4 (2.5) — Skeletal peloidal wackestone — Tidal pond (subtidal)

Mud-dominated lithology with very abundant, small peloids and common fossils. Fossils are mostly articulated ostracodes and pelecypods. Matrix is highly dolomitized.

Sample is similar in general appearance to ISR 11, but lacks strong indicators of inland algal marsh deposition.

CS 3 (2.0)	Skeletal mudstone	Tidal pond (subtidal)

Non-fenestral, non-laminated, featureless lime mud with some pelecypod molds and ostracodes. Only slightly dolomitized.

CS 2 (1.5)	Dolomudstone	Tidal pond (subtidal)

Highly dolomitized, mottled mudstone. Contains no fauna or recognizable allochems.

CS 1 (?*)	Fenestral mudstone (altered to diagenetic grainstone)	Inland or high algal marsh (high intertidal to supratidal)

Fenestral mudstone with "crinkled fenestral lamination", more similar to Mosheim than typical Five Oaks. Very similar to ISR 13 and TH 7.4, but contains more dolomite than either of those samples. Has very well-developed "diagenetic grainstone" texture caused by intense fenestral alteration of original muddy sediment. Portions of this sample consist of mud lumps that fit together in jigsaw puzzle fashion, separated by thin, curving hairline fenestrae (shrinkage or desiccation cracks). In other areas, the lumps are more rounded and separated, and some micrite lumps have concentric micritic coatings that are more dense than the nucleus ("caliche pisoids"). The diagenetic grainstone texture and abundance of pisoids attests to vadose alteration during extended subaerial exposure. Fenestrae are typically large and irregular and filled with drusy, equant calcite cements. Also contains a few vertical burrows. Contains essentially no fossil debris. *Position above post-Knox unconformity from which sample was collected was not recorded.

Red House Branch Section

The Red House Branch Section is located on both sides of the Red House Branch embayment of Cherokee Lake (Holston River), southeast of U.S. Highway 11W in Hawkins County, Tennessee. The section lies in the NE 1/4, NW 1/4 of the Russellville 7.5 minute topographic quadrangle. This section was used to represent the Hawkins Belt, where the basal Middle Ordovician section consists of a very thin Mosheim facies (4.2 meters) and a thin Lenoir section (17.8 m). The section is overturned and highly fractured due to its proximity to the Saltville Fault. Nine samples were collected from the Red House Branch section for this study, and six thin sections were prepared. The samples are numbered RHB 1 - 9, beginning at the Knox unconformity.

Sample # (Position)	Carbonate Rock Classification	Depositional Subenvironment

Lenoir Formation

RHB 9 (4.2)	Argillaceous skeletal wackestone	Shallow subtidal offshore marine

Typical basal Lenoir limestone. Collected from immediately above the sharp erosional surface that separates the Mosheim Member from the overlying main body of the Lenoir

Formation. Local relief on the erosional surface is about 0.5 m. Grayish brown lithology consists of nodules of fossiliferous limestone surrounded by laminae of dolomitized calcareous argillite. Also contains fairly abundant black specks of organic or mineral (?) material.

Mosheim Member

RHB 8 (4.2) — Mudstone — Tidal pond (subtidal)

Dove gray, featureless lime mudstone. Very few fenestrae, no lamination. Highly fractured (shattered), with fractures filled with white calcite. (No thin section)

RHB 7 (4.0) — Mudstone — Tidal pond (subtidal)

Dove gray mudstone with abundant vugs. Vugs are irregular in shape, and are filled with equant calcite cement, although some are floored with geopetal sediment. Contains very few fenestrae. Contains abundant fractures and bed-parallel stylolites.

RHB 6 (3.3) — Mudstone — Tidal pond (subtidal)

Medium gray mudstone with few fenestrae. Contains some vugs (3 to 5 mm across) filled with calcite cement that is white in hand sample. Sample is highly fractured, and contains abundant bed-parallel and bed-normal stylolites. (No thin section)

RHB 5 (2.5) — Fenestral mudstone — Algal marsh (intertidal)

Dove gray, fenestral mudstone. Fenestrae are small and irregular in shape, but most occur in bed-parallel layers that give the rock a vague lamination probably analogous to the "crinkled fenestral lamination" described from the high algal marshes on the Andros Island tidal flat (Hardie and Garrett, 1977).

RHB 4 (1.5) — Mudstone — Low algal marsh (intertidal)

Dove gray mudstone with very few fenestrae. Larger (3 to 5 mm) calcite-filled vugs are very common. (No thin section)

RHB 3 (0.7) — Mudstone — Low algal marsh (intertidal)

Same as RHB 4. Highly fractured with abundant stylolites. Some of the larger spherical fenestrae are lined with fibrous calcite cement, then filled with equant calcite. Other voids are completely occluded by equant cement. Some burrows are filled with peloids and small intraclasts that occur in a wide array of sizes.

RHB 2 (0.5) — Fenestral intraclastic packstone — Inland or high algal marsh (highest intertidal to supratidal)

Dove gray packstone with very abundant irregular and laminoid fenestrae. Orientation of fenestrae give the rock "crinkled fenestral lamination." Matrix is not muddy, but consists of discrete, depositional intraclasts with some peloids. Contains abundant caliche pisoids. Contains some calcite-filled vugs larger than fenestrae. Also contains a few lithoclasts of beige dolostone and brown chert, apparently derived from the

underlying Mascot Formation. Fractures cut diagonally across the sample (oblique to bedding).

RHB 1 (0.0) — Fenestral intraclastic grainstone — Inland algal marsh (supratidal)

Collected from immediately above the post-Knox unconformity. Matrix is not muddy at all, but consists entirely of discrete, depositional mud intraclasts. Represents sediment washed onto the Knox surface during initial marine transgression. Contains abundant fenestrae and abundant larger calcite-filled vugs up to 1 cm in diameter.

RHB 0 (0.0) — Conglomerate — Depression-fill

Sample is a piece of conglomerate collected from a filled depression on the Knox surface. Contains chert, dolostone, and limestone clasts. Interclastic space is filled with coarsely-crystalline calcite cement.

Bethel Valley Section

The Bethel Valley section is in the St. Paul belt, the northwesternmost strike belt sampled in this study. The basal strata of the Chickamauga Group in this strike belt are assigned to the Tumbez Formation, which is overlain by shales of the Eidson Member of the Lincolnshire Formation. Here, the basal Middle Ordovician strata are quite different lithologically from the basal peritidal deposits of the strike belts to the southeast. Tumbez lithologies are dominated by reddish, argillaceous limestones and partly silicified, conglomeratic dolostones. The Andros Island-type humid tidal flat deposits that are typical of the Five Oaks / Mosheim units are not represented in the St. Paul belt. For this reason, the sample descriptions provided below do not include an interpretation of the precise tidal flat depositional subenvironment in which each sample was deposited. Fourteen samples were collected and made into polished slabs, and eight thin sections were prepared from of those. The samples are numbered on the basis of their position (in meters) above the Knox unconformity.

Sample # (Position) — Lithology/Description

Tumbez Formation

BV 6.2 (6.2) — Mottled burgundy/gray peloidal skeletal packstone. Contains white chert-like "nodules" that are actually the red calcareous alga *Solenopora*, which encrusts other fossils. Also includes *Hedstoemia*, calcispheres, as well as pelecypods and ostracodes Occurs immediately beneath red shales of the Eidson Member.

BV 5.7 (5.7) — Gray, medium-crystalline (sucrosic) dolostone with nodules of burgundy-colored, *in situ* chert. (No thin section)

BV 5.2 (5.2) — Maroon-colored, terrigenous clastic siltstone or mudstone. Appears to have very low carbonate content. Overlies 1.7 m of reddish-brown shale. (No thin section)

BV 3.7 (3.7)	Greenish-gray, sucrosic dolostone with nodules of burgundy-colored, *in situ* chert. Very similar to BV 5.7. (No thin section)
BV 2.6 (2.6)	Mottled beige and burgundy skeletal wackestone, with small angular clasts of silicified dolostone. Also contains small acicular clasts (?) of chert and skeletal fragments that include pelecypods, trilobites, bryozoans, ostracodes, and rare echinoderm grains. Matrix is lime mud.
BV 2.1 (2.1)	Gray sucrosic dolostone, very similar to BV 5.7 and BV 3.7, but lacks chert. (No thin section)
BV 1.8B (1.8)	Burgundy-colored, argillaceous limestone with abundant angular clasts of yellow and beige dolostone. (No thin section)
BV 1.8A (1.8)	Mottled burgundy and gray limestone with very abundant angular chert and dolostone clasts. Very similar to BV 2.6.
BV 1.7 (1.7)	Mottled burgundy and gray chert. Appears to be a silicified version of BV 1.8A. Contains abundant sub-angluar clasts of red chert and beige dolostone in a limestone matrix that, in most places, has undergone partial silicification.
BV 1.1 (1.1)	Conglomeratic dolostone, very similar to the basal dolostone at the Idol section (ISR 1). Clasts are composed of chert and dolostone. Dolostone lithoclasts are composed of finely-crystalline dolomite whereas the matrix is more coarsely-crystalline. The basal 3 cm of the sample has been silicified, but dolostone clasts are still visible within the silicified portion. The dolomite clasts appear to be "floating" in a translucent chert matrix. White calcite cements are present in the non-silicified portion.
BV 0.4 (0.4)	Beige dolostone, with distinct stromatolitic algal lamination. Laminations are bed-parallel, with gentle undulations. In places, laminations are disrupted by bioturbation. Lamination is not associated with fenestrae, and is more typical of Knox-type algal lamination than the Mosheim/Five Oaks lamination. Sample contains no calcite at all.
BV 0.2 (0.2)	Conglomerate, with clasts composed of beige and brown dolostone, gray limestone, and blue to brown, translucent chert. Matrix is entirely dolomite, probably detritus reworked from the underlying Knox Group. Clasts are small, mostly less than 1 cm. Carbonate clasts are sub-round, but chert clasts are sub-angular. Shelter pores beneath clasts are filled with white calcite cement. Sample is identical to RV 0.6 (Raccoon Valley Section).
BV 0.1	Conglomerate, identical to BV 0.2, except that there is less cement-filled shelter (0.1) porosity. (No thin section)
BV 0.0 (0.0)	Conglomerate, very similar to BV 0.2, and also very similar to basal comglomerates of Raccoon Valley and other sections. Consists of clasts of dolostone and chert with lime peloids and abraded ostracode and pelecypod shells in a matrix of detrital dolomite. Some clasts have been rounded, but most are quite angular. Most clasts are small (0.1 to 1 cm), but a small portion are as large as 3 cm. Shelter pores beneath clasts are filled with calcite cement. Collected from immediately above the post-Knox unconformity, which is very sharp at this outcrop.

Raccoon Valley Section

The Raccoon Valley section, along with the Bethel Valley Section, occurs in the St. Paul strike belt. As in Bethel Valley, the lowermost strata of the Chickamauga Group are assigned to the Tumbez Formation. The total thickness of the Tumbez at this outcrop is unknown, but the basal 5.5 m are exposed above the post-Knox unconformity. The Andros Island-type humid tidal flat deposits that are typical of the Five Oaks / Mosheim units are uncommon in the basal Chickamauga strata in the St. Paul belt. For this reason, the sample descriptions provided below do not include an interpretation of the precise tidal flat depositional subenvironment in which each sample was deposited. It should be noted, however, that some of the Tumbez lithologies are very similar to some of the conglomeratic, dolomitic lithologies of the Blackford Member of the Five Oaks. Also, the Raccoon Valley section does contain some laminated, fenestral limestones that indicate that some of the Tumbez strata were deposited in a tidal flat environment. Twenty samples were collected and made into polished slabs, and thin sections were prepared from twelve of those. The samples were numbered based on their inferred position (in meters) above the inferred position above the Knox unconformity, which proved to be 0.5 meter higher than initially thought. The lower two samples are from the Mascot Formation (Knox Group).

Sample # (Position)	Lithology/Description
Tumbez Formation	
RV 6.0 (5.5)	Conglomeratic dolostone. Matrix consists of beige, finely-crystalline dolostone. Contains abundant subrounded to subangular clasts of lighter-colored dolostone and red, blue, and brown chert. (No thin section)
RV 5.3 (4.8)	Sample consists of two distinct lithologies separated by a sharp, scalloped erosional surface. Relief on the surface is only about 1 cm. The upper lithology is a conglomeratic limestone that extends upward to the position of the overlying sample (RV 6.0), becoming more dolomitic upwards. Clasts in the upper lithology consist of brown chert, beige dolostone, and dove-colored lime mudstone. The chert and dolostone clasts do not appear to have been derived from the underlying lithology, but the limestone clasts do. The lower lithology is a dove-colored lime mudstone with few fenestrae and no apparent lamination. The mudstone contains a few vertical burrows floored with yellow dolomitic internal sediment, and filled with clear equant calcite cement. These cements appear to be truncated at the erosional surface that occurs at the top of the lower mudstone lithology.
RV 5.1 (4.6)	Dove gray limestone that consists of intercalations of lime mudstone and peloidal grainstone. Mudstone portions contain vertical burrows filled either with clear equant calcite cement or internal sediment composed of dolomite clasts and lime peloids and intraclasts.
RV 5.0 (4.8)	Sample consists of two very similar limestone lithologies separated by a sharp, scalloped erosional surface. Relief on the erosional surface is about 2 cm. The

upper lithology is the same as the intercalated peloidal grainstone / mudstone described above (RV 5.1). Contains randomly-oriented irregular fenestrae and vertically-oriented, calcite cement-filled burrows. The lower lithology is fenestral mudstone similar to typical Mosheim. Fenestrae are filled with clear, equant calcite cement.

RV 4.5 (4.0) Sample consists of two similar limestone lithologies separated by a sharp, scalloped erosional surface. Relief on the erosional surface is about 0.5 cm. The upper lithology is a fenestral, intraclastic, peloidal packstone with abundant irregular and vertically-oriented, cement-filled fenestrae and a few 1 cm-sized chert clasts. The lower lithology is a non-fenestral lime mudstone that also contains abundant vertical cement-filled burrows.

RV 3.8 (3.3) Sample consists of two similar limestone lithologies separated by a sharp surface (partially obscured by a stylolite). The upper lithology is a conglomeratic limestone that consists of chert, dolostone, and limestone clasts in a peloidal intraclastic packstone matrix. The lower lithology is a lime mudstone that contains dolomitized burrows and abundant stylolites. The sample is very similar to RV 5.3. (No thin section)

RV 3.7 (3.2) Beige dolostone, finely-crystalline with vague horizontal lamination. (No thin section)

RV 3.1 (2.6) Medium-gray, intraclastic/skeletal lime packstone. Clasts include blue chert and light to dark brown lime mudstone. Slightly dolomitized, with rhombs scattered throughout the lithology.

RV 3.0 (2.5) Conglomeratic limestone. Clasts consist of limestone and dolostone with minor chert. Interclastic voids are filled with equant calcite cements. (No thin section)

RV 2.9 (2.4) Sample consists of two distinct lithologies separated by a sharp surface. The upper lithology is the same conglomeratic limestone as the overlying sample (RV 3.0), but with larger clasts and larger cement-filled voids. The lower lithology is an algally-laminated lime mudstone or peloidal packstone. (No thin section)

RV 2.8 (2.3) Sample consists of intercalated laminae of lime mudstone and skeletal, intraclastic packstone. Mud laminae are slightly dolomitized.

RV 2.4 (1.9) Conglomeratic, intraclastic skeletal packstone, with intercalated lime mud laminae. Similar to RV 2.8, but contains clasts of chert and dolostone. Matrix is mostly intraclastic packstone. Some of the muddy laminae are dolomitized. Clear equant calcite cements fill shelter pores beneath clasts and rare vugs.

RV 1.7 (1.2) Laminated beige/gray limestone. Consists of layers of mudstone intercalated with layers of peloidal packstone. (No thin section)

RV 1.5 (1.0) Conglomeratic, intraclastic/skeletal packstone. Very similar to RV 2.4. Clasts (up to 3 cm diameter) consists of dolostone and chert Matrix is almost free of dolomite.

RV 1.2 (0.7) Conglomerate, with clasts including beige dolostone (some of which have dedolomitization rims, and some of which are silicified), chert, and limestone. The matrix is peloidal, intraclastic packstone.

RV 0.9 (0.4) Laminated peloidal skeletal packstone. Very similar to BV 6.2 (Bethel Valley section). Skeletal fragments are mostly abraded ostracodes and pelecypods. Contains more skeletal material than RV 2.4 Lime packstone layers are intercalated with layers of detrital dolomite crystals.

RV 0.7 (0.2) Dolomitic conglomerate, consisting of limestone and dolostone clasts in a dolomitized lime mud matrix. (No thin section)

RV 0.6 (0.1) Conglomeratic dolostone, with clasts consisting primarily of dolostone, chert, and minor limestone. Matrix consists of coarse dolomite rhombs. Very similar to the basal conglomerates at the Idol and Bethel Valley sections. Collected from immediately above the post-Knox unconformity.

Mascot Formation

RV 0.5B (0.0) Light greenish-gray / beige dolostone. Contains large clasts of very angular chert. Occurs immediately beneath post-Knox unconformity, and represents the top of the Mascot Formation (Knox Group). (No thin section)

RV 0.5A (-0.1) Medium-gray dolostone. Consists of alternations of mudstone and peloidal intraclastic packstone. Contains calcite cement-filled vugs. Sample is identical to the uppermost Knox at the Idol Mine section. Beneath this lithology is a monotonous, thick section of interbedded limestone and dolostone ("ribbon limestone") characteristic of the Mascot Formation.

Boyd's Creek Road Section

The Boyd's Creek Road section contains a complete section of the Mosheim that is very well exposed, from basal conglomeratic strata to the sharp contact with the Lenoir Formation. The Mosheim is exposed on the gentle hillside facing Boyd's Creek Road, and also in an old quarry. The Knox unconformity is exposed approximately five meters from the road, and is difficult to see due to superficial lithologic similarity between the upper dolomitic limestones of the Mascot Formation and the dolomitized lower Mosheim strata. The upper Mosheim contact is exposed in the yard of the nearby house. The Mosheim at this section is very typical in terms of its lithostratigraphic sequence and its overall thickness (13.3 m). 27 samples were collected from this outcrop and made into polished slabs, and thin sections were prepared for 23 of these. The samples are numbered from BCR 1 - BCR 23 (duplicates of some intervals are indicated by letters after the number). The lower six samples (BCR 1 - BCR 6 are from the upper Mascot Formation (Knox Group).

Sample # (Position)	Carbonate Rock Classification	Depositional Subenvironment

Lenoir Formation

BCR 23 (13.4) — Skeletal wackestone — Shallow offshore marine (subtidal)

Dark gray wackestone with abundant, open marine fauna. Collected from immediately above the base of the main body of the Lenoir Formation.

Mosheim Member

BCR 22 (13.3) — Fenestral mudstone — Low algal marsh (intertidal)

Mud-dominated lithology collected from immediately beneath the erosional surface that forms the contact between the Mosheim and the overlying Lenoir. Contains a minor amount of small, abraded fossil fragments. Contains common irregular fenestrae, but no laminoid fenestrae, and no hint of lamination.

Contains fairly abundant large gastropod molds and perhaps some solution vugs. Fenestrae and most of the smaller vugs are filled with equant calcite cement, but some of the larger molds and vugs are lined with cloudy, fibrous calcite cement, and some are floored with marine sediment that is more fossiliferous than the mudstone matrix. This internal sediment also contains some round oncoid or peloid-like clasts. The internal sediment is overlain within voids by a thin layer of crystal silt and pisoids, and this layer is then overlain by clear, very fine crystals of equant calcite cement, which fills the remaining void space. Some of the larger voids contain coarsely-crystalline calcite in the centers Under cathodoluminescence (CL), the fibrous cement fringe is non-luminescent, the crystal silt/peloid layer is luminescent, and the equant calcite is dull and zoned.

BCR 21 (13.0) — Fenestral mudstone — Low algal marsh (intertidal)

This sample is just like BCR 22, except that dissolution vugs are more abundant. More of these vugs are lined with fibrous calcite cement, but fewer contain fossiliferous marine internal sediment. Under CL, most pores have the characteristic sequence of non-luminescent outer (first generation) cement, followed by a thin brightly-luminescent zone that outlines the initial black crystals, followed pore the dull, vaguely zoned equant calcite that fills the pore centers. Where present, the fibrous cements that fringe the outside of some pores are dull, and similar in luminescence to the pore-filling equant calcite.

BCR 20 (11.0) — Skeletal wackestone / Fenestral mudstone (altered to diagenetic grainstone) — Tidal pond/low algal marsh (intertidal) / High algal marsh (highest intertidal to supratidal)

Sample consists of two lithologies separated by a vague, non-erosional surface. The upper few mm of the lower lithology beneath this surface are bleached. The upper lithology is a skeletal wackestone, with abundant, very fine fossil fragments that include sponge spicules and ostracode valves. The upper lithology lacks fenestrae, but does contain some large laterally-oriented, stromatactis-like voids that are floored with internal sediment and filled with equant calcite. Under CL, this equant calcite is zoned,

and has a pendant distribution, with early generations of cement having grown downward from the roof of the void.

The lower lithology is a highly-fenestral lime mudstone, with very abundant irregular and laminoid fenestrae and a minor amount of interparticle porosity. The lower lithology contains abundant pisoids and well-developed diagenetic grainstone texture. Some pores are floored with internal sediment and a minor amount of vadose silt. All other pore space is filled with equant cements, which under CL are zoned and show unequivocal pendant distributions. There is no evidence of non-selective dissolution, and very little dolomite (<1%).

BCR 19 (9.0)	Fenestral mudstone	Low algal marsh (low intertidal)

Medium-gray lime mudstone, only slightly fenestral. Contains several calcite cement-filled vugs, some of which are floored with internal geopetal sediment. (No thin section)

BCR 18 (7.5)	Skeletal wackestone Fenestral mudstone (altered to diagenetic grainstone)	Tidal pond/low algal marsh (intertidal) High algal marsh (highest intertidal to supratidal)

Sample consists of two lithologies separated by a sharp, erosional surface. The upper lithology is a mottled wackestone with areas of clotted, peloidal texture. Much of the fossil debris (mostly gastropods and pelecypods) in the upper lithology has been leached, and most of the porosity (now filled) was moldic. There are a few burrows and a few fenestrae. All cements in the upper lithology are equant.

The lower lithology is a fenestral mudstone that has been altered to a diagenetic grainstone with abundant pisoids. Fenestrae include both laminoid and irregular morphologies. No lamination. As in the upper lithology, all pore-filling cements are equant calcite. Under CL, many of the fenestra-filling cements have pendant distributions. Some of the larger pores have a bright zone (or two) of cement which follows initial non-luminescent cement crystals. Smaller pores are filled entirely with non-luminescent calcite. Diagenetic (vadose) silt occupies much of the intergranular space. Rare fossil fragments in the upper lithology are not leached as in the lower portion.

Cements as well as depositional particles have been truncated at the erosional surface that caps the lower lithology, and the upper mm of the lower lithology has been bleached. This bleached surface appears to contain some vertically-oriented algal filaments. The surface may be analogous to the "paper crusts" described from the inland algal marsh on Andros Island (Hardie and Garrett, 1977).

BCR 17 (6.0)	Fenestral mudstone	Low algal marsh (low intertidal)

Medium-gray mudstone, fewer fenestrae than BCR 18. Very similar to BCR 19. (No thin section)

BCR 16 (5.0)	Fenestral mudstone (altered to diagenetic grainstone)	High algal marsh (highest intertidal to supratidal)

Highly-fenestral mudstone, with well-developed diagenetic grainstone texture and abundant pisoids. Both laminoid and irregular fenestrae are abundant, but if any

lamination was originally present, it has been obliterated by diagenetic, fenestral alteration. Pisoids in this sample are very large (up to 1 cm), and many are composite grains with clotted, peloidal interiors. All cements are equant calcite, with drusy fabric. The muddy sediment contains a minor amount of pyrite, but very little dolomite.

BCR 15 (3.5) — Fenestral mudstone (altered to diagenetic grainstone) — High algal marsh (highest intertidal to supratidal)

Originally a fenestral mudstone, now completely altered diagenetically to a pisolitic grainstone. No lamination. Virtually all mud is in the form of mud lumps, many of which are concentrically-laminated pisoids. The lithology was at one time very porous, as up to 50% of the rock volume is now calcite cement. Porosity types include fenestral, intergranular, and moldic (after gastropods). Cements are primarily equant calcite, but micritic, meniscus cements are also quite abundant at the points of contact between mudlumps and pisoids. The larger equant calcite cement-filled pores show the characteristic zonation under CL: an initial generation of non-luminescent (black) crystals lining pores, followed by one thin brightly-luminescent zone, followed by dull, vaguely-zoned cement in the pore center. Smaller pores are filled entirely with non-luminescent equant cement. Dull luminescent diagenetic crystal silt is fairly common in fenestrae, but interestingly does not occur on the floor of the pores, but well up into the cement sequence. Contains virtually no dolomite, and no pendant cements.

BCR 14 (2.2) — Fenestral mudstone — High algal marsh (highest intertidal)

Medium-gray mudstone, with moderately abundant fenestrae. Also contains a few larger vugs that are filled with white equant calcite. (No thin section)

BCR 13 (1.3) — Fenestral mudstone — Inland or high algal marsh (highest intertidal to supratidal)

Non-laminated mudstone with abundant irregular and laminoid fenestrae, and trains of vertically-oriented, spherical "bubble" fenestrae (gas escape paths?). Also contains some moldic and interparticle pores. All pores are filled with non-luminescent, equant calcite cement. Mud between fenestrae has been rounded diagenetically into discrete "clasts" (autoclasts), but alteration has not progressed to the "diagenetic grainstone" stage. Matrix mud is slightly dolomitized, more so than in overlying samples, but significantly less than underlying mudstones. Contains some fossil debris (leached) and a few dolomite clasts.

BCR 12B (1.0) — Fenestral mudstone — Inland or high algal marsh (highest intertidal to supratidal)

Medium-gray, non-laminated, fenestral mudstone, collected from the stratigraphically lowest, true fenestral mudstone bed in the Boyd's Creek Road section. Abundant laminoid and irregular fenestrae separate lumps of mud that appear to have been produced during early fenestral alteration. The few true clasts of depositional origin that are present serve as nucleii for round, concentrically-laminated, but poorly-developed (incipient) caliche pisoids. It appears that the process of alteration of this sediment to diagenetic grainstone/pisolite was arrested before completion. Dolomite is very rare. There are some micritic, meniscus cements in the interparticle space between mudlumps, but all other cements are equant calcite. Some of the equant cements seem

to have pendant distributions, but this does not stand out under CL because all cements are non-luminescent.

BCR 12 (1.0)	Fenestral intraclastic packstone	Inland or high algal marsh (highest intertidal to supratidal)

This fenestral packstone is similar in many ways to the overlying fenestral mudstones, but differs in that the matrix in this sample is not mud, but consists of peloids and small intraclasts composed of lime mud. These allochems, unlike those in some of the overlying samples, are true clasts of depositional (not diagenetic) origin--most are rounded and do not have a fitted fabric. Also, this sample contains zones of arched laminae ("wavy fenestral lamination") produced by alternation of dark organic-rich zones and lighter dolomitic zones. Dips on these arching laminae of up to 20 suggests binding of the peloidal sediment by cyanobacterial mats. The peloidal matrix is only slightly dolomitized. Fenestrae are extremely abundant, and include laminoid and irregular shapes. Crystal silt is abundant on the floors of fenestrae, but all cements are non-luminescent equant calcite.

BCR 11B (0.6)	Fenestral intraclastic packstone	Inland or high algal marsh (highest intertidal to supratidal)

Medium-gray fenestral limestone. Most fenestrae are filled with reddish-brown internal sediment rather than with calcite cement. Otherwise similar to other fenestral mudstones in this sequence. (No thin section)

BCR 11 (0.6)	Fenestral intraclastic packstone	Inland or high algal marsh (highest intertidal to supratidal)

Matrix consists of tightly-packed, small muddy intraclasts and peloids, and in most places has been thoroughly dolomitized. Certain zones within the rock are relatively undolomitized, and these zones seem to grade into the more heavily dolomitized portion. Dolomite rhombs cut across cements between intraclasts, suggesting that dolomitization followed early cementation. Contains abundant small laminoid fenestrae, many of which have been coalesced into long horizontal voids that give the rock a distinctive "crinkled" or "wavy fenestral lamination" indicative of deposition on the highest intertidal to supratidal portions of the tidal flat. Most voids are fenestrae, and the sample contains very few solution-enlarged vugs. All cements are small equant calcite crystals, which do not have the clarity of most equant cements in the Mosheim. Cements are all non-luminescent.

BCR 10B (0.5)	Fenestral intraclastic packstone	Inland or high algal marsh (highest intertidal to supratidal)

Sample is representative of the basal Mosheim at this and most other outcrops. Matrix is highly dolomitized peloidal, intraclastic packstone, with very little loose mud. Contains some small undolomitized limestone lithoclasts, that are presumably redeposited Knox detritus. Laminoid and irregular fenestrae are both very abundant, with the laminoid slightly more common, but the orientation of fenestrae is not consistent enough to give the rock any lamination. Porosity of the lithology was very high, as about 40% of the rock volume is occupied by cement. Cements (except in fractures) are all non-luminescent equant calcite. Vertical fractures are filled with

baroque dolomite and ferroan calcite that clearly post-dates all other void-filling cements.

BCR 10A (0.5) — Fenestral intraclastic packstone — Inland or high algal marsh (highest intertidal to supratidal)

Very similar to BCR 10B, but contains more intraclasts and lithoclasts. Clasts are small (1 to 3 mm) and generally quite round, although some are angular. Intraclasts are micritic, peloidal, or composed of skeletal material (especially *Hedstroemia* algae). Voids are very abundant, and most are fairly large (commonly up to 4 mm), spherical "bubble" fenestrae, but some are clearly leached allochems, some of which have micritic envelopes. Laminoid fenestrae are not common, but enough are present to give the rock a vague, arched lamination ("wavy fenestral lamination"). Most voids are filled with non-luminescent, equant calcite, but some (especially the larger ones) have an initial lining of cloudy, fibrous calcite. Cement occupies 40 to 45% of the rock volume in this sample. Although there is evidence of dissolution, there is no clear evidence that this occurred in the vadose zone.

BCR 9 (0.4) — Fenestral peloidal packstone — Inland or high algal marsh or levee backslope (supratidal)

Very similar to samples immediately above and below, but contains well developed disrupted flat lamination. This sample contains the best lamination observed anywhere in the Mosheim Member. Laminae are produced by alternation of dark, organic-rich mud layers and lighter, thoroughly dolomitized peloidal layers. Lamination is enhanced by horizontally-oriented laminoid fenestrae that have coalesced into sheet cracks, some of which stretch across the slide. The sample also contains vertical mudcracks that connect one sheetcrack to the underlying one, and break up the sediment layers into "flat pebbles" that are somewhat rounded at each end. All pores are filled with equant calcite cement, most of which is entirely non-luminescent. The largest pores contain brightly luminescent cements that outline non-luminescent first-generation cement, and dull pore-central cements.

BCR 8 (0.0) — Conglomeratic fenestral grainstone — Inland or high algal marsh (highest intertidal to supratidal)

Matrix consists of highly dolomitized peloids and muddy intraclasts, with no loose mud. Contains abundant lithoclasts of dolostone and chert that are presumably redeposited Knox detritus. Knox dolomite clasts differ from dolomitized intraclasts in that the Knox clasts are lighter-colored, finer-grained, and anhedral to subhedral, whereas the *in situ* clasts are composed of medium-crystalline, euhedral rhombs. Also contains rare echinoderm grains and molds of gastropod shells indicated by micritic envelopes. Pores include both fenestrae and intraparticle voids (keystone vugs), all of which are filled with very clear, equant calcite that is non-luminescent (black) under CL. No pendant cement distributions or unequivocal indicators of vadose alteration (such as crystal silt) were observed

BCR 7 (0.0) — Fenestral dolomudstone — Inland or high algal marsh (highest intertidal to supratidal)

Three samples (7A, 7B, and 7C) were collected from the same interval and are very similar (also very similar to BCR 10A,B). BCR 7A is highly fenestral, highly

dolomitized mudstone with abundant mud intraclasts. Fossil fragments are very rare (one bryozoan fragment, a few trilobite fragments, and some gastropod molds). Also contains a few lithoclasts of Knox dolostone, which is differentiated from Mosheim dolostone as described above. Matrix dolomite is medium-crystalline and strikingly euhedral. Fenestrae are predominantly laminoid, but irregular fenestrae are also very abundant. All pores are filled with very clear, equant calcite cement. Cement occupies 30 to 35% of the rock volume.

BCR 7B is just like 7A and 10A, except that fenestrae are dominantly irregular rather than laminoid. Large fenestrae (2 to 5 mm) are common. 7C contains mostly very small (1 to 2 mm) irregular fenestrae, but also contains some almost perfectly spherical "bubble" fenestrae.

BCR 7D (0.0) Conglomeratic dolostone Depression fill

Conglomerate in dolomite matrix, collected from a shallow (0.2 m) depression on the Knox surface just below the stratigraphic level of BCR 7A, B, C. Very similar to basal conglomeratic dolostones of the Douglas Lake Member. Matrix appears to be pervasively dolomitized lime mud. Dolomite is medium- to coarsely-crystalline and sub- to euhedral. Interestingly, the peloids and small lime mud intraclasts supported in this matrix are undolomitized. Does not contain fenestrae, but does contain some subround pores that may be leached fossil shell fragments or solution vugs. All pores in the matrix are filled with equant calcite cement, but cements in the Knox dolostone lithoclasts include silica in addition to equant calcite.

Mascot Formation

BCR 1 - 6 These samples were collected from the upper four meters of the Mascot Formation that underlies the Mosheim beneath the post-Knox unconformity. The Mascot in this area consists of light gray, non-fenestral, intraclastic lime grainstone interbedded with dark gray, finely-crystalline dolostone and burrow-mottled dolomitic limestone. The light gray limestone portions of the Mascot are superfically quite similar to the Mosheim, and have led to speculation that the contact between the Mascot and Mosheim in this strike belt is conformable (e.g. Ruppel, 1979). This suite of samples, however, clearly shows that the post-Knox unconformity is present in this outcrop belt between the Mascot and the Mosheim. The limestone portions of the Mascot are tidal flat deposits, but can be differentiated from the Mosheim in that the Mascot samples lack fenestrae, which are all but ubiquitous in the Mosheim.

Deep Springs Section

The Deep Springs section is exposed on the north shore of Douglas Lake, and can only be observed when the water level is down. An extensive exposure of Douglas Lake Member conglomerates and shaly dolomitic limestones is exposed beneath the Mosheim Member, and the outcrop is one of the best places to observe paleokarst features along the Knox unconformity. The upper contact between the Mosheim and Lenoir is also very well exposed, and can be traced laterally for tens of meters. Samples were collected at approximately one-meter intervals, depending upon exposure, and also at lithologic changes. A total of 24 samples were collected from this outcrop and made into polished slabs, and thin sections were prepared for 13 of these. Samples DS 1 through DS 3 are from the upper Mascot Formation (Knox Group) and samples DS 4 through DS 6 are from the fissile, shaly limestones of the Douglas Lake Member. Thin sections were not prepared from the Mascot or Douglas Lake Member samples. A measured section for the Deep Springs Section is provided in Shanmugam (1978).

Sample # (Position)	Carbonate Rock Classification	Depositional Subenvironment
Lenoir/Mosheim Contact		
DS 24 (24.4)	Argillaceous skeletal packstone Fenestral mudstone	Adjacent offshore marine (subtidal) Low algal marsh (low intertidal)

Three samples collected from same interval. Samples contain the contact between the Mosheim and the overlying Lenoir. The contact is sharp and erosional, with up to 8 cm relief at this outcrop. Cements as well as depositional grains are truncated at this surface. The basal Lenoir is very dark gray, very fossiliferous packstone. The uppermost Mosheim is medium-gray, non-laminated, highly-fenestral lime mudstone. Fenestrae are very small and irregular; laminoid fenestrae are absent. Mud is somewhat organized into rounded lumps surrounded by thin void spaces, but development toward diagenetic grainstone texture is poor. Does not contain pisoids. Fenestrae are filled primarily with very small, equant calcite. Pyrite is fairly common in some of the fenestrae. The sample also contains abundant unbroken, equant calcite-filled ostracode shells, and several large vugs, some of which are floored with beige-colored internal sediment (not similar to the overlying Lenoir sediment), while others are lined with brownish, cloudy, fibrous calcite cement and then filled with equant calcite. Fractures are abundant, and filled with coarsely-crystalline, ferroan equant calcite cement.

Under CL, it is clear that the equant calcite cements filling void spaces in this sample were precipitated in several generations. The ostracodes are filled almost entirely with non-luminescent (black) cement, whereas the fenestrae contain only a very few small subcrystals of non-luminescent cement. These subcrystals are outlined by a thin zone of brightly-luminescent cement, and then the center of the void is filled with dull (sometimes vaguely zoned) calcite. Where pyrite occurs, it is usually associated with the dull, pore-central cement. Where fenestrae are truncated by the erosional surface at the top of the Mosheim, all cement zones are truncated. Fracture-filling ferroan cements are invariably unzoned and more dull than the pore-central dull cement in fenestrae. Cements in pores in the Lenoir are all unzoned, dull orange, and similar to the pore-central cements in the Mosheim fenestrae.

Mosheim Member

DS 23 (24.4) — Mudstone — Tidal pond/low algal marsh margin (low intertidal)

Sample collected from just beneath the top of the Mosheim consists of medium gray, non-laminated, lime mudstone with very few small irregular fenestrae. Fenestrae are filled either with beige internal sediment or equant calcite. As above, contains several whole ostracode shells filled with white equant calcite, and large internal sediment-filled dissolution vugs. Also contains abundant stylolites that are cut by a large diagonal fracture that is filled with ferroan calcite. Luminescence of cements is the same as in DS 24.

DS 22 (24.1) — Mudstone — Tidal pond/low algal marsh margin (low intertidal)

Very similar to DS 23. One very large vug (3 cm across) is filled with brown internal sediment just like the overlying Lenoir. This internal sediment contains open marine fossils and clasts of gray mudstone like the Mosheim matrix. It is presumed that this void was connected to the surface (0.3 m above this sample), and was filled with Lenoir-like sediment during deposition of the Lenoir.

DS 21 (23.3) — Fenestral mudstone — Low algal marsh (intertidal)

Beige/gray non-laminated mudstone with abundant irregular fenestrae (no laminoid fenestrae). Dissolution vugs and gastropod molds are also common. Cements in vugs, fenestrae, and inside gastropod chambers are cloudy and look fibrous or bladed, but cements in shell molds are tiny and have greater clarity. One large gastropod mold is filled with multiple generations of fibrous cement. Under CL, almost all pores contain an initial generation of non-luminescent crystals, which is rimmed by a single, thin, brightly luminescent zone, and then pore-central, dull (or vaguely subzoned) equant crystals. Pyrite is also present as a cement phase, and occurs within the dull pore-central calcite. There are at least two generations of veins, one of which is bed-parallel and filled with white calcite, and a younger generation that cuts the bed-parallel set diagonally and is filled with gray equant calcite cement. The calcite filling both vein sets is ferroan and dull orange under CL.

DS 20 (22.8) — Mudstone — Tidal pond/low algal marsh margin (low intertidal)

Mottled gray lime mudstone with abundant black (organic?) matter. Contains irregular fenestrae, but in lesser abundance than above. No lamination or laminoid fenestrae. Contains abundant vugs, most of which are filled with fibrous cements, but all other voids are filled with equant calcite cements that show the same characteristics under CL as DS 21. Abundant bed-parallel veins cross-cut all other features.

DS 19 (21.2) — Fenestral mudstone — Low algal marsh (intertidal)

Black, non-laminated, highly fenestral mudstone, similar to other Mosheim fenestral mudstones except for the very dark color. Irregular fenestrae are abundant in a wide range of sizes. Vertically-oriented burrows, gastropod molds, and ostracodes are fairly

common. Voids are filled with very fine, equant calcite cement, although some are floored with lighter-gray internal sediment. No evidence of non-selective (vuggy) dissolution or extended vadose alteration.

DS 18 (20.6) — Fenestral mudstone — Low algal marsh (intertidal)

Identical to DS 19.

DS 17 (20.0) — Mottled limestone — Tidal pond (subtidal)

Black and gray mottled "ribbon" limestone, possibly partly dolomitic. Rock is brecciated, with numerous fractures in random directions. All fractures are filled with white calcite, some with multiple generations of cement. (No thin section)

DS 16 (18.7) — Fenestral mudstone — Low algal marsh (intertidal)

Black fenestral mudstone, very similar to DS 18, 19. Gastropod molds are filled with internal sediment. Contains several voids that are larger than fenestrae (vugs?) and filled with internal sediment, and cloudy, brownish cements that appear to be fibrous calcite, but are actually very fine equant cements, as in DS 19. Large bed-normal veins are filled with coarse, white equant calcite, except for some areas that are lined with clear calcite.

DS 15 (17.9) — Fenestral mudstone — Low algal marsh (intertidal)

Black, fenestral mudstone very similar to DS 16, 18 and 19. (No thin section)

DS 14 (16.8) — Mudstone — Tidal pond/low algal marsh margin (low intertidal)

Dove gray mudstone with few fenestrae , but several cement-filled burrow tubes. (No thin section)

DS 13 (15.8) — Mudstone — Tidal pond/low algal marsh margin (low intertidal)

Dove gray mudstone just like DS 14, but with almost no fenestrae and fewer burrows. (No thin section)

DS 12 (14.0) — Fenestral mudstone — Low algal marsh (intertidal)

Dove gray fenestral mudstone, with abundant, small, irregular fenestrae. Contains no laminoid fenestrae or lamination, no dissolution vugs. All pores are filled with fine, equant calcite cement. Fractures are filled with clear equant cement.

DS 11 (12.0) — Fenestral mudstone — Low algal marsh (intertidal)

Medium-gray fenestral mudstone very similar to DS 12, but with more fractures, most of which are perpendicular to bedding. (No thin section)

DS 10 (10.7)	Mudstone	Tidal pond/Low algal marsh margin (subtidal to low intertidal)

Dove gray mudstone with rare fenestrae, but with a few large vugs filled with equant calcite cement. Under CL, the cements filling these voids have the typical pore-filling sequence of initial pore-rimming non-luminescent (black) crystals outlined by a brightly-luminescent zone, the the pore center is filled with dull, subzoned cement.

DS 9 (9.6)	Mudstone	Tidal pond/Low algal marsh margin (subtidal to low intertidal)

Dove gray mudstone essentially identical to DS 10. Fenestrae are rare and small, but large vugs filled with white calcite are common. One vug is filled with an unknown black material. Contains several almost bed-normal fractures filled with clear calcite cement. (No thin section)

DS 8 (8.0)	Mudstone	Tidal pond/low algal marsh margin (subtidal to low intertidal)

Medium to dark gray mudstone with rare fenestrae, similar to DS 9 and 10. Contains several vugs filled with dark brownish, fibrous calcite cement. Also has very abundant black stylolites. (No thin section)

DS 7 (7.2)	Fenestral mudstone	Low algal marsh (intertidal)

Brownish-gray nodular lime mudstone with abundant small, irregular fenestrae. Nodular appearance is produced by an abundance of bed-parallel stylolites.

DS 6 (6.4)	Mudstone	Tidal pond/low algal marsh margin (subtidal to low intertidal)

Dark gray mudstone with rare fenestrae, but with large stromatactis-like vugs filled with brownish fibrous calcite and white equant calcite cements. Also contains numerous subhorizontal stylolites. Collected from the stratigraphically lowest bed of Mosheim-like fenestral limestone. Grades downward into more argillaceous, nodular, shallow subtidal limestones assigned to the Douglas Lake Member.

Douglas Lake Member

Underlying the Mosheim at the Deep Springs locality is a lens-shaped body of argillaceous, dolomitic limestone that closely resembles the main body of the Lenoir. The thickness of this unit varies from 0 to as much as seven meters, and can be seen to pinch out laterally, placing fenestral mudstones of the Mosheim Member directly on the Mascot. On the basis of its position beneath the Mosheim, and its laterally-discontinuous, depression-filling distribution, Shanmugan (1978) assigned this basal portion of the Middle Ordovician sequence to the Douglas Lake Member. Shanmugam reported a sharp, unconformable contact with underlying dolostones of the Knox Group at the base of this nodular sequence. The post-Knox unconformity was not directly observed at the specific point where this suite of samples was collected because it occurred in a covered interval.

DS 5 (5.2) — Nodular mudstone — Shallow restricted subtidal lagoon

Medium gray, burrow-mottled, nodular, argillaceous limestone very similar to the main body of the Lenoir Formation, but without fossils. Appears to be dolomitic, but that has not been confirmed by petrography or geochemical methods. (No thin section)

DS 4 (4.6) — Nodular mudstone — Shallow restricted subtidal lagoon

Dark gray, very argillaceous, nodular lime mudstone. As above, this sample closely resembles the Lenoir, but fossils are rare and limited to ostracodes and trilobite fragments. Metalliferous (manganese?) nodules are fairly common. (No thin section)

DS 3 (4.0) — Nodular mudstone — Shallow restricted subtidal lagoon

Dark gray, very argillaceous, nodular lime mudstone identical to DS 4. Argillite content increases significantly downward beneath this sample, such that samples are shaly and easily weathered. No samples were collected from the shaly interval. Beneath the shaly interval, which is several meters thick, the next rocks outcropping are dolostones interpreted to be in the Knox Group. (No thin section)

Mascot Formation (Knox Group)

DS 2 — Black, medium-crystalline, argillaceous dolostone. Collected ten meters beneath DS 3, or about six meters beneath the top of the Knox Group. Strongly resembles the dolostone portions of the upper Mascot at the Boyd's Creek Road section (especially BCR-4), but is more argillaceous here. (No thin section)

DS 1 — Beige, nodular, mottled, finely-crystalline dolostone, with abundant fractures and stylolites. Collected one meter beneath DS 2. (No thin section)

DS 0 — Beige, medium-crystalline dolostone. Collected two meters beneath DS 1. Typical Mascot dolostone. (No thin section)

Fish Hatchery Road Section

At the Fish Hatchery Road location, the basal portion of the Mosheim Member and its contact with the Knox Group are not exposed, but occur beneath a three-meter thick covered interval. Eleven meters of the Mosheim is exposed above this covered interval, so the total thickness of the Mosheim Member at this location does not exceed approximately thirteen meters. Stratigraphic position given for each sample is the distance in meters above the covered interval. The contact with the overlying main body of the Lenoir Formation is well-exposed, and is very sharp and planar. This erosional surface has about 7 cm of relief across the outcrop. Twenty-one samples were collected from this section and made into polished slabs, and thin sections were prepared from nine of those.

Sample # (Position)	Carbonate Rock Classification	Depositional Subenvironment

Lenoir Formation

FH 20 (11.2) — Skeletal wackestone — Shallow offshore marine (subtidal)

Dark gray argillaceous wackestone with abundant, open marine fauna. Typical lithology of the main body of the Lenoir Formation. (No thin section)

FH 19 (11.1) — Skeletal wackestone — Shallow offshore marine (subtidal)

Same as above, with very abundant wispy stylolites that give the lithology its characteristic nodular appearance. (No thin section)

FH 18 (11.0) — Skeletal packstone — Shallow offshore marine (subtidal)

Brown, oxidized, very argillaceous packstone with abundant, open marine fauna. Collected from immediately above the base of the main body of the Lenoir Formation.

Mosheim Member

FH 18B (10.9) — Fenestral mudstone (altered to diagenetic grainstone) — High algal marsh (highest intertidal to supratidal)

Medium gray, highly fenestral mudstone collected from uppermost Mosheim, just beneath the Mosheim/Lenoir contact. Irregular and laminoid fenestrae are very abundant, but the laminoid variety are dominant and give the rock vague "crinkled fenestral lamination". Muddy matrix has been highly altered through fenestral alteration, but the diagenetic grainstone texture is not well developed. Contains abundant caliche-type pisoids. Matrix contains no dolomite. Fenestrae are filled with non-ferroan, equant calcite cement that has the following luminescence zonation under CL: Only the tiny, first generation crystals adjacent to the pore walls have alternating bright and non-luminescent zones. The vast majority of cements (and all pore centers) are dull luminescent. There are no fibrous cements and no vadose silt in this sample. Very small fractures are abundant and are filled with finely-crystalline, ferroan calcite cement.

FH 17 (10.8) — Fenestral mudstone — Low algal marsh (intertidal)

Medium gray mudstone contains abundant irregular fenestrae, but no laminoid fenestrae. This sample has not been altered to the diagenetic grainstone texture and lacks pisoids. Vertical, smooth-walled burrows and gastropod molds are common, and these as well as all fenestrae are filled with non-ferroan, equant calcite cement. Fractures are filled with ferroan calcite cement. Contains no vadose silt or internal sediment in pores. Luminescence of cements is the same as in FH 18.

FH 16 (10.6) — Fenestral mudstone — Low algal marsh (intertidal)

Very similar to FH 17; contains a few large micritic intraclasts, but matrix is all mud with no peloids. Also contains abundant irregular fenestrae and gastropod molds, some of which have been enlarged by dissolution. All pores are filled with equant calcite;

internal sediment, fibrous cements, and vadose silt are absent. Luminescent zonations of cement are similar to FH 18, but there are two thin zones of brightly-luminescent cement alternating with non-luminescent zones in the crystals that rim the pore walls. All other cements have dull luminescence. Fractures are filled with dull luminescent, ferroan calcite cement.

FH 15 (10.2) — Fenestral mudstone — Low algal marsh (intertidal)

Dove gray fenestral mudstone. Irregular fenestrae are abundant, and many are filled with light gray internal sediment, but most are filled with equant calcite cement. Contains abundant stylolites, some of which are associated with pyrite. (No thin section)

FH 14 (9.9) — Mudstone — Tidal pond/low algal marsh margin (low intertidal)

Dove gray mudstone, with rare fenestrae, but with fairly common larger equant calcite cement-filled vugs. Bed-parallel and bed-normal stylolites are very abundant. Fractures clearly cross-cut stylolites. (No thin section)

FH 13 (9.3) — Fenestral mudstone (altered to diagenetic grainstone) — High algal marsh (highest intertidal to supratidal)

Just like FH 18B, with abundant caliche-type pisoids, but with diagenetic grainstone texture not as well-developed. Matrix contains alot of peloids. Contains abundant laminoid fenestrae, but any original lamination has been obscured by intense fenestral alteration. Also, this sample is not as highly fractured as FH 18. There is a minor amount of dolomite associated with stylolites in this sample.

FH 12 (8.4) — Mudstone — Tidal pond/low algal marsh margin (low intertidal)

Dove gray featureless lime mudstone with very few fenestrae. Contains very abundant subhorizontal stylolites. No fossils are apparent in polished slab. (No thin section)

FH 11 (7.2) — Fenestral mudstone — Low algal marsh (intertidal)

Dove gray fenestral mudstone. This is the most characteristic lithology of the Mosheim Member. Contains abundant, small, irregular fenestrae filled with equant calcite. Also contains a few large burrows or solutional vugs filled with equant calcite and very abundant stylolites. (No thin section)

FH 10 (6.2) — Fenestral mudstone — Low algal marsh (intertidal)

Dove gray fenestral mudstone, very similar to FH 16. Contains several subangular to rounded micritic intraclasts, some of which contain *Girvanella* (?) filament molds that are filled with calcite. Fenestrae are abundant and all irregular, and some laminoid fenestrae wrap around the intraclasts. All voids are filled with fine, equant calcite cement. Also contains a few burrows that are filled with equant calcite, except for a few which are floored with crystal silt and a few which are filled with fecal pellets. Stylolites are abundant, and occur in many orientations. Under CL, cement luminescence is very similar to that of FH 16. Most pores contain an initial generation

of non-luminescent crystals, then a generation that consists of three alternating bright- and non-luminescent cement zones, and a final pore-central generation of dull cement.

FH 9 (5.6) — Fenestral mudstone — Low algal marsh (intertidal)

Dove gray fenestral mudstone, essentially just like FH 10. (No thin section)

FH 8 (4.4) — Fenestral mudstone — Low algal marsh (intertidal)

Just like FH 9 and 10. (No thin section)

FH 7 (3.8) — Fenestral mudstone — Low algal marsh (intertidal)

Dove gray fenestral mudstone, very typical Mosheim, just like FH 8, 9, and 10. Contains a large fracture filled with brownish equant calcite cement. (No thin section)

FH 6 (2.9) — Fenestral mudstone — High algal marsh/levee backslope (highest intertidal to supratidal)

Dove gray, fenestral, peloidal mudstone, with very abundant irregular and laminoid fenestrae. Orientation of laminoid fenestrae give the rock a vague "wavy fenestral lamination". Also contains some vertical burrows. Some of the smaller fenestrae are floored with crystal silt, but all remaining pore space is filled with very clear, typically coarsely-crystalline equant calcite. Luminescent zonation is more complex in this sample than above, with five brightly luminescent zones alternating with non-luminescent zones. Even the smallest fenestrae contain multiple bright zones. The matrix mud contains a minor amount of dolomite, but most of the dolomite in the sample is styloreactate along stylolites.

FH 5 (2.0) — Fenestral mudstone — Low algal marsh (intertidal)

Dove gray fenestral mudstone, very similar to FH 17. Matrix is entirely mud, with no clasts of any kind. No alteration of the matrix to pisoids. Fenestrae are irregular, but not as abundant as in the overlying samples. Fenestrae are larger than average (3 to 6 mm). There is also some moldic porosity after gastropods and some whole ostracodes. All pores are filled with equant calcite cement, but there is a minor amount of intercrystalline pyrite or hydrocarbon material within the equant calcite. Large bed-normal fractures and other smaller parallel fractures are filled with dull-luminescent equant calcite.

FH 4 (1.4) — Fenestral mudstone — Low algal marsh (intertidal)

Dove gray fenestral mudstone, with fenestrae dominated by the irregular shape. Also contains a few larger calcite-filled vugs. (No thin section)

FH 3 (1.1) — Mudstone — Tidal pond/low algal marsh margin (low intertidal)

Dove mudstone with a few irregular fenestrae. (No thin section)

FH 2 (0.2)	Mudstone	Tidal pond/low algal marsh margin (low intertidal)

Dove mudstone similar to FH 3. A few fenestrae are filled with internal sediment. (No thin section)

FH 1 (0.0)	Mudstone	Tidal pond (subtidal)

Dove gray featureless mudstone. No fenestrae or lamination. Collected from the lowest exposed Mosheim at this outcrop.

Nina Section

At the Nina section, the Mosheim Member is 18.7 m thick. The lower contact with the Knox Group is very sharp here, with 0.3 m (1 ft) of relief. The upper contact of the Mosheim Member with the main body of the Lenoir at this locality differs from all others in the study area in that this contact is gradational. The uppermost Mosheim, rather than being composed of high intertidal to supratidal fenestral mudstones typical of the upper Mosheim, consists of nodular wackestones that grade upward into more open marine, but otherwise similar, skeletal packstones of the Lenoir. It is believed that the upper Mosheim at Nina was deposited in a depositional subenvironment such as a tidal channel mouth where the beach ridge that normally marks the tidal flat/adjacent marine depositional interface (and the Mosheim/Lenoir contact) is not present. Nina is the only outcrop where this gradational type of contact exists between the Mosheim and Lenoir. Twenty-eight samples were collected from the Nina section, and 27 of those were made into polished slabs. Twenty-one thin sections were prepared. Four thin section (NR 6 - NR 9) were made of the Knox unconformity at this section. Samples NR 1 - NR 5 are from the upper Mascot Formation (Knox Group).

Sample # (Position)	Carbonate Rock Classification	Depositional Subenvironment
Lenoir Formation		
NR 28 (18.8)	Argillaceous, skeletal packstone	Shallow offshore marine (subtidal)

Argillaceous, nodular, skeletal packstone collected from just above the Mosheim/Lenoir contact, which is recognizable, but not sharp and erosional at this location. Typical basal Lenoir.

Mosheim Member

NR 27	Skeletal peloidal packstone	Tidal channel mouth bar (subtidal) (18.7)

Collected from top of Mosheim, this sample is a beige-gray, non-fenestral, non-laminated, argillaceous packstone. Contains abundant argillaceous laminae that give the lithology a somewhat nodular appearance. Resembles Lenoir and contains a diverse,

open marine fauna (bryozoans, brachiopods, red and green algae, trilibites, and echinoderms), but contains fewer fossils than Lenoir. Allochems are primarily peloids in a slightly dolomitized, muddy matrix. Poloids have vague borders, and merge into matrix. Very little porosity, but what there is is inter- and intraparticle. All pore space is filled with equant calcite.

NR 26 (18.2) — Skeletal peloidal packstone — Tidal channel mouth bar (subtidal)

Same as NR 27. (No thin section)

NR 25 (18.0) — Skeletal peloidal packstone — Tidal channel mouth bar (subtidal)

Light gray packstone, very similar to NR 26 and 27, but with lower argillaceous content. As above, very low porosity. Contains abundant bed-normal fractures filled with calcite cement.

NR 24 (16.7) — Fenestral mudstone — Low algal marsh (intertidal)

Dove gray fenestral mudstone, collected from the stratigraphically highest typical Mosheim lithology. Contains fairly abundant irregular fenestrae and larger vugs, most of which are filled with equant calcite, but some of the large vugs appear to contain some cloudy, fibrous calcite cement. (No thin section)

NR 23 (15.7) — Fenestral mudstone — Low algal marsh (intertidal)

Dove gray, non-laminated, fenestral mudstone, typical Mosheim. Matrix is all mud (no peloids). Contains abundant irregular fenestrae, and no laminoid fenestrae. Fossils are limited to rare ostracodes and gastropod molds. Virtually all porosity is fenestral, although some appear to be solution-enlarged. Some fenestrae contain some internal sediment and rarely, crystal silt, but the vast majority of the porosity is filled with equant calcite cement. Dispersed within the matrix in this sample are many "nodules" of a mineral that appears to be gypsum. These nodules of gypsum in the matrix are clearly authigenic, and are approximately the same size as the fenestrae (about 0.5 mm), but are not believed to fill fenestrae, but probably grew displacively in the matrix. The nodules are very rough-edged and extremely finely-crystalline. Also,gypsum occurs as a cement in one gastropod mold. This mold is floored by the following sequence of materials: gypsum (?), celestite, and crystal silt, then the remaining pore space is filled by zoned, luminescent equant calcite. This is the only sample in the Mosheim in which evaporite minerals have been observed. Under CL, the crystal silt is entirely non-luminescent (darker than the matrix mud, but not as black as some non-luminescent zones in the equant calcite). The equant calcite shows alternating zones of non- and brightly-luminescent cement, but the final pore-filling cement generation is dull under CL. The celestite does not luminesce, but has a faint bluish color (vivid blue under crossed nicols).

NR 22 (14.7) — Fenestral intraclastic mudstone — Low algal marsh (intertidal)

Dove gray fenestral mudstone with uncommon intraclasts that are slightly darker than the matrix. Also contains some white, equant calcite-filled vugs that are larger than fenestrae. Similar to NR 23. (No thin section)

NR 21 (13.2) — Fenestral mudstone — Low algal marsh (intertidal)

Dove gray, non-laminated, fenestral mudstone, very representative of typical Mosheim. Essentially just like NR 23, but lacks gypsum nodules, and contains more crystal silt within fenestrae. Fenestrae are larger than normal, and may be solution-enlarged. All fenestrae are filled with equant cement, some of which exhibits nice pendant morphologies under CL (non-luminescent crystals hanging from fenestra ceilings.)

NR 20 (11.7) — Fenestral mudstone — Low algal marsh (intertidal)

Dove gray mudstone with abundant irregular fenestrae and some larger calcite-filled vugs. Also contains a vertically-oriented burrow filled with internal sediment and white equant calcite. Abundant stylolites. (No thin section)

NR 19 (9.7) — Peloidal skeletal wackestone — Tidal channel mouth or pond (subtidal)

Medium-gray, mottled limestone similar to NR 26 and 27, but not argillaceous or nodular. Intraclasts are of a lighter gray color than the matrix. Fossil fragments (especially calcareous algae) are more abundant than in NR 26 and 27. Open marine fauna suggests open communication with the open marine environment Contains no fenestrae and no lamination, and no evidence of subaerial exposure.

NR 18 (6.9) — Fenestral mudstone (altered to diagenetic grainstone) — High algal marsh (highest intertidal to supratidal)

Dove gray, highly fenestral mudstone with well-developed diagenetic grainstone texture and abundant caliche pisoids. Pisoids are up to 2 mm in diameter. All cements appear to be equant calcite. For more information see description of NR 17 (No thin section)

NR 17 (6.9) — Fenestral mudstone (altered to diagenetic grainstone) — High algal marsh (highest intertidal to supratidal)

Dove gray, highly fenestral mudstone with well-developed diagenetic grainstone texture and abundant caliche pisoids. Fenestrae are primarily laminoid, with irregular fenestrae also common. Laminoid fenestrae are coalesced into sheet cracks up to 4 cm long, and give the rock "crinkled fenestral lamination" which is unusual in the Mosheim. Pisoids are very large and very abundant. Micritic meniscus cements are common between pisoids and mud lumps, but all other cements are equant calcite. Some crystal silt is present on the floors of some fenestrae. Under CL, smaller fenestrae are filled with non-luminescent (black) cements, whereas some of the larger pores are rimmed with small crystals that have alternating bright and non-luminescent zones. Pore central cements are typically dull luminescent. Crystal silt has exactly the same luminescence as the mud matrix.

NR 16 (5.9) — Fenestral mudstone — Algal marsh (intertidal)

Classic Mosheim fenestral lithology, with rare pisoids, but no diagenetic grainstone texture. Irregular fenestrae are very abundant, and many of these are very large. There is no other type of porosity. Very many of the fenestrae are floored with diagenetic crystal silt that is lighter colored than the rock matrix, but all remaining porosity is filled with equant calcite. Under CL, the equant cement has some non-/bright-/dull-

luminescent zonations, as described above. Crystals do not show any pendant distributions, but grew from all sides of the pore equally. Pore centers are filled with vaguely subzoned, dull luminescent crystals. The internal sediment on the floors of some fenestrae has the same character under CL as the muddy matrix.

NR 15 (4.7)	Fenestral mudstone	High algal marsh (high intertidal to supratidal)

Similar to NR 16, but contains abundant pisoids. (No thin section)

NR 14 (3.2)	Fenestral mudstone	High algal marsh (highest intertidal to supratidal)

Dove gray fenestral mudstone with abundant laminoid and irregular fenestrae. Coalescence of laminoid fenestrae give the rock "wavy" or "crinkled fenestral lamination" similar to NR 17, but this sample lacks sheet cracks and does not have the diagenetic grainstone texture or pisoids. Fenestrae contain no internal sediment or crystal silt, and all pores are filled with non-luminescent, equant calcite cement. Matrix contains quite a bit of dolomite, compared with overlying samples (but does not exceed about 2%).

NR 13 (2.7)	Mudstone	Low algal marsh/tidal pond margin (low intertidal)

Dove gray mudstone with far fewer fenestrae than the overlying samples. Fenestrae are organized into vertically-oriented trains of gas escape buddles Contains fairly common vugs and burrows that are floored with brownish internal sediment and filled with clear equant calcite. Quite similar to NR 11 and 12, which are described below. (No thin section)

NR 12 (1.7)	Mudstone	Tidal pond (subtidal)

Medium-gray, non-fenestral, non-laminated, basically featureless peloidal mudstone. Very similar to NR 21 and NR 23. Contains some small fossil debris, rare whole ostracodes and micritic intraclasts. Contains rare burrows or vugs that are partially filled with laminated, peloidal and non-peloidal internal sediment that is beige and laminated when viewed on the polished slab surface. All remaining pore space is filled with equant calcite. Intergranular cement within the internal sediment burrow fills is brightly luminescent, but all other cement is non-luminescent.

NR 11 (0.5)	Mudstone	Tidal pond (subtidal)

Non-fenestral, non-laminated mudstone that is virtually identical to NR 12. Also very similar to NR 19, but this sample contains more fossil fragments (limited to ostracodes, pelecypods, and gastropods), most of which have been leached and replaced with calcite cement. Contains vugs that are floored with laminated, peloidal and non-peloidal marine sediment.

NR 10 (0.1)	Conglomeratic fenestral packstone	Inland or high algal marsh (supratidal)

Highly fenestral packstone lithology consisting of dolomitized muddy peloids and intraclasts with abundant, subround dolostone lithoclasts. Collected from a 0.3 m (1 ft) thick conglomeratic layer immediately above the Knox unconformity. Lithoclasts are derived from the Knox Group, and have dedolomite reaction rims. Irregular fenestrae are very abundant, and are filled entirely with non-luminescent (black under CL) equant calcite cement.

Mosheim/Mascot contact (Knox unconformity)

NR 6, 7, 8, 9 (0.0) These samples all contain the sharp, unconformable contact between the Mosheim Member (upper lithology) and the Mascot Formation of the Knox Group (lower lithology). Mosheim consists of highly fenestral conglomerates like NR 10. Pores in the basal Mosheim are combination of fenestrae and shelter pores beneath dolostone lithoclasts. All pores are filled with very clear, coarsely-crystalline, equant calcite that is entirely non-luminescent. Some pores contain a minor amount of internal sediment. Mascot consists of dark gray, intercalated limestone and dolostone ("ribbon limestone").

Mascot Formation (Knox Group)

NR 5 (-0.4) Dark gray laminated dolostone. Contains very large (up to 5 cm) vugs filled with baroque dolomite. Similar to upper Knox at the Dandridge locality.

NR 4 (-0.8) Light gray, intercalated peloidal/intraclastic grainstone and lime mudstone.

NR 3 (-1.3) Light gray intraclastic wackestone.

NR 1 (-1.4) Light gray, interbedded dolomitic limestone and chert.

Nina-B Section

The Nina-B section, as used by Shanmugam (1978), is located xxx feet from the main Nina section. Only the basal 5 m of the Mosheim is exposed here, but that part of the unit, and its basal contact with the Knox Group is exceptionally well-exposed. The post-Knox unconformity is very striking here, with up to 0.5 m relief, and with a 0.5 m thick conglomeratic zone overlying the unconformity. The conglomerate includes clasts derived from the Mascot Formation up to 0.3m (1 ft) in diameter. Although the entire Mosheim is not exposed here, eight samples were collected from this basal portion, and six thin sections were prepared.

Mosheim Member

NBR 6 (3.0) — Fenestral mudstone — Algal marsh (intertidal)

Dove gray mudstone.with abundant, but very small, irregular fenestrae. Contains several argillaceous laminae. (No thin section)

NBR 5 (2.0) — Fenestral mudstone — High algal marsh/levee backslope (supratidal)

Fenestral mudstone with well-developed "disrupted flat lamination" produced by bed-parallel orientation of laminoid fenestrae between non-fenestral mud crusts. Also contains an abundance of very large (up to 5 mm) voids filled with clear equant calcite. Fenestrae are also filled with equant calcite.

NBR 4 (1.2) — Fenestral mudstone — Inland or high algal marsh (supratidal)

Dove gray fenestral mudstone with very abundant laminoid and irregular fenestrae. Laminoid fenestrae are coalesced into bed-parallel laminae, and give the rock "crinkled fenestral lamination". All fenestrae are filled with non-luminescent equant calcite cement. Matrix contains a fair amount of dolomite.

NBR 3 (1.0) — Fenestral mudstone — Inland or high algal marsh (supratidal)

Dove gray laminated fenestral mudstone, collected from immediately above the basal conglomeratic zone. Very similar to NBR 4. (No thin section)

NBR 2, 2B (0.5) — Conglomeratic fenestral mudstone — Inland or high algal marsh (supratidal)

Conglomerate consisting of lithoclasts of dolostone and limestone embedded in a fenestral mudstone matrix. Dolostone clasts have dedolomite rims. Also contains some anhydrite and gypsum clasts that are probably allogenic (derived from Knox). Some of the fenestrae are very large (4 mm) here. Matrix is highly dolomitized. All fenestrae are filled with non-luminescent, clear equant calcite cement. These samples are very similar to the basal conglomerate at the other Nina section.

NBR 1B (0.1) — Conglomeratic fenestral mudstone — Inland or high algal marsh (supratidal)

Conglomerate just like NBR 2 and 2B. Collected from just above the post-Knox unconformity. Dolomite clasts are very large (several cm).

Mosheim/Mascot contact (Knox unconformity)

NBR 1 (0.0) — Sample contains the Knox unconformity, with Mosheim conglomeratic fenestral mudstone overlying dark gray, laminated dolostone of the Mascot Formation. The unconformity is sharp and very irregular.

John Sevier Highway Section

Several samples were collected from the side of John Sevier Highway beside the entrance to the American Limestone Quarry. The Knox unconformity is very well exposed at this location, and the seven samples collected were from the unconformity and the basal 0.5 m of the Mosheim. Thin sections were made from all seven. Because the strata are essentially flat-lying at this locality, only the basal few meters of the Mosheim are exposed along the side of the road, and no attempt was made to collect additional samples from this site.

Sample # (Position)	Carbonate Rock Classification	Depositional Subenvironment

Mosheim Member

JS 3A,B,C (0.3) — Conglomeratic intraclastic packstone — Inland or high algal marsh (supratidal)

This sample is similar to the basal conglomeratic fenestral lithologies at the Boyd's Creek Road section. The matrix, rather than consisting of mud, consists of mud peloids and small lime mud intraclasts, and in this sample is highly dolomitized. Lithoclasts of Mascot dolostone are abundant in a variety of sizes, and show evidence of dedolomitization, especially around the clast edges. This is especially apparent on the polished slab surface.

Fenestrae are very abundant, and are all irregular and quite large. Interparticle and shelter pores (beneath dolostone lithoclasts) are also abundant. There is no compelling evidence of dissolution. Porosity was at one time as high as approximately 40%, as evidenced by the large percentage of rock volume now occupied by cement. Cements types (in decreasing order of abundance) include equant calcite, fibrous calcite, and baroque dolomite. Fibrous calcite cements commonly form isopachous linings of pores or pendant morphologies beneath clasts. Baroque dolomite is intergrown with equant calcite crystals, especially in som of the larger pores. The distribution of baroque dolomite cement is not limited to pore centers, but it often lines pores, with fibrous calcite occupying the pore center. This suggests that this dolomite cement was not a late stage (burial) cement, as baroque dolomite typically is, but was a very early phase, precipitated essentially in the depositional environment. Under CL, cements show the typical zonation sequence, with non-luminescent crystals lining pores, outlined by a single thin zone of brightly-luminescent cement, followed by pore-filling dull subzoned equant calcite. Fibrous cements that line pores are entirely non-luminescent (black). Baroque dolomite cements are very dull red to non-luminescent.

JS 2 (0.1) — Conglomeratic fenestral dolostone — Inland or high algal marsh (supratidal)

This highly fenestral sample was collected from immediately above the Knox unconformity. The lithology is unique for the Mosheim in that it consists entirely of dolomite. All matrix, all clasts, and all cements are dolomite. Fenestrae are filled with coarsely-crystalline, baroque dolomite cement, as described in JS 3, but here the dolomite cement completely occupies every pore. The matrix is pervasively dolomitized with dolomite rhombs that are considerably more coarsely-crystalline than in the underlying Knox dolostones. Under CL, the baroque dolomite cements differ from the

matrix dolomite in that the baroque dolomite cement is non-luminescent, whereas the matrix dolomite luminesces dull red. Some fenestrae are lined with dull red dolomite crystals.

Mosheim/Mascot contact (Knox unconformity)

JS 1A,C (0.0) Conglomeratic fenestral dolostone Inland or high algal marsh (supratidal)

These samples contain the post-Knox unconformity within them, with basal Mosheim conglomeratic, fenestral dolostones overlying dark gray, laminated fine-grained dolostone of the Mascot Formation. The basal Mosheim in these samples is identical to JS 2, and consist entirely of dolostone, with all fenestrae filled with baroque dolomite cement.

JS 1B (0.0) Conglomeratic fenestral dolostone Inland or high algal marsh (supratidal)

This sample was collected at the same stratigraphic level as JS 1A and 1C, but a few feet away laterally. Like those samples, this sample contains the post-Knox unconformity, and consists of conglomeratic fenestral dolostone (Mosheim) overlying Mascot dolostone. In this sample, however, the majority of cements in the basal Mosheim are calcite rather than baroque dolomite. Also, the matrix is not as thoroughly dolomitized (the mud matrix is dolomitized, but many of the peloids and intraclasts are not). Cements in this sample are predominantly equant calcite, which is quite coarse, but fibrous calcite cements are also common. Fibrous cements typically line pores or occur as a pendant fringe beneath lithoclasts in shelter pores, but in some cases the entire pore is filled with fibrous cement. Baroque dolomite cements are present in some pores, and as in JS 3, the baroque dolomite occurs intergrown with equant calcite, and does not always occupy a pore-central position.

It should be noted that the Knox unconformity is very sharp when viewed on the polished slab surface of these samples, but in thin section, the unconformity surface is more vague, as if the surface between the two dolomitic lithologies "healed" duing diagenetic alteration. In thin section, the contact is recognized by a noticeable difference in the size of the dolomite rhombs, with the Mosheim dolomite more coarsely-crystalline.

VITA

Keith Eric Roberson was born on December 11, 1959 in Detroit, Michigan. At the age of eight, he moved with his family to Hamilton, Alabama, and graduated from Hamilton High School in 1977. Mr. Roberson attended the University of Alabama in Tuscaloosa from 1977 to 1982, graduating with a Bachelor of Science degree in Geology in May 1982. During 1982 and 1983, Mr. Roberson made a living as a professional bluegrass musician in Tennessee. In 1983, he enrolled as a graduate student in the Department of Geology at the University of Alabama, and studied the stratigraphic relationships of the post-Knox unconformity in the Alabama Appalachians as his Master's thesis topic. Mr. Roberson was employed with the Alabama Geological Survey from 1985 to 1986. He attained the Master of Science degree in Geology from the University of Alabama in May 1988. In 1986, Mr. Roberson married Jennifer L. Tobola, and moved to Knoxville, Tennessee to begin the Ph.D. program in Geology at the University of Tennessee. Mr. Roberson lived in Knoxville from 1986 until 1991, and for his Ph.D. dissertation, studied the depositional and diagenetic history of the basal Middle Ordovician carbonate rocks in East Tennessee. In 1991, Mr. Roberson accepted a job as an environmental geologist with International Technology (IT) Corporation in Los Alamos, New Mexico. In 1992, Mr. Roberson transferred with IT Corporation to Las Vegas, Nevada, accepting a position as a hydrogeologist to study and model the groundwater flow system and potential contaminant migration beneath the Nevada Test Site. Mr. Roberson successfully defended his Ph.D. dissertation at the University of Tennessee in December, 1993.